# PLANE STRAIN FAILURE CHARACTERISTICS OF A SATURATED SAND

Thesis submitted to the

University of London

(Imperial College of Science and Technology)

for the degree of

Doctor of Philosophy in the Faculty of Engineering

by

Derek H. Cornforth, B.Sc.(Durham), M.S.(Northwestern, U.S.A.)

July, 1961.

## ABSTRACT

The shear strength of Brasted sand in plane strain compression tests is compared with the strength under standard triaxial compression and extension conditions. Large size test specimens were used in all the tests. Comparing the drained strengths at the same placement density, the standard triaxial compression and extension tests agree to a common strength-density curve. The strength-density curve for plane strain has a similar shape to the triaxial curve but the plane strain strength is always higher, the difference in strength increasing progressively from $\frac{1}{2}^{\circ}$ in loose sand to $4^{\circ}$ in the densest specimens. It is concluded that the external strain condition is a major factor influencing the shear strength of dilatant soils.

The ultimate strength of the sand is approximately constant at all densities and has the same value in plane strain and triaxial compression tests.

The intermediate principal stress at failure in plane strain increases with increasing placement density. At all times during shear, it remains considerably less than one-half the sum of the other two principal stresses. A marked similarity in the behaviour of the major and intermediate principal stress ratios is noted.

The axial strain at failure in plane strain is always considerably less than in the corresponding triaxial tests. The volume change characteristics are also different, but the measurements are probably affected by friction between the specimen and loading platens.

Moisture content determinations on tested and untested specimens enabled the changes of density during shear to be measured. Movements of water to the central failure zone occurred in both drained and undrained tests. The moisture content determinations also revealed porosity variations within the soil resulting from the compaction technique.

The results of the undrained tests are interesting but inconclusive. Further research is needed to elaborate the points made in the discussion on these tests.

Two theoretical solutions involving dilatancy terms are examined for validity. In the final chapter, a rational empirical method of extending the Brasted sand plane and symmetric strain correlation to other cohesionless soils is put forward.

ACKNOWLEDGEMENTS

This Thesis describes research work carried out in the Civil Engineering Department (Professor of Civil Engineering : A. W. Skempton, F.R.S., D.Sc., M.I.C.E.) of Imperial College between October, 1957 and December, 1959. The delay in publication of the work is regretted, but is the result of writing the Thesis on a part-time basis.

The author is indebted to Dr. A. W. Bishop, Reader in Soil Mechanics, who supervised the research. Dr. Bishop showed considerable interest in the experimental work and offered sound advice on the test programme and techniques; he also gave many helpful suggestions in the preparation of the text. Other members of the College staff to offer assistance include Dr. R. E. Gibson, Mr. D. Evans, Mr. N. Scott and Miss J. Kinnerley.

The author also wishes to thank his present employers, the Directors of Soil Mechanics Ltd., who made the research work possible by financial aid through the Soil Mechanics Ltd. Bursary. Other present and former members of the Company who have helped in the Thesis preparation are Mr. S. Jacobs, Mr. A. C. Meigh, Mr. T. G. Clark, Mr. N. Simons and Miss B. Pankhurst.

Finally, thanks to my wife who has endured "plane strain" in the various roles of friend, fiancée, wife and mother, and who has willingly allowed our small flat to be used as a Drawing Office over such a long period. She also typed the first, and one half of the final, drafts of the text.

## LIST OF CONTENTS


| | |
|---|---|
| Title Page | i |
| Abstract | ii |
| Acknowledgements | iv |
| List of Contents | v |
| General Information | ix |

CHAPTERS — Page

Chapter 1. INTRODUCTION — 1

The triaxial test. Limited application of triaxial test. The plane strain condition. Plane strain apparatus. Aims of thesis.

Chapter 2. THE STRENGTH OF SANDS IN VARIOUS THREE-DIMENSIONAL STRESS SYSTEMS UNDER DRAINED CONDITIONS — 7

A. The standard triaxial (axial) extension test.
B. The standard shear box and its modifications. Roscoe; Peltier.
C. Special shear research apparatuses. Kjellman; Jakobson; Habib; Daniel; Kirkpatrick; Wood; Kummeneje; metallurgists.

Research test requirements. Theories of shear strength in sands :- Mohr-Coulomb; Kirkpatrick; Roscoe, Schofield and Wroth; Caquot; Bishop. Summary.

Chapter 3. DESCRIPTIONS OF APPARATUS — 28

Plane strain apparatus. Standard triaxial compression apparatus. Standard triaxial extension apparatus.

Chapter 4. DESCRIPTION OF BRASTED SAND — 32

Chapter 5. TEST PROGRAMME — 33

$K_o$-Consolidation.
Plane Strain Tests.
Drained tests:- Series A, Series B, Series C.
Undrained tests:- Series D.

Standard triaxial tests.
Drained tests (compression) :- Series E
Series F
Drained tests (extension) :- Series G
Undrained tests (compression) :- Series H
Undrained tests (extension) :- Series J

Chapter 6. PREPARATION OF SPECIMENS, TEST PROCEDURE, AND CALCULATIONS 39

I Plane Strain Tests.
Specimen preparation. Test procedure.
II Standard Triaxial Tests.
Specimen preparation. Test procedure.
III Shear Test Calculations.
All tests. Plane strain tests. Standard triaxial extension tests.

Chapter 7. COMMENTS ON MOISTURE CONTENT DETERMINATIONS, COMPACTION AND CONSOLIDATION 56

Moisture content and density. Non-uniformity of specimen density. Non-uniformity of compaction densities. Correlation of densities measured in plane strain and standard triaxial tests. Consolidation volume changes.

Chapter 8. DRAINED TEST RESULTS AND DISCUSSION 68

I Plane Strain Tests: Typical curves from Series A. End-of-test observations. Factors affecting strength. Ultimate strength. Intermediate principal stress.
II Standard Triaxial Compression Tests: Factors affecting strength. Ultimate strength.
III Comparison between Plane Strain and Standard Triaxial Compression Tests.
IV Volume Changes during Shear: Uniformity of volume changes. Onset of dilation. Uniformity of volume changes in plane strain. Progressive failure. Volume changes and ultimate strength.
V Standard Triaxial Extension Tests.
VI Strength and Strain Conditions during Shear: Development of shear strength in intergranular structure.
VII Theoretical Solutions: A. Energy Term Hypothesis. Test results. B. Simple Shear Failure Zone Hypothesis. Compression tests. Extension tests. Test results. Interpretation of dilatancy terms.

Chapter 9. UNDRAINED TEST RESULTS AND DISCUSSION 117

I Plane Strain Tests: Stress-strain curve.
Strength at maximum principal stress ratio.
Strength at maximum deviator stress.
Explanation of undrained strength.
II Standard Triaxial Tests: Explanation of undrained strength.
III Undrained Conditions in the Laboratory and Field.

Chapter 10. A PRACTICAL METHOD OF ESTIMATING THE STRENGTH OF SANDS UNDER PLANE AND SYMMETRIC STRAIN CONDITIONS. 135

Introduction. Theoretical solutions. Empirical solutions. Method for relating plane and symmetric strain tests. Example of design method. Uses of the design method. Extension of the correlation to other soil types. Relative porosity, relative density & relative dry density.

References 156

APPENDICES

1. Calibration of measuring devices 161

(a) Proving rings
(b) Manometers and pressure gauges
(c) Plane strain end clamp

2. Method of making rubber membranes 163

3. Rubber membrane corrections 164

Plane strain, Standard triaxial.

4. Effect of errors in measurements 166

Plane strain. A. errors in porosity. B. errors in strength. C. errors in the measurement of $\sigma_2$.
Standard triaxial compression.
A. errors in porosity.

5. Typical plane strain test computation 170

Test No. BS-P-24.

6. Alterations to the plane strain apparatus 173

End clamp. Loading head. Cell base plate.

7. Results and discussion of standard shear box tests 175

8. Some notes on the packing of sands 177

9. Factors suggesting the significance of the ultimate strength in the dilatancy contribution to shearing resistance. 180

10. Graphical presentation of shear test results 182

11. Kaolinite tests 183

Introduction. Consolidation characteristics. Measurement of $K_o$. Shear strength. In conclusion.

## GENERAL INFORMATION

### Test results

The larger part of the volume of the Thesis comprises the shear test results, which are reproduced in graphical form at the end of the book (Appendix 10). The plane strain test specimens have the prefix 'P'. The standard triaxial test specimens, having a cylindrical shape, have the prefix 'C'. Every completed shear test is included, and the numbers after the prefix are in chronological sequence.

### Reference to drawings, etc.

The photographs, tables, drawings and graphs referred to in the text are to be found at the end of each Chapter. They are always in the following order:-

Plates (photographs)
Tables
Figures (drawings and graphs)

Each item is identified by two numbers; the first number is the Chapter or Appendix e.g. Plate 3-2 denotes the second photograph to be located after the text of Chapter 3. Appendices are differentiated from Chapters in this system by use of the prefix 'A' e.g. Fig. A9-1.

### Terminology and symbols

Suffixes are as follows:-

1 denotes major principal axis (e.g. $\sigma_1$)
2 denotes intermediate principal axis
3 denotes minor principal axis
o denotes quantitative value under initial placement condition (e.g. $n_o$)
c denotes quantitative value under full consolidation load condition immediately prior to shear (e.g. $\frac{\Delta V}{V_c}$)
f denotes quantitative value at maximum deviator stress condition (e.g. $\{\epsilon_1\}_f$)

| | |
|---|---|
| $\sigma$ | normal stress |
| $\tau$ | shear stress |
| $u$ | pore-water pressure (relative to atmospheric pressure) |
| $\epsilon$ | linear strain |
| $\frac{\Delta V}{V}$ | volumetric strain |
| $\mu$ | coefficient of friction |
| $\phi$ | angle of shearing resistance |
| $\nu$ | Poisson's ratio |
| E | Young's modulus (or modulus of deformation) |
| e | voids ratio |
| n | porosity |
| $\gamma$ | density |
| G | average specific gravity of soil particles |

Effective stresses are calculated as $\sigma' = \sigma - u$

where $\sigma'$ = effective normal stress

$\sigma$ = total normal stress

The term 'axial' refers to the stresses and strains in the vertical direction on all types of test.

## Chapter 1 INTRODUCTION

### The triaxial test

The techniques of the triaxial (or cylindrical) compression test have become firmly established in the field of soil mechanics. The increasing use of the test in research and commercial laboratories is a clear indication that most engineers regard it as having greater merit than any other shear test method.* A detailed description of the equipment and test procedure is to be found in a textbook by Bishop & Henkel (1957).

Briefly, the advantages of the triaxial test are:-

(i) the principal stresses acting on the soil are approximately known at all times during the test.

(ii) the drainage conditions can be controlled.

(iii) the zone of rupture is not rigidly imposed on the soil.

On the debit side, owing to friction on the loading platens, the soil specimen deforms into a barrel shape during shear and results in a slightly non-uniform distribution of stress.

A large amount of basic research has been devoted to the shear strength of soils. The historical development of our present knowledge has been treated in Theses by Hafiz (1950), Bjerrum (1954), Wroth (1958) and Hirschfeld (1958). The most important result has been experimental proof that the behaviour of soil is governed by the effective stresses applied to it, although the exact mechanism of effective stress is not yet known (Skempton, 1960). In saturated soils, the effective stress $\sigma'$ is equal to the applied stress $\sigma$ less the neutral stress of the pore-water $u$. If the test results are expressed in terms of the modified Coulomb equation

---

* the triaxial apparatus is useful for simulating non-failure conditions which occur in soil mechanics e.g. $K_o$ (zero lateral strain) tests, constant factor of safety tests, dissipation tests, permeability tests. The sample shape is also an advantage in tests on undisturbed soils recovered from boreholes.

$\tau = c' + (\sigma - u)\tan\phi'$, the effective strength parameters of the soil mass, $c'$ and $\phi'$, are mainly controlled by:-

(i) the properties of the soil grains (i.e. soil minerals, particle shape, surface phenomenon, etc.).

(ii) the packing of the soil grains (i.e. relative density, stress history, etc.).

Limited application of triaxial test

The fluid pressure surrounding the soil in the triaxial test represents two of the three principal stresses. Although the soil can be taken along several different stress paths to failure, the results of these tests are only strictly applicable to soil problems in which such a symmetry of stress conditions exist; for example, the axis of square and circular footings, piles. Few engineers are aware of this limitation to the triaxial test. The commonly accepted Mohr-Coulomb criterion of failure tacitly assumes that the intermediate principal stress $\sigma_2'$ has no effect on the shear strength $\frac{1}{2}(\sigma_1' - \sigma_3')$ of soil. This assumption has never been satisfactorily proved by experiment and the wide adoption of the triaxial test has inhibited research on unequal stress conditions. It is sometimes argued that the condition $\sigma_3 < \sigma_2 < \sigma_1$ would lead to a higher strength which could be used as an additional factor of safety in design, but the results of triaxial extension tests in which $\sigma_3 < \sigma_2 = \sigma_1$ (see Chapter 2) have not supported this claim.

The plane strain condition

Many practical soil failures approximate to a condition of plane strain in which no movement takes place along one of the principal axes. The three principal stresses have different values, with the intermediate principal stress acting along the axis of zero deformation. Some of the design problems in this group are earth dams, embankment and cuttings for roads and railways, foundation excavations, retaining walls and strip footings.

It is clear that a majority of stability analyses fall into the category of two-dimensional strain problems yet, at the present time, design methods use the value of the shearing resistance obtained from

standard triaxial compression test data. This practice should not be condemned for routine foundation problems. The triaxial test is simple to perform commercially and the available evidence, including correlation with actual failures in the field, does not suggest any radical changes in strength under other intermediate principal stress relationships. However, there is an increasing number of large earthwork projects in civil engineering practice. Stability calculations for these projects are based on limit design and a marginal factor of safety against failure. The quantities of soil placed during the construction of an earth dam are so large that improved accuracy in design is an important economic factor. The recent advances in methods of stability analysis (Bishop, 1955; Little & Price, 1958) and the field measurement of pore-water pressures (Armstrong, 1945; Penman, 1956; Conference on Pore Pressure and Suction in Soils, 1960) should be coupled with a better knowledge of the shear strength under the appropriate stress-strain conditions.* Finally, it is worth mentioning that a knowledge of the plane strain condition is important in the development of design methods because the reliability of a design method can only be checked on an actual shear failure; that is, on a stability analysis with a known safety factor of 1.0. In this case, the strength value used in the calculations must correspond with the type of failure which took place.

In summary, research on the plane strain condition in soils is justified on three points, namely:-

(i) basic research; to gain further understanding of soil behaviour with particular reference to unequal principal stress conditions.

(ii) earth dams and other large-scale earthworks; to compare the plane strain effective strength parameters with the corresponding parameters determined from triaxial test data.

---

* the plane strain condition is only one consideration; other factors include the shape of the slip interface, the rotation of the principal stresses along the potential slip interface, progressive failure, non-homogeneity of constructional materials, etc.

(iii) design methods; to aid in the development of improved design methods for the plane strain condition.

There is now a widespread interest in the general effect of the intermediate principal stress on the shear strength of soils and it was one of the subjects discussed at the 4th International Conference on Soil Mechanics in London, 1957. Almost all of the published work has been carried out on cohesionless materials. The resulting data is contradictory and will be discussed in some detail in Chapter 2. The main difficulty seems to be the design of a suitable apparatus for varying the three principal stresses independently of each other. Another problem which arises in comparative studies on cohesionless soils is to ensure that the placement or consolidated densities are comparable between tests employing different shapes of specimens.

Plane strain apparatus

An apparatus has been developed at Imperial College which measures the shear strength of soils for the important condition of plane strain. The working principles of the apparatus were conceived by Dr. A. W. Bishop and Dr. C. C. Wood, and the constructional details have been presented by Wood (1958). The test specimen is nominally 16 inches long, 4 inches high and 2 inches wide, thus retaining the same height:width ratio as the standard triaxial test specimen. An outstanding design feature of the apparatus is a strain control device (hereafter termed "the end clamp") which is placed in contact with the plane ends of the specimen. During a shear test, the device maintains plane strain and the necessary additional stresses applied to the ends of the specimen are measured directly using a null technique. The values of the intermediate principal stress for plane strain, being measured for the first time, are of special interest.

One of the aims of this thesis is to compare the plane strain shear parameters with those of the standard triaxial test. To do this, the test results must be sufficiently accurate that any measured differences in the soil characteristics cannot be attributed to errors in technique or apparatus. Hence, emphasis has been placed on the accuracy of experiment and measurement. End friction on the plane strain specimen is reduced by coating the areas with a thin layer of

silicone grease. The effect of end friction on the measured strength is further minimized by making the test specimen long relative to the other two dimensions. In applying the deviator stress, ram friction in the vertical direction is practically eliminated by the use of rotating bush assemblies on both the plane strain and standard triaxial cells.

The triaxial test specimen has a nominal diameter of 4 inches and height of 8 inches, the volume thus being similar to the plane strain test specimens. The use of large specimens for research has several advantages:-

(i) the density of the soil can be measured with a relatively high degree of accuracy.
(ii) the rubber membrane correction is negligible.
(iii) the failure plane area is large, reducing the effects of imperfectly formed specimens.

Aims of thesis

The original programme envisaged the testing of a typical normally consolidated clay and a typical sand. Much of the author's time was spent in an attempt to overcome the technical difficulties of testing a large specimen of clay. The choice of clay, Supreme Kaolin, proved to be an unfortunate one as the data obtained from preliminary tests was inconsistent. Certain aspects of the problem are presented in Appendix II.

The main body of this Thesis is concerned with the shear strength properties of a typical sand. The background of research on the shear strength of cohesionless soils in the triaxial test is fairly well known. The tests carried out may be subdivided into two main groups:-

(i) tests to determine the mechanical properties of the soil.
(ii) tests to determine the influence of the triaxial apparatus on the measured characteristics.

It is assumed that the reader will be familiar with most of these investigations. For brevity, it is not proposed to summarise the conclusions at this stage but, instead, to refer to the relevant information as the subjects are discussed in the latter part of the

Thesis. The principal sources of reference have been the Triaxial Shear Report (1947), Kolbuszewski (1948), Taylor (1948), Hafiz (1950), Eldin (1951), Nash (1953), Penman (1953), Shockley (1953), Bishop (1954), Fraser (1957), Kummeneje (1957) & Bjerrum, Kringstad & Kummeneje (1959).

The plane strain research has been limited to one sand, but many of the conclusions are likely to be of general validity for cohesionless soils. Brasted sand was chosen for the research work as a considerable amount of data had already been obtained on this sand through previous experiments at Imperial College (Kolbuszewski, Hafiz, Eldin & Fraser).

The objects of the present research work are:-

(i) to compare the strength, together with associated strain and volume change characteristics, of fully saturated Brasted sand under plane strain and axially symmetric strain conditions.

(ii) to measure the value of the intermediate principal stress in plane strain.

(iii) to assess the importance of the intermediate principal stress on the shear strength of cohesionless soils.

(iv) to consider the possibility of relating the strengths of cohesionless soils in a general stress-strain system.

## Chapter 2 THE STRENGTH OF SANDS IN VARIOUS THREE-DIMENSIONAL STRESS SYSTEMS UNDER DRAINED CONDITIONS

Many special types of test apparatus have been built for investigating the shear strength properties of soils under different stress-strain conditions. A survey of the published results does not show any general agreement about the influence of the intermediate principal stress on strength. In this chapter, a summary of the individual contributions will be presented. For convenience, they may be divided into three distinct groups, as follows:-

A. The standard triaxial extension test
B. The standard shear box and its modifications
C. Special shear research apparatuses

A. The standard triaxial (axial) extension test gives the strength of soil at the upper limiting value of the intermediate principal stress. The cell pressure represents both the intermediate and major principal stresses. The two most common techniques to cause failure are (i) keeping the cell pressure constant and reducing the axial stress, and (ii) keeping the axial stress constant and increasing the cell pressure. The test is of special importance as there are few methods of measuring strength when the intermediate principal strain is compressive.

The standard triaxial compression and extension test specimens are prepared in the same manner, and the measured densities are subject to the same degree of experimental error. For this reason, the comparative accuracy of carefully prepared specimens should be extremely good. In the measurement of strength, however, the extension test is particularly sensitive to errors and much more scatter of the test results is to be expected. There are two main reasons for errors in the measured strength of extension test specimens. Firstly, there is a tendency for the test specimens to undergo a localized reduction in cross-sectional area in the failure zone. The strength of such a specimen will be underestimated if the stress calculations assume that the specimen has retained the shape of a right circular cylinder during shear. One method of obtaining a more correct value for the strength

is to calculate the area of a plane passing symmetrically through the centre of the neck at an angle of $(45 + \frac{1}{2}\phi)^\circ$ to the vertical axis of the specimen. The test is stopped immediately after the maximum deviator load has been attained and the necked zone of the specimen is measured. Eldin (1951) measured the actual area of the failure plane in this manner and showed that the error of assuming the right cylindrical shape at failure was much greater in the extension test than in the compression test at the same axial failure strains. Necking is most prevalent in loose sand specimens.

The second source of error is that the measured value of the minor principal stress is affected by errors of the deviator stress in the extension test. To illustrate this point, suppose that a proving ring calibration is in error by 2% at failure when the true stresses on the soil are:-

$$\sigma_1 - \sigma_3 = 100.0 \text{ lb./sq.in.}$$
$$\sigma_3 = 30.0 \text{ lb./sq.in.}$$
$$\therefore \frac{(\sigma_1 - \sigma_3)}{\sigma_3} = 3.33 \ (\phi = 38{\cdot}7^\circ)$$

The effect on the measured strength in a compression and an extension test due to the error in the ring calibration would be:-

| | Compression | Extension |
|---|---|---|
| $\sigma_1 - \sigma_3$ = | 102.0 lb./sq.in. | = 102.0 lb./sq.in. |
| $\sigma_3$ = | 30.0 lb./sq.in | = 28.0 lb./sq.in. |
| $\therefore \frac{(\sigma_1 - \sigma_3)}{\sigma_3}$ = | 3.40 $(\phi = 39{\cdot}0^\circ)$ | = 3.65 $(\phi = 40{\cdot}2^\circ)$ |

It is clear from the above calculation that, for deviator stress measurements, the normal range of scatter which occurs in the compression test will be magnified 3 to 5 times in the extension test; that is, by the ratio of the principal stresses at failure (approximately). Hence, the usual factors which can influence the correct measurement of the deviator stress achieve a greater significance in the extension test. Apart from the proving ring calibration already mentioned, rubber membrane effects, piston friction or failure to accurately record the maximum deviator stress are worthy

of mention. It is also noteworthy that a constant error in the cell pressure measurement would not affect the comparison of strength in the two types of test.

To sum up, great care must be taken in the measurement of the deviator stresses in the standard triaxial extension and compression tests if a good comparison is to be made between the tests. The correlation of porosities in the two types of test is not a problem as the specimens are prepared in an identical manner.

The results of published comparisons between the extension and compression tests on sands are summarized in Table 2-1 together with the graphs of Eldin (1951) and Peltier (1957) on Figure 2-1. Eldin's results were corrected for the reduction in area of the failure plane due to necking. Kirkpatrick claims that necking did not occur in his test specimens until after failure had taken place. The French experimenters, Habib (1953) and Peltier (1957) do not mention area corrections in their publications. A photograph of a failed extension test specimen in Habib's Paper showed that considerable necking had occurred. It is doubtful, however, whether area corrections could account for the differences in strength of approximately $7^{\circ}$ measured in their tests.

The general conclusion from the previous work on the standard triaxial extension test is that the strength is about the same or somewhat lower than that of the corresponding compression test. This may seem to be a surprising result in view of the fact that the intermediate principal stress is equal to the major principal stress in the extension test. It suggests that the strength of sands does not depend on the average principal stress acting on the soil.

B. The standard shear box and its modifications This well-known test apparatus is illustrated on Fig. 2-2. The box is separated into two halves at the mid-height and takes a soil specimen nominally 6 cm. square and 2 cm. thick. The lower half of the box rests in a tank which is caused to slide horizontally on two ball bearing tracks by a constant rate-of-strain loading jack. The reaction is transmitted from the top half of the shear box to a calibrated proving ring. The normal load is applied to the horizontal square section of the specimen by means of a

loading cap and lever system. A dial gauge, set on the centre of the top cap, measures the vertical deformation of the specimen during shear.

For many years, the shear box (or direct shear test) was accepted as a standard method of measuring the shear strength of soils and, consequently, a good deal of data has been collected on the behaviour of sands in the test. It is extremely simple to carry out the test and the drainage path is conveniently short, which reduces the duration of drained tests on clay.

In the last decade, however, the shear box has gone out of favour as a standard test because of its theoretical and practical limitations. Some of the disadvantages are:-

(i) failure is progressive, developing from the ends of the box to the middle.

(ii) friction between the specimen and sides of the box make the principal stresses difficult, if not impossible, to evaluate. There is also a continual change in orientation of the principal stresses throughout the shearing process.

(iii) under light normal loads, parts of the specimen may be subjected to tensile stresses (Roscoe, 1953).

(iv) at large strains, the normal load acts over the whole of the top half of the box but only over part of the lower half of the box.

(v) it would be difficult to adapt the shear box to measure pore-water pressure changes during a shear test, although constant volume undrained tests have been carried out by Taylor (1951).

(vi) the shear box test is not as versatile as the standard triaxial compression test; that is, stress and drainage conditions cannot be varied to simulate different types of failure.

(vii) the soil must fail in a pre-determined zone of shear.

(viii) there is some controversy as to whether the horizontal shearing stress is the shear stress on

the failure plane or on the plane of maximum shear.

The final disadvantage is less well-known than the others and bears closer examination. The usual interpretation of the failure stresses is that in which the normal and shearing stresses are taken to be the stresses on the plane of failure, as outlined, for example, by Taylor (1948). However, Hill (1950) in a footnote to his book on plasticity, openly disagrees with this interpretation on theoretical grounds. He argues that the deformation of the soil in a shear box is so constrained as to be effectively a simple shear in a narrow zone. If the material is isotropic, the directions of maximum shear stress and maximum shear strain-rate must coincide (De Saint-Venant's Principle) and hence the shear stress measured in the test is the maximum shear stress of the material; that is, the radius of the Mohr circle. In this case, the line tangential to the Mohr circle and passing through the origin of the Mohr diagram will have a greater slope in Hill's interpretation of the shear box result than in the interpretation of Taylor (Fig. 2-2). De Jong (1959) showed that there are theoretical grounds for believing that the directions of maximum shear stress and maximum shear strain-rate do not necessarily coincide for granular materials. In his theoretical work on the statics and kinematics of soils, he claims that the two directions can differ within the range $\pm \phi$ for cohesionless soils but that they coincide for $\phi = 0$ materials. Most plasticity theories disregard the volume changes which occur in the failure zone of soils.

It is not proposed to summarize the test data obtained from shear boxes but the test is of some interest because the soil is sheared in plane strain. Comparisons of the strength of various sands in the shear box and triaxial compression apparatus are tabulated in Table 2-2. All the tests reported in the table were carried out on small test specimens so that the accuracy of the density correlation may not be particularly good. The strengths of the shear box specimens are based

on the usual (Taylor) interpretation of the failure stresses. The normal stresses at failure in the two types of test were similar in all cases.

Almost every possible combination of conclusions have been reached and there is little that one can say in summarizing them except, perhaps, that the two tests give approximately similar values of strength at comparable porosities. However, if the Hill interpretation of the shear box test is correct, it is likely that the strength of a sand in plane strain will be very much greater than the strength in the comparable triaxial compression test.

Roscoe (1953) has built a modified form of shear box in which the soil specimen fails in simple shear (Fig. 2-3). The box retains the dimensions of the small standard shear box but two opposite sides of the box are hinged so that they rotate parallel to each other during shear. A rubber membrane is placed between the specimen and the sides of the box and friction is considerably reduced by applying a thin layer of silicone grease to the outer surface of the membrane. A series of tests on striped plasticine showed that the box produced a simple shear distortion on this material. No results of shear strength tests on soils have been published yet but it is understood from Wroth (1958) that considerable difficulties were experienced in reaching the maximum deviator stress on all but the densest sands and that the ultimate strength of the sand was never attained. To avoid fouling during the test, the top loading cap has to be initially level with the upper edges of the box. However, when the sides of the box rotate from the initial vertical position, the volume of the box decreases whereas a sand specimen usually increases in volume during a shear test. The net result is that a certain portion of the specimen rises out of the box and is no longer subject to simple shear strain or any lateral stresses (Fig. 2-3). There is a possible danger of failure taking place along the line D'C'. Other disadvantages of the Roscoe shear box are that, like its predecessor, it is not as versatile as the triaxial compression test and the normal stress is not uniform throughout the specimen when the box is in an extended position.

Peltier (1957) describes a shear box in which the two halves are

separated at the mid-height in the same way as the standard shear box but in which the two vertical sides at right-angles to the line of shear can be moved horizontally and are loaded independently of the normal and shearing stresses (Fig. 2-3). The moveable sides are lubricated in some undisclosed manner to reduce friction between the specimen and sides of the box and each of the four half-sides are loaded by a lever system prior to the test. The vertical normal stress is applied by a piston. The specimen is then sheared to failure in the usual manner. No details are given of any individual test results. The form of equation chosen to relate the three stresses (Fig. 2-3) is somewhat indefensible as the test range values of the stress $\sigma_2$ are not stated. It is implied in the Paper that the equation will hold for all values of $\sigma_2$. The Peltier shear box is also subject to all the disadvantages listed for the standard shear box.

C. Special shear research apparatuses The results and conclusions of this final section are much more difficult to evaluate than in the earlier sections, where the same types of test were carried out by several different operators on many soils. In the present section, each piece of apparatus is unique and there is often little published comment on its performance. Hence, the reliability of the apparatus can only be assessed in the most general terms. The correlation of densities is another important consideration in comparative studies, particularly if the test specimen is of a different shape or size.

Kjellman (1936) reported some test results on an apparatus built in 1933 and which tests a cubical specimen of 6.2 cm. side (Fig. 2-4). In each principal direction, the specimen is compressed between a frictionless steel piston and a steel reaction plate on the opposite side of the specimen. The pressure is transferred to the specimen, on each side of the cube, by 100 No. 0.6 cm. square section brass rods with plane ends bearing on the specimen and spherical ends in contact with the end of a piston or reaction plate. The rods reduce friction on the sides of the specimen during shear, the rods being free to move laterally as the specimen deforms. The apparatus is supported by a cast-iron frame. Each piston is loaded by a lever system, a suspended water tank being used in preference to weights. The applied pressure is read directly

from the water level in the tanks, the maximum pressure being 13 kg./sq.cm. The advantage of the water tanks pressure system is that a smooth transition of pressures can be achieved. In constant average principal stress tests, a closed hydraulic system is used, water being transferred from tank to tank according to the test requirements. No membrane is used for coarse sand specimens, but for clays a thin rubber membrane is stretched over the specimen to prevent soil squeezing out between the rods.

The shear test results on dry German standard sand are tabulated in Fig. 2-4. The strengths of the sand in the two tests having an intermediate principal stress greater than the minor principal stress were appreciably higher than the strength measured in test 3, which had the same stress system as the standard triaxial compression test. He concluded that the difference in strength was due to the influence of the intermediate principal stress. It is interesting to note from Kjellman's curves that the small amounts of intermediate principal strain at failure in tests 1 and 2 were approximately the same in magnitude but of different sign.* The ratio of the intermediate to the sum of the other two principal stresses in these two tests are 0.42 and 0.50 respectively. It may be deduced, therefore, that the failure relationship $\sigma_2 = 0.46(\sigma_1 + \sigma_3)$ would occur in a test under plane strain conditions.**

It is probable that Kjellman's apparatus is better suited for the investigation of small principal strains rather than for tests carried to failure. The initial clearance between each loading rod in his apparatus is only 0.02 cm. so friction between the specimen and the rods must increase considerably when the clearance has been eliminated at a

---

* presumably the compressive strain in test 2 was insufficient to cause fouling between adjacent sets of rods.

** as tests 1 and 2 have different stress histories, it must be assumed that this factor has no effect on the relation between the three principal stresses at failure.

principal compressive strain of 3.2%.* On the other hand, if the clearance between the rods increases to more than the sand particle sizes during a shear test, the sand grains will move into the gaps.

Jakobson (1957) used Kjellman's apparatus for his investigation of the modulus, Poisson's ratio, compressibility and strength of two uniform, coarse, medium dense sands. The intermediate principal stress was kept equal to either the major or the minor principal stress in all the tests. The tests were not carried to failure, owing to the limited range of movement in the apparatus, but Jakobson deduced the strength of the sands by extrapolating his curves to a modulus value of zero. Part of his test data has been replotted to a linear scale on Fig. 2-5. There is too much scatter in the results to warrant a confident extrapolation to a definite failure strength but the general trends of the points on the graphs are indicated by broken lines. It does seem likely that the failure strengths of both sands would be greater when the intermediate principal stress is equal to the major principal stress than when it is equal to the minor principal stress. The same result would also seem apparent in the unloading tests, although there is less data available at small modulus values. This set of data, therefore, conflicts with the conclusions reached in comparing the standard triaxial compression and extension tests. Jakobson concluded that the intermediate principal stress has a considerable influence on the shear strength of sands.

Habib (1953) describes a torsion test for investigating the influence of the intermediate principal stress on the strength of soils (Fig. 2-6). The torsion test specimens are similar in shape to the standard triaxial test specimens except that the cross-sectional area is increased at the ends of the specimen to prevent failure occurring at these points. In the drained torsion test, the cell pressure and axial stress are held constant under equilibrium conditions. The soil specimen is then failed by applying a torque to the top cap so that the specimen is twisted relative to the stationary base spigot. The shear

---

* in the standard triaxial compression test, failure occurs at a major principal compressive strain of 4 to 15%, depending on the initial density of the sand.

stress produced by the torque in the plane of the axial stress is calculated from plastic theory and has complementary values in the planes, mutually perpendicular to it, represented by the cell pressure. The specimens have a spiral failure zone (Fig. 8-17).

Habib compared the results of a series of drained torsion tests on loose Fontainebleau sand with corresponding standard triaxial compression and extension tests (Fig. 2-6d). The shear strength of the sand attained a maximum value when the parameter $\lambda$ was 0.22, and the strength results show a steady transition between the limiting values of the intermediate principal stress. A series of Mohr circles were drawn for each test series having a constant ratio between the cell and axial pressures, and the cohesion intercept on the Mohr diagram was taken to be the constant rubber membrane correction.* The rubber membrane correction, calculated in this way, varied from 7 to 13% of the total shearing resistance.

No values are given of the porosities measured in the two types of test specimen but the specimens are probably sufficiently similar in shape to give a good density correlation for soil placed in an identical manner. The torque test, however, is open to some criticisms. The distribution of the axial stress is non-uniform and the thickened ends of the specimen must have a considerable influence on the torque measurements. The shape of the test specimen makes it difficult to measure the density accurately. Finally, the distribution of the shear stress produced by the torque varies from zero at the centre to a maximum at the circumference of the specimen. It is not known to what extent the concepts of plasticity, adopted for the computations of shearing resistance, are valid for the interpretation of shear tests on granular soils.

Daniel (1954) carried out experiments on two uniform dry sands

---

* this assumes that the true Mohr envelope for sands is a straight line passing through the origin of the Mohr diagram and that the rubber membrane correction is independent of the cell pressure. A similar argument, in general terms, was put forward in the Triaxial Shear Report (1947).

using a steel box $3\frac{1}{2}$ inches high x $1\frac{3}{4}$ inches square with moveable rectangular sides so that the stresses normal to the sides of the box could be varied independently. The sides of the box were connected together by rubber jointing material, the rubber being folded inwards before the sand was poured into the box (Fig. 2-7). The lateral pressures were applied to the soil through a system of weights and levers. The apparatus was adapted to be used in the standard triaxial framework, the vertical pressure being added through a plunger. The vertical load was measured on a proving ring.

The apparatus did not behave entirely satisfactorily. Opposite pairs of strain dial gauges gave inconsistent readings and each type of test was repeated several times to obtain average readings. The porosity of the sand in each test was not measured, although attempts were made to place the soil at a constant density. The box tests were not carried to failure, the strengths of the sands being deduced from the extrapolated asymptotic values of the stress-strain curves. The comparison between the standard triaxial compression tests and tests at equal lateral pressures in the box showed a reasonable measure of agreement. The maximum principal stress ratios for the two sands were approximately 5.0 and 4.6, suggesting that the sands were densely compacted. The strengths obtained under non-equal stress conditions were surprisingly high, and maximum principal stress ratios of up to 12.6 were recorded. Daniel did not discuss the likely effects of wall friction or the corner joints on the test results.

Kirkpatrick (1954, 1957) describes a hollow thick cylinder shear test in which the specimen is subjected to three unequal principal stresses. The test specimens are nominally 6 inches high and the outer and inner diameters of the cylinder are 4 inches and $2\frac{1}{2}$ inches respectively. A soil specimen is failed by holding the cell pressure on the outer wall of the cylinder at a constant value and increasing the inner (bore) pressure. The dimensions of the specimen were chosen in the design so that the differences of bore and outside pressures acting on the sealed end of the specimen would bring the axial stress at failure to a value approximately mid-way between the average values of the tangential and radial stresses i.e. $\sigma_2 \simeq \frac{1}{2}(\sigma_1 + \sigma_3)$. Rubber

membranes cover both walls of the thick cylinder specimens and are ingeniously sealed at the top and base. The outside pressure is supplied from a constant head mercury tank and the inner pressure is applied by a foot controlled pump, both pressures being measured by mercury manometers. The stress system is shown on Fig. 2-7. The test is stopped immediately after failure has occurred. The dimensions of the specimen are then measured and the measurements used for the calculation of the stresses acting on the soil at failure. The apparatus can be easily adapted to provide an axial stress additional to that produced by the bore and outside pressures.

Kirkpatrick carried out a series of drained shear tests on a saturated, uniform, medium sand. He investigated the strength characteristics of the sand under three different stress systems and compared the results with the Mohr-Coulomb criterion of failure and the criteria of von Mises and Tresca extended so that the maximum shear stress is a function of the mean normal stress on the failure plane. The data is presented as a plot in a plane at right-angles to the space diagonal $\sigma_1 = \sigma_2 = \sigma_3$ . This method is commonly adopted for the study of yield in metals (Nadai, 1950) and is outlined at a later stage in the chapter. A set of thick cylinder tests were carried out on uniform, very dense Loch Aline sand using cell pressures varying from 14.4 to 54.8 lb./sq.in. The angle of shearing resistance in the individual tests varied from $39.9^\circ$ to $42.7^\circ$, the average values of the angle and the consolidated porosity being $41.2^\circ$ and 35.6% respectively.* There was no evidence of any variation in the angle of shearing resistance due to the different cell pressures. This friction angle was approximately $2^\circ$ higher than the angle measured in the standard triaxial compression and extension tests at 35.1% porosity (Fig. 2-7). One, or occasionally two, vertical cracks appeared in the side of the specimen at failure. On examination of the specimen after failure, it seemed that one side of the crack had rotated outwards along a shear trajectory, while the remainder of the specimen had retained its

---

* the angle of shearing resistance was based on the assumption that the average radial stress was equal to half the sum of the bore and outside (cell) pressures.

circular shape (Fig. 8-17). The measured volumetric strains in the thick cylinder tests, typically 0.45% expansion, were much less than the corresponding volume increases, of approximately 7.5%, measured in the triaxial compression tests. This suggested that the failure zone was confined to the deformed wedge of material in the crack. Kirkpatrick concluded that the Mohr-Coulomb criterion provides a reliable means of estimating the strength of sands under conditions of full drainage. However, he suggested that the general condition of yield in sand may depend to some extent on strain.

An advantage of the thick cylinder as a shear test is that two of the stresses are applied by fluid pressures. The only frictional forces present in the test are at the ends of the cylinder. The main disadvantage of the test is that the radial and tangential stresses at failure have maximum values at the inner wall, and minimum values at the outer wall whereas the axial stress is constant at all parts of the cylinder wall. Therefore, the relation between the intermediate principal stress and the sum of the other two principal stresses is not constant throughout the specimen but varies from approximately 0.4 at the inner wall to 0.6 at the outer wall, If the strength of sand is dependent on the value of the intermediate principal stress, the thick cylinder test will only give an average strength over a range of intermediate principal stress relationships. Another disadvantage is that the calculation of the friction angle is complicated by the non-uniform distribution of the radial stresses, the actual distribution being dependent on the friction angle (Fig. 2-7). Therefore, it is necessary to calculate directly, or by a series of approximations, the value of the average radial stress which is mathematically compatible with the distribution of the radial stresses and the known values of the average tangential stress and the failure stresses at the bore and outside of the thick cylinder. Fortunately, the radial stresses do not vary appreciably from a linear distribution in Kirkpatrick's apparatus, so the error in assuming a straight line relationship between the bore and outside pressures was not great.

A few points call for comment with regard to the experimental work. The first point is that the dimensions of the specimen may change

between failure and measurement, due to the release of the external stresses on the soil. Secondly, the difference in strength between the thick cylinder and standard triaxial tests would have been greater if they had been compared at the same porosity. For example, the measured strengths in the thick cylinder and triaxial tests at 35.6% porosity, based on the rate at which the sand strength was changing with respect to its porosity,* would be $41.2^{\circ}$ and $38.3^{\circ}$ respectively. This represents an 18% increase in the strength of the soil in the thick cylinder test. Despite these minor criticisms, the experimental work has obviously been performed with great care. The fairly wide scatter of the individual test results, due to the use of small size specimens, is largely offset by carrying out many tests at approximately the same density, thus giving the research work a good comparative accuracy.

Wood (1958) carried out undrained tests at Imperial College in the plane strain apparatus described in Chapter 3. The soil used in the tests was a well-graded granular fill material from Glen Shira, Scotland, re-compacted at optimum + 3% moisture content.

A series of plane strain undrained tests with pore-water pressure measurements was compared with a series of 4 inch diameter cylindrical samples of the same compacted soil in the standard triaxial apparatus. The main results are summarized in Fig. 2-8. Interpretation of the data is complicated by a slight difference in initial dry densities between the two types of test and also by the two failure criteria of undrained tests. The Mohr envelopes were drawn to a statistical line of best fit and show that both the effective stress shear parameters, $c'$ and $\phi'$, are higher under plane strain conditions. However, the plane strain test specimens exhibited less dilatancy than the triaxial specimens with the result that the pore-water pressures at failure were greater. Thus, the triaxial test specimens had a greater strength at failure, despite having lower effective stress parameters. The axial (major principal) strains in the plane strain test varied from

---

* information supplied in private correspondence with Dr. Kirkpatrick.

4 to 10% at the maximum deviator stress compared with a range of 15 to 18½ % in the triaxial tests.

The value of the intermediate principal stress was measured throughout the plane strain test. The ratio of the effective intermediate to the effective major principal stresses remained at approximately the $K_o$ value of the soil at all stages. The ratio of the effective intermediate principal stress to the sum of the other two principal stresses, often assumed to be 0.5 in theoretical work on the plane strain condition, was found experimentally to be approximately 0.31 at both failure criteria. This is probably the first time that the intermediate principal stress has been accurately measured under strictly plane strain conditions.

The Norwegian Geotechnical Institute has constructed an apparatus which tests a specimen of similar shape to that of the Imperial College plane strain apparatus. It was deliberately designed in a much simpler form than the Imperial College apparatus and cannot, therefore, be expected to compete in accuracy. The Norwegian apparatus is illustrated in Fig. 2-9. The test specimen is nominally 4 cm. wide, 12 cm. high and either 30 cm. or 60 cm. in length. The end edges of the specimen are slightly rounded to a radius of 1 cm. There is no form of restraint to maintain the length constant during the shear test but the friction between the specimen and the loading plates is sufficient to induce a plane strain type of failure. The specimen is not enclosed in a cell and the effective lateral pressure is obtained by applying a vacuum to the lower end of the specimen via a long porous stone. The negative internal pressure is held constant during a test and it is measured at the top and bottom of the specimen by two mercury manometers. Vertical deformations during the shear test are measured by two dial gauges, one at each end of the specimen. A third vertical dial gauge was inserted at the centre of the 60 cm. long specimen. The vertical load is applied to the soil through a central ram which bears on a circular plate 8 cm. in diameter. The ram is guided in its alignment by the supports to the cross-bar loading head of the triaxial testing machine. Volume changes are measured by a water-filled burette but they are not very reliable as it is difficult to hold the vacuum pressure constant.

Kummeneje (1957) carried out a series of shear tests on dry Valgrinda sand in the apparatus and compared the results with a corresponding set of tests on large (8 cm. diameter, 20 cm. high) and small (3.6 cm. diameter, 8 cm. high) standard triaxial compression test specimens. The sand contained medium but mainly fine sand particle sizes and the individual grains were generally of well-rounded and polished quartz. The same constant strain rate of 8% per hour was used for both types of test. The sand was tested at three porosities - loose, medium and dense - and at negative pressures of 0.2, 0.5 and 0.8 kg. per sq.cm. The smaller standard triaxial specimens were tested at cell pressures of $\frac{1}{2}$, 1 and 2 kg. per sq.cm. The results (Fig. 2-10) showed that the plane strain type of failure gave a higher strength than the corresponding standard triaxial tests at all the porosities in the test range. Surprisingly, the greatest difference in strength, of 3 to 4 degrees, was measured on the medium dense specimens.

A visual examination of the failed specimens usually showed a failure zone extending along the whole length of the specimen, passing from near the base plate on one side of the specimen to near the top plate on the other side. The three vertical dial gauges showed that the top loading plate did not bend appreciably during the shear test but one end of the specimen tended to deform more than the other in many tests. At failure, the left-hand side dial gauge occasionally registered a vertical strain of up to 50% greater than the right-hand gauge.* The vertical strains at failure in the plane strain type of test were generally somewhat lower than the strains in the vacuum standard triaxial tests at comparable porosities and appreciably less than those measured in the standard triaxial tests using cell pressures. The volume change measurements were erratic but tended to show that the standard triaxial tests on dense specimens had greater percentage increases in volume at failure.

The influence of the intermediate principal stress on strength

---

* this tilting of the top plate indicates slightly eccentric loading by the vertical ram and may produce a more progressive failure in the denser specimens than specimens failed with a uniform distribution of shearing load.

has also interested metallurgists. Lode (1926) carried out tests on thin-walled tubes of iron, copper and nickel, subjected to axial tension combined with an internal hydraulic pressure. He found that the friction angle in tension and compression tests were identical but, when $\sigma_2 = \frac{1}{2}(\sigma_1 + \sigma_3)$, a 15% greater strength was measured. Bridgmann (1946) carried out two-dimensional compression tests on long prismatic specimens without longitudinal end restraint. The deviation from the plane strain condition at failure was less than 1% and the strength of the metals were 10-13% greater than the corresponding symmetric strain test specimens.

Research test requirements

The individual contributions, which have just been reviewed, represent some ingenious methods of varying the three principal stresses in failing granular soils. Often, however, the final result is only of nominal interest because the technical difficulties of the problem have been overlooked. There are two essential factors in making a satisfactory comparison between different types of shear test, namely:-

1. an apparatus which will not impose errors on the measured soil properties. No apparatus achieves all the ideal requirements which are sought but in the standard triaxial apparatus, for example, there is fairly general agreement that most of its so-called drawbacks do not appreciably affect the measured strengths (e.g. Taylor, 1941; Penman, 1953; Kummeneje, 1957). It is, therefore, a suitable test for comparing strength properties. Most other shear test devices have not been so thoroughly examined for "apparatus errors".

2. the measurements must be as accurate as possible, to minimize the scatter. Advantages in comparative work can be gained from (i) use of large size test specimens (ii) test specimens of the same shape (iii) carrying out a large number of tests to investigate one variable (iv) an independent check on the measured densities in specimens of different shape (v) the principal stresses being measured directly.

Theories of shear strength in sands

Comparison of test results under different stress conditions

requires some form of shear strength theory.

The Mohr-Coulomb criterion of failure assumes that the yield of soils is independent of the value of the intermediate principal stress acting on the soil. As there has been no convincing information to the contrary, this assumption is widely accepted in the field of soil mechanics.

Kirkpatrick (1954, 1957) has suggested a method of plotting the yield stresses of a three-dimensional stress system on a two-dimensional co-ordinate diagram.

In Fig. 2-11, the three principal stresses are shown with a space diagonal $\sigma_1 = \sigma_2 = \sigma_3$. For a standard triaxial test, two of the principal stresses are represented by the cell pressure and a two-dimensional figure can be drawn with one axis representing $\sqrt{2}.\sigma_c$, the vector sum of the two equal principal stresses.* If we consider the strength of sand to increase linearly with the normal stress on the plane of failure, two straight lines can be drawn to represent the yield criteria for the standard triaxial compression and extension tests. A right section from the space diagonal at O' cuts the strength envelope lines at A and A'. The right section represents a plane of equal average principal stress. Any combination of principal stress conditions having the same average principal stress can be plotted on a common right section and the perimeter of the section represents the failure condition in the soil. Experimental data is adjusted to a common average principal stress.

The Mohr-Coulomb criterion of failure in sand is shown as a yield surface on Fig. 2-11. The shape of the surface is that of a hexagonal pyramid with its apex at the origin. Right sections of the surface increase proportionally to the square of the distances from the origin, the distance of the yield surface from the space diagonal being dependent on the angle of shearing resistance and the mean stress on the

---

* the use of the space diagonal has also been adopted by Henkel (1959, 1960) for the correlation of shear tests on clays.

section. The section is not symmetrical with respect to the space diagonal O-O', despite the diagram representing a constant angle of shearing resistance at all values of the intermediate principal stress. The amount of eccentricity depends on the angle of shearing resistance (Fig. 2-11).

Roscoe, Schofield and Wroth (1958) have put forward a general hypothesis on the nature of yield in both cohesive and cohesionless soils. It is an extension of Hvorslev's (1937) classic work on the shearing resistance of remoulded saturated clays. Hvorslev showed that the peak shear stress at failure, $\tau_f$ , of such a soil is a function of the effective normal stress $\sigma_f'$ , and of the voids ratio $e_f$ in the plane of failure and this function is independent of the stress history in the soil. Roscoe, Schofield and Wroth have accepted these three independent variables as being fundamental parameters,* except that the shear stress is corrected for the additional work which is done by, or against, the cell pressure throughout the test (Bishop, 1954).

The results of a shear test are plotted on a diagram which has the three variables as mutually perpendicular axes. Each shear test gives a succession of points which form a loading path on the diagram. Briefly, Roscoe et al. suggest the following behaviour in soils:-

1. that the yield condition in soils can be defined by a surface in $(\tau, \sigma', e)$ space. The yield surface is bounded by the two stress reference planes, $\tau = 0$ and $\sigma' = 0$, and by the extreme conditions of density which the soil can experience. A drained yield surface for tests carried out on equal diameter steel balls in the simple shear box, designed by Roscoe (1953), is shown in Fig. 2-12. For the steel balls, a constant relationship holds between the normal stress and corrected shear stress irrespective of the placement density, but the strength and total range of voids ratios are relatively small.

2. that continuous yielding of a specimen can be represented by a loading path which rises to the yield surface after only a slight

---

* any equivalent system can be substituted for the above parameters e.g. average principal effective stress in place of the effective normal stress; water content, porosity in place of voids ratio.

distortion of the specimen and, thereafter, remains on the surface until it reaches a specific end point at large strains. The end points from all such tests define a unique line on the yield surface. Soil at this ultimate condition is said to be in a critical voids ratio (C.V.R.) state. The end point in a drained test is the ultimate state at which any further increment of shear distortion will not change the voids ratio.* In the undrained test, the loading path lies in an e = constant plane. However, the effective stress alters to bring the specimen into the ultimate state such that the voids ratio of the test becomes a critical voids ratio. The loading paths of a typical dense specimen, starting at P', and of a typical loose specimen, starting at P, are shown in Fig. 2-12.

3. that the above two concepts hold for both the drained and undrained conditions, giving one unique yield surface and C.V.R. line, and is also likely to hold for all other conditions of drainage.

At the present time, no satisfactory results have been obtained to define a unique drained and undrained yield surface for the same cohesionless soil. The parameters are difficult to apply directly to any practical problem and several points are in need of further clarification e.g. are the effective normal stress and average principal effective stress interchangeable parameters, and how does one adequately define the limits of packing? The Roscoe et al. Paper points out that there are many inherent difficulties in analysing triaxial test data on soils.**

Theoretical solutions concerning the nature of shear strength in granular materials have usually aimed at relating the angle of internal friction, $\phi_f$ , with the coefficient of friction, $\mu$ , acting between

---

* this definition also defines the Casagrande (1938) upper limiting critical density.

** they are:- difficult to set up loose specimens, fracture of the soil particles during shear, limited test range of densities in the undrained test due to cavitation, localized region of failure in the drained test making the parameters difficult to measure, inaccuracy of the triaxial test results at large strains.

the grains.* Equal diameter spheres are adopted as the model of soil grains and the analysis is based on energy considerations. Caquot (1934) has derived the relationship $\tan \phi_f = \frac{1}{2}\pi.\mu$ . More recently, Bishop (1954), has obtained general expressions taking into account the variation of the intermediate principal stress. For the triaxial compression test, he suggests $\sin \phi_f = \frac{15\mu}{(10 + 3\mu)}$ and for the plane strain condition, assuming $\sigma_2 = \frac{1}{2}(\sigma_1 + \sigma_3)$, the relationship is $\sin \phi_f = \frac{3}{2}\mu$ . Using a typical value of $\mu$ obtained in work directed by Dr. Bishop (Hafiz, 1950) the angle of internal friction for a sand under plane strain conditions would be approximately 5 degrees higher than that of the standard triaxial compression test.

The packing of the sand grains is assumed to have no influence on the value of $\phi_f$. Quite apart from the validity of the energy approach, however, there is some controversy regarding the value of the coefficient of friction, $\mu$ , of quartz grains (Tschebotarioff and Welch, 1948; Hafiz, 1950; Penman 1953).

Summary

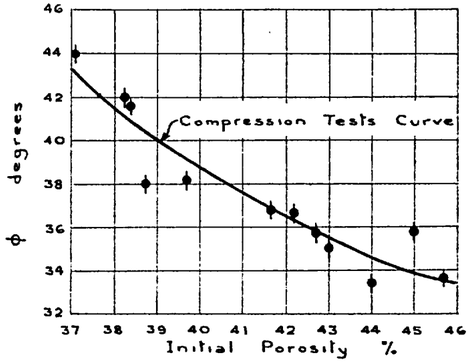
The research work of Kirkpatrick (1954), Kummeneje (1957) and Wood (1958) all give evidence that the shear strength parameters of soils under plane strain conditions are likely to be higher than the corresponding parameters of the triaxial compression test. The theoretical solution of Bishop (1954) supports this view.

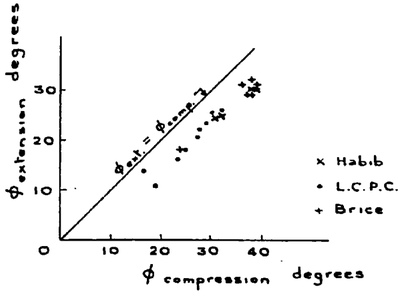
---

* "the angle of internal friction" is the angle of the Mohr envelope for the strength of soils at constant volume. A correction is applied to the results of drained shear tests in which the specimen volume is changing at failure (Bishop, 1954).

| Source | Extension Test Data | Conclusions |
|---|---|---|
| Taylor (1941) | Franklin Falls sand. Wide range of densities tested. Uniform, fine.<br>Extension test specimens :-<br>1·4 in. dia. × 3 in. long (18 No.)<br>1·0 in. square × 2·6 in. long (16 No.)<br>2·0 in. square × 5·2 in. long (5 No.) | Comparing maximum principal stress ratios at the same (i.e. consolidated) densities :-<br>1. Small square section extension specimens are approx. 15% lower than corresponding compression tests. (small cylindrical extension specimens are lower still)<br>2. Large square section extension specimens are approx. 12% lower at highest porosities and 6% greater at lowest porosities. |
| Eldin (1951, 1953) | Brasted sand. Uniform, medium-to-fine fraction.<br>Extension test specimens :-<br>1·5 in. dia. × 3 in. long<br>Wide range of densities. | $\phi_{compression} = \phi_{extension}$ over complete range of densities tested.<br>See graph → |
| Habib (1953) | Leucate<br>A well-graded river sand } Porosities not measured but specimens given same amounts of compaction.<br>Fontainebleau sand, loose | Leucate :- $\phi_{comp.} = 38°$, $\phi_{ext.} = 30°$<br>River sand :- $\phi_{comp.} = 39°$; $\phi_{ext.} = 30°$<br>Fontainebleau :- $\phi_{comp.} = 31°$, $\phi_{ext.} = 24\frac{1}{2}°$ |
| Kirkpatrick (1954, 1957) | Loch Aline sand. Uniform, medium<br>Extension test specimens :-<br>1·5 in. dia. × 3 in. long (18 No.) at 4 different densities covering the full range of packing. | $\phi_{compression} = \phi_{extension}$ over complete range of densities tested. |
| Peltier (1957) | Summary of work carried out by 3 French research establishments (including Habib) on several cohesionless materials - few details available on experimental techniques. | $\phi_{compression} = \phi_{extension} + 7°$ (approx.) for all materials tested.<br>See graph → |

TABLE 2-1. COMPARISON OF DRAINED EXTENSION AND COMPRESSION TESTS ON SANDS.




Upper graph - Eldin (1951)

Lower graph - Peltier (1957)

FIG. 2-1

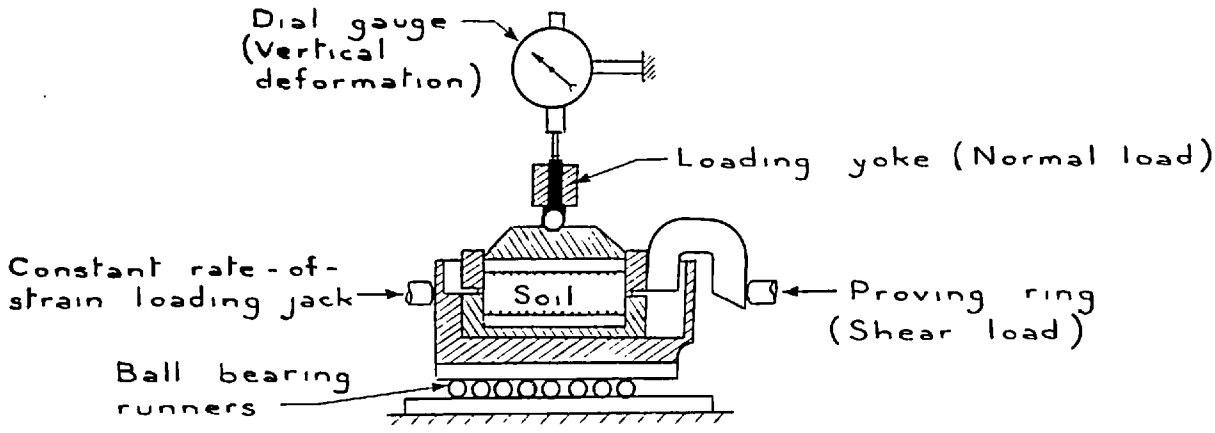
| Source | Sand | Conclusions |
|---|---|---|
| Casagrande and Albert (1932) | Franklin Falls sand | Loose :- $\phi$ triaxial < $\phi$ shear box by 2°<br>Dense :- $\phi$ triaxial > $\phi$ shear box by 3° |
| Taylor (1939) | Ottawa standard sand | Loose :- $\phi$ triaxial < $\phi$ shear box by 2° at low pressures and by $\frac{3}{4}$° at high pressures.<br>Dense :- $\phi$ triaxial < $\phi$ shear box by 4° at low pressures and by $\frac{3}{4}$° at high pressures. |
| Triaxial Shear Report - U.S.W.D. Rutledge (1947) | Franklin Falls sand | $\phi$ triaxial > $\phi$ shear box by approx. 10% in strength. Triaxial specimens saturated, shear box specimens dry. |
| Hafiz (1950) | Stone Court sand | Loose :- $\phi$ triaxial > $\phi$ shear box by 1° (dry)<br>Dense :- $\phi$ triaxial > $\phi$ shear box by $2\frac{1}{2}$° (dry) |
| Nash (1953) | Uniform river sand | Loose :- $\phi$ triaxial > $\phi$ shear box by 2°<br>Dense :- $\phi$ triaxial < $\phi$ shear box by 4° |

TABLE 2-2

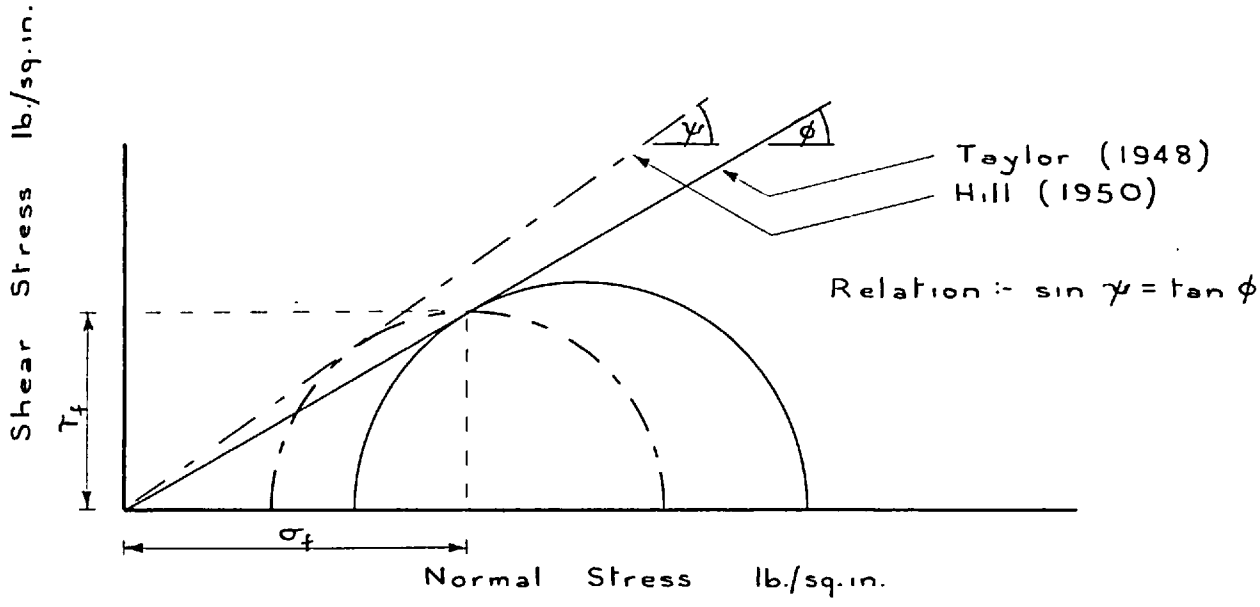
## COMPARISON BETWEEN STANDARD TRIAXIAL COMPRESSION TESTS AND STANDARD SHEAR BOX TESTS

Standard triaxial test specimen :- nominally $1\frac{1}{2}$ in. diameter, 3 in. high.

Standard shear box test specimen :- various dimensions.



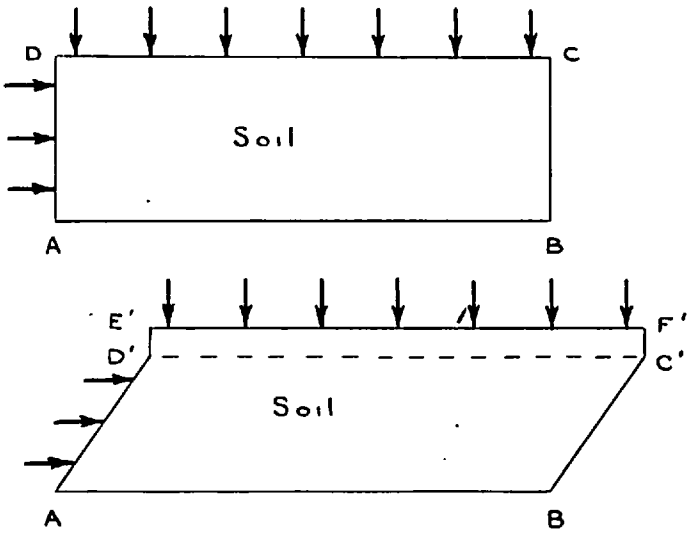

A. Elevation of shear box.



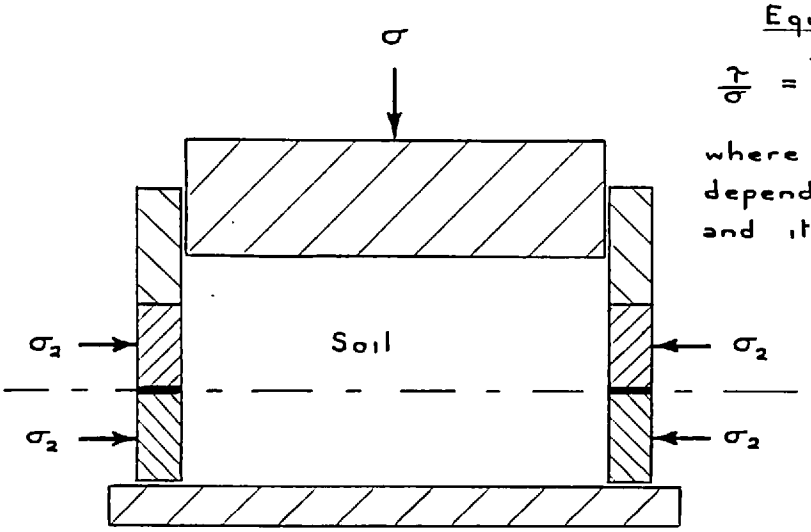

B. Dual interpretation of test results.

SHEAR BOX

FIG. 2 - 2




A. Roscoe (1953)




B. Peltier (1957)

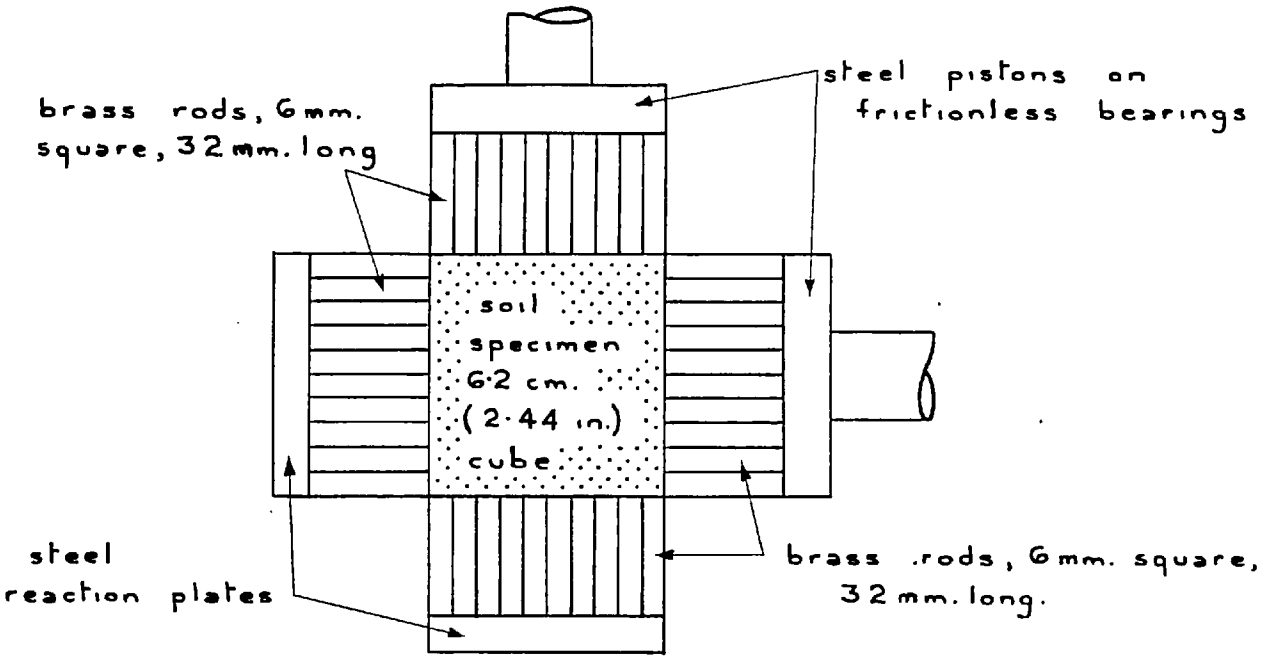
Equation :-

$$\frac{\tau}{\sigma} = A + B \cdot \frac{\sigma_2}{\sigma}$$

where A, B are constants dependent on the soil and its density.

## MODIFICATIONS TO THE SHEAR BOX

FIG. 2 - 3




(a) Specimen loading arrangement in 2-dimensions.

| Test | | | Failure values | | |
|---|---|---|---|---|---|
| No. | Consol. | Shear | Stresses | $\phi_d$ | $\frac{\sigma_2}{\sigma_1+\sigma_3}$ |
| 1 | $\sigma_2 = \sigma_3 \triangleq K_o \sigma_1$ | $\sigma_1$, $\sigma_2$ constant $\sigma_3$ reduced to failure. | $\sigma_1$ = 12·00 kg./cm.$^2$ $\sigma_2$ = 6·00 kg./cm.$^2$ $\sigma_3$ = 2·27 kg./cm.$^2$ | 43° | 0·42 |
| 2 | all-round pressure | $\sigma_2$ constant, $\sigma_1$ increased & $\sigma_3$ decreased ($J$ constant) | $\sigma_1$ = 10·13 kg./cm.$^2$ $\sigma_2$ = 6·00 kg./cm.$^2$ $\sigma_3$ = 1·87 kg./cm.$^2$ | 43° | 0·50 |
| 3 | all-round pressure | $\sigma_1$ increased, $\sigma_2 = \sigma_3$ decreased ($J$ constant) | $\sigma_1$ = 9·70 kg./cm.$^2$ $\sigma_2$ = 2·65 kg./cm.$^2$ $\sigma_3$ = 2·65 kg./cm.$^2$ | 35° | 0·21 |

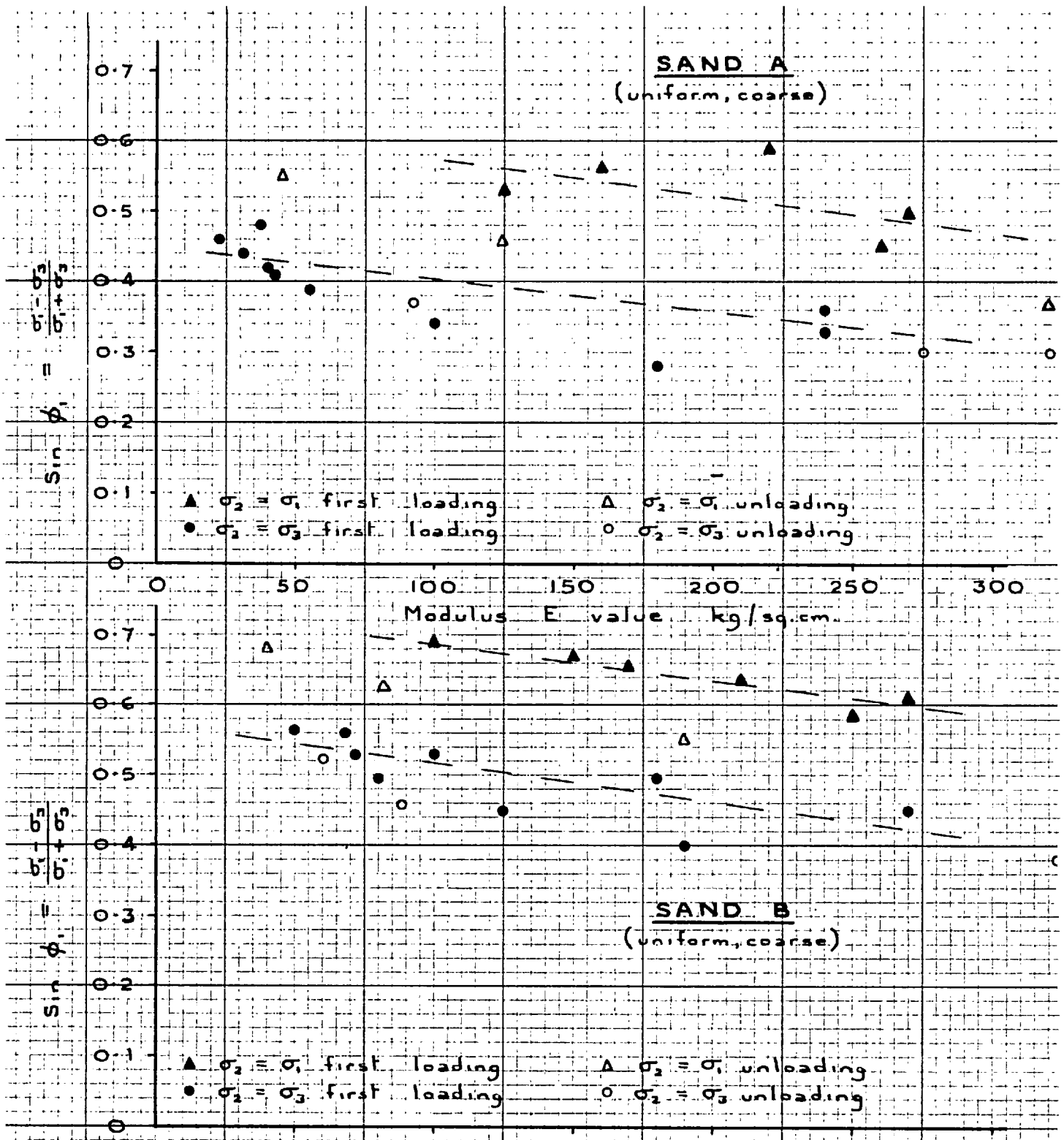
N.B. $J = \frac{1}{3}(\sigma_1 + \sigma_2 + \sigma_3)$

(b) Test results on dry German standard sand

$K_o$ (first loading) = 0·52
Grain size = 1 m.m.
Void ratio = 0·67 (medium dense ?)

KJELLMAN (1936)

FIG. 2-4




JAKOBSON (1957)

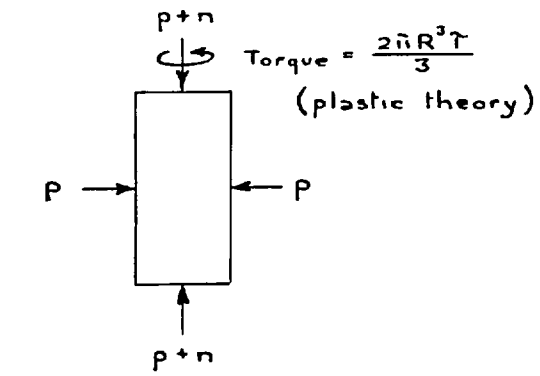
Kjellman (1936) "Triaxial" apparatus

$\sin \phi_1 \rightarrow \sin \phi_d$, as $E \rightarrow 0$

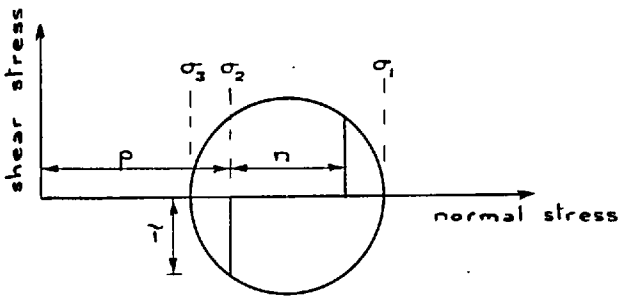
Sand A (German) – void ratio range 0·61 → 0·65

Sand B (Swedish) – void ratio range in tests 0·69 → 0·72.

FIG. 2 – 5

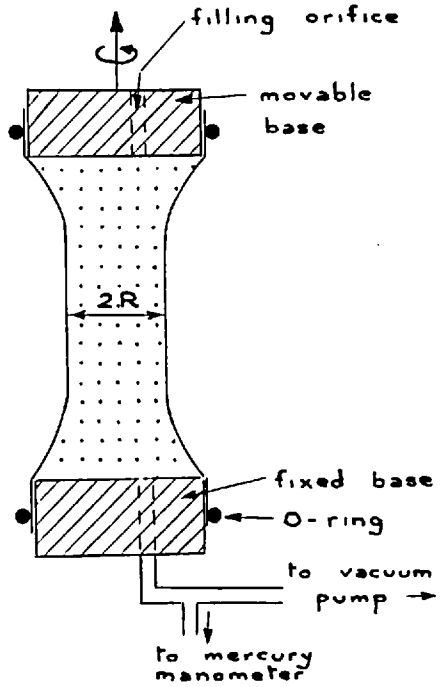



(a) Stress System




$$\lambda = \frac{\sigma_2 - \sigma_3}{\sigma_1 - \sigma_3}$$

(b) Mohr Diagram



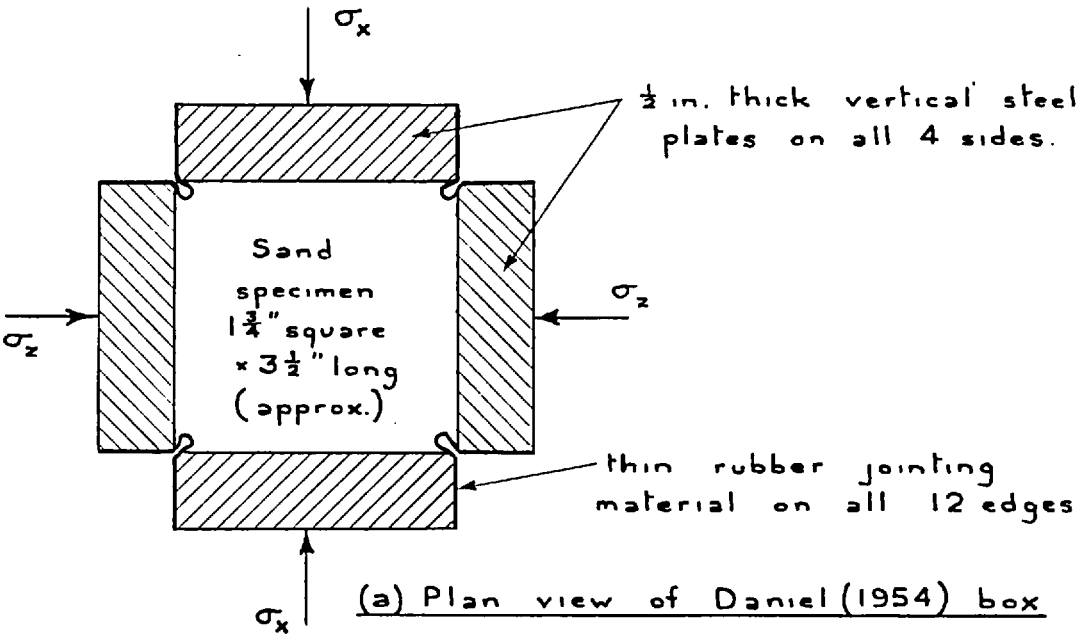

(c) Torsion Test Specimen

| | Comp.ⁿ | Torsion | | | | | Tensⁿ |
|---|---|---|---|---|---|---|---|
| Cell pressure kg./cm.² | 5 | 5 | 5 | 5 | 5 | 5 | 5 |
| Axial stress kg./cm.² | 16 | 13 | 10 | 5 | 4 | 3 | 2 |
| Total couple kg.-cm. | 0 | 33·9 | 43·5 | 32·5 | 25·5 | 17·5 | 0 |
| Total shearing resistance $\tau$ kg./cm² | 0 | 3·09 | 3·96 | 2·96 | 2·32 | 1·59 | 0 |
| Correction to $\tau$ kg./cm² | 0 | 0·2 | 0·3 | 0·4 | 0·3 | 0·2 | 0 |
| Angle of shearing resistance $\phi$ ° | 32 | 33 | 36 | 31 | 28 | 27 | 25 |
| Parameter $\lambda$ | 0 | 0·09 | 0·22 | 0·50 | 0·62 | 0·80 | 1 |

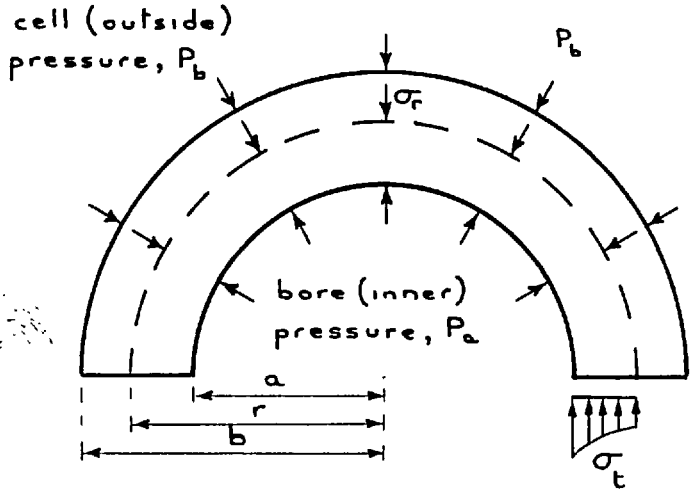
(d) Relation between $\phi$ and $\lambda$

HABIB (1953)

FIG. 2 - 6




(a) Plan view of Daniel (1954) box




Let $\sigma_3/\sigma_1 = \lambda$, then

$$\sigma_r \text{ (av.)} = \sigma_1 = \frac{P_b}{\lambda}\left\{\frac{b^\lambda - a^\lambda}{(b-a)\,b^{(\lambda-1)}}\right\}$$

$$\sigma_t \text{ (av.)} = \sigma_3 = \frac{P_b\,b - P_a\,a}{b-a}$$

$$\sigma_{ax.} = \sigma_2 = \frac{P_b\,b^2 - P_a\,a^2}{b^2 - a^2}$$

In test specimen, $a = 1\frac{1}{4}$ inches, $b = 2$ inches

(b) Half plan view of Kirkpatrick's (1954, 1957) thick cylinder stress system

| Test | Average Consolidated Porosity, $n_c$% | Angle of Shearing Resistance | Ratio $\left\{\frac{\sigma_1 - \sigma_3}{\sigma_3}\right\}_f$ |
|---|---|---|---|
| Std. triaxial compression | 35·1 | 39° | 3·37 |
| Std. triaxial extension | | 38·8° | |
| Thick cylinder | 35·6 | 41·2° | 3·85 |

(c) Summary of average strengths - Kirkpatrick (1954, 1957)

DANIEL (1954) & KIRKPATRICK (1954, 1957)

FIG. 2 - 7

| Failure Criteria | Shear Strength Parameters | | | | Ratio $\frac{\sigma_2'}{\sigma_1' + \sigma_3'}$ | Increase in strength of plane strain specimen at $\sigma = 30$ lb/sq.in. |
|---|---|---|---|---|---|---|
| | PLANE STRAIN | | STD. TRIAXIAL | | | |
| | $c'$ lb./sq.ft. | $\phi'$ degrees | $c'$ lb./cu.ft. | $\phi'$ degrees | | |
| $(\sigma_1' - \sigma_3')_{max}$ | 270 | 36·9° | 30 | 35·1° | 0·31 | 14 % |
| $\sigma_1'/\sigma_3'$ max | 250 | 41·9° | 130 | 37·2° | 0·31 | 18 % |

Soil :- Glen Shira Fill

Description :- Brown, well-graded gravelly silty SAND

Compaction properties :-

Optimum moisture content = 10·5 %

Maximum dry density = 125·4 lb./cu.ft.

Specific gravity = 2·77

Coefficient of earth pressure at rest, $K_o$ (Fraser, 1957) = 0·36

Compaction :- Equivalent Proctor effort per unit volume at optimum + 3 % moisture content.

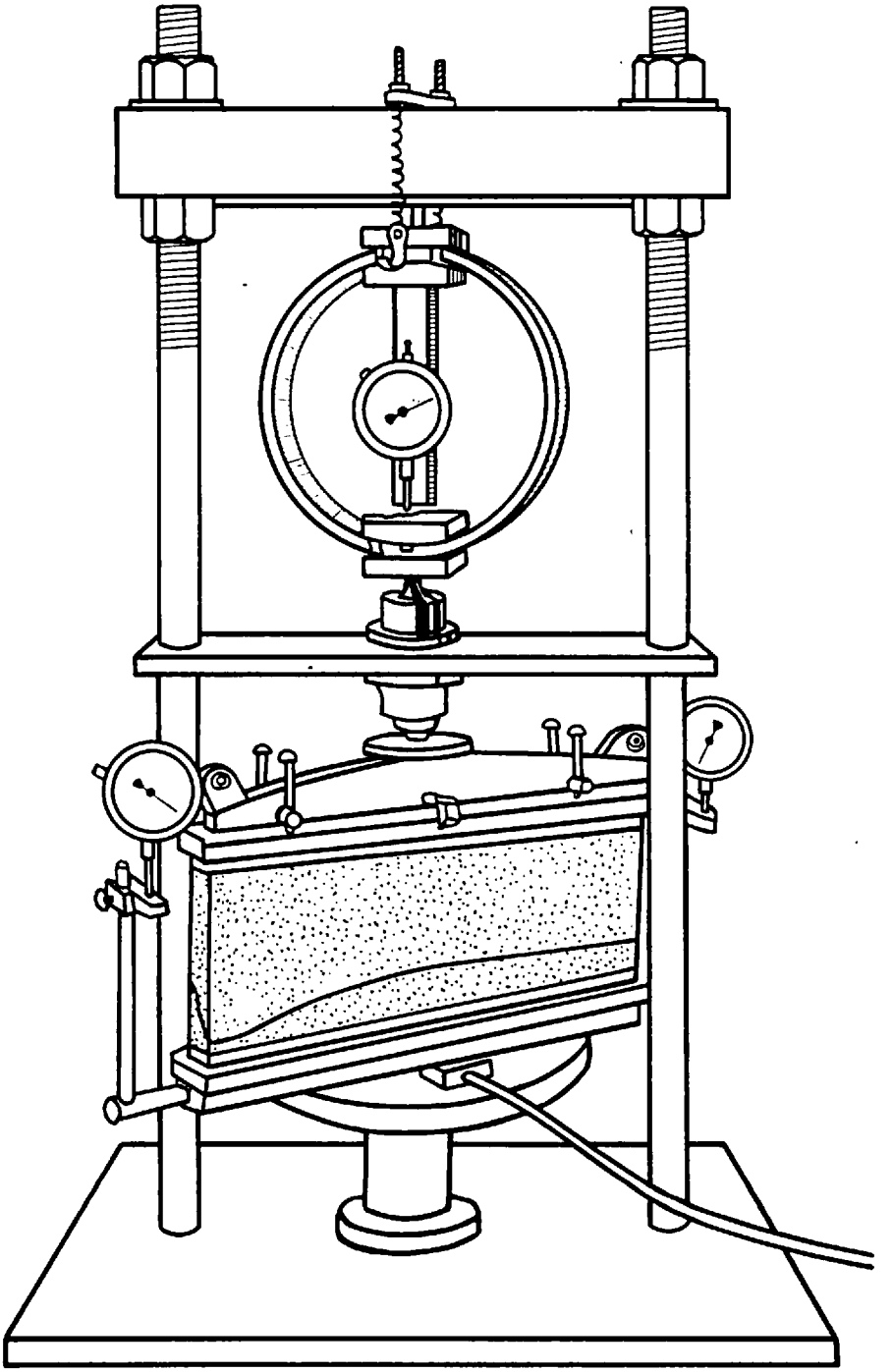
| | Plane Strain | Standard Triaxial |
|---|---|---|
| Number of tests | 8 | 11 |
| Average initial dry density (lb./cu.ft.) | 120·9 | 119·4 |
| Average initial moisture content (%) | 13·3 | 13·6 |
| Average consol. dry density (lb./cu.ft.) | 122·5 | 122·2 |
| Pore-water pressure coefficient $\bar{B}$ (Bishop, 1954) for $\sigma_1' = 140$ lb./cu.ft. | 0·34 | 0·19 |
| Axial strain at failure, $\epsilon_1$ (%) | 4 to 10 % | 15 to 18½ % |

## WOOD (1958)

Imperial College, London, Plane Strain apparatus, designed by Dr. A.W. Bishop & Dr. C.C. Wood.

Test specimens :- Plane Strain – 16" × 4" × 2"
Std. Triaxial – 8" × 4" dia.

FIG. 2 - 8

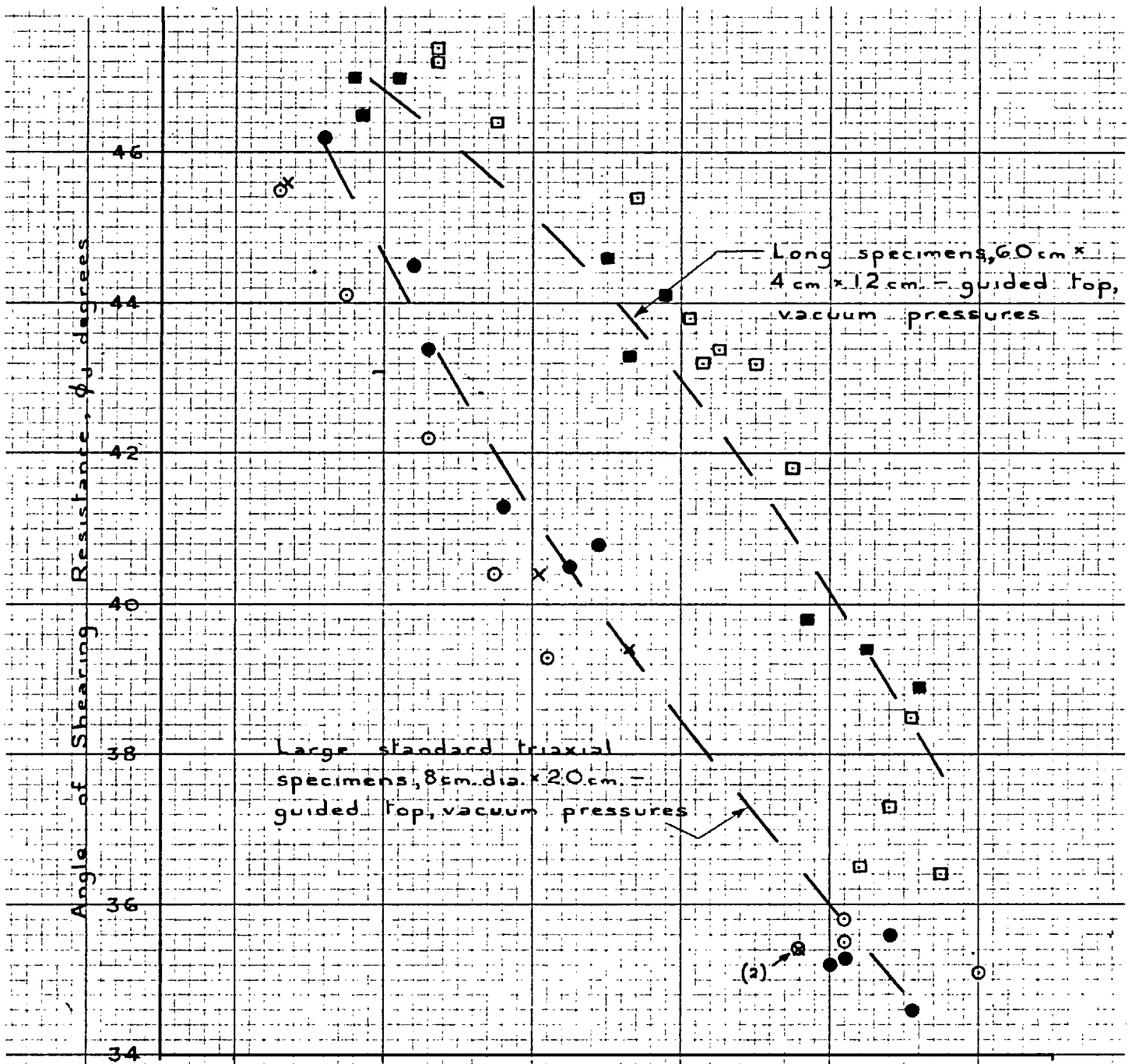


NORWEGIAN GEOTECHNICAL INSTITUTE

PLANE STRAIN APPARATUS

Reproduced by permission of Dr. L. Bjerrum, Director, N.G.I.

FIG. 2 - 9




NORWEGIAN GEOTECHNICAL INSTITUTE – KUMMENEJE (1957)

(Reproduced by kind permission of Dr. L. Bjerrum, Director)

Key

■ Plane strain type 60 cm. x 4 cm. x 12 cm. – vacuum

□ Plane strain type 30 cm. x 4 cm. x 12 cm. – vacuum

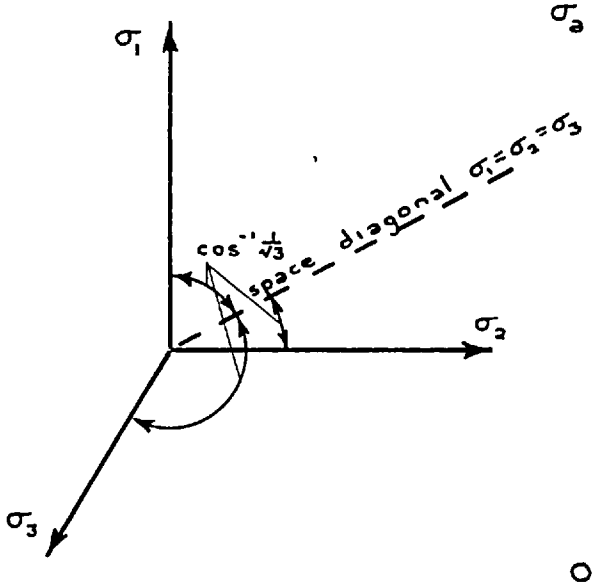
● Standard triaxial 8 cm. dia. x 20 cm. – guided top cap – vacuum

⊙ Standard triaxial 8 cm. dia. x 20 cm. – free top cap – vacuum

x Standard triaxial 3·6 cm. x 8 cm. – cell pressures

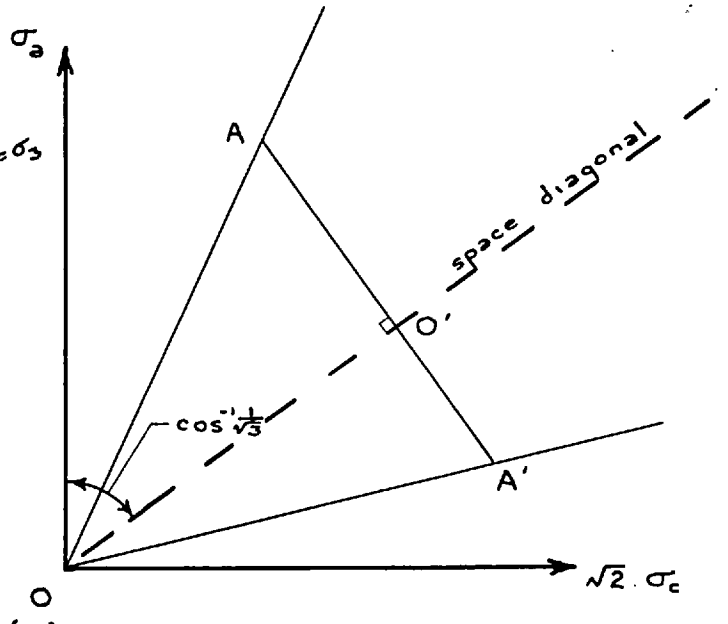
In the above graph, no distinction is drawn between tests at different cell pressures.

FIG. 2-10



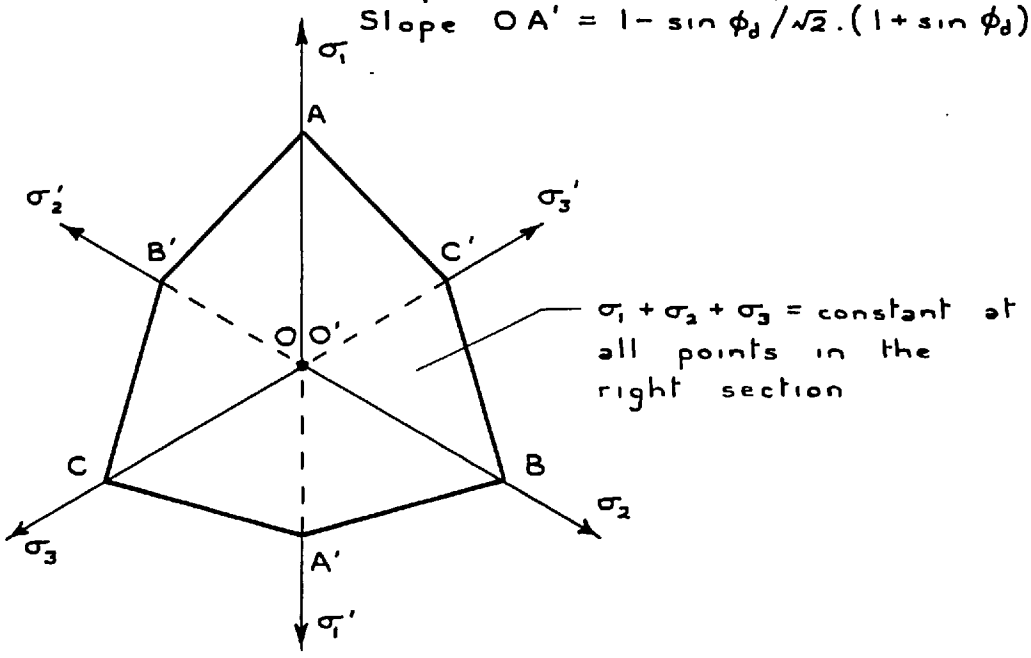

(a) Space diagonal and the Principal Stresses

Space diagonal makes an angle $\cos^{-1}\frac{1}{\sqrt{3}}$ to the three principal stresses.




(b) Section of Mohr-Coulomb Surface for Std. Triaxial Test

$\sigma_a$ = axial stress
$\sigma_c$ = cell pressure
Slope $OA = 1+\sin\phi_d / \sqrt{2}.(1-\sin\phi_d)$
Slope $OA' = 1-\sin\phi_d / \sqrt{2}.(1+\sin\phi_d)$

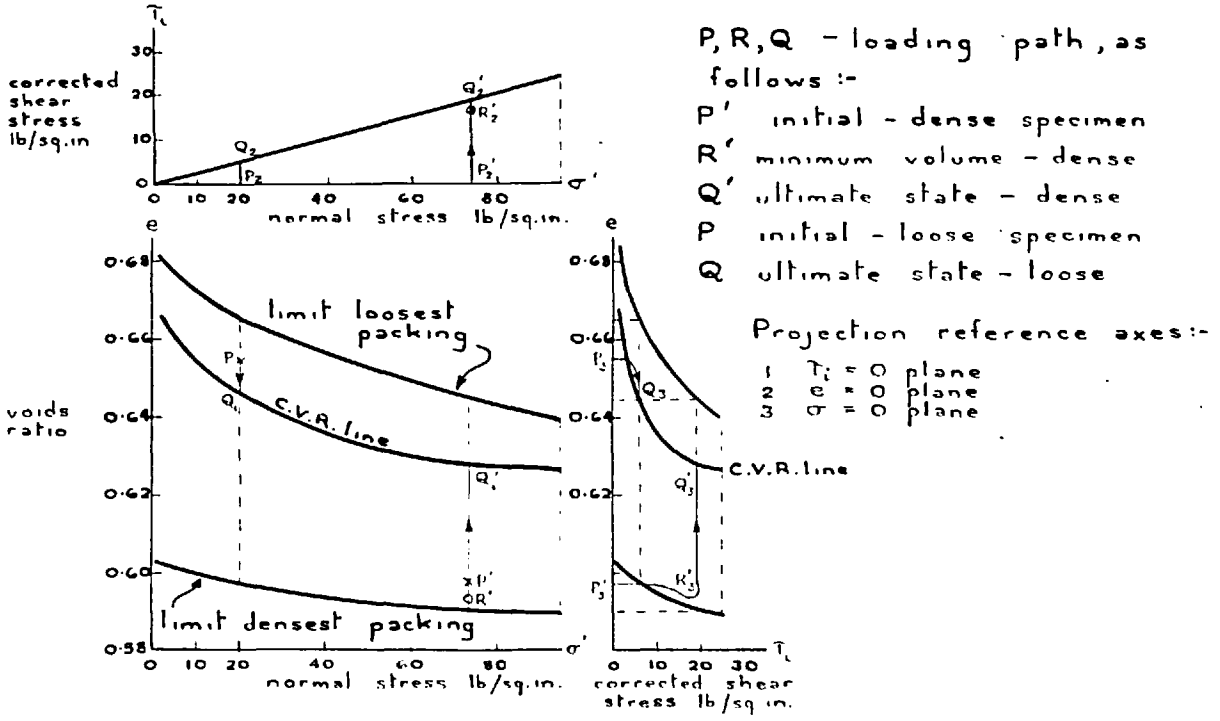



(c) Right Section of Mohr-Coulomb Surface of Yield

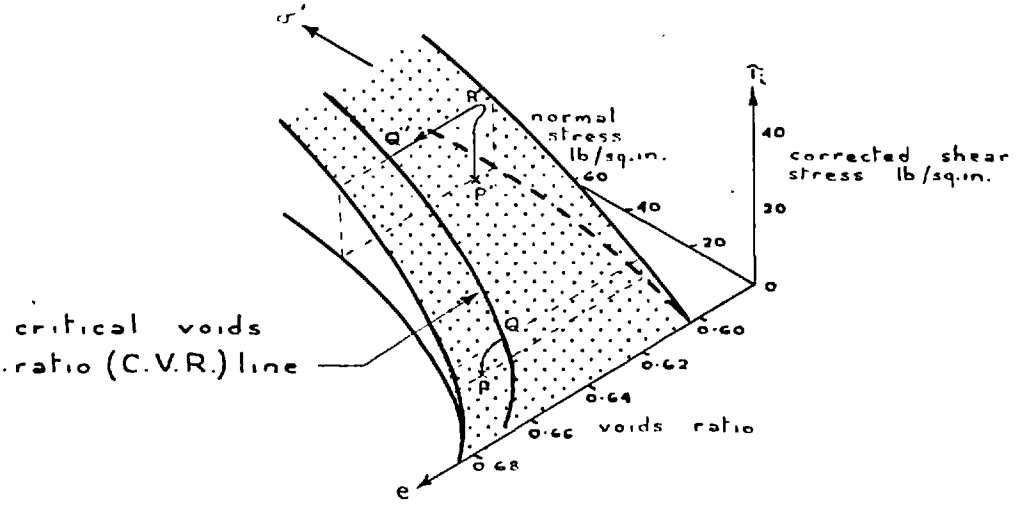
Note : $O'A = O'B = O'C > O'A' = O'B' = O'C'$

## PRESENTATION OF SHEAR STRENGTH DATA - KIRKPATRICK (1957)

FIG. 2 - 11




(a) Projections of drained yield surface on reference axes




(b) Isometric projection of drained yield surface

## ROSCOE, SCHOFIELD & WROTH (1958)

Drained yield surface for 1 m.m. steel balls, from results of Simple Shear Box tests. Surface is a plane containing the e-axis and inclined at constant angle to the other two planes.
Loading path for drained tests in σ = constant plane.

FIG. 2 - 12

## Chapter 3 DESCRIPTIONS OF APPARATUS

### Plane strain apparatus

The plane strain apparatus was designed by Dr. A. W. Bishop, assisted by Dr. C. C. Wood, and full details of the apparatus, together with the working drawings, are described in Wood's thesis (1958). To ease the operational procedure, some slight modifications were made to the original design but the working principles are essentially the same. The alterations are listed in Appendix 6. A general view of the apparatus is shown in Plate 3-1. Sections through the cell are shown on Fig. 3-1.

The test specimen is nominally 16 inches long, 4 inches high and 2 inches wide but the apparatus can be easily adapted to test specimens less than 16 inches long. The specimen is placed on the lower platen which consists of a bronze plate with a rubber ring recessed into the lower surface. In setting up a sample, the edges of the rubber membrane are placed between the platen and the cell base plate. The lower platen is then screwed to the base plate and seals the membrane. A similar arrangement is used to seal the upper edges of the membrane between the upper platen and the upper bearing plate, the two metal parts being positioned by locating pins. The upper bearing plate is flanged to increase its rigidity against bending. Screwed to the top of the lower platen and beneath the specimen is a perspex sheet which holds 4 porous stones ($1\frac{1}{2}$ in. diameter) with a small connecting channel between them. A copper tube, passing through the lower platen, connects the porous stones with a burette or null indicator.

The cell enclosing the specimen consists of three parts:- the cell cap plate, cell body and cell base plate. The cap and base plates are made of brass and the body casting is of bronze. The base plate centres onto the pedestal of the standard triaxial apparatus and is provided with 4 legs for use when the plate is standing on the laboratory bench. The cell body casting is fitted with 6 perspex observation windows. Machined recesses in its upper and lower flanges each hold an O-ring which form a watertight seal around the perimeter of the cell when the three units are tightened together by the 16 tie bars. When the apparatus is being assembled, 2 of the tie bars are

used for guides as the cell body and cell cap plate are lowered into position by the overhead crane. The cell cap plate holds the twin $\frac{3}{4}$ in. diameter stainless steel rams which load the upper bearing plate through hemispherical contacts at the quarter points of the upper platen. The honed bronze sleeves surrounding the rams are rotated continuously during a test by means of a worm gear, driven by a small electric motor. This arrangement eliminates errors in the measurement of the vertical load due to friction between the ram and bushing. Each ram has a separate proving ring mounted between the top of the ram and the head of the testing machine. Adjusting screws allow both proving rings to be set to zero at the start of a test. An arm and dial gauge is attached to each ram to measure vertical movements of the specimen. Cross-links are attached to the arms of the vertical dial gauges to prevent the rams and gauges from being turned around by the rotation of the bronze sleeves. Table 3-1 shows that the loading arrangement works satisfactorily, each ram taking approximately 50% of the total load and vertical deformation. An oil lead is fitted to each ram housing.

A strain control device (end clamp) maintains the plane strain condition during shear. It consists of 2 plates in contact with the ends of the specimen and connected by 4 symmetrically placed tie bars (Figs. 3-1, 3-2; Plates 6-3, 6-4). The plates are made of anodised aluminium and are covered with a thin layer of silicone grease before being placed in contact with the membrane. Tests by Wood (1958) in a shear box showed that coefficient of friction between the plates and the membrane is then $\mu = 0{\cdot}018$ .* Further calculations showed that the maximum error in the deviator stress at failure due to end friction is of the order of 0.3% and can be neglected.

One end of the clamp incorporates a pressure measuring device. This consists of a cell with a fairly stiff rubber diaphragm. A rigid metal disc is attached to the diaphragm such that the rubber forms a slightly flexible annulus (Fig. 3-2b). The disc bears against the facing plate in contact with the end of the specimen. The space

---

* more recent tests by Mr. N. Wade gave $\mu = 0{\cdot}024$ (see Appendix 6).

behind the diaphragm is filled with de-aired water and a nylon tube connects the device with a null indicator. The additional stresses required for plane strain are measured by a null method similar to that adopted for measuring pore-water pressures (Bishop & Henkel, 1957). However, it is necessary to apply a correction (Appendix 1) to the level of the mercury thread in the null indicator during the test to allow for the elastic distortions of the tie bars, rubber, and nylon tubing. The end clamp is supported by 4 springs set in perspex sheets. The height of the springs and hence the position of the clamp can be altered by placing brass plugs in the spring seatings. There is also a small clearance between the end plates of the clamp and the two platens so that there is no interference during a shear test. Observations have shown that the sand grains in the clearances do strain uniformly with the rest of the specimen.

Stabilizing bars are fitted to the plane strain apparatus. A bar bolted to the cell cap plate passes through a frictionless guide in the head of the testing machine and keeps the cell vertical. A second bar extends horizontally backwards from the cell cap plate and engages in a guide fixed to the column of the testing machine. This prevents horizontal rotation of the apparatus.

The apparatus used for applying and measuring the cell pressure, pore-water pressure and vertical deviator stress are exactly the same as for the standard triaxial test and are fully described in Bishop & Henkel (1957).

Standard triaxial compression apparatus

The apparatus used at Imperial College for testing 4 inch diameter triaxial specimens is described in Bishop & Henkel (1957). The cell used in the present tests has a flat top and is fitted with a rotating bush assembly to eliminate vertical friction, identical in design to those used in the plane strain apparatus (Plate 3-2).

Standard triaxial extension apparatus

The loading cap for extension tests is shown on Fig. 3-3. Tensile loads of up to 1200 lb. were required to fail the large

diameter specimens and some modifications to the triaxial apparatus were necessary. For an extension test, the motor is reversed so that the pedestal moves downwards at a constant rate-of-strain. The method of measuring the tensile loads is illustrated in Plate 3-3 and Fig. 3-4. A circlip inserted near the top of the ram transmits the tensile forces to a loading yoke which then measures the load in compression via a proving ring placed between the yoke and the head of the testing machine. A frictionless guide between the ring and the yoke keeps the proving ring vertical. As all the test specimens were consolidated under $K_o$ conditions before shearing, a second proving ring was placed between the ram and the head of the testing machine. When consolidation is in progress, the vertical rods of the loading yoke pass freely through holes in the horizontal arm attached to the ram. For the extension part of the test, the nuts on the rods (below the arm) are tightened, bringing the two parts into contact.

The cell is held onto the pedestal by two clamps which pass completely round the cell, one on each side of the ram housing. The pedestal is held onto the screw jack of the loading machine by a steel pin in double shear.

## Key to Plate 3-1

### Plane strain cell

1. The cell, consisting of three units held together by 16 tie bars.
2. Ram housing.
3. Proving ring.
4. Axial deformation dial gauge.
5. Oil lead to ram.

### Measurement of the intermediate principal stress

6. Valve leading to the end clamp.
7. Null indicator.
8. Bourdon-type pressure gauge (0 to 300 lb./sq.in.).
9. Hand-operated screw ram control.

### Measurement of the minor principal stress (cell pressure)

10. Hand-operated screw ram control.
11. Bourdon-type pressure gauge (0 to 150 lb./sq.in).
12. Mercury manometer (0 to 25 lb./sq.in.).
13. Constant pressure mercury pot.
14. Ratchet winch for altering the level of the mercury pot.

### Measurement of the pore-water pressure

15. Valve leading to porous stones at base of specimen.
16. Bourdon-type pressure gauge (0 to 150 lb./sq.in.).
17. Null indicator.
18. Mercury manometer (0 to 22 lb./sq.in.).

### Accessories to the triaxial apparatus

19. Manual control and clutch of the vertical loading jack.
20. Multi-speed gear box and electric motor.
21. Volume change measuring unit of cell water.
22. Drive to rotating bush.
23. Electric motor for rotating bush.

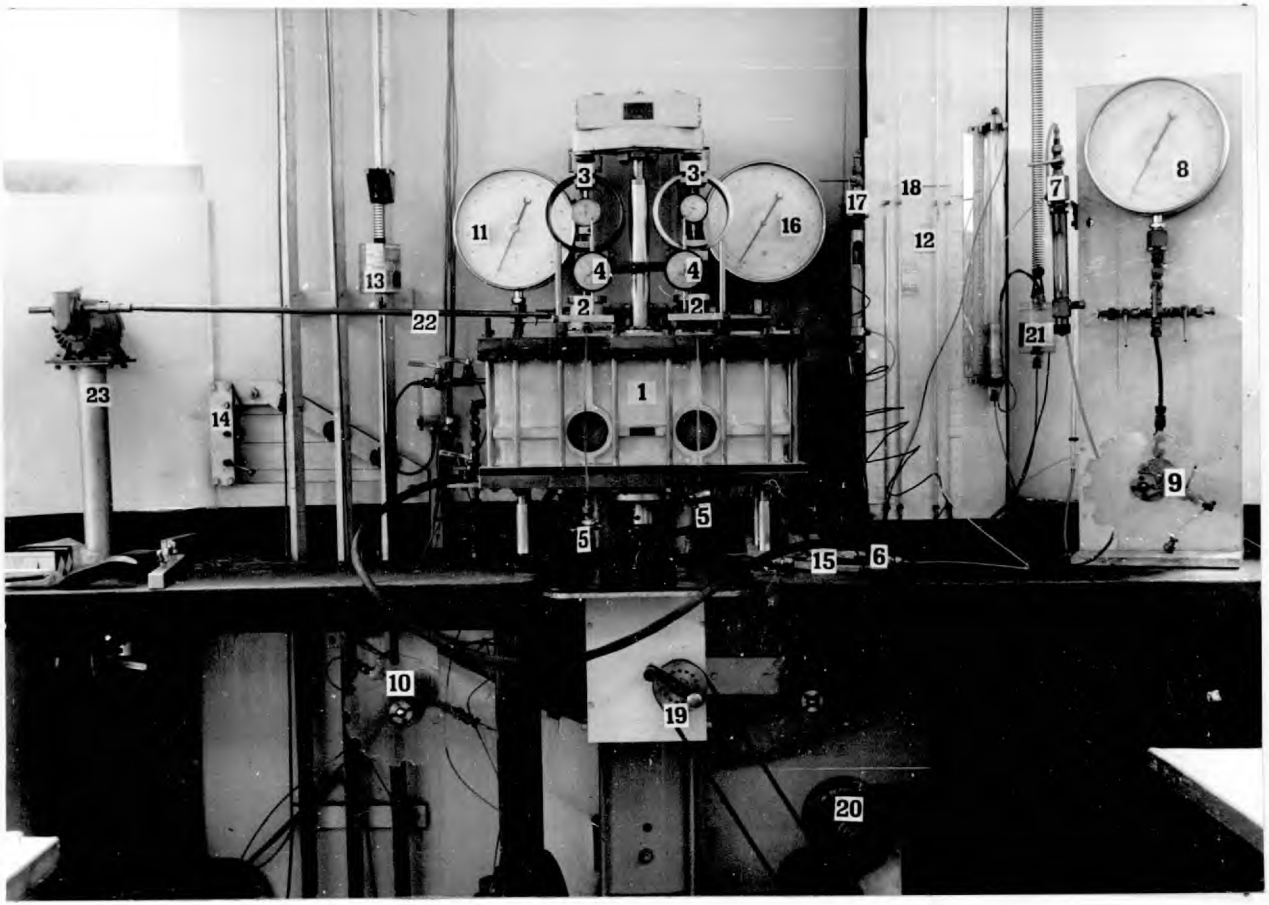



PLATE 3-1 GENERAL VIEW OF PLANE STRAIN APPARATUS

FOR A CONSOLIDATED - UNDRAINED TEST

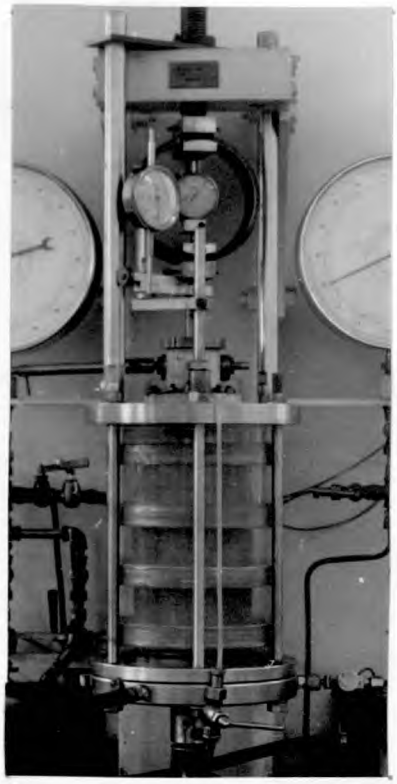


PLATE 3-2

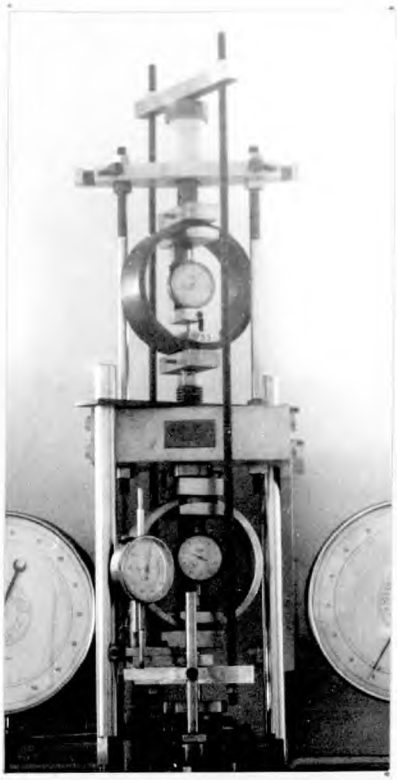


PLATE 3-3

STANDARD TRIAXIAL APPARATUS

PLATE 3-2 General view of large cell for 4" diameter specimens with rotating bush.

PLATE 3-3 Axial extension loading yoke. The clamps which hold the cell to the pedestal are not shown.

Table 3-1 Behaviour of Plane Strain Apparatus at Failure

| Ring 133 on left-hand side | | Test No. | Ring 332 on right-hand side | |
|---|---|---|---|---|
| Load | Vertical Dial | | Load | Vertical Dial |
| lb. | $10^{-3}$ in. | | lb. | $10^{-3}$ in. |
| 1930 | 129.8 | 6 | 2020 | 129.4 |
| 2204 | 87.6 | 8 | 2238 | 84.4 |
| 1760 | 91.5 | 9 | 1786 | 90.3 |
| 1816 | 164.1 | 10 | 1859 | 167.5 |
| 2301 | 89.0 | 11 | 2330 | 85.2 |
| 3163 | 75.3 | 12 | 3130 | 75.3 |
| 2112 | 113.0 | 13 | 2139 | 110.4 |
| 2366 | 86.5 | 19 | 2396 | 82.1 |
| 1753 | 134.2 | 20 | 1819 | 132.2 |
| 1908 | 130.5 | 21 | 1911 | 129.9 |
| 1791 | 117.5 | 22 | 1819 | 117.2 |
| 2967 | 63.0 | 23 | 3035 | 57.5 |
| 2182 | 84.7 | 24 | 2281 | 78.9 |
| 2070 | 92.5 | 25 | 2091 | 90.5 |
| 2414 | 58.8 | 26 | 2505 | 59.5 |
| 2882 | 47.0 | 27 | 2929 | 45.6 |
| 1472 | 111.6 | 28 | 1452 | 114.0 |
| 2231 | 115.0 | 29 | 2260 | 115.4 |
| 2741 | 99.5 | 30 | 2786 | 95.7 |
| 2576 | 73.4 | 31 | 2561 | 71.4 |
| 518 | 92.3 | 32 | 540 | 85.5 |
| 1101 | 125.0 | 33 | 1129 | 126.2 |
| 1072 | 90.3 | 34 | 1071 | 85.9 |

For the above 23 test results:-

Total load on ring 133 (L.H.S.) = 47,330 lb. (49.6%)
on ring 332 (R.H.S.) = 48,087 lb. (50.4%)
Total dial movement (L.H.S.) = 2.272 in. (50.5%)
(R.H.S.) = 2.230 in. (49.5%)

Table 3-1 (continued)

| Ring 332 on left-hand side | | Test No. | Ring 133 on right-hand side | |
|---|---|---|---|---|
| Load | Vertical Dial | | Load | Vertical Dial |
| lb. | $10^{-3}$ in. | | lb. | $10^{-3}$ in. |
| 3036 | 63.6 | 5 | 3087 | 58.0 |
| 1852 | 156.7 | 14 | 1793 | 152.3 |
| 2660 | 52.6 | 15 | 2717 | 51.2 |
| 2957 | 55.0 | 16 | 2925 | 53.8 |
| 3233 | 64.5 | 17 | 3358 | 58.9 |
| 2181 | 91.3 | 18 | 2182 | 92.8 |
| 3491 | 79.8 | 35 | 3573 | 75.2 |

For the above 7 test results:-

Total load on ring 332 (L.H.S.) = 19,410 lb. (49.7%)
on ring 133 (R.H.S.) = 19,635 lb. (50.3%)
Total dial movement (L.H.S.) = 0.564 in. (51.0%)
(R.H.S.) = 0.542 in. (49.0%)

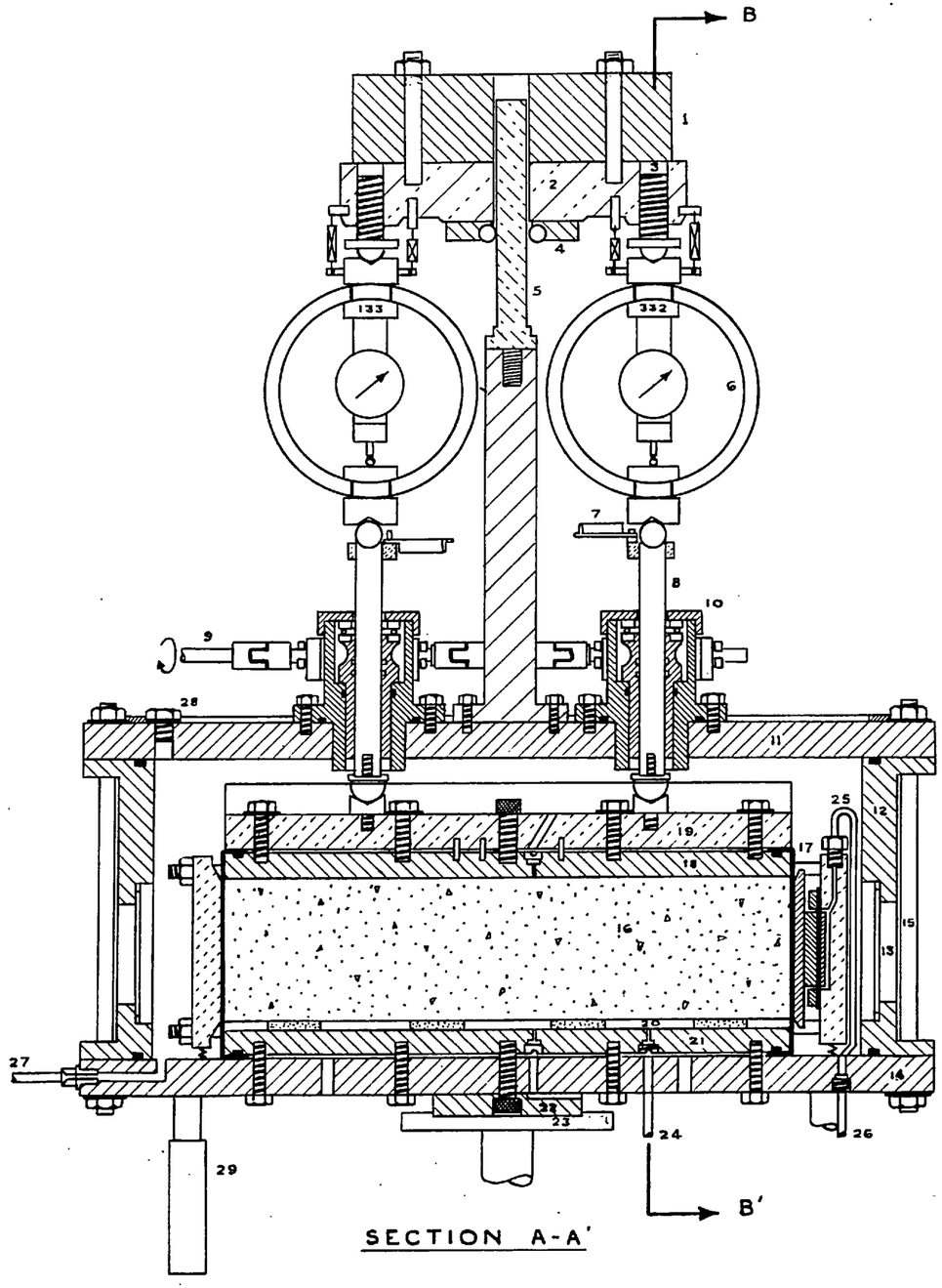
---

Summarizing all 30 test results:-

Left-hand side ring carried 49.6% of total load.
Left-hand side dial gauge recorded 50.6% of total dial gauge readings.

For the 5 test results in which the plane strain end clamp was omitted from the test:-

Left-hand side ring carried 50.0% of total load.
Left-hand side dial gauge recorded 50.6% of total dial gauge readings.




SECTION A-A'

SECTION B-B'

## SECTION A-A'

1 Head of triaxial apparatus
2 Head adaptor bar
3 Adjusting screw
4 Frictionless guide
5 Vertical guide bar
6 Proving ring
7 Anti-rotation links
8 Vertical loading ram
9 Vertical friction eliminator (rotating bush type)
10 Ram housing
11 Cell cap plate
12 Cell body casting
13 Perspex observation window
14 Cell base plate
15 Tie bar (16 No.)
16 Soil specimen
17 Rubber membrane
18 Upper platen
19 Upper bearing plate
20 Porous stones in perspex holder
21 Lower platen
22 Locating disc plate
23 Pedestal of triaxial apparatus
24 Lead from soil specimen
25 End clamp (see Fig. 3-2)
26 Lead to null indicator of intermediate principal stress
27 Cell pressure lead
28 Air release valve
29 Leg

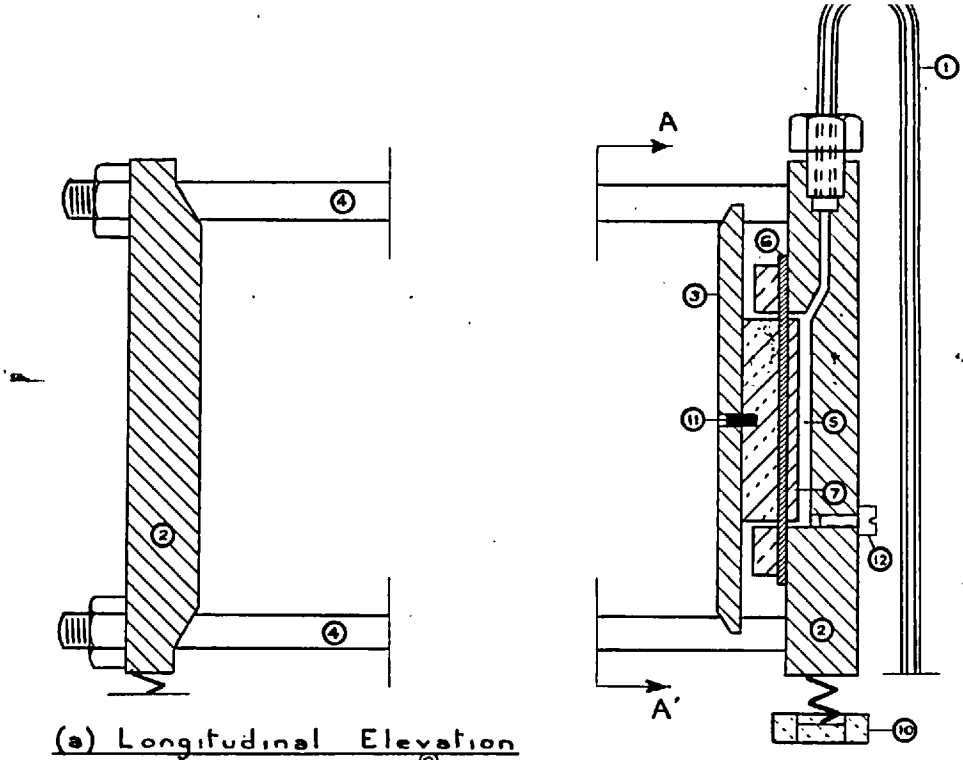
## SECTION B-B'

30 Horizontal guide bar (in centre of apparatus - added to B-B' as an extra)
31 Dial gauge for axial deformation
32 Arm for vertical dial gauge
33 Castor oil lead to ram

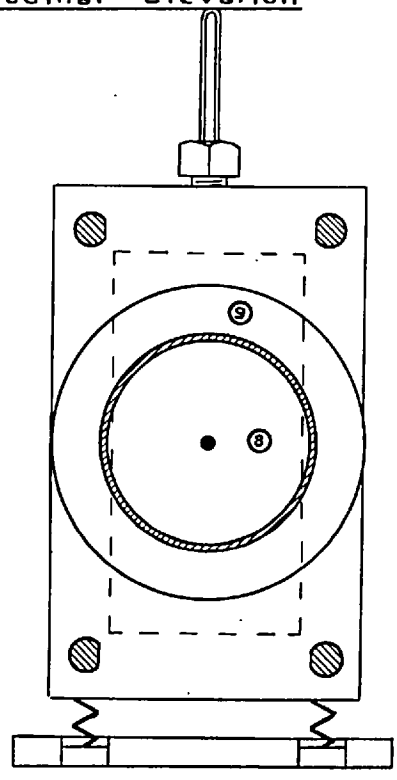
# PLANE STRAIN APPARATUS - ASSEMBLY DRAWING

Scale :- One-Quarter Full Size

FIG. 3-1




(a) Longitudinal Elevation



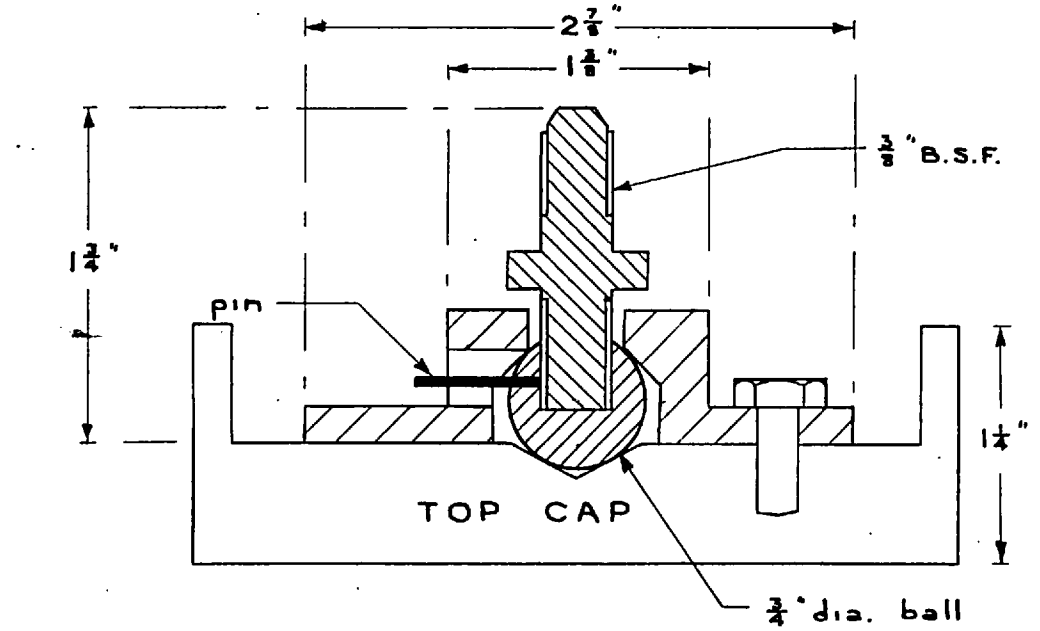

(b) Section A-A' without Facing Plate

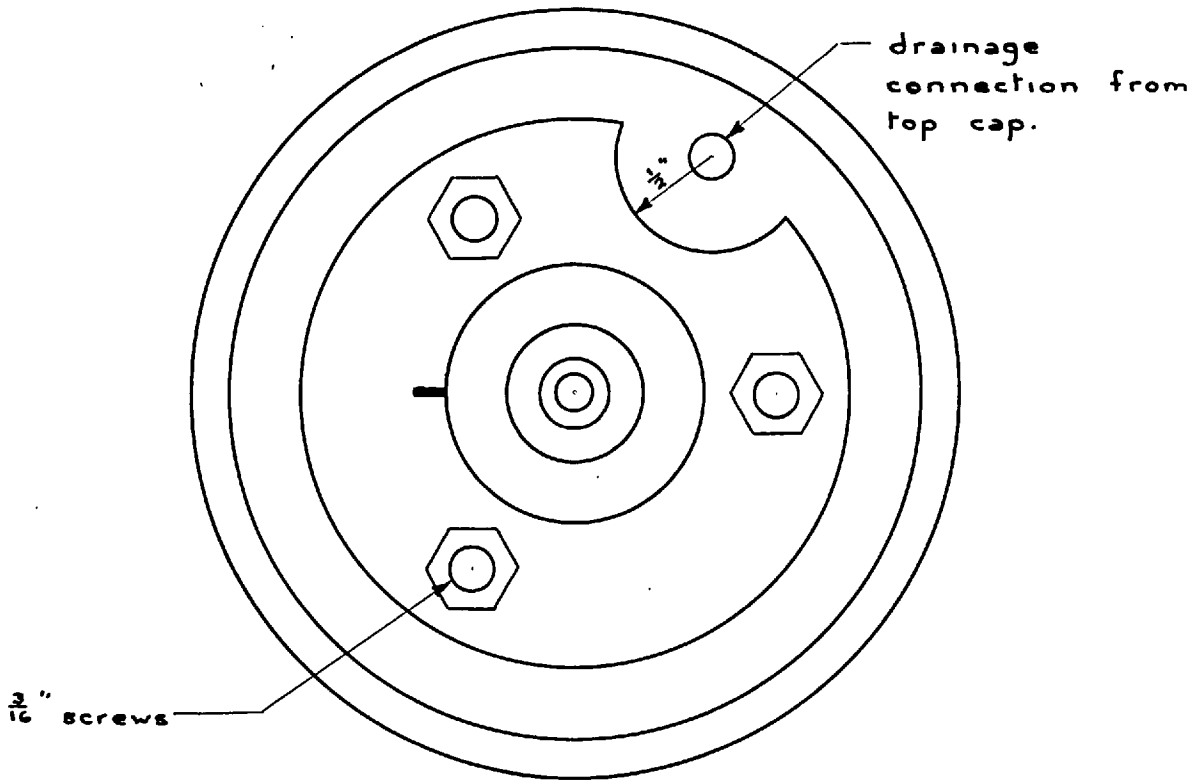
① Nylon tube to null indicator
② End plates
③ Facing plate
④ Tie bars
⑤ Pressure cell (water-filled)
⑥ Diaphragm
⑦ Stiffening Plate
⑧ Loading Plate
⑨ Diaphragm retaining ring
⑩ Clamp support, comprising springs, perspex seatings & brass adjusting plugs
⑪ Locating dowel for facing plate
⑫ Air release screw

## PLANE STRAIN END CLAMP

Scale :- Half Full Size

FIG. 3 - 2

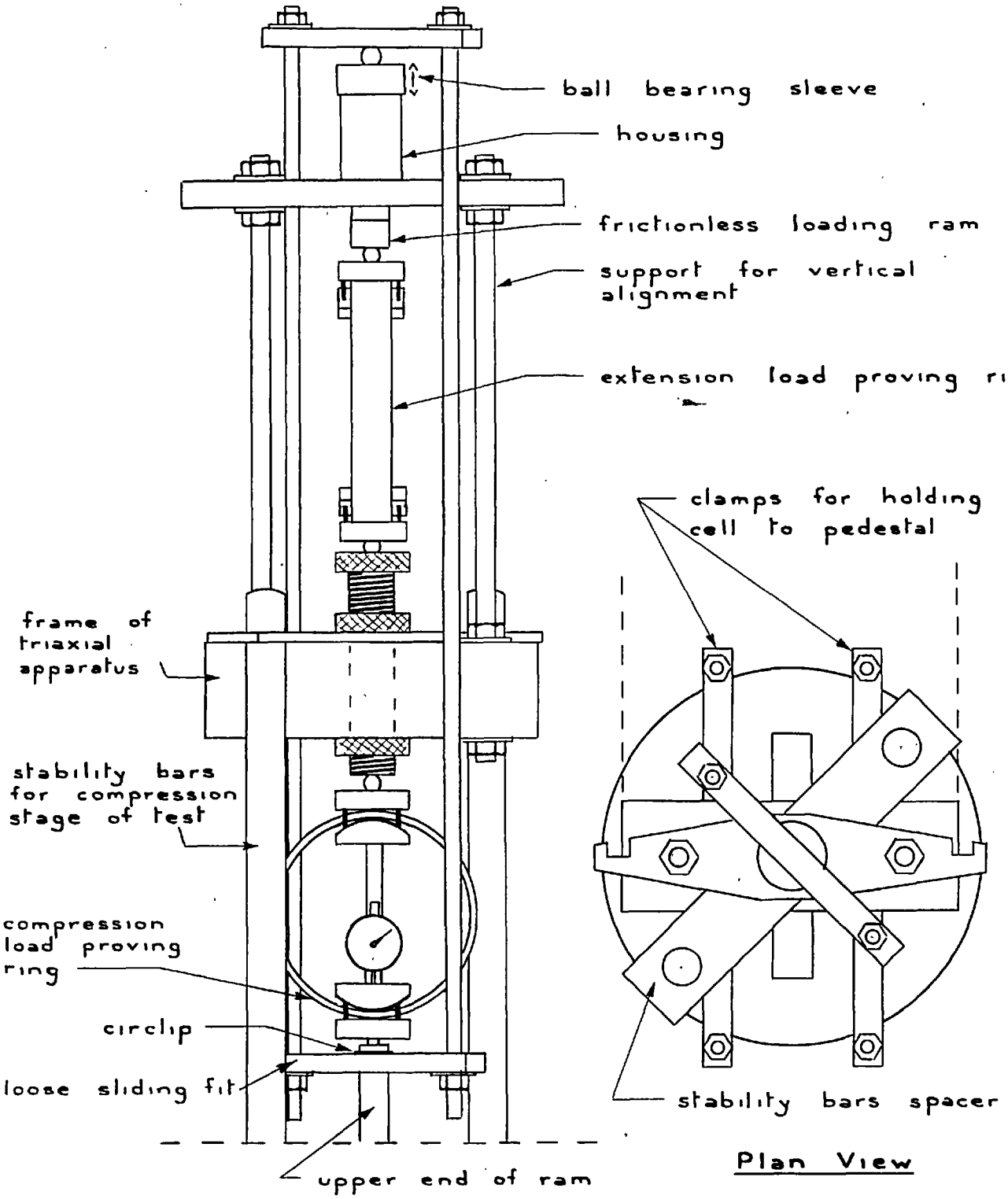



## TENSION FITTING FOR TOP CAP

Stainless steel components.

FIG. 3 - 3




## EXTENSION TEST - AXIAL LOADING APPARATUS

One-quarter full size, approximately.

FIG. 3-4

## Chapter 4 DESCRIPTION OF BRASTED SAND

The sand used in the test programme was obtained from a deposit being worked adjacent to the River Darent near Brasted, Kent. It is a medium-to-fine uniform sand with angular grains. It consists of quartz with a slight trace of mica. There is no organic matter present.

This sand has been used in research work by Kolbuszewski (1948), Hafiz (1950), Eldin (1951) and Fraser (1957). Approximately 12000 gm. of the sand were available in the laboratory and, as 5000 gm. of sand was used for each experiment, the same grains of sand were sheared many times in the course of testing 30 plane strain and 33 large triaxial specimens, as well as many other incidental tests. The grading curve prior to the test programme and a second curve obtained towards the end of the programme are shown on Fig. 4-1. There has obviously been some breakdown in the size of the grains. The shear tests were run in groups to prevent changes in the particle size distribution from affecting the measured $\phi$ - porosity relationship within each group. The effect of particle breakdown in the comparison between groups is more difficult to assess but a consideration of all the test results does not suggest that there was any serious effect from this source.

The specific gravity of the sand was measured after the sand had been immersed under water for a period of 24 hours. The value adopted throughout the test programme was 2.684, an average of 4 determinations. (The specific gravity determinations were not accurate to the fourth significant figure).

The limiting densities of the sand were measured and gave the following results:-

| | Voids Ratio | Porosity (%) | Dry Density (lb./cu.ft.) |
|---|---|---|---|
| Rapid tilt test on dry sand | 0.792 | 44.2 | 93.4 |
| Vibration of saturated sand by Kango hammer technique | 0.475 | 32.2 | 113.5 |

The detailed procedures for these tests are given by Kolbuszewski (1948) and are referred to in Chapter 10.

# PARTICLE SIZE DISTRIBUTION

LOCATION No.....  BORE HOLE No.....  SAMPLE No.....

DATE OF TEST.....  DESCRIPTION Brasted Sand

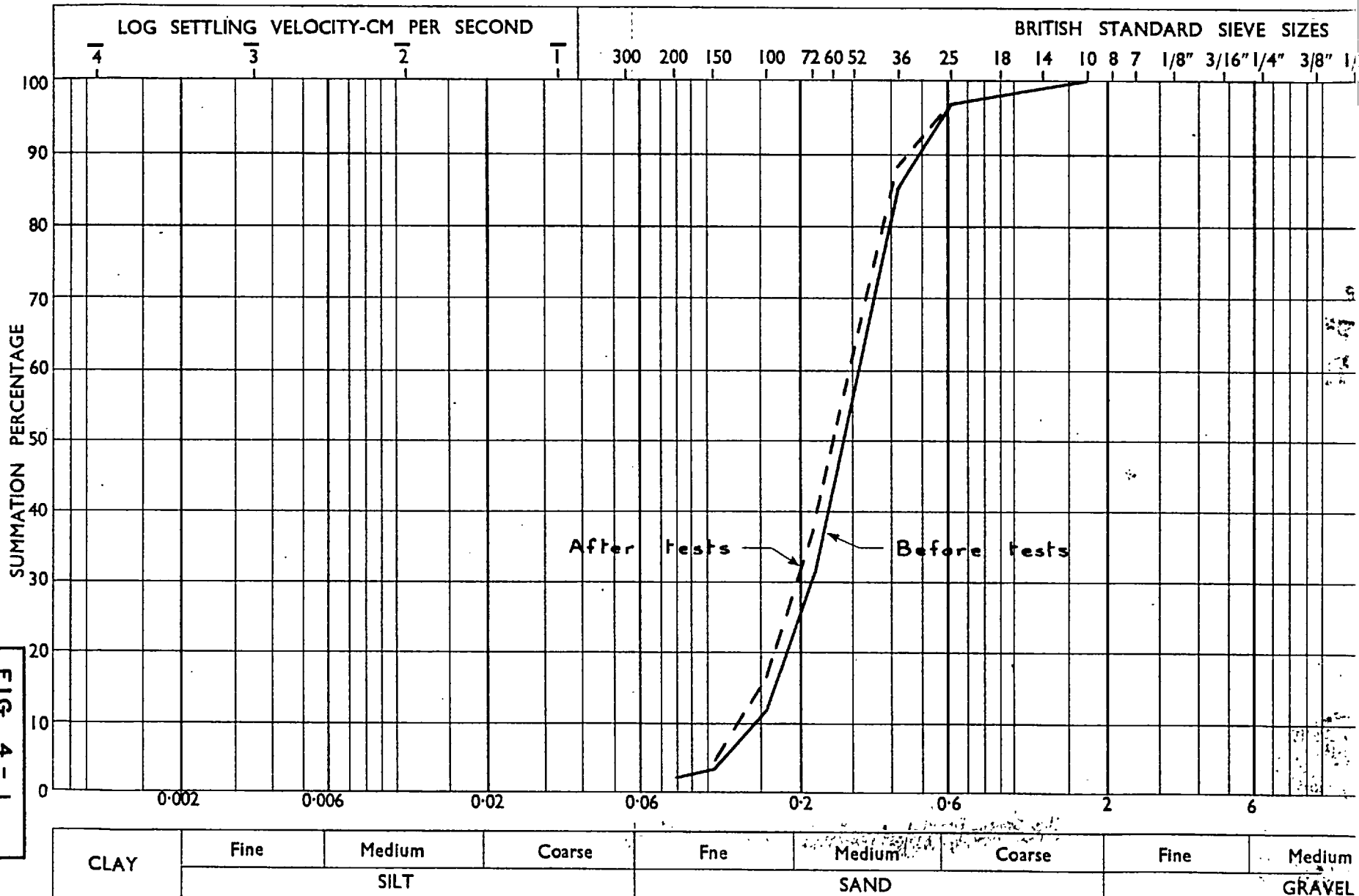



FIG. 4 - 1

## Chapter 5 TEST PROGRAMME

All the tests described in this thesis were carried out on saturated sand. This has the advantage that the volume changes within the specimen can be measured directly and with greater accuracy than in tests on dry sand. Furthermore, the porosity of the denser plane strain and standard triaxial test specimens were correlated, independently of the measured weight and dimensions, by means of moisture content determinations. This provided a direct check on the accuracy of the research work. A possible disadvantage of saturation is that pore pressure changes may occur during supposedly drained tests. Comparatively slow shearing rates were adopted to ensure complete dissipation.

### $K_o$ - consolidation

To test a soil in the plane strain apparatus, any consolidation of the soil must be carried out under conditions of zero lateral strain ($K_o$) because the end clamp used to keep plane strain in the subsequent shearing phase is placed in position before the start of consolidation. To maintain consistency in experimental technique, the standard triaxial compression and extension test specimens were also consolidated with no lateral yield.*

---

* the classical view of natural sedimentation is that of a horizontally bounded semi-infinite mass of soil subjected to a uniform rate and intensity of deposition at the interface between the soil and water. At any point within the soil mass, the stresses on the soil are governed by the strain condition; that is, by the condition that no overall horizontal movements can take place during consolidation. The relationship between the minor and major principal stresses in this system is termed the coefficient of earth pressure at rest, $K_o$, defined by:-

$$K_o = \frac{\sigma_3'}{\sigma_1'}$$

where $\sigma_3'$ = effective horizontal stress

$\sigma_1'$ = effective overburden stress

A lateral strain indicator for measuring the $K_o$ stresses in soil has been devised by Dr. A. W. Bishop at Imperial College. Fraser (1957) found that the $K_o$ values of sand and other granular media remained fairly constant over a wide range of stresses. The $K_o$ values on a particular soil do, however, vary with the placement density and saturation.

Triaxial shear tests on sands consolidated under $K_o$ stresses and under all-round pressures have been compared by Bishop & Eldin (1953), Fraser (1957) and Bjerrum, Kringstad & Kummeneje (1959). In all cases, it was found that the drained strength was unaffected by the type of consolidation.

## Plane Strain Tests

### Drained tests. Series A - cell pressure constant, axial stress increased

All the specimens were sheared at a constant cell pressure of 40 lb./sq.in. with drainage to a burette at atmospheric pressure. After consolidation, the axial stress was increased at a constant machine rate-of-strain until failure occurred (maximum deviator stress). Several tests were continued beyond failure to the ultimate strength.

This is the most important set of plane strain tests as the test conditions are comparable with those of the most common standard triaxial test. The placement density of the sand was varied over a wide range so that the strength-density curve could be defined.

### Drained tests. Series B - axial stress constant, cell pressure decreased

The average principal stress was decreased during the shear stage of the tests, giving the sand a different stress history to the tests of Series A. The tests were designed to give a cell pressure at failure of approximately 40 lb./sq.in.i.e. each test specimen was consolidated until the vertical stress had reached the value corresponding to failure in Series A (for the same placement density). The cell pressure was approximately 70 lb./sq.in. at this point. As the cell pressure was decreased, the axial stress was increased by an equal amount using the manual control of the screw jack. The cell pressure was decreased initially by 5 lb./sq.in and then in progressively smaller amounts. The response of the test specimen to the stress changes was practically instantaneous but 10 minutes were allowed after each decrement for the axial strain to reach full equilibrium. When failure was imminent, the motor was switched on and failure took place

at a constant rate-of-strain, the cell pressure remaining constant at failure.

The author believes that the above method gives the operator better control of the measurements during this test. However, the technique is open to criticism on the grounds that the final stages of failure do not strictly adhere to the prescribed test conditions. Two of the later tests were carried out using a manual control of both the cell pressure (via the screw ram) and the deviator stress to failure. The test results obtained by the two techniques do not show any measureable differences which can be attributed to the techniques.

Drained tests. Series C - cell pressure constant, axial stress increased (omission of end clamp)

This test series was identical to Series A except that the strain control device was left off the specimen. Series C was designed to find out by experiment whether friction at the ends of the specimen was sufficient to increase the measured shear strength of the soil. The changes in length at the end of the test were measured on some of the specimens.

Undrained tests. Series D - cell pressure constant, axial stress increased

In undrained tests, the maximum principal stress ratio and maximum deviator stress are not usually coincident (Holtz, 1947). Tests in Series D may be divided into two categories:-

(a) tests in which an attempt was made to reach the maximum deviator stress.

(b) tests designed to reach a maximum principal stress ratio with an effective minor principal stress of approximately 40 lb./sq.in.

As the maximum principal stress ratio generally occurs earlier than the maximum deviator stress in dilatant cohesionless soils (Taylor, 1939; Bishop & Eldin, 1950; Penman, 1953), tests with objective (a) were consolidated to lower effective consolidation stresses than tests with objective (b). However, it was not possible to attain the

maximum deviator stress in the denser specimens. The maximum principal stress ratio was achieved in all the tests and Series D marks an important step forward to increasing knowledge about the undrained test. This is the first time that it has been possible to shear saturated sand specimens over such a wide range of placement densities.

After consolidation, the specimens were sheared at a constant rate-of-strain. In some of the denser specimens, an initial positive pore pressure was created, prior to shear, by raising the cell pressure under undrained conditions. The pore pressures were measured by the usual null technique.

## Standard Triaxial Tests
(abbreviated descriptions)

**Drained tests. Series E - cell pressure constant, axial stress increased**

Cell pressures:- 40 lb./sq.in., 60 lb./sq.in.
Axial loading at constant rate-of-strain.
Comparable with plane strain Series A.
Total number of tests in Series E 40 lb./sq.in. - 8
60 lb./sq.in. - 8

**Drained tests. Series F - axial stress constant, cell pressure decreased**

Test designed for cell pressure at failure of approximately 40 lb./sq.in.
Application of cell and axial stresses by manual control.
Comparable with plane strain Series B.

This test simulates the type of failure which occurs in excavation work. The test has been compared with the more common triaxial test (Series E) on several previous occasions. The Triaxial Shear Report (1947) and Bishop & Eldin (1953), the latter using Brasted sand, found that the drained strength of cohesionless soils was independent of this form of stress history, but Fraser (1957) measured slightly higher strengths on Brasted sand when the lateral pressures were decreased to failure.

Drained tests. Series G - cell pressure constant, axial stress decreased (axial extension tests)

Cell pressures of 130 - 140 lb./sq.in. were used so that the tensile load on the specimen could be accurately measured by the 6000 lb. capacity proving ring which had been used in all the other tests.

Each specimen was consolidated under $K_o$ stresses to a lateral pressure of 130 - 140 lb./sq.in. The deviator stress was then removed leaving the specimen under an all-round pressure. The motor was switched on and the specimen failed by reducing the axial compressive stress. In this case, the cell pressure is both the intermediate and major principal stresses at failure. This test series was included to study the effect of the intermediate principal stress on strength. It is probably the first time that extension tests have been attempted on 4 inch diameter specimens of cohesionless soil.

Undrained tests. Series H - cell pressure constant, axial stress increased

Axial loading at constant rate-of-strain. Pore pressures measured at base of specimen using null technique. Maximum deviator stress never attained, even under loose placement densities. Cell pressure raised under undrained conditions to increase pore pressures before and during shear.*

---

* cohesionless soils cannot usually maintain lower pore pressures than approximately - 14 lb./sq.in. When the pore pressure approaches absolute zero, air dissolved in the water comes out of solution at an increasing rate. A saturated specimen ceases to remain at constant volume and the phenomenon is termed cavitation (Bishop & Eldin, 1950). In general, it is advisable to keep the pore pressures positive i.e. greater than atmospheric pressure.

Bishop & Eldin (1950) proved experimentally that loose saturated sand behaves as a "$\phi = 0$" material in the undrained test, providing that the soil does not cavitate. This conclusion was later confirmed by Penman (1953) on loose silt and Nash (1953) on fine sand. Soil specimens which do cavitate show an increasing strength with increasing cell pressures as the effective minor principal stress is unable to increase when the pore-water pressure reaches minus 1 atmosphere. This probably explains the earlier observations of certain soils having "$c - \phi$" characteristics in the undrained test.

Undrained tests. Series J - cell pressure constant, axial stress decreased (axial extension tests)

Procedure similar to Series G, except that specimens were sheared under undrained conditions.

---

The total number of shear tests reported in the Thesis are:-

| | Plane Strain | Triaxial Compression | Triaxial Extension |
|---|---|---|---|
| Series A | 13 | | |
| Series B | 4 | | |
| Series C | 5 | | |
| Series D | 8 | | |
| Series E | | 16 | |
| Series F | | 5 | |
| Series G | | | 6 |
| Series H | | 4 | |
| Series J | | | 2 |
| Total | 30 | 25 | 8 |

---

The order of carrying out the test series has some importance because:-

(i) experimental techniques tend to improve with time. There is also a possibility that the technique might inadvertently alter slightly with time.

(ii) the strength-density curves may alter slightly due to the constant re-use of the soil

The chronological order is given by the following list:-

1. Series E (60 lb./sq.in.) 2. Series A & Series C 4. Series B
5. Series D 6. Series E (40 lb./sq.in.) & Series F 8. Series H
9. Series G 10. Series J.

# Chapter 6 PREPARATION OF SPECIMENS, TEST PROCEDURE, AND CALCULATIONS

## I Plane Strain Tests

### Specimen preparation

The sand was saturated by weighing out 5000 gm. of dry soil and slowly pouring it into a large shallow tray of boiling water. The sand was boiled for at least one hour and then allowed to cool overnight.

To prepare the test specimen, the cell base plate was taken off the pedestal of the triaxial machine and stood on its legs. The perspex holder, which positions the 4 porous stones, was screwed to the base platen and sealed around the perimeter with plasticine. The membrane was sealed between the lower platen and the cell base plate. The base plate was then moved onto the pedestal of the machine. De-aired water was run into the membrane to a depth of 1 to 2 inches and the porous stones were placed in the holder. All the air bubbles trapped between the membrane and the lower platen were removed. The sand former (Plate 6-1) was carefully positioned around the lower platen, and the rubber membrane was stretched and held by turning the top face of the membrane over the recessed edges of the former. The membrane was mainly retained in position by the corners of the former and a little french chalk was rubbed onto the former at these points to prevent slippage of the wet membrane during the subsequent specimen preparation. Small clips were used to hold up the membrane at the mid-length of the former.

Saturated sand was transferred from the tray into the former, using a scoop, and spread evenly beneath the water. For placing loose specimens, the former was completely filled with water so that the sand was deposited with a low velocity of fall and low intensity of deposition. The sand was densified by a small mechanical vibrator which was placed on the base of the former. The upper surface of the sand was open to the atmosphere during vibration. This technique allowed the sand to be placed and vibrated in several layers (see later) but the

ends of the specimen were not as well developed, in general, as in an earlier compaction method.* Different densities were obtained by varying the vibration time and the amplitude of the vibrator. The sand remaining in the tray after making the specimen was dried and weighed to the nearest gram.

The upper surface of the sand was levelled and the upper platen gently lowered onto it. The rubber membrane was turned over the recessed O-ring of the upper platen and sealed by screwing the upper bearing plate to the platen. Care was taken to avoid trapping air bubbles inside the rubber membrane. Despite the use of clips, it was difficult to prevent the membrane from sagging along the length of the specimen. The result was that the right-angled upper edge of the membrane did not always fit perfectly to the right-angled edge of the upper platen and some excess water, and an occasional small air bubble, were trapped between the membrane and the upper platen** (Plates 6-2, 6-3, 6-4). The air bubbles remained between the upper platen and membrane throughout the tests, but some of the excess water was pushed out during consolidation by the increasing cell pressure.

To ensure consistency in all the plane strain tests, the bolts connecting the upper bearing plate to the upper platen were well tightened down. It required great care to do this without appreciably disturbing the soil structure, particularly on the looser specimens. The weight of the two loading plates puts an initial deviator stress of 0.6 to 0.7 lb./sq.in. at the top of a specimen.

---

* in the early tests, the membrane was sealed to the top cap before vibration took place and the specimen was allowed to drain through a burette connected to the base. During vibration, there was a tendency for the sand grains to be trapped between the membrane and upper platen and a risk of the abrasive sand grains or upper platen piercing the membrane. Furthermore, wrinkling of the membrane occurred in the preparation of dense specimens. The technique was withdrawn in favour of the above vibration method.

** this could probably be avoided by making membranes which increase slightly in depth from the ends to the mid-length.

The valve at the base of the specimen was opened and the level of the burette was adjusted so that the water level in it corresponded to the mid-height of the sample. The burette was then lowered by 2 ft., placing a negative pressure of slightly less than 1 lb./sq.in. on the soil. The wing nuts of the former were taken off, the shanks removed and the sides of the former slid off slowly.*

The width of the specimen was measured using a special device developed by Wood (Plate 6-2). Six equally spaced measurements at each of three different levels were taken and the maximum difference between the 18 readings was usually only 0.005 inches. The average width, including the membrane, of almost 80% of the test specimens was 2.097 in. $\pm$ 0.002 in. The dial gauge was checked by a gauge length of 2.000 inches after each measurement. The height of the specimen was measured by a steel rule to the top of the loading plate, the height for each reading being estimated to 0.01 centimetres. Three readings were taken on each side of the specimen - at the centre and approximately one-sixth the distance from the ends. The length of the specimen was measured on all the early tests but, as it was found to be invariable relative to the accuracy of measurement, it was decided to adopt an overall length (including the membrane) of 16.10 inches for all the tests. Readings of the volume burette were taken before and after measurement. The ends of the specimen were slightly rounded on the side edges. This "lost" volume was estimated by filling the space between the end plates of the former and the specimen with soft plasticine, the volume of the plasticine being measured by water displacement. The volume varied from 4 to 11 cc., the average value being about 7 cc. (0.3% of the total volume). This may have influenced the measured value of the intermediate principal stress as the end plates

---

* the former should not be pulled back or the specimen is liable to collapse. For easy removal of the former, the area of contact between the membrane and the former should be either perfectly dry or saturated. It is difficult to keep the area dry but the saturated state can be brought about by wetting the outside of the membrane at the setting-up stage, followed by a liberal dose of water from a squeeze bottle just before removing the former.

were not in contact with the full cross-sectional area of the specimen. However, this seems to be extremely unlikely as there was no indication of any change in configuration at the ends of the specimens after the shear test had been completed. An allowance for the rounded ends was made in the calculation of the initial volume and horizontal cross-sectional area of the specimen.

Test procedure

The ends of the rubber membrane enclosing the specimen were smeared with a light coating of silicone grease. The end clamp was then carefully placed in position with the contacting plates adjusted so as to leave an equal gap between the upper and lower platens. The null indicator of the intermediate principal stress device was set to zero. A slight positive water pressure was placed on the null indicator through the screw ram such that the mercury in the null indicator rose by approximately 0.4 inch. The four bolts of the end clamp were tightened evenly by hand until the mercury level in the null indicator had returned to the zero mark. This placed a small deviator stress of approximately 0.25 lb./sq.in. on the ends of the specimen and ensured a good contact between the specimen and end plates. A time interval of 30 minutes was allowed to ensure that this deviator stress did not decrease. Two views of the end clamp are shown on Plates 6-3 and 6-4.

The remainder of the apparatus was assembled for testing (Fig. 6-1). The cell was filled with de-aired water and castor oil was fed to the rams via leads passing through the ram housing. The air bleed valves at the top of the cell were closed and the cell pressure set to atmospheric pressure. Any zero correction on the mercury manometer was noted. The rams were lowered until one of them had established contact with a hemispherical seating on the loading plate, the adjusting screws above the proving rings being used where necessary to bring the second ram into contact. The motor attached to the arm of the friction eliminators was switched on, the dial gauges set to zero, and the specimen was ready for consolidation.

At this stage, the initial porosity of the specimen was known

from the dry weight of sand used in the test. The corresponding value of $K_o$ was abstracted from Fraser's (1957) curve for saturated Brasted sand (Fig. 6-2). The cell pressure was increased in stages and the calculated value of deviator stresses necessary to maintain the $K_o$ condition at each cell pressure were simultaneously applied to the specimen by hand using the manual control of the loading screw jack. As each cell pressure was applied, an equal pressure had to be added to the pressure diaphragm of the end clamp and, if the specimen was consolidating correctly, the mercury in the null indicator returned to the zero mark. In some tests, however, there was a small lateral deviator stress on the specimen at the end of the consolidation stage. Readings of the volume change and vertical dial gauges were taken at cell pressures of 1, 2, 4, 7, 10, 15, 20, 25, 30, 40, etc. lb./sq.in. The response of a specimen to change in the external stresses was practically instantaneous but approximately 10 minutes were allowed after each increase of cell pressure to establish static equilibrium. The burette was raised to the mid-height of the specimen at a cell pressure of 4 lb./sq.in. An allowance for the weight of the loading plates was made in the calculation of the deviator stress but no allowance was made for the self-weight of the specimen. Hand loading was preferred to constant rate-of-strain loading as it allows the operator better control of the consolidation. The difficulty in applying a constant stress ratio at a constant rate-of-strain is that the compressibility of the test specimen changes appreciably during the test. For example, if the motor speed is set to bring the specimen to full consolidation in 2 hours, few readings can be taken in the first hour but in the final 10 to 15 minutes the cell pressure has to be raised at an increasing rate to keep pace with the increases in deviator stress. Thus, the test is apt to become out of control at the most crucial stage.

The time taken to apply the consolidation stresses by hand was approximately 2 hours and a further 1 hour was allowed under the final consolidation loads before starting the shear test. The consolidated end area, volume and height of the specimen were calculated. If the specimen had consolidated correctly, the initial cross-sectional area

multiplied by the change in height should equal the change in volume. As discussed in the next Chapter, it is probable that there are slight errors in both the change in height (due to cell expansion) and change in volume (due to entrapped water outside the soil which is expelled during consolidation). However, for calculation purposes, the changes in height and volume were taken from these measured changes, but the cross-sectional area of the specimen after consolidation was assumed to be unchanged from the initial measurement.

Throughout a shear test, readings were taken of both the axial deformation dial gauges, both proving rings and the volume change burette. The stress in the diaphragm of the plane strain end clamp was controlled manually by the hand-operated screw ram. The mercury level in the null indicator was kept at the calibrated mark corresponding to the pressure difference between the diaphragm and the cell. In the undrained tests, a second null indicator was operated in a similar manner and readings of the pore-water pressures were taken from the manometer and Bourdon gauge. The results were calculated as the test was carried out, sets of readings being generally taken at intervals of 0.25% axial strain up to failure. Some tests were stopped at failure but the majority were continued until the ultimate condition had been reached.

There was sometimes a slight time lag in the response of the pressure diaphragm so that, for example, the maximum value of the intermediate principal stress occurred one reading later than the maximum major principal stress, although the latter may have only shown a slight decrease at this point. In general, however, the intermediate principal stress measuring device behaved extremely well, as can be seen from the graphs in Appendix 10. At frequent intervals, the device was de-aired and re-calibrated. The calculated intermediate principal stress value includes the initial (placement) prestress and any additional stress on the soil at the end of consolidation i.e. some of the shear tests start with a small lateral deviator stress on the ends of the specimen.

The cell pressure gauge was very consistent throughout the test programme and was checked as far as 25 lb./sq.in. by the mercury

manometer. The cell pressure reading was always checked at failure. From time to time, the length of the specimen was measured at the end of the test to prove that no change in length had occurred during shear. On one occasion, the whole specimen was re-measured at the end of the test and its dimensions and volume were in excellent agreement with the corresponding values computed from the initial measurements and subsequent changes.

At the end of a test, the motor clutch was disconnected and the deviator stress was taken off the specimen. The valve connecting the burette to the specimen was kept open. In the case of undrained tests, the null indicator was disconnected and a burette substituted at the end of the test prior to removing the deviator stress. The level of the burette was lowered 2 feet below the mid-height of the specimen. The cell pressure was reduced to zero and the specimen was allowed to expel or take in as much water as it wished,* but was finally under a small negative pressure which held it intact.

The apparatus was dismantled and care was taken to see that the specimen was not disturbed during these operations. The plane strain end clamp was carefully removed and the width of the failure zone, which was clearly marked on the ends of the specimen in tests continued to the ultimate condition, was measured and its position noted. All oil, silicone grease, and water adhering to the membrane and metallic parts were removed by a damp cloth.

---

* the effect of the removal of the external stresses on the volume changes is interesting. The results of a dense specimen (P-23), which was sheared to the ultimate stress, and those of a medium dense specimen (P-24), in which shearing was stopped shortly after reaching the peak deviator stress, are shown on Figure 6-3. The result of taking off the deviator stress was similar in both cases. At first a small amount of water was sucked in by the sand but as the stress reduced to zero the specimen started to expel water. It is remarkable that a reduction in the total stresses produces a decrease in the volume of the specimens. When the cell pressure was taken off, water was sucked into both specimens. These volume changes are typical for all the plane strain tests. The volume changes which occurred in the earlier part of the test are plotted on the graph for comparison.

The following procedure was adopted for many of the denser specimens. The valve leading to the burette was closed. The upper bearing plate was removed and the membrane peeled off the specimen, leaving the sand exposed. The upper platen was carefully removed and 3 moisture content samples were taken at each of 3 different levels of the specimen:- top, middle and bottom. Great care was taken to ensure that the structure of the soil was undisturbed during the removal of the membrane and loading plates. The soil structure becomes progressively more sensitive as the density becomes looser. It was not possible to remove the membrane from the looser specimens without expelling pore water. The limit for successful sampling was found to be the initial porosity of 40%. The method thus covered two-thirds of the total density range.*

The remainder of the sand was placed in a large tray and oven-dried. Before dismantling the rest of the apparatus, the membrane was sealed again between the two loading plates. Measurements were taken of the height of the assembly, without a specimen, in an identical manner to the procedure at the start of the test. The height of the specimen was obtained by deducting this latter average height from the average height measured prior to shear. The measurement at the end of the test was a check on the value used in the pre-shear calculations.

The weight of dry sand used in the test can be calculated by two methods - firstly, by subtracting the weight of dry soil which was not used in the test from the 5000 gm. which was originally placed in the tray of boiling water, and secondly, by adding together the dry weights from the moisture content determinations and the remainder of the specimen after the test. The two results did not, in general, agree as some soil was lost during the test (8 gm. on average). It was assumed that as much sand was lost before the specimen was set up as after the specimen was taken down, and the average dry weight of sand was used

---

* the grading curve of the soil will probably govern the density range for which moisture contents can successfully be taken. The finer the soil, the greater the range.

in the calculations. The maximum amount of sand lost during a test was 15 gm. and if all this quantity had been lost either before or after the specimen was measured, the resulting error in porosity would be 0.11%. Allowance was made for the sand which was trapped between the edges of the lower platen and the membrane. This sand was collected in a separate dish for drying. The plasticine used to seal off the joint between the perspex porous stone holder and the lower platen served as an effective stop which prevented large quantities of sand from being vibrated down these edges. Nevertheless, an average of 14 gm. of soil was carried into these regions and would have affected the measured porosity if they had not been taken into account.

The moisture content of the sand was determined after drying the sand in an oven for 24 hours at a temperature of 105-110°C. The porosity of the sand was then calculated by assuming that the sand was fully saturated. The average of the nine determinations was taken to be the average porosity of the whole specimen at the end of the test. This value was compared with the porosity at the end of the test calculated from the initial dimensions of volume and weight together with the volume changes which took place during the test. The comparison is given in Fig. 7-1 and shows, on average, a good agreement between the two independent methods.

## II Standard Triaxial Tests

To avoid undue repetition, the preparation of specimens and test procedures in the standard triaxial tests are shortened to explain only the main points in the technique.

### Specimen preparation

The preparation of a 4 inch diameter specimen is illustrated on Plates 6-5, 6 & 7, and is almost self-explanatory. The rubber membrane is first sealed to the base pedestal of the triaxial cell with rubber O-rings. De-aired water is run into the membrane to a depth of 1 to 2 inches, entrapped air bubbles are removed, and a coarse-grained porous stone placed under the water. A three-part split mould, held together by an encircling link chain, is set in position on the base of the

triaxial cell. The supports are adjusted to make the mould vertical (checked by a spirit level) and keep the lower edge of the mould just above the porous stone. The mould had a slightly smaller diameter than the porous stone and this prevented sand from passing down between the membrane and pedestal.

Saturated sand was spread evenly under the water and the soil was densified by the mechanical vibrator, placed on top of the split mould. The top cap had a larger diameter than the mould and would not pass down inside the mould collar. Hence, sufficient sand was used to make the level of the vibrated surface slightly below the upper edge of the mould. Next, a thick porous stone was gently lowered into position on top of the sand. The membrane was slipped off the collar, the collar was removed, and the top cap placed and sealed to the specimen.

The above technique was changed for the extension tests, which required a perfect fit between the sand and top cap. Strips of polythene sheeting were glued to the joints of the split mould to increase its diameter and thus allow the top cap to pass inside the mould. It was necessary to apply a vacuum to the inside of the mould to hold the membrane flat against the sides of the mould near the top. After vibration, the surface of the sand was carefully levelled by a special tool and the top cap was added directly to the sand. The extension test specimens were slightly shorter than the compression test specimens.

The outside burette was lowered by 2 feet, placing a negative pore-water pressure on the soil. The split mould was then removed. The diameter of the specimen was measured to 0.001 inch at 6 equidistant levels on each of 3 equidistant points around the circumference of the specimen, using the measuring device developed at Imperial College (see Bishop & Henkel, p.86 ). The diameter, including the membrane, of more than two-thirds of the compression test specimens was $4.007 \pm 0.003$ inches. The dial gauge was checked against a steel gauge length of 3.995 inches after each measurement. A steel rule was used to measure the height of the specimen and end caps (to 0.01 cm.) at 4 equidistant points around the circumference. The height of the

end caps and porous stones alone was subtracted from the total height to give the height of the specimen.

Test procedure

The remainder of the apparatus was assembled for the test. The porosity of the specimen was estimated from the weight of dry soil used in the test, and the corresponding $K_o$ stresses applied to the soil by hand in an identical manner to the plane strain tests. At the end of the consolidation stage, the volume and height of the consolidated specimen were calculated.

The machine rate-of-strain was set at 0.006 inches/minute or 4½% of the specimen height per hour. This speed is 2½ times faster than the rate used for the plane strain tests. The different rates are unlikely to make any measurable effect on the strength (Casagrande & Shannon, 1948). After the shear test, the stresses were removed. The valve to the burette remained open, the burette having been placed 2 feet below the mid-height of the specimen.

Most of the extension test specimens were sheared at the same cell pressure. For drained extension tests, the range of failure loads is comparatively small as any increase in deviator stress decreases the minor principal stress. Therefore, the proving ring was very carefully calibrated over the range of extension test failure loads. The special calibration showed a good agreement with the more general calibration of the ring shown on Appendix 1, Fig. A1-1.

Moisture content samples were taken on the denser specimens at the end of the test. For triaxial specimens, 2 moisture contents were taken at each of 5 equidistant levels of the specimen so that each pair of moisture contents represented an equal proportion of the total volume. The average moisture content value was converted to final porosity, assuming complete saturation, and the result was compared with the final porosity calculated from the weight-volume measurements, allowing for the volume changes which occurred during the test (Fig. 7-1).

The weight of dry sand used in the test calculations was assumed to be the average between the deduced weight (i.e. weight not used in

test deducted from the original amount of soil weighed out) and the weight of soil recovered at the end of the test. The amount of soil lost during a test was 4 gm. on average.

## III Shear Test Calculations

### All tests

Porosity was calculated as follows:-

$W_d$ = average dry weight of sand in the specimen

$V$ = calculated volume of specimen

$V_s$ = volume of specimen occupied by sand

$$= \frac{W_d}{G\gamma_\omega}$$

where $G$ = average specific gravity of Brasted sand = 2.684

$\gamma_\omega$ = unit weight of water

$V_v$ = volume of voids in the specimen

$$= V - V_s$$

$e$ = voids ratio

$$= \frac{V_v}{V_s}$$

$n$ = porosity

$$= \frac{e}{(1+e)}$$

Vertical deviator stress was calculated as follows:-

$$(\sigma_1 - \sigma_3) = \frac{\text{Net load}}{A_s}$$

where $(\sigma_1 - \sigma_3)$ = vertical deviator stress

$A_s$ = average cross-sectional area

$$A_s = \frac{A_c\left(1 + \frac{\Delta V}{V_c}\right)}{(1 - \epsilon_1)}$$

where $A_c$ = consolidated area of specimen

= original area of specimen for $K_o$ consolidation, $A_o$

$\frac{\Delta V}{V_c}$ = volumetric strain and is negative for consolidation volume changes, positive for expansive volume changes

$\epsilon_1$ = vertical linear strain and is positive for compression tests, negative for extension tests

Net load = $(L + W) - A_r . \sigma$

where $L$ = load measured on proving ring and is positive in compression, negative in extension

$W$ = dry weight of top cap, etc. = 21 lb.

$A_r$ = cross-sectional area of ram

$\sigma$ = cell pressure

In addition, the following formulae were used in the stated tests:-

Plane strain tests

Lateral deviator stress $(\sigma_2 - \sigma_3)$ was calculated as follows:-

Pressure difference between end clamp cell and plane strain cell = $(g - \sigma_3)$

where $g$ = corrected Bourdon gauge reading (calibrated against the plane strain cell pressure)

$$(\sigma_2' - \sigma_3') = (g - \sigma_3) \frac{A_D}{A_E}$$

where $A_D$ = cross-sectional area of diaphragm plate
= 3.55 sq.in.*

$A_E$ = cross-sectional area of the end of the specimen in sq.in.
= $A_{EC}\left(1 + \frac{\Delta V}{V_c}\right)$

To give the reader some idea of the quantities measured in the plane strain test, a worked example of a typical consolidated-drained test is presented in Appendix 5.

---

* this is the area of the rigid disc attached to the rubber diaphragm. The effective area of the diaphragm is slightly larger and the values of the intermediate principal stress quoted in the Thesis are underestimated by approximately 1% (Appendix 4).

Standard triaxial extension tests

In the extension tests, uniform necking occurred in the failure zone and it was quite evident that a substantial error would be made in the calculations of strength if the average cross-sectional area over the whole length of the specimen was used. As soon as the maximum deviator stress had been reached in an extension test,* the test was stopped. The apparatus was dismantled and the diameter of the soil specimen was measured, at 3 equidistant points of the circumference, by a travelling microscope. Readings were generally taken at 2 cm. intervals along the length of the specimen but the intervals were shortened to $\frac{1}{2}$ cm. in the necked area.

There was no visible failure plane at the maximum deviator stress condition. In the calculations, it was assumed that a failure plane would make an angle of $(45 + \frac{1}{2}\phi)^\circ$ degrees to the vertical axis and that its centroid would coincide with the centre of the specimen's least diameter i.e. that the failure plane would pass symmetrically through the necked zone. First, however, it is necessary to guess the correct value of $\phi$ so that the vertical depth of the potential failure plane can be determined. There are several methods of proceeding from this point. Eldin (1951) plotted the perimeter of the potential failure plane and measured the area of the plane. This area can then be converted to an equivalent horizontal cross-sectional area. This method is laborious and may not be particularly accurate for planes which approximate to a circular shape. Equivalent horizontal areas can also be obtained from average diameters in the potential failure zone, based on Simpson's Rule and the arithmetic mean. A comparison of these three methods has been made for Specimen C-43, which was the least dense of the 6 drained extension tests. This particular test will be considered in more detail as it exhibited far more necking than any of the other tests and thus presented the most difficult case. However, one further complication will be mentioned first. When the external stresses are released at the end of the test, additional changes take

---

* the one exception was specimen no. C-43 - see later.

place in the volume and axial strain of the specimen; hence, the diameters measured by the travelling microscope are not the same as the corresponding diameters at failure. A correction has been derived on the following assumptions:-

(i) that the ratio of the necked area to the average specimen area remains the same between failure and measurement.

(ii) ignoring any change in the direction of the potential failure plane, due to the change in axial strain from failure to measurement.

Let $A_{fn}$ = equivalent average area in the failure zone at failure

$A_f$ = average area of specimen at failure

$A_{dn}$ = equivalent average area in the failure zone after dismantling apparatus

$A_d$ = average area of specimen after dismantling apparatus

$A_o$ = average area of specimen at start of test

$A_c$ = average area of specimen after consolidation

Then $A_c = A_o$, for $K_o$ consolidation

$$A_f = \frac{A_o\left\{1 + \left(\frac{\Delta V}{V_c}\right)_f\right\}}{\left\{1 + (\epsilon_1)_f\right\}}$$

$$A_d = \frac{A_o\left\{1 + \left(\frac{\Delta V}{V_c}\right)_d\right\}}{\left\{1 + (\epsilon_1)_d\right\}}$$

From assumption (i)

$$\frac{A_{fn}}{A_f} = \frac{A_{dn}}{A_d}$$

i.e. $$A_{fn} = \left\{\frac{A_f}{A_d}\right\} \cdot A_{dn}$$

$$\frac{A_f}{A_d} = \text{area correction factor} = \frac{\left\{1 + \left(\frac{\Delta V}{V_c}\right)_f\right\}\left\{1 + (\epsilon_1)_d\right\}}{\left\{1 + \left(\frac{\Delta V}{V_c}\right)_d\right\}\left\{1 + (\epsilon_1)_f\right\}}$$

Note The area correction factor is independent of errors in the $K_o$ value nor is it necessary to measure $A_d$.

The total vertical depth of the failure zone is $D.\tan(45 - \frac{1}{2}\phi)$ where D is the horizontal diameter of the specimen at the vertical extremities of a potential failure plane.

Calculations for extension test specimen C-43 This was the only extension test specimen to be sheared beyond failure. When the test was stopped, the deviator load was starting to drop off sharply (Fig. A10-46) with a corresponding increase of necking.

Direct measurements (average over whole length of specimen) :-

| | $\epsilon_1 = -9.0\%$ (failure) | $\epsilon_1 = -12.0\%$ (end of test) | |
|---|---|---|---|
| Measured $(\sigma_1 - \sigma_3)$ = | 89.49 | 85.88 | lb./sq.in. |
| Membrane correction = | -0.15 | -0.20 | lb./sq.in. |
| Net $(\sigma_1 - \sigma_3)$ = | 89.34 | 85.68 | lb./sq.in. |
| $\sigma_1$ = | 130.0 | 130.0 | lb./sq.in. |
| $\therefore \sigma_3$ = | 40.66 | 42.32 | lb./sq.in. |
| $\therefore \frac{(\sigma_1 - \sigma_3)}{\sigma_3}$ = | 2.198 | 1.933 | |
| i.e. $\phi_d$ = | 31.60° | 29.45° | |

The amount of necking had clearly altered between 9% and 12% axial extension and it would have been unrealistic to correct the maximum deviator stress values for the area reductions measured after the test had been stopped at a later stage. Hence, corrections have been applied to the readings at 12% strain. This will result in a slight under-estimate of the "true" failure stresses.

$$\left(\frac{\Delta V}{V_c}\right)_f = -1.28\% \; ; \qquad \left(\frac{\Delta V}{V_c}\right)_d = -1.74\%$$

$$(\epsilon_1)_f = -12.0\% \; ; \qquad (\epsilon_1)_d = -7.92\%$$

Area correction factor = 0.968

| | $A_{dn}$ (sq.in.) | $A_{fn}$ (sq.in.) | $\phi_d{}^\circ$ |
|---|---|---|---|
| Plot of potential failure plane | 10.835 | 10.480 | 33.20 |
| Simpson's Rule (9 diameters) | 10.747 | 10.405 | 33.60 |
| Arithmetic Mean (9 diameters) | 10.787 | 10.443 | 33.40 |

A fourth method is to use only the travelling microscope measurements to relate the necked area to the average area and assume that the same ratio holds for the end of test stress values. For the plot of a potential failure plane:-

$$\frac{A_{dn}}{A_d} = 0.933 \; ; \qquad \phi_d = 33.00^\circ$$

In summary, the four methods of correcting the stresses in specimen C-43 agree reasonably well. They increase the shear angle by amounts varying from $3.6^\circ$ to $4.2^\circ$. The error of assuming uniform strain at the maximum deviator stress conditionsis approximately $2^\circ$.

The deviations between the four methods are likely to be much less for the remainder of the extension tests* (except C-46). For simplicity, these tests were corrected from the arithmetic mean of the microscope readings in the failure zone, as follows:-

| Specimen No. | 44 | 45 | 46 | 47 | 48 |
|---|---|---|---|---|---|
| $\phi_d$, uniform strain - degrees | 39.05 | 33.70 | 33.35 | 40.35 | 36.30 |
| $\phi_d$, corrected for necking - degrees | 40.05 | 34.50 | 36.50 | 40.75 | 37.05 |
| Increase in $\phi_d$ - degrees | 1.00 | 0.80 | 3.15 | 0.40 | 0.75 |

* there will obviously be no difference between the first 3 methods if necking does not occur.

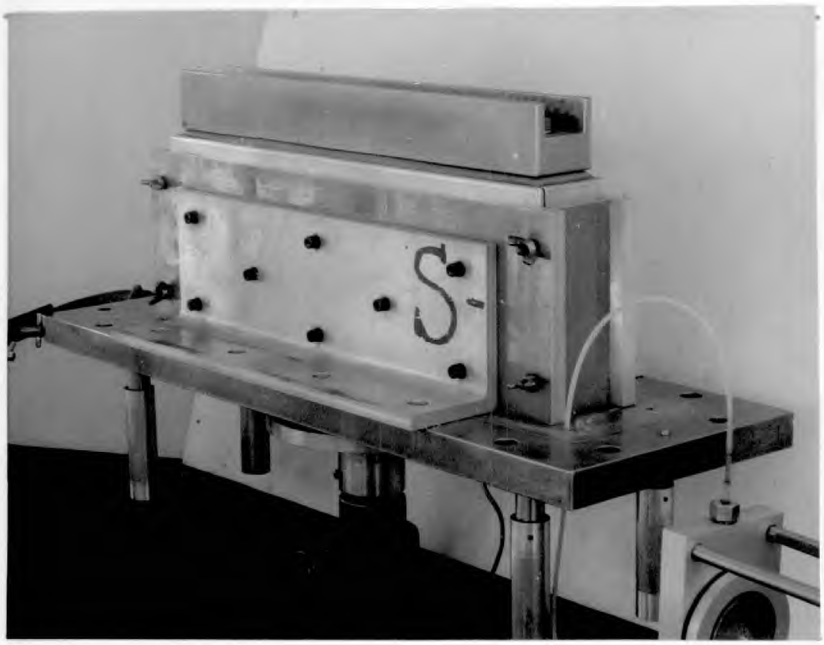


PLATE 6-1 Specimen in former with top cap in position

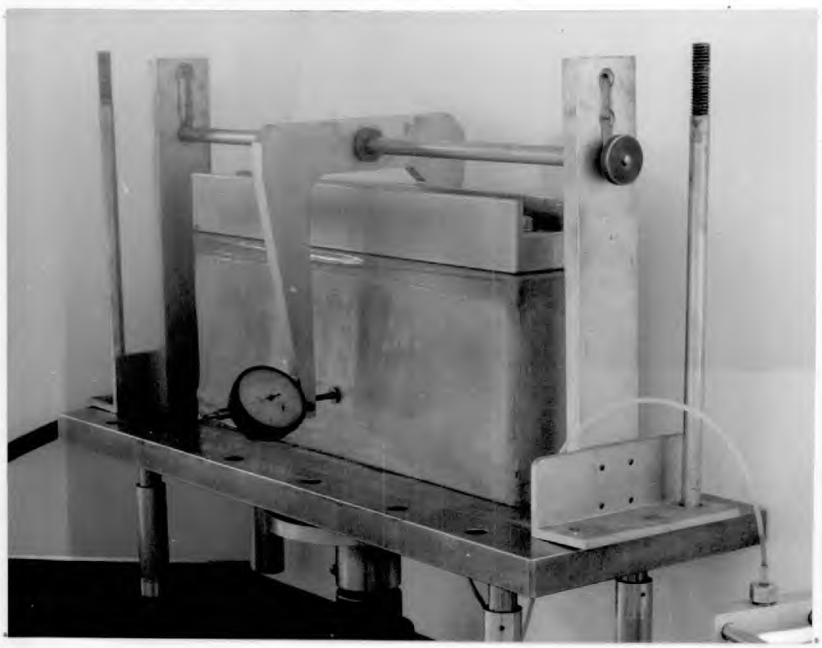


PLATE 6-2 Measurement of specimen width

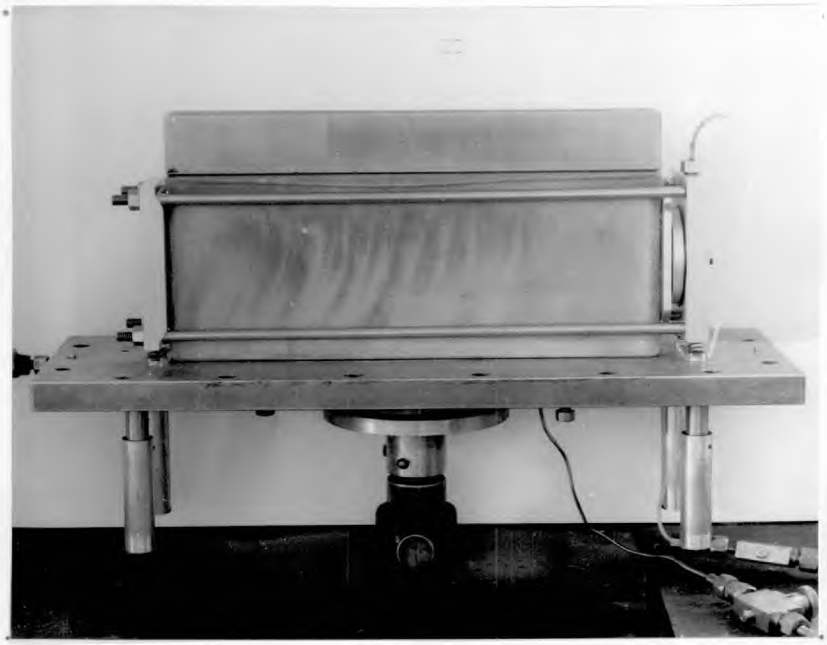


PLATE 6-3

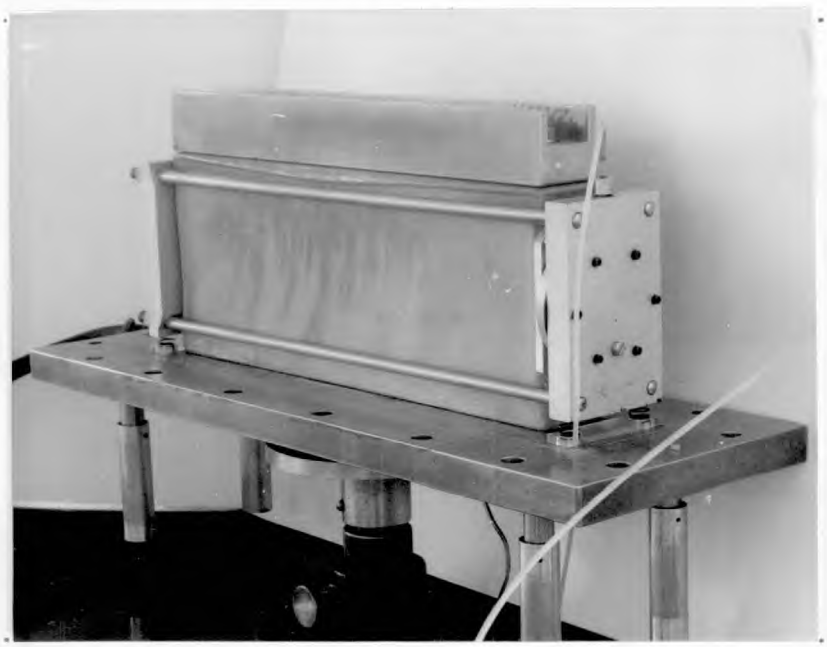


PLATE 6-4

PLANE STRAIN END CLAMP (P-26)



PLATE 6-5

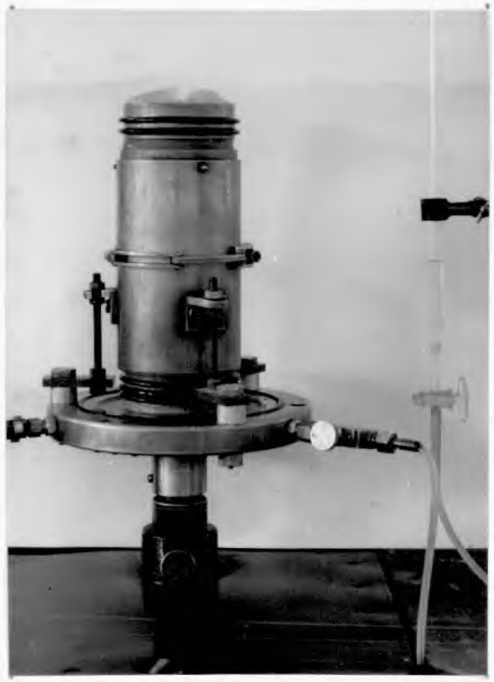


PLATE 6-6



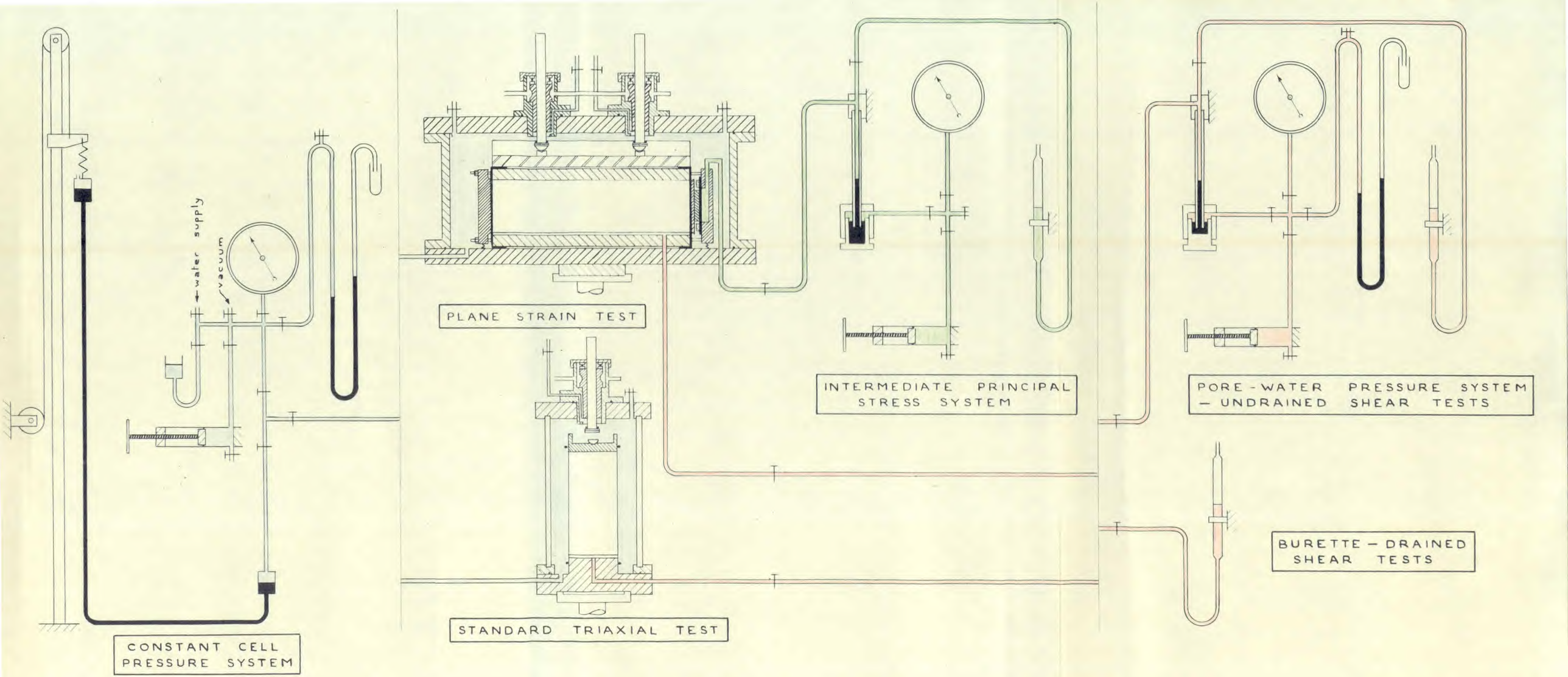
PLATE 6-7

PREPARATION OF STANDARD TRIAXIAL COMPRESSION SPECIMENS FOR TESTING

PLATE 6-5 Split mould on pedestal with membrane turned back.

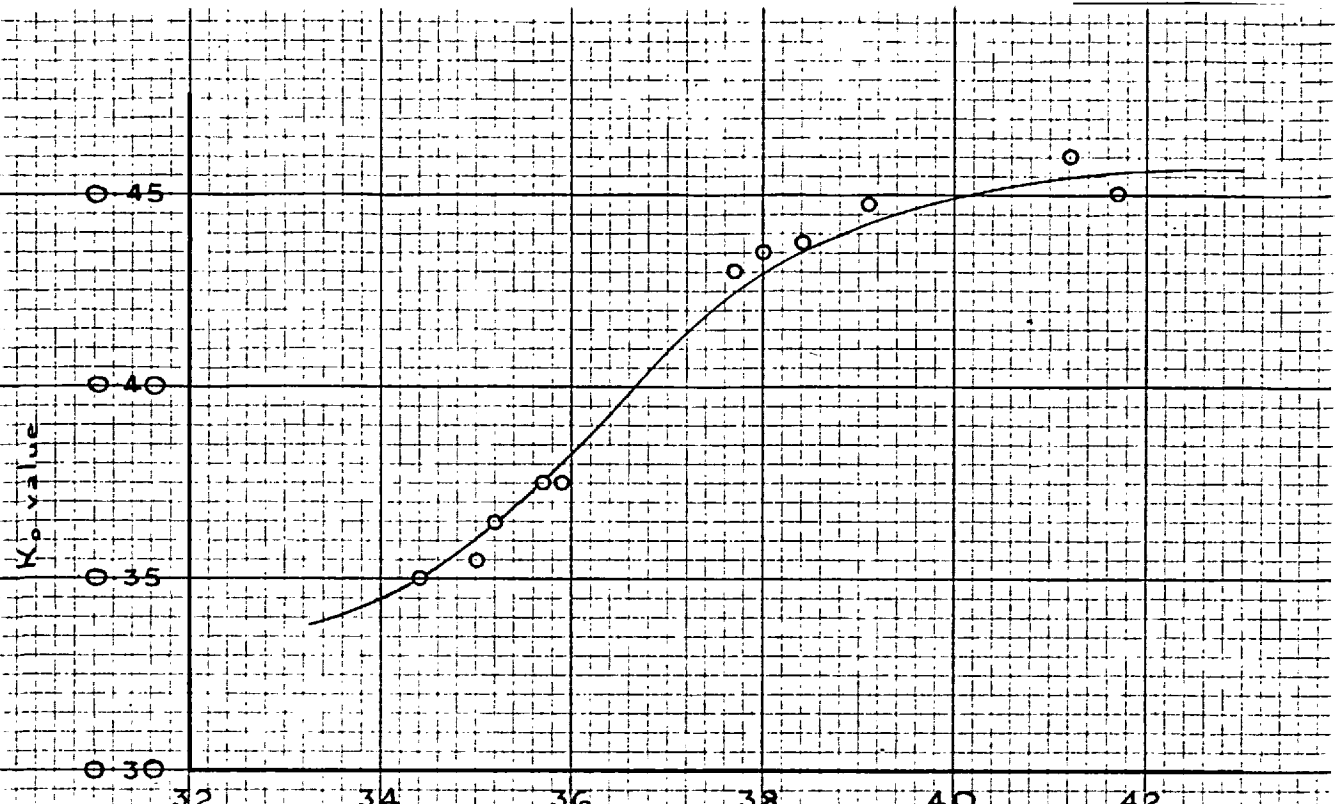
PLATE 6-6 Top cap in position.

PLATE 6-7 Specimen ready for testing.




DIAGRAMMATIC LAY-OUT OF APPARATUS FOR SHEAR TESTS

FIG. 6-1




| Initial Porosity | $K_o$ Value | $\frac{J}{\sigma_3}$ | $\mu = \frac{K_o}{1+K_o}$ |
|---|---|---|---|
| 34·0 | 0·345 | 1·633 | 0·257 |
| 35·0 | 0·360 | 1·593 | 0·265 |
| 36·0 | 0·384 | 1·535 | 0·277 |
| 37·0 | 0·410 | 1·480 | 0·291 |
| 38·0 | 0·430 | 1·442 | 0·301 |
| 39·0 | 0·442 | 1·421 | 0·307 |
| 40·0 | 0·449 | 1·409 | 0·310 |
| 41·0 | 0·454 | 1·401 | 0·312 |
| 42·0 | 0·456 | 1·398 | 0·313 |
| 43·0 | 0·457 | 1·396 | 0·314 |

## VARIATION OF $K_o$ WITH POROSITY IN SATURATED BRASTED SAND - FRASER (1957)

The same sand was used in the above tests and the tests carried out in this thesis.

$J$ = average principal stress
$= \frac{1}{3}[\sigma_1 + \sigma_2 + \sigma_3]$

FIG. 6 - 2

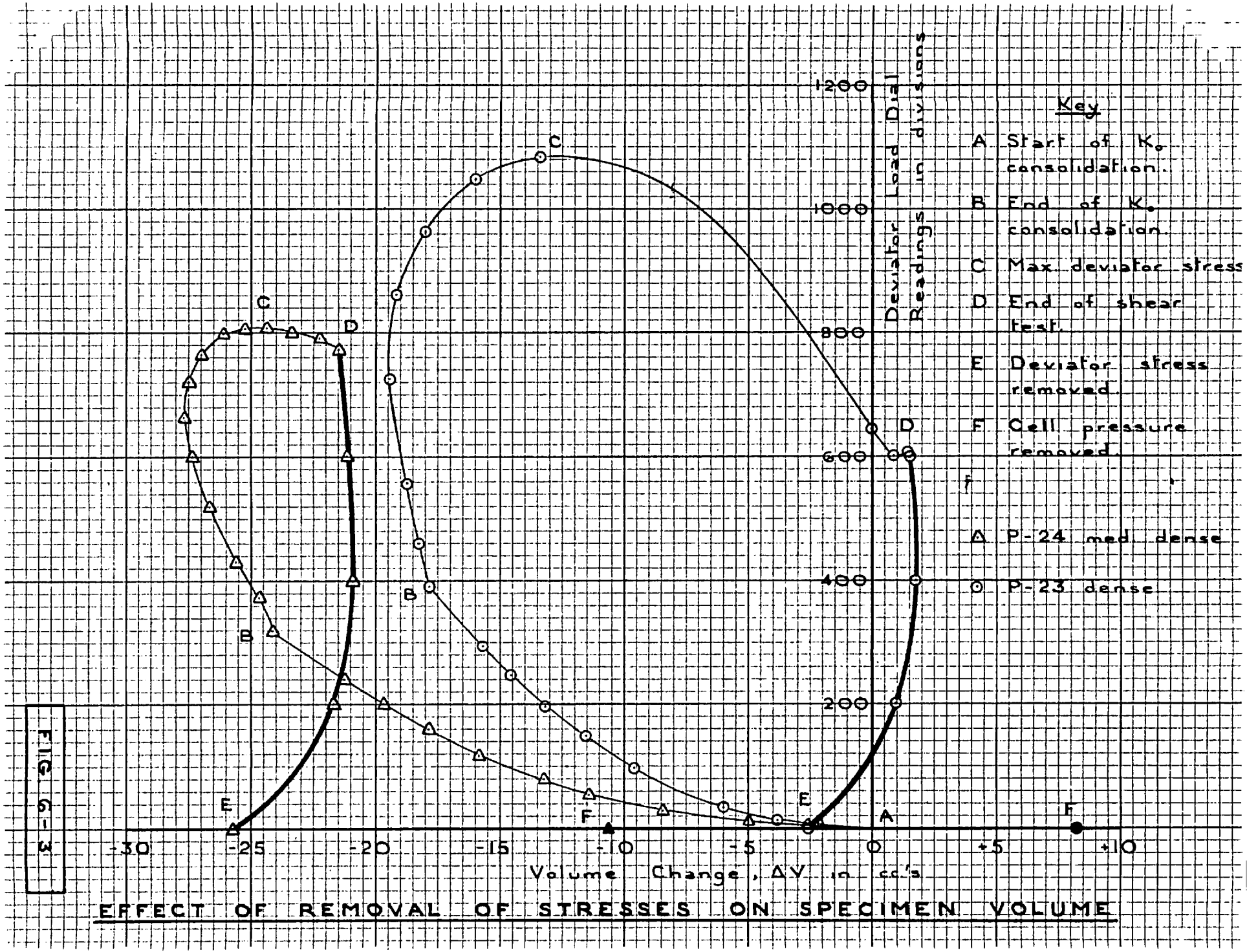



FIG 6-3

EFFECT OF REMOVAL OF STRESSES ON SPECIMEN VOLUME

## Chapter 7 COMMENTS ON MOISTURE CONTENT DETERMINATIONS, COMPACTION AND CONSOLIDATION

### Moisture content and density

The moisture content determinations, referred to in Chapter 6, proved to be a valuable guide in four respects:-

(i) for measuring the variations in density within the specimen due to the compaction technique.

(ii) for showing the changes in density within the specimen which occur during shear.

(iii) for independently correlating the density measurements taken in the plane strain and standard triaxial tests, having different specimen shapes (see Chapter 3).

(iv) a guide to assessing the reliability of any individual test density computed from weight - volume measurements.

### Non-uniformity of specimen density

Variations of density within sand specimens at failure have been measured by the Waterways Experiment Station (Shockley, 1953). Vertical and circumferential lines were drawn at 1 cm. intervals on the rubber membrane of triaxial specimens. The markings were observed during the shear test. It was found that the density at the centre of the specimen increased and the density at the ends decreased, irrespective of the initial density of the soil. The results were qualitatively checked by freezing the sheared specimens and measuring the density of segments by displacement methods. The variations in density were attributed to end restraint.

The technique of moisture content determinations allowed the variations of density within specimens to be measured both before and after shear tests. The results can be examined separately, or compared in a simple manner by adjusting the initial porosities to a common base.

To assess density changes during shear, the method adopted was as follows:-

Two specimens were prepared using the same compaction technique. Both specimens were measured under placement conditions and, in the majority of cases, the initial densities agreed to within 0.3% porosity. One specimen was then consolidated and sheared to failure, and the duplicate specimen was taken down immediately after the initial measurements. Moisture content samples were taken at corresponding positions in the two specimens.

It is clearly impossible to compact two specimens to exactly the same density so, to make a comparison, the author evolved a technique which can be termed the method of adjusted porosities. The calculations for a standard triaxial test are illustrated on Fig. 7-2, which gives two typical comparisons for soil compacted to the same initial density but which were prepared by different compaction techniques. In these tests, 2 moisture content determinations were made at each of 5 different levels in each specimen.

The 2 moisture contents taken at the same level are averaged and the average value is converted to porosity, assuming that the soil is fully saturated. The summation mean of the porosities is then calculated and a suitable integer of porosity is chosen for the compaction technique e.g. 38% for the 4 specimens on Fig. 7-2. For the duplicate compaction specimen, the porosity values at each level are adjusted by a constant amount - the difference between the integer value and their summation mean - to give the adjusted initial porosities. For the shear test specimens, the change in the average porosity throughout the complete test is calculated from the burette volume changes, and this amount is added to the integer value of porosity to give the summation mean of the adjusted final porosities. The adjusted porosities are rounded off to the nearest 0.1% and the two sets - initial and final - are subtracted to obtain the porosity changes at different levels in the specimen.

The moisture content values recorded on Fig. 7-2 may be regarded as being typical examples. On average, moisture contents (and porosities)

taken at the same level differed by 0.5% although the median, at a lower value, would probably give a better criterion of variation.

To make the analysis of a particular compaction technique statistically sound, several tests on compacted and sheared specimens would have to be carried out. None of the data presented in this Chapter truly satisfies this condition, but sufficient comparison tests on single specimens have been made to indicate some broad conclusions relating to density distributions within a specimen. The main danger is to avoid placing undue emphasis on any one comparison.

Non-uniformity of compaction densities

The author was astonished to discover that variations occur on initial compaction which can account for a substantial part of the failure density variations. Some of the compaction test results are given on Fig. 7-3. In the upper table, it is seen that, in general, the porosities are least at the top of the specimen, increase to a maximum near the middle and tend to decrease slightly towards the bottom.

It became apparent in the early stages of the research work that the plane strain specimens did not dilate as much as the standard triaxial tests. This indicated that the plane strain specimens were unlikely to undergo large changes of porosity during shear. Therefore, to make the best use of limited time, the main investigation of compaction densities (and, of course, end-of-shear densities) was concentrated on the standard triaxial specimens.

The initial compaction densities for standard triaxial specimens are given on Figs. 7-3, 7-5 & 7-6. On Fig. 7-3 a , it is seen that a dense sand compacted in a single layer, C-20, had a maximum vertical porosity variation of 3.3%. This is mainly due to the low porosity at the top of the specimen, which is at a relative porosity of almost 100%. The average relative porosity of the whole specimen is approximately 75%. For a dense specimen vibrated in 4 equal layers, C-30, the maximum porosity range was 3.0% but the middle porosity of 36.9% is uncommonly high and the actual variation is probably slightly more than 2%. The medium dense specimen C-35, which was also vibrated in 4 layers, has

slightly less variation. In this test, and most of the other specimens vibrated in 4 layers, the time of vibration for each layer was varied in an attempt to make the density more uniform. Altogether, 6 compaction specimens were prepared by vibration in 4 equal layers. The general trend is that specimens with a higher average porosity have lower variations in porosity, but the trend is less marked than one might expect. Hence, it is concluded that vibration in 4 equal layers produces a slightly more uniform density than vibration in 1 layer but does not eliminate porosity variations in the compacted soil.

Specimen C-35A was tamped in 4 layers to a medium density, giving each layer an equal number of tamps. The resultant porosity analysis showed a similar variation to that of a vibrated specimen. Fig. 7-3c shows that the lateral variations in porosity are negligible for standard triaxial tests.

The only compaction test on a plane strain specimen was the dense specimen P-36, in which the moisture contents were taken at carefully measured points in the soil. The average vertical porosity variation is less than 1% but the porosity contour lines on Fig. 7-3b show that the maximum variation was more than 2%. The porosity is a maximum near the centre and is least at the edges. For plane strain specimens generally, it is probable that the compaction variations in density are little different from the end of test porosities. The latter do not show as much longitudinal variation as specimen P-36 but it must be pointed out that the possibility of longitudinal variations, in addition to vertical variations, was not fully appreciated until the systematic sampling of the final two plane strain specimens. Hence, the order in which the moisture contents appear on the author's data sheets may not be a completely reliable guide to their longitudinal position in the specimen.

Checking back through the earlier records, there were 2 instances where whole-depth block moisture content samples had been taken at or near to the ends of failed specimens. In both cases, the block sample had a lower porosity than the summation mean porosity of the 9 smaller

moisture contents, as follows:-

| | P-23 | P-24 |
|---|---|---|
| Porosity of block sample (%) | 35.6 | 37.6 |
| Average final porosity (%) | 36.9 | 38.5 |

On balance, it seems reasonable to conclude that the longitudinal variations in porosity shown on Fig. 7-3b are typical.

The shape of the porosity contour lines suggest that density variations during compaction may be attributed to the phenomenon observed by Mogami and Kubo (1953). They placed layers of dyed sand in a transparent tank and applied a vertical sinusoidal vibration to the surface. The sand moved with an irregular motion to form a spiral shape, the centre of the spiral coinciding with the centre of the tank.

It is a well-known fact that loose sands cannot be densified by static loading. Vibration and tamping produce a fluid condition in the sand so that the grain-to-grain contacts no longer exist, as in quick-sand, and the sand is shaken into a denser packing. However, it would appear from the present investigation that there is danger of a turbulent motion being set up in the vibrated sand which results in density variations within the compacted layer. Vibration in several layers reduces this effect,* but does not eliminate it. No method was devised for achieving uniform placement density. All the later test specimens, beginning with P-18 and C-21, were compacted by vibration in 4 equal layers.

For both plane strain and standard triaxial specimens, less vibration time was required for a 4-layer compaction to achieve a given average density than a 1-layer compaction. Furthermore, less vibration time was required for a plane strain specimen to achieve a given average density than for a standard triaxial specimen. This may be due to the

---

* perhaps because the top of each successive layer is vibrated to a dense state and thus made more difficult to set in motion during the later vibrations.

closer proximity of the walls of the specimen former in the plane strain test which inhibit convection of the sand.

It is obviously desirable to begin a shear test with a uniform density throughout the specimen. The dilemma is that high densities can only be achieved by dynamic methods. Dynamic methods produce a turbulent motion in the sand-water fluid which, through frictional boundary conditions or the form of energy transfer, result in non-uniform densities within the sand. One possible solution is to deposit dry sand through a funnel into the sand former. By controlling the rate and intensity of deposition, the density of the sand specimen can be varied (Kolbuszewski, 1948) and should be uniform. De-aired water can then be passed slowly up through the sand so that the soil structure is not disturbed. This will not saturate the sand but saturation can be completed by applying a back (pore-water) pressure of 50 to 70 lb./sq.in. to dissolve the remaining air voids into solution. The soil can be considered saturated when the pore-water pressure coefficient B (Skempton, 1954) under undrained conditions approaches unity* for ambient stress change. The specimen drains against the back pressure during a drained shear test.**

It would seem likely that density variations in saturated sand may have unwittingly affected the results of previous research work. The main problem in the present context is to try to assess the extent of its effect on the comparison between plane strain and symmetric strain tests. The plane strain specimens are probably the least affected because, although the range of variation is similar to the standard triaxial specimens, there is a smaller percentage of the soil at the extreme

---

* as the coefficient B depends on both the degree of saturation and the compressibility of the soil skeleton, it is more difficult to achieve high B values in soil which is densely packed.

** theoretically, the water containing dissolved air can be replaced by de-aired water, using differential back pressures. The cell and back pressures are then progressively reduced until the back pressure can be replaced by a drainage burette. In practice, the method is not satisfactory for research work.

values of the range. In almost all of the tests, the failure plane passed through the whole depth of the specimen, so the measured strength approximately represents the average (secant) strength over the range of porosities in the specimen. Assuming a maximum porosity variation of 2%, the measured secant strength over-estimates the strength of a uniformly dense specimen by less than 0.1 degrees at all porosities. This statement is also true for the standard triaxial compression tests. However, in this case, the shape of the failure plane is such that a greater part of the failure plane passes through the middle of the specimen than through the ends. The initial average density of soil on the failure plane may be slightly less than the initial average density of the whole specimen. Assuming that this error could be as much as 0.3% in porosity, the strength would be under-estimated by 0.2 to 0.4 degrees, depending on the average density.

For the axial extension tests, the problem is more complex. The extremities of the failure plane are confined within a zone less than one-third of the total height of the specimen. The effects of porosity variations on extension test strengths will be discussed in Chapter 8.

Correlation of densities measured in plane strain and standard triaxial tests

The measurement of porosities is extremely sensitive to errors in the linear dimensions of the test specimen. Therefore, when specimens of different shape are tested and their strength is to be compared, how can one ascertain the accuracy of porosity measurement and, in particular, the comparative accuracy between the two specimen shapes? Unless it is fairly certain that a plane strain specimen measured to a porosity of 35% (say) is at the same actual density as a cylindrical specimen also measured to a porosity of 35%, a discussion concerning the effect of porosity variations during compaction is meaningless.

The moisture content determinations* were originally taken to

---

* for convenience of presentation, all the data relating to these moisture contents are grouped together at the end of this chapter.

provide an independent method of checking the measured densities of the plane strain and cylindrical specimens. It is now convenient to examine more closely the average values of Fig. 7-1, dealing with the comparison of (i) densities calculated from moisture content determinations and (ii) densities calculated from direct measurements. For each type of test, the average values agree to within 0.2% in porosity but the differences are of opposite sign; i.e. in terms of the moisture contents, plane strain and cylindrical test specimens thought to be at the same porosity from direct measurements may differ by almost 0.4% in porosity. However, there are a number of reasons to suggest that the difference is unlikely to be so great.

In the plane strain tests, the number of moisture content determinations (9) was probably not sufficient to obtain a good "average" value for the whole specimen. The moisture content determinations per unit volume is 3.7 per litre in the plane strain tests compared with 6.2 per litre in the standard triaxial tests. Furthermore, longitudinal porosity variations in the plane strain specimens were not anticipated; to show the order of error which might occur in a 9 determinations test, the final two densely compacted plane strain test specimens had 18 moisture contents taken from them (Fig. 7-6). These two tests showed that if moisture contents had been inadvertently taken at the quarter points rather than the "equal volume" position at the one-sixth points, which is possible in the earlier tests, the average porosity would have been over-estimated by 0.11% and 0.34% in the tests. Although the errors were quite small, it would tend to bring the average values closer together on Fig. 7-1. On the other hand, it is unlikely that the moisture contents were taken any nearer to the ends of the specimen, which would have had the effect of increasing the discrepancy between the average porosities in the plane strain tests.

Turning to the standard triaxial test comparisons, it is noticeable that wide variations occur in specimens C-7 to C-16 inclusive, which were tests carried out at cell pressures of 60 lb./sq.in. and are, therefore, only of passing interest to the main theme of the Thesis. Furthermore, these test results were the first attempts to take moisture

content determinations from the undisturbed sand structure and are probably less reliable than the later tests in which the technique had matured. If these first 4 results are ignored, the average values of the porosities calculated from the two independent sources show excellent agreement (37.16% - 37.19%).

In summary, the technique of taking moisture content determinations in the test specimens has shown that a plane strain specimen measured at the same average porosity as a cylindrical specimen may actually be at a slightly looser density. The difference may be as much as 0.4% in porosity but, for reasons given in the preceding discussion, it is unlikely to be so great. In an earlier discussion it was stated that the average initial density on the failure plane of a standard triaxial compression test may be slightly looser than the average initial density of the whole specimen. Hence, in using the porosity values determined from weight-volume measurements, the two possible sources of error tend to cancel each other out. Although these errors cannot be overlooked, the author has accepted the weight-volume measurements for determining the initial densities, believing that they give the greatest comparative accuracy between the two types of compression test.

Consolidation volume changes

A second method of independently relating the densities of the plane strain and cylindrical specimens is through the volume changes which take place during consolidation. Specimens at the same density and subjected to the same stress conditions should have the same volumetric strains. On Fig. 7-7, the volumetric strains are plotted for cell pressures of 40 lb./sq.in. and it is immediately obvious that there is a considerable difference between the two types of specimen. For dense sand, the volumetric strain recorded for plane strain tests is approximately 30% greater than the corresponding standard triaxial compression tests and approximately 50% greater than the extension tests; for loose sands, the differences are not so great. The variations for a given specimen type are so great that this method cannot be a suitable way of correlating specimen densities.

The principal source of error is the free water entrapped inside the rubber membrane but outside the soil structure (Fig. 7-8). In all the plane strain specimens, the right-angled upper edge of the rubber membrane did not fit perfectly to the upper platen along the whole length of the specimen. A considerable volume of water can be trapped in this space which will be pushed out as the increasing cell pressures flatten the membrane against the platen. Fortunately, it is unlikely to affect the volume changes measured in the shear tests. A typical example of the folds, which remain at the middle of the top edge of a specimen after compaction, is illustrated on Plates 6-2, 3 & 4. The volume change for this specimen, P-26, is ringed by a broken line on Fig. 7-7. Water is also trapped between the lower platen and the rubber membrane.

The volume changes which take place in the consolidating sand are so small that the sum total of all the water trapped outside the soil can have a considerable influence on the total volume change. The increasing cell pressure can displace the water voids at the surfaces of the specimen so that the surface appears pitted relative to its initially smooth surface. The plane strain specimens have a greater surface area per unit volume than the standard triaxial specimens and are likely to be more affected. The juncture between the specimen and top cap is another region of entrapped water and unnaturally high voids ratios.

The standard triaxial extension test specimens show distinctly lower volumetric strains during consolidation than the corresponding compression test specimens. This can be attributed to (i) omission of the thick upper porous stone and (ii) the extreme care taken to ensure a perfect joint between the top cap and specimen, to avoid necking at this point. Therefore, of the three types of test, the extension test specimens have the least, and most reliable, volume change readings during consolidation. If these results are accepted as correct, a typical plane strain specimen contains approximately 6 ml. of entrapped water.

Very complete records were kept of the volume changes during consolidation, with readings at 10 cell pressure increments up to

40 lb./sq.in. For extension specimens, an additional 6 readings were taken between the cell pressures of 40 and 130 lb./sq.in. Most of the entrapped "free" water will be removed at the lower cell pressures. This is confirmed on the lower part of the graph, Fig. 7-7, on which is plotted some of the volumetric strain increments between the average principal stresses of 15 and 45 lb./sq.in. The increments were abstracted from plots of the individual test results, not shown. The percentage difference between the two types of compression test specimens (plane strain - standard triaxial) is reduced to less than 10% over this stress range.

As there is little data available on the compressibility of sands, the author hopes to investigate these points in greater detail at a later date. It may be possible to relate compressibility with the relative porosity or some other parameter. Using the extension test results as a basis, the other curves representing specimens with greater amounts of entrapped "free" water can be brought into the family of curves to give results which will be sufficiently accurate for practical purposes.*

Finally, for $K_o$ consolidation, the cross-sectional area of the specimen should remain constant and it follows that the burette volume changes should equal the volume changes calculated from the measurements of vertical deformation. The comparison is given on Table 7-1 (a), (b) & (c). It shows good agreement, on average, for each type of test but the agreement is fortuitous in view of the preceding remarks on the burette volume changes. The dial gauge readings are in error when the cell pressure changes because the rigid arm, which is in contact with the dial gauge spindle, is connected to the cell. The cell top distorts under pressure (Fraser, 1957) so that the measurements over-estimate the true vertical deformations. The amount of error depends upon the position of the spindle on the arm and, presumably, the tightening of the cell tie bars.

---

* porosity variations within the compacted specimen will also affect the compressibility curves.

For the extension tests, two clamps were placed symmetrically around the cell, one on each side of the upright supporting the horizontal dial gauge arm, to hold the cell in contact with the pedestal of the machine. The clamps will have affected the pattern of bending in the cell top plate. In these tests, the average volumetric strain calculated from the dial gauge readings is approximately 15% less than the burette readings.

Table 7-1 Volume changes during consolidation

(a) Plane Strain

| Test No. | Volume changes for cell pressure change of 0 - 40 lb./sq.in. | | Volume changes for cell pressure change of 7 - 40 lb./sq.in. | |
|---|---|---|---|---|
| | Calculated - Dial Gauge cc. | Measured - Burette cc. | Calculated - Dial Gauge cc. | Measured - Burette cc. |
| P-11 | 28.45 | 25.20 | 18.95 | 13.70 |
| P-12 | 19.70 | 20.85 | 14.95 | 11.25 |
| P-13 | 21.35 | 27.45 | 14.25 | 16.05 |
| P-14 | 30.60 | 32.00 | 19.85 | 20.70 |
| P-15 | 19.85 | 19.65 | 13.05 | 10.50 |
| P-16 | 18.80 | 17.35 | 13.85 | 9.60 |
| P-17 | 18.90 | 17.10 | 12.65 | 8.20 |
| P-18 | 19.05 | 22.15 | 12.80 | 13.20 |
| P-19 | 18.85 | 19.80 | 12.05 | 12.20 |
| P-20 | 35.90 | 40.75 | 22.30 | 21.60 |
| P-21 | 31.70 | 33.30 | 20.65 | 19.75 |
| P-22 | 36.55 | 39.45 | 25.30 | 21.90 |
| P-23 | 18.85 | 17.85 | 13.75 | 9.90 |
| P-24 | 21.70 | 24.10 | 14.10 | 12.65 |
| P-25 | 27.85 | 26.95 | 17.55 | 16.15 |
| P-26 | 19.65 | 21.25 | 13.05 | 12.05 |
| P-28 | 30.20 | 34.40 | 20.40 | 20.65 |
| P-29 | 24.30 | 33.20 | 16.55 | 15.95 |
| Average | 24.57 | 26.27 | 16.45 | 14.78 |
| Volume Strain % | 1.02 | 1.09 | 0.68 | 0.61 |

Table 7-1 (contd.)

(b) Standard Triaxial Compression

| Test No. | Volume changes for cell pressure change of 0 - 40 lb./sq.in. | | Volume changes for cell pressure change of 7 - 40 lb./sq.in | |
|---|---|---|---|---|
| | Calculated - Dial Gauge cc. | Measured - Burette cc. | Calculated - Dial Gauge cc. | Measured - Burette cc. |
| C-7 | 14.65 | 11.90 | 8.80 | 6.95 |
| C-8 | 14.20 | 15.05 | 8.30 | 9.35 |
| C-9 | 9.70 | 9.25 | 5.85 | 5.90 |
| C-10 | 14.00 | 18.35 | 7.40 | 10.20 |
| C-12 | 28.20 | 23.30 | 15.85 | 14.90 |
| C-15 | 17.60 | 10.25 | 5.75 | 6.65 |
| C-16 | 12.80 | 8.95 | 5.75 | 6.75 |
| C-21 | 26.10 | 25.30 | 14.40 | 14.60 |
| C-22 | 19.55 | 22.35 | 14.05 | 14.35 |
| C-23 | 23.35 | 24.05 | 13.35 | 14.15 |
| C-25 | 12.05 | 13.95 | 7.30 | 8.45 |
| C-26 | 13.80 | 16.45 | 8.20 | 9.55 |
| C-27 | 9.10 | 12.15 | 4.90 | 7.00 |
| C-28 | 10.80 | 11.15 | 5.05 | 6.90 |
| C-29 | 13.05 | 11.25 | 8.20 | 7.40 |
| C-31 | 11.80 | 11.05 | 6.10 | 6.95 |
| C-32 | 9.95 | 10.30 | 5.40 | 6.50 |
| C-33 | 8.30 | 11.40 | 4.90 | 7.05 |
| C-34 | 17.55 | 10.85 | 6.30 | 6.95 |
| C-36 | 12.45 | 12.70 | 6.65 | 7.95 |
| C-40 | 12.55 | 11.00 | 6.35 | 7.00 |
| Average | 14.84 | 14.33 | 8.04 | 8.83 |
| Average (excluding C-15 & C-34) | 14.55 | 14.73 | | |
| Volume Strain % | 0.90 | 0.91 | 0.50 | 0.55 |

Table 7-1 (contd.)

(c) Standard Triaxial Extension

| Test No. | Volume changes for cell pressure change of 0 - 40 lb./sq.in. | | Volume changes for cell pressure change of 7 - 40 lb./sq.in | |
|---|---|---|---|---|
| | Calculated - Dial Gauge cc. | Measured - Burette cc. | Calculated - Dial Gauge cc. | Measured - Burette cc. |
| C-43 | 13.55 | 17.95 | 8.55 | 11.55 |
| C-44 | 8.05 | 8.00 | 5.35 | 5.20 |
| C-45 | 10.40 | 10.90 | 7.00 | 7.15 |
| C-46 | 7.55 | 9.50 | 5.25 | 6.15 |
| C-47 | 7.50 | 8.05 | 5.05 | 5.20 |
| C-48 | 7.70 | 8.40 | 5.25 | 5.45 |
| Average | 9.13 | 10.47 | 6.08 | 6.78 |
| Volume Strain % | 0.62 | 0.71 | 0.41 | 0.46 |

| PLANE STRAIN | | |
|---|---|---|
| Test Number | $n_d$ calculated from :- % | |
| | 9 No. water contents | weight - volume |
| P - 8 | 39·75 | 39·92 |
| P - 12 | 36·57 | 36·48 |
| P - 13 | 39·60 | 39·30 |
| P - 15 | 37·25 | 37·09 |
| P - 16 | 35·67 | 36·09 |
| P - 17 | 34·98 | 34·86 |
| P - 18 | 39·67 | 39·34 |
| P - 19 | 38·64 | 38·17 |
| P - 23 | 36·90 | 36·72 |
| P - 24 | 38·55 | 38·53 |
| P - 25 | 39·54 | 39·50 |
| P - 26 | 38·41 | 37·87 |
| P - 27 | 37·36 | 36·49 |
| P - 30 | 38·10 | 37·92 |
| P - 31 | 35·75 | 34·62 |
| P - 34 | 37·95 | 37·83 |
| P - 35 | 35·23 * | 35·56 |
| P - 36 | 34·65 * | 34·53 |
| Average | 37·48 | 37·27 |

* 18 No. water contents

| STANDARD TRIAXIAL | | |
|---|---|---|
| Test Number | $n_d$ calculated from :- % | |
| | 10 No. water contents | weight - volume |
| C - 7 | 36·84 | 37·34 |
| C - 9 | 36·26 | 36·90 |
| C - 13 | 38·07 | 39·26 |
| C - 16 | 36·43 | 37·15 |
| C - 29 | 35·82 | 35·41 |
| C - 31 | 35·39 | 35·62 |
| C - 33 | 38·89 | 38·85 |
| C - 36 | 38·54 | 38·60 |
| C - 38 | 38·21 | 38·10 |
| C - 40 | 38·58 | 38·72 |
| C - 44 | 35·46 | 35·93 |
| C - 46 | 37·18 | 37·56 |
| C - 47 | 35·39 | 35·62 |
| C - 48 | 36·81 | 37·03 |
| C - 50 | 38·64 | 38·46 |
| C - 30 | 35·38 | 34·69 |
| C - 35 | 37·91 | 37·87 |
| C - 35 A | 37·66 | 37·65 |
| C - 48 A | 36·00 | 36·37 |
| C - 50 A | 38·98 | 38·91 |
| Average | 37·12 | 37·30 |

## POROSITIES MEASURED AT THE END OF THE TESTS

$n_d$ is the average porosity (in %) after dismantling the apparatus at the end of the test.

FIG. 7 - 1

Compaction by VIBRATION :- 4 layers 8 sec., 10 sec., 10 sec., 6 sec.

| Position in Specn | INITIAL (C-35) Moisture Content % | Average Moisture % | Average Porosity % | Adjusted Porosity % | FINAL (C-33) Moisture Content % | Average Moisture % | Average Porosity % | Adjusted Porosity % | Change in Porosity - Initial to Final % |
|---|---|---|---|---|---|---|---|---|---|
| Top | 21·44<br>22·41 | 21·92 | 37·04 | 37·14 | 21·79<br>21·71 | 21·75 | 36·86 | 36·53 | - 0·6 |
| Quarter | 23·14<br>22·68 | 22·91 | 38·08 | 38·18 | 23·49<br>21·73 | 22·61 | 37·77 | 37·44 | - 0·7 |
| Middle | 22·83<br>22·24 | 22·54 | 37·69 | 37·79 | 25·62<br>25·58 | 25·60 | 40·73 | 40·40 | + 2·6 |
| Quarter | 22·60<br>22·87 | 22·73 | 37·89 | 37·99 | 25·25<br>24·75 | 25·00 | 40·16 | 39·83 | + 1·8 |
| Bottom | 23·54<br>23·73 | 23·64 | 38·82 | 38·92 | 23·73<br>23·51 | 23·62 | 38·80 | 38·47 | - 0·5 |
| | Σ mean = 37·90 38·00<br>Measured $n_o$ = 38·03 | | | | Σ mean = 38·86 38·53<br>Measured $n_o$ = 38·19<br>Measured $n_d$ = 38·72 } ↑ 0·53 | | | | |

Compaction by TAMPING :- 4 layers, each given 9 tamps.

| Position in Specimen | INITIAL (C-35 A) Moisture Content % | Average Moisture % | Average Porosity % | Adjusted Porosity % | FINAL (C-36) Moisture Content % | Average Moisture % | Average Porosity % | Adjusted Porosity % | Change in Porosity - Initial to Final % |
|---|---|---|---|---|---|---|---|---|---|
| Top | 21·07<br>21·16 | 21·11 | 36·17 | 36·51 | 22·39<br>21·83 | 22·11 | 37·24 | 37·32 | + 0·8 |
| Quarter | 22·82<br>22·13 | 22·47 | 37·62 | 37·96 | 23·77<br>23·66 | 23·72 | 38·90 | 38·98 | + 1·0 |
| Middle | 22·96<br>22·94 | 22·95 | 38·12 | 38·46 | 23·85<br>24·43 | 24·14 | 39·32 | 39·40 | + 0·9 |
| Quarter | 22·93<br>22·42 | 22·67 | 37·83 | 38·17 | 22·99<br>23·37 | 23·18 | 38·35 | 38·43 | + 0·3 |
| Bottom | 23·47<br>23·21 | 23·34 | 38·52 | 38·86 | 24·32<br>23·00 | 23·66 | 38·84 | 38·92 | + 0·1 |
| | Σ mean = 37·66 38·00<br>Measured $n_o$ = 37·81 | | | | Σ mean = 38·54 38·62<br>Measured $n_o$ = 37·95<br>Measured $n_d$ = 38·57 } ↑ 0·62 | | | | |

## POROSITY CHANGES DURING SHEAR - TYPICAL EXAMPLE OF CALCULATIONS

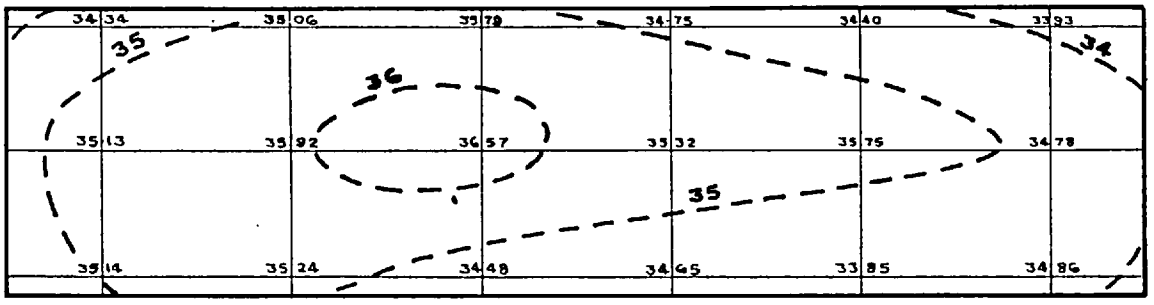
$n_o$ - initial porosity

$n_d$ - final porosity, based on the initial porosity and volume changes during shear.

FIG. 7 - 2

| C-20 Vibration in 1 layer STANDARD TRIAXIAL | C-30 Vibration in 4 layers STANDARD TRIAXIAL | P-36 Vibration in 4 layers PLANE STRAIN | Position in Specimen | C-35 Vibration in 4 layers STANDARD TRIAXIAL | C-35A Tamped in 4 layers STANDARD TRIAXIAL |
|---|---|---|---|---|---|
| 32·8 | 33·9 | 34·7 | Top | 37·1 | 36·5 |
| 35·2 | 35·4 | | Quarter | 38·2 | 38·0 |
| 35·7 | 36·9 | 35·6 | Middle | 37·8 | 38·5 |
| 36·1 | 34·5 | | Quarter | 38·0 | 38·2 |
| 35·4 | 34·4 | 34·7 | Bottom | 38·9 | 38·9 |
| Σ mean = 35·0 | 35·0 | 35·0 | | 38·0 | 38·0 |
| Max. diff. = 3·3 | 3·0 | 0·9 | | 1·8 | 2·4 |

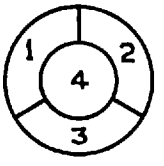
(a) Vertical variations (Plane Strain, Standard Triaxial)

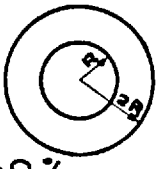



(b) Longitudinal variations (Plane Strain):- P-36, $n_o$ = 35·0 %

| Position in Specimen | Area 1 | Area 2 | Area 3 | Average of Areas 1,2,3 | Area 4 |
|---|---|---|---|---|---|
| Top | 35·1 | 34·2 | 35·1 | 34·8 | 35·0 |
| Quarter | 35·8 | 35·9 | 36·1 | 35·9 | 36·3 |
| Middle | 37·0 | 36·5 | 36·5 | 36·7 | 36·3 |
| Quarter | 36·7 | 36·8 | 38·2 | 37·2 | 36·1 |
| Bottom | 35·8 | 35·4 | 34·7 | 35·3 | 36·3 |
| Σ mean = | | | | 36·0 | 36·0 |

Plan view




(c) Lateral variations (Standard Triaxial):- C-48A, $n_o$ = 36·0 %

## POROSITY VARIATIONS ON INITIAL COMPACTION – PLANE STRAIN & STANDARD TRIAXIAL

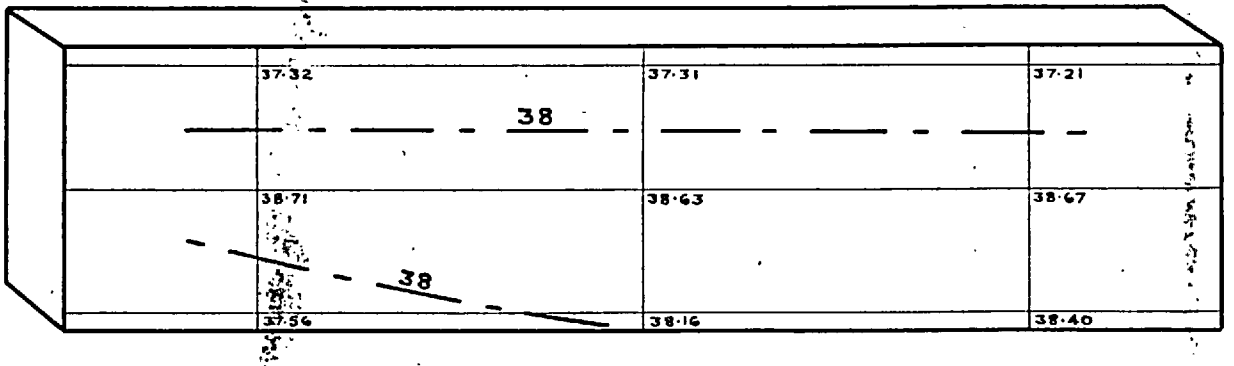
All the above porosities are "adjusted porosities" as outlined in the typical calculation on Fig 7-2. The figures were then rounded off to the nearest 0·1 %, and are given on the tables in this form.

FIG. 7-3

| COMPACTION:- 1 layer 20 minutes (heavy) | | | | | | |
|---|---|---|---|---|---|---|
| Position in Specimen | Initial C-20 $n_o$ % | Final C-7 $n_d$ % | Final C-9 $n_d$ % | Final C-16 $n_d$ % | Final (Average) $\bar{n}_d$ % | Porosity Changes $(\bar{n}_d - n_o)$% |
| Top | 32·8 | 32·3 | 33·2 | 32·3 | 32·6 | -0·2 |
| Quarter | 35·2 | 35·3 | 35·1 | 35·3 | 35·2 | 0 |
| Middle | 35·7 | 37·6 | 37·8 | 37·9 | 37·8 | +2·1 ← max. bulge |
| Quarter | 36·1 | 37·4 | 37·3 | 37·3 | 37·3 | +1·2 |
| Bottom | 35·4 | 35·7 | 36·1 | 36·4 | 36·1 | +0·7 |
| Average | 35·0 | 35·7 | 35·9 | 35·8 | 35·8 | +0·8 |

(a) Standard Triaxial Compression

All the above shear tests were stopped at the maximum deviator stress.



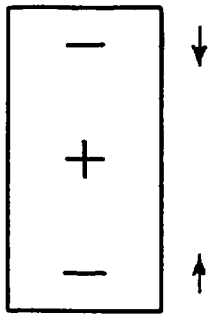

(b) Plane Strain Compression

The drawing shows the average values of the porosity at different points within the specimen for 10 drained tests, some of which were stopped at the max. deviator stress and some at the ultimate stress.

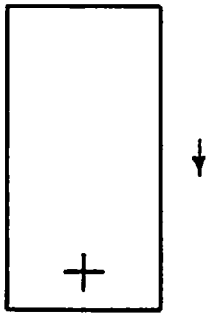
## POROSITY CHANGES DURING SHEAR – DRAINED COMPRESSION TESTS

FIG. 7 – 4

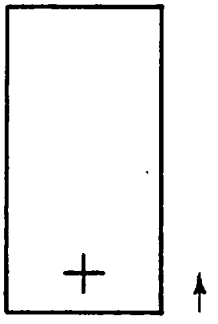
Movement of Water
(Diagrammatic)



(a) Shear test



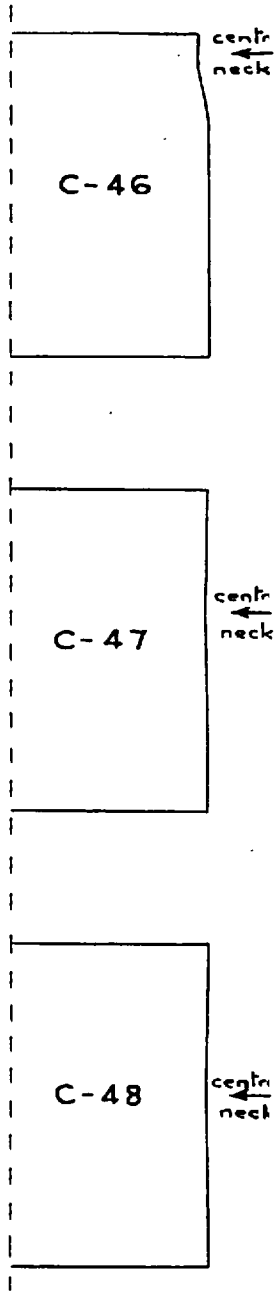
(b) Release deviator stress



(c) Release cell pressure

| Initial Conditions – Porosity $n_o$ % | Final Conditions – Porosity $n_f$ % | Change in Porosity $(n_f - n_o)$ % |
|---|---|---|
| 37·8 | 37·1 | −0·7 |
| 37·9 | 35·6 | −2·3 |
| 38·8 | 37·3 | −1·5 |
| 37·6 | 38·7 | +1·1 |
| 37·9 | 38·4 | +0·5 |
| Σ = 38·0 | Σ = 37·4 | Σ = −0·6 |
| 34·5 | 33·3 | −1·2 |
| 34·2 | 34·3 | +0·1 |
| 36·0 | 35·4 | −0·6 |
| 35·4 | 35·9 | +0·5 |
| 35·0 | 35·9 | +0·9 |
| Σ = 35·0 | Σ = 35·0 | Σ = 0 |
| 35·8 | 34·3 | −1·5 |
| 37·0 | 35·9 | −1·1 |
| 37·6 | 37·7 | +0·1 |
| 38·0 | 38·0 | 0 |
| 36·6 | 37·2 | +0·6 |
| Σ = 37·0 | Σ = 36·6 | Σ = −0·4 |

Diameters of Failed Specimens
(Scale :- 1 in. = 10 cm.)




## POROSITY CHANGES DURING SHEAR – EXTENSION TESTS

Levels :- A top ; B quarter ; C mid-height ;
D quarter ; E bottom.

Porosity values are calculated from the average of two moisture contents.

FIG. 7 – 5

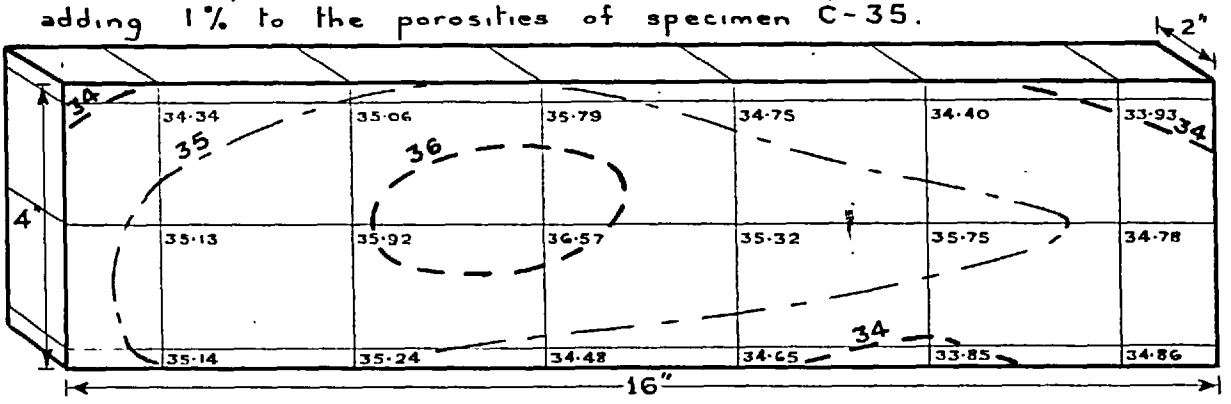
| Position in Specimen | COMPRESSION TESTS | | | EXTENSION T. | |
|---|---|---|---|---|---|
| | Adjusted Porosities | | Adj. Por. | Adjusted Porosities | |
| | Initial C-35 | Final C-38 | Final C-39 | Initial C-50A | Final C-50 |
| Top | 37·1 | 35·2 | 36·2 | 38·2 | 37·5 |
| Quarter | 38·2 | 39·4 | 40·9 | 38·6 | 39·0 |
| Middle | 37·8 | 38·8 | 39·7 | 39·5 | 39·9 |
| Quarter | 38·0 | 39·1 | 39·5 | 39·7 | 39·0 |
| Bottom | 38·9 | 37·3 | 38·7 | 39·1 | 39·7 |
| Average | 38·0 | 38·0 | 39·0 | 39·0 | 39·0 |

max. bulge

max. necking

(a) Standard Triaxial tests

There is no "initial" specimen corresponding to the compaction used for specimen C-39, but it can be approximated to by adding 1% to the porosities of specimen C-35.




(b) Plane Strain tests :- Initial P-36 (upper drawing) and Final P-35 (lower drawing) } n = 35·0%

## POROSITY CHANGES DURING SHEAR - UNDRAINED TESTS

To aid the analysis, the average adjusted porosities - "initial" & "final" - on the above diagrams, are equal.

Changes in porosity during shear

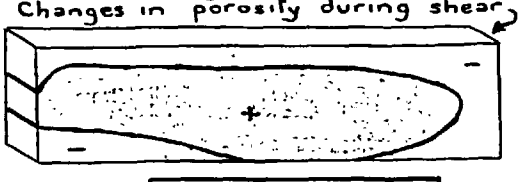
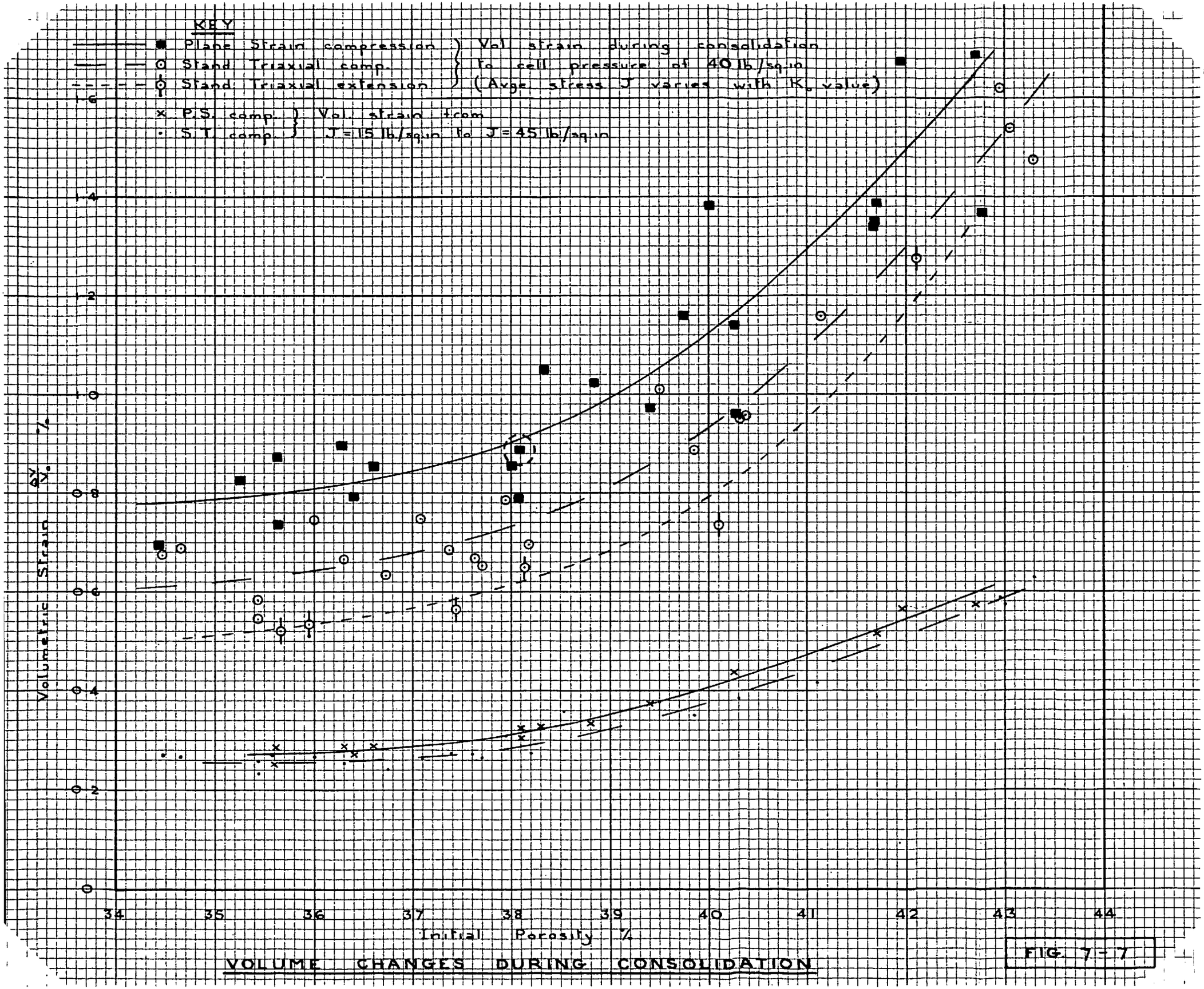
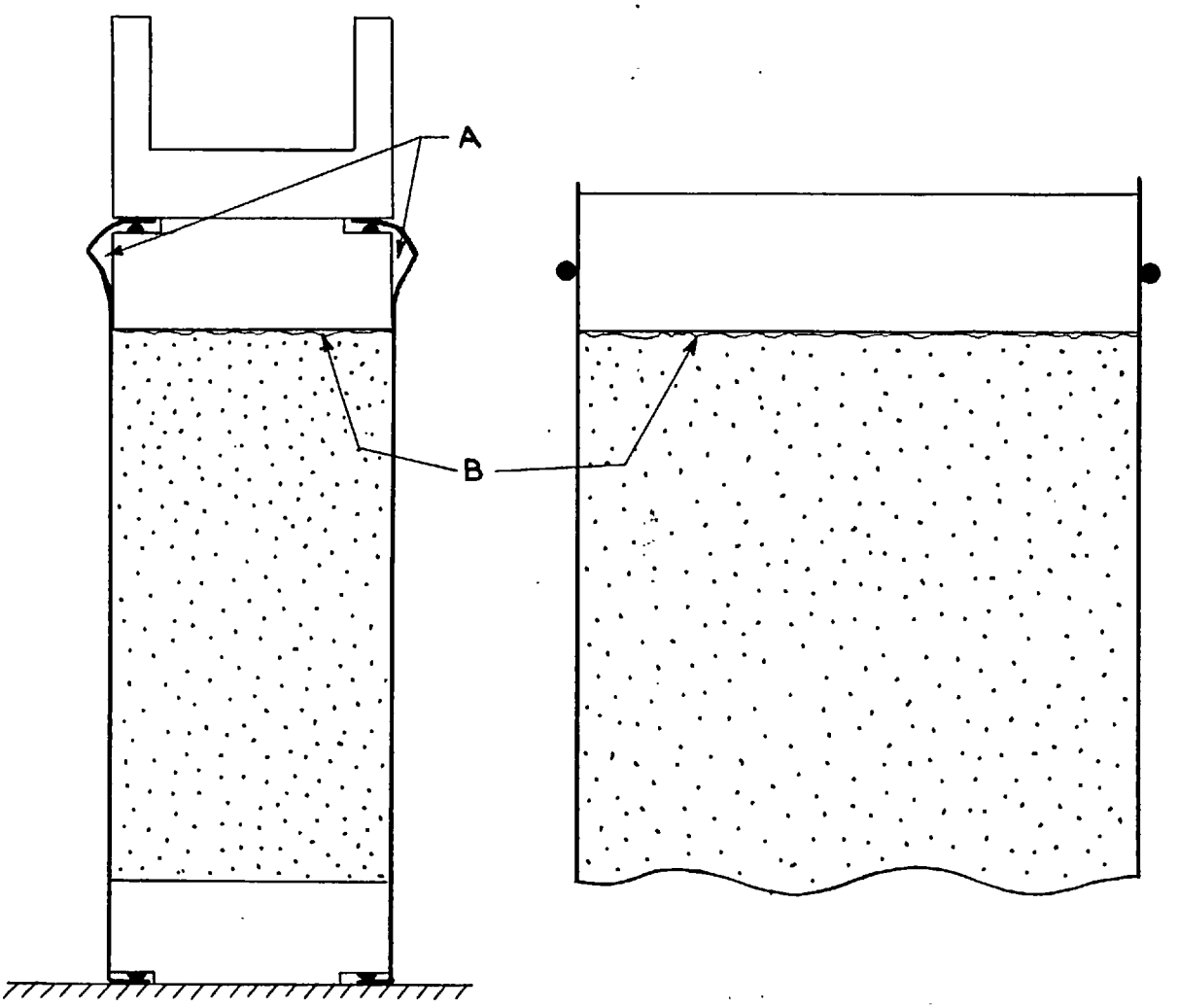



FIG. 7-6




VOLUME CHANGES DURING CONSOLIDATION

FIG. 7-7




(a) Plane Strain (b) Standard Triaxial

## SOURCES OF ERROR IN VOLUME CHANGE MEASUREMENTS

A - Water trapped between the membrane fold and upper platen. Affected by cell pressure only.

B - Water trapped by irregular surface. For equally rough surfaces, plane strain specimen will trap twice as much water (per unit volume) as a standard triaxial specimen.

FIG. 7 - 8

## Chapter 8 DRAINED TEST RESULTS AND DISCUSSION

The main object of the testing programme was to compare the failure characteristics of the plane strain and standard triaxial compression tests and, in particular, the measured strength-density relationships. In all cases, the strength is represented by the apparent angle of shearing resistance, assuming that the Mohr envelope to the stress circle passes through the origin. The initial porosity refers to the porosity, calculated from weight and linear dimensions, of the soil immediately after compaction with the specimen under a small negative head. Before making the comparison, the results of each test series will be examined separately.

### I. Plane Strain Tests

#### Typical curves from Series A

The result of a typical plane strain test on a medium dense sand is shown on Fig. A10 - 12*. In this test, the cell pressure was held constant and the axial stress was increased to failure. The strains, linear and volumetric, were calculated from the start of the shear test proper, at the end of the consolidation stage.

The stress-strain curves have the same characteristic shape as a standard triaxial specimen. Both the major and intermediate principal stresses rise to a peak value at approximately the same strain and then decrease until they reach a fairly constant residual stress.

The relationship between the intermediate and the other two principal stresses are shown on the graph. On this curve, the value of $\sigma_2/(\sigma_1+\sigma_3)$ rises slightly to failure and remains fairly constant thereafter. In many tests this ratio remains almost constant throughout the test. It is clear, therefore, that the

---

* the test results, Appendix 10, are to be found at the back of the thesis.

intermediate principal stress in plane strain is not equal to one-half the sum of the other two principal stresses, a relation which is sometimes assumed in theoretical considerations.

The shape of the volume change curve is also similar to that of the standard triaxial test. The specimen consolidates initially, reaches a minimum volume and then dilates until the ultimate condition is reached.

In a dense sand, the reduction in axial load occurs in a spectacular manner after failure (Fig. A10-17). The deflection of the proving rings stores up elastic energy which is sufficient to apply an appreciable axial strain to the specimen without the aid of the triaxial machine strain rate. Consequently, the axial strain in specimen P-17 (Fig. A10-11) increased from 1.4% to 2.9% within a few seconds and no readings could be taken during this period*. In some instances, the stress release is so severe that a kink of low strength appears in the stress-strain curve due to a dynamic condition. The stress quickly increases and levels off at the ultimate value.

Typical curves for a loose specimen are shown on Fig. A10-14. The peak stresses become much less pronounced with decreasing density. There is very little dilatancy volume change in this specimen.

---

* however, the elastic expansion of the proving rings does not completely account for this large change in strain. On specimen P-17 (Fig. A10-11), for example, the average strain dial gauge reading during the run-down of stress was 0.070 in. The elastic expansion of the proving rings was 290 division = 0.029 in. and allowing for one minute to have elapsed between the strain values of 1.4% and 2.9%, the pedestal of the machine would have risen only 0.001 in. The balance of 0.040 in., equivalent to an axial strain in the specimen of 0.9%, remains to be accounted for and is probably mainly due to the elastic deflection of the G-frame triaxial apparatus.

End-of-test observations

When the cell body casting was removed at the end of a test, it was found that there was no visible failure zone in tests which were stopped at strains just beyond failure. However, after the run-down of stress had occurred, at or near the ultimate condition, the two edges of the failure zone could be seen along the whole length of the specimen. On removal of the end plates, the membrane was seen to be discoloured along the zone of failure and the width of the failure zone was clearly marked (Fig. 8-17). The width of the zone varied from 1½ to 5 mm. but was, in general, wider and less distinctly defined in the looser than in the denser specimens. The failure surface was not always flat, but was usually slightly curved, probably as a result of progressive failure or porosity variations with depth. An average slope of the failure surfaces gave good agreement with the theoretical slope of $\left(45 + \frac{1}{2}\phi\right)$ degrees to the horizontal. The shape of each observed failure zone is recorded on the graphs, together with the width of the failure zone. The inner surface of the membrane in contact with the failure zone during shear was scoured and rough to the touch afterwards. This indicates that considerable agitation of the sand grains had occurred in this zone, but not elsewhere in the specimen. (This, of course, produces the discolouration of the membrane.)

It was noted that one edge of a failure zone always passed through an upper or lower joint between specimen and platen, probably due to the stress dis-continuity set up at these points by horizontal shearing forces. The other sheared edge did, in general, outcrop on the opposite side of the specimen, but in some of the denser specimens, it intersected the opposite platen, despite an average height: width ratio of 2.2. Hence, interference from the platens may have a slight influence on the shear strength of the dense specimens.

Factors affecting strength

The failure characteristics of Series A are shown on Fig.8-1. The results are as one would expect; the shear strength increased as the specimen density increased, axial strain at failure increased as the specimen density decreased and the volume changes at failure show that the dense samples have expanded when failure has been reached and that the looser samples have decreased in volume. On the same graph are shown the results of four early tests which are of doubtful accuracy - numbers6, 7, 8 and 10. These four tests are not consistent with the test results obtained later and will be omitted from later discussions. They are merely included for completeness. It is difficult to locate the exact sources of error, but it is thought that one or both of the following reasons are responsible. Firstly, the original springs supporting the end clamp were too soft and in some early tests the end clamps were in contact with the lower platens. This may have affected the measured stresses and this appears to have happened in test 10 (Fig. A10-5) where the ultimate value of the intermediate principal stress is very much higher than in any other test. After test 10 had been completed, the old springs were removed and replaced by springs which supported the end clamp at the correct level mid-way between the upper and lower platens. The second possibility affecting the early test results was the measurement of the porosity. The technique of measuring the height of the specimen was improved in later tests. In general, the failure characteristics of axial strain and volume change support the view that specimens 6, 7 and 8 were denser than their measured porosities in relation to the later plane strain tests (Fig. 8-1). The maximum slopes of the volume change curve for these specimens are offset to the right of the summary curve shown on Fig. 8-12(a).

Specimen 7 was affected by an experimental error such that the vertical consolidation load was not uniformly distributed over the length of the specimen. The stress-strain curve of this test has not been plotted.

The results of Series C, in which the end clamp was omitted, are also shown on Fig. 8-1. There is no noticeable difference between the strengths measured with and without the end clamp. As it was apparent that the shear strengths in plane strain were somewhat higher than the corresponding shear strengths in the standard triaxial test, it would be expected that the results of tests without an end clamp would give a lower strength-density curve if the test specimen was insufficiently long to induce a plane strain type of failure. Also, the measured strength in Series A would again be higher than the strength in Series C if there had been an appreciable shear force produced by the end clamp at the ends of the specimen. As the two series of tests give identical strength-density curves, it is concluded that neither of these possibilities has exercised much influence.

To sum up, a plane strain strength will be obtained if the specimen is made sufficiently long relative to its width, and the shear force between the end plates and the specimen has a negligible effect on the measured strength; this conclusion agrees with the calculations based on the measured coefficient of friction (see Chapter 4).

The other failure characteristics are slightly affected by the omission of the end clamp. In Series C, three of the five tests show a slight increase in axial strain at failure and three results have a slightly greater increase in volume at failure.

In Series C, two of the four specimens in which the failure plane was visible, the plane could only be seen over the central 13 to 14 in. and not at the ends. Plate 8-3 shows a specimen with a failure plane along the whole length. This photograph clearly illustrates the formation of two soil wedges at the ultimate condition; in this case, there is a slight outward displacement of the lower part of the upper wedge. The discolouration of the membrane is just visible, but this effect was more apparent in tests using the end clamp.

The increased length of three specimens in Series C were as follows :-

| Specimen No. | | P-11 | P-13 | P-15 |
|---|---|---|---|---|
| Initial porosity | (%) | 38.3 | 39.7 | 36.6 |
| Test stopped at | | fail-to-ult. | failure | ultimate |
| Length at top | (in) | - | 16.13 | 16.11 |
| mid-height | (in) | 16.21 | 16.19 | 16.25 |
| bottom | (in) | - | 16.13 | 16.11 |
| average | (in) | - | 16.15 | 16.16 |
| Average longitudinal strain | (%) | - | 0.3 | 0.4 |
| Average lateral strain | (%) | 2.5 | 1.6 | 4.8 |

The most significant result is P-13, which showed that the average longitudinal strain at failure was approximately 20% of the lateral strain. It suggests that the strength measured under strictly plane strain conditions is applicable to practical stability problems which approximate to plane strain.

---

The results of Series B, in which the axial stress was held constant and the cell pressure decreased to failure, are compared with Series A on Fig. 8-2. The test was arranged so that the cell pressure at failure in Series B was approximately the same as that in Series A, so that any effect of cell pressure on

strength would not invalidate the results. The strength curves do not show any appreciable differences between the two testing techniques and it is concluded that the strength of the sand is not affected by the stress history in comparing these cases.

The other failure characteristics are noticeably affected by the stress history. The volume changes are more positive in Series B, in which the effective stresses during shear are being decreased. The axial strains of Series B are appreciably lower than the corresponding strains of Series A, particularly in the denser specimens.

The specimens of Series B have been consolidated under a greater average principal stress before shear than those of Series A. If an allowance is made to each result of Series B for the additional axial strain and volume change which takes place after the consolidation stresses in Series A have been exceeded, the results of the two test series correspond more closely. The values of volume change and axial strain corrected in this way are shown by crosses on Fig. 8-2, and it is seen that the corrected values of Series B agree reasonably well with the corresponding curves of Series A.

Two of the individual test results of Series B are shown on Fig. A10-16. The intermediate principal stress remained approximately constant in these tests as the cell pressure was reduced to failure. When the test results are plotted in the form of stress ratios, it is apparent that the resulting curves are similar to those in Series A where the cell pressure was held constant and the axial stress increased to failure. We note again that the ratio $\frac{\sigma_3}{(\sigma_1 + \sigma_3)}$ is approximately constant throughout the test and is always considerably less than 0.5. The two deviator stress ratios reach constant ultimate values.

The ratio $\sigma_2/\sigma_3$ at failure is slightly higher in Series B than in Series A, probably due to a time lag in the response of the null mercury thread of the intermediate principal stress. This would account for the slightly higher value of $\sigma_2$ measured in Series B, as $\sigma_2$ was approximately constant in this test, but was continuously increasing in Series A. The author does not regard the difference as being of any significance.

Summarising the above discussions, it has been argued that the measured deviator stresses in the two test series do not show any appreciable differences. The volume changes and axial strains are also similar if an allowance is made to the results of Series B for the additional changes which took place in its consolidation history. Hence, the three principal stresses and the three total linear strains are uniquely defined at failure for a given initial density and are unaffected by the different stress histories.

This result is comparable with the research work of Fraser (1957) on the effects of stress history and volume changes in Brasted sand. Fraser found that, for sand specimens at the same initial density, the volume changes during ambient stress consolidation and $K_o$ consolidation were approximately equal at equal values of average principal stress (Fig. 8-22). In a further series of tests, he consolidated several pairs of soil specimens under $K_o$ and ambient stresses to the same value of average principal stress; then, holding the average principal stress constant, he increased the principal stress ratio until dilatancy began (Fig. 8-22). The test results showed that soils at the same initial density undergo approximately equal volume changes during shear by the time dilatancy occurs, irrespective of the type of consolidation or stress history during shear.

Fraser was mainly interested in the compressibility characteristics of the sand in the early stages of a shear test up to the onset of dilation. However, Fig. 8-12 shows that the rate of dilation at failure is the same in Series A and B at corresponding placement densities, so it is reasonable to infer that, had Fraser continued his investigation of volume changes up to failure, the uniqueness of the stress and strain relationships at failure would have been established for his tests, which were also subjected to different stress histories.

Ultimate strength

The ultimate condition is attained at an axial strain of only 3 to 6%, depending on density, and can be measured with good accuracy. It does show a slight decrease as straining is continued, but from observations, it seems likely that this apparent drop in strength may be attributed to the calculation of cross-sectional area of the failure plane as the two wedges of soil separate, i.e. once the ultimate condition has been reached, the actual area probably remains approximately constant (e.g. simple shear) but calculations of deviator stress based on changes in the axial strain assume that the area is increasing; hence, the apparent decrease in the calculated deviator stress.

Fig. 8-3 shows the ultimate strength values of all plane strain specimens and it is clear that they are independent of the placement density of the test specimens. The average value of the ultimate strength is slightly lower than the lowest peak strength measured in either the plane strain or standard triaxial compression tests. The significance of this remark will be made apparent later in the thesis.

Intermediate principal stress

The intermediate principal stress results are shown on Fig. 8-4(a). The value of the principal stress ratio $\frac{\sigma_2}{\sigma_3}$ at failure decreases as the density of the specimen decreases. The ultimate value of this ratio is constant and independent of the specimen density. The two curves approach each other at the looser densities; therefore, the ratio $\frac{\sigma_2}{\sigma_3}$ has much in common with the ratio $\frac{\sigma_1}{\sigma_3}$ .

It was noted earlier that, when the major principal stress was held constant and the cell pressure decreased to failure, the intermediate principal stress remained approximately constant during shear. As the consolidated condition was $\sigma_2 = \sigma_3 = K_o \sigma_1$, the relationship $\frac{\sigma_3}{\sigma_1} = K_o$ is apparent. This relationship was suggested by Wood (1958). The curve relating these two values, Fig. 8-4(b), shows that the $K_o$ value would slightly over-estimate the measured value of $\sigma_2$.

A second failure relationship for the intermediate principal stress can be derived from elastic theory, as follows :-

The linear principal strains, $\epsilon$ , are

$$\epsilon_1 = \frac{1}{E}\left\{\sigma_1 - \nu(\sigma_2 + \sigma_3)\right\} \qquad \ldots\ldots\ldots\ldots\ldots\ldots(1)$$

$$\epsilon_2 = \frac{1}{E}\left\{\sigma_2 - \nu(\sigma_1 + \sigma_3)\right\} \qquad \ldots\ldots\ldots\ldots\ldots\ldots(2)$$

$$\epsilon_3 = \frac{1}{E}\left\{\sigma_3 - \nu(\sigma_2 + \sigma_1)\right\} \qquad \ldots\ldots\ldots\ldots\ldots\ldots(3)$$

where $\nu$ = Poissons ratio;
$E$ = Young's modulus

For $K_o$ conditions, $\epsilon_2 = \epsilon_3 = 0$, and $\sigma_2 = \sigma_3$

From (3), $\sigma_3 - \nu(\sigma_1 + \sigma_3) = 0$

$\therefore\quad \frac{\sigma_3}{\sigma_1} = K_o = \frac{\nu}{(1-\nu)}$

or $\nu = \frac{K_o}{1 + K_o}$ $\qquad \ldots\ldots\ldots\ldots\ldots\ldots(4)$

For plane strain conditions, $\epsilon_2 = 0$

From (2), $\sigma_2 = \nu (\sigma_1 + \sigma_3)$

Substituting (4), $\sigma_2 = \frac{K_o}{(1+K_o)} (\sigma_1 + \sigma_3)$

This intermediate principal stress relationship is plotted on Fig. 8-4(c), and shows that the values of intermediate principal stress determined by this method slightly under-estimate the measured values. This curve also shows that the ratio of the intermediate principal stress to the sum of the other two principal stresses varied from approximately 0.27 for the denser specimens to 0.36 for the looser specimens. The results are similar to the values of intermediate principal stress measured by Wood (1958) on a partly saturated compacted fill material (see Chapter 2, page 21).

## II. Standard Triaxial Compression Tests

It is not considered necessary to deal with the standard triaxial results in too much detail.

### Stress-strain curves

The author was particularly interested to determine the point in the test where the failure zone was first seen. Careful observations were made during several tests. Examples are given on the stress-strain curves of Figs. A10-35,-37,-40,-41,-45, the appearance of the zone coinciding with a marked drop in the deviator stress to the ultimate value and a rapid levelling off in the volume change curve. Recalling the points made about the plane strain tests again, there was no visible failure zone at the maximum deviator stress condition, but the zone was distinctly marked at the ultimate condition. Therefore, it would seem reasonable to expect that the failure zone also appears immediately prior to the rapid drop of deviator stress in the plane strain tests.

Another observed similarity with the plane strain tests was that the failure zone always passed through an edge at the juncture between the soil and end caps in the standard triaxial compression tests. This observation has been made many times by the author since the completion of the present investigation. It is probably the result of the high shear stresses developed at these junctures due to friction between the soil and loading caps.

Factors affecting strength

The results of test series E are plotted on Fig. 8-5. The strength-density curve shows the well-known trend of increasing strength with increasing density. There only appears to be a slight and insignificant difference between the angles of shearing resistance computed from shear tests at cell pressures of 40 lb/sq.in. and 60 lb/sq.in. This was the only variation of the cell pressure in the research work, so that it is impossible to reach any general conclusion regarding the effect of different cell pressures on shear strength. Surprisingly, perhaps, the volume change and axial strain failure characteristics are very similar at the same placement density in the tests at different cell pressures.

In Series F, the axial stress was held constant and the cell pressure decreased to failure, the test being so arranged that the cell pressure at failure in Series F was approximately 40 lb/sq.in. The results of this series are compared with Series E (at a constant cell pressure of 40 lb/sq.in.) in Fig. 8-6. The strength curves in the two test series appear to be coincident and it is concluded that the strength of the sand is not affected by the different stress histories. Test C-40 was carried out as a repeat of test C-28.

The volume changes at failure in Series F are more positive than those of Series E, but there is little difference between the axial strains at failure. If an allowance is made for the additional strains and volume changes which take place in Series F after the equivalent consolidation in Series E has been exceeded, the failure characteristics of the two test series correspond more closely to each other. The volume changes and axial strains corrected in this way are shown by crosses on Fig. 8-6, and there is excellent agreement. Therefore, the total stress-strain conditions at failure are unique for a given specimen density in a similar way to the comparable plane strain test series A & B. It is worth mentioning, however, that this conclusion would not have been so apparent from the triaxial test results alone.

Ultimate strength

Large axial strains were required to reach the ultimate strength of the standard triaxial tests and the author was hesitant about plotting any values for it. The result depends partly upon the axial strain used to define the ultimate stress on the soil, but eight values are shown on Fig. 8-7. Assuming that the ultimate strength is independent of density, the average value is approximately equal to the shear strength of the loosest specimens; it is $0.7^{\circ}$ higher than the average ultimate strength measured in the plane strain tests.

## III. Comparison between Plane Strain and Standard Triaxial Compression Tests

Test Series A and E are compared on Fig. 8-8, and some general comments can be made. The strength of the plane strain specimens are always greater than the strength of the corresponding triaxial specimens at the same placement density. The difference varies from approximately $\frac{1}{2}^{\circ}$ at the looser densities to more than $4^{\circ}$ for the dense specimens. It should also be noted that the

shape of the strength-density curves are similar, i.e. concave uppermost. The standard triaxial specimens have a greater positive volume change at failure, but the volume change curves for the two types of test tend to converge at the looser porosities. The axial strains at failure in the standard triaxial test are almost three times greater than those of plane strain specimens at the same density.

The difference in compressive strength between plane strain and standard triaxial compression specimens at different placement densities is shown graphically on Fig. 8-9. The plane strain specimens showed a higher strength ranging from 2½% to 28% over the test range of porosities.

Individual plane strain and standard triaxial tests at three different densities are plotted to the same scale on Fig. 8-10. The comparison accentuates many of the points which have been noted in the preceding discussion of the test results. A surprising result is that the modulus at the start of the shear stage appears to be lower in plane strain.

It has already been concluded that the failure characteristics of the drained compression tests under plane strain conditions, at a given specimen density, are unique provided test Series B are corrected in the manner described in that section. In a similar way, the test Series E and F for the triaxial results also produce a unique set of conditions at failure. By combining the results of all the drained tests onto a single graph, a better comparison of the failure characteristics can be made than by comparing test Series A and E alone. The resultant curves are shown on Fig. 8-11 and it will be seen that the points noted on the Series A and E comparison are more clearly substantiated.

The failure characteristics of Brasted sand in the two types of test have been discussed in some detail. It is now necessary to consider certain other factors which are relevant to a further discussion on the shear strength of the sand.

## IV. Volume Changes during Shear

A theoretical approach to the analysis of volume changes in shear tests was attempted by Eldin (1951). He postulated that the volume changes were comprised of three components (Fig. 8-23) which, in the sum, give the total volume change, as follows :-

(i) a volume change due to changes in the average principal stress acting on the soil. This component can be calculated by extrapolating the plot of volume changes during the consolidation stage of the test.

(ii) a dilatancy component which he assumed to be directly proportional to the shear strain and having a slope equal to the maximum rate of dilation, occurring at failure. This component is almost independent of the average principal stress but the slope increases with increasing density.

(iii) a volume change due to structural breakdown in the soil, associated with the mobilization of friction. Eldin deduced that its maximum value at failure, was proportional to the average principal stress and that its curve was similar in shape to the corresponding change in principal stress ratio during shear. The structural breakdown component is negligible in dense sands but increases at an increasing rate for looser sands.

Later research has shown that some of Eldin's concepts require modification but, nevertheless, they form a valuable contribution in attempting to understand the volume changes which take place during shear. These volume changes play an important role in the present analysis. Two questions to be discussed at this stage are :-

(i) are the measured volume changes uniformly distributed throughout the test specimens?

(ii) what is the relation between the mobilization of friction and volume changes?

Uniformity of volume change

There can be little doubt that the volume changes which have taken place when the ultimate condition is reached are not uniformly distributed throughout the test specimens, but the uniformity of the volume changes at failure (maximum deviator stress) is more difficult to assess. A specimen at failure has no visible failure plane and the appearance of the plane at a later stage was accompanied by a rapid drop in the rate of dilation, which had been remarkably constant up to this point. The appearance of the failure plane may mark the beginning of non-uniform shear conditions.

The evidence in support of non-uniform volume changes at failure is probably more convincing. The best evidence is provided by the porosity changes within the specimen during shear, analysed from moisture content determinations taken at the end of the test. They have shown that the triaxial specimens become much looser in the centre than at the ends, implying that dilation occurs mainly in the central portion.

There is a wealth of evidence collected during the investigation to support this view but, for brevity, only one example will be cited. On Fig. 7-4(a), the porosity variations with depth are given for three standard triaxial compression tests, specimens C-7, C-9, C-16. In all cases, the soil was densely compacted by the same compaction technique and was dilating rapidly at failure, when the test was stopped. The porosities measured at each level are extremely consistent and the average values have been compared with an untested "twin" specimen, C-20. The final column of the table shows that the porosity at the mid-height of the average specimen gained approximately 2% at failure whereas

the whole specimen gained only 0.8% in porosity. The maximum bulging of the specimens occurred at or near the mid-height, corresponding with the maximum increase in porosity. It confirms the measurements of porosity variations within sheared sand specimens made by the Waterways Experiment Station (Shockley, 1953; Hvorslev, 1957) referred to in Chapter 7, page 56.

Finally, there is one further point to be cleared up and it is that the bottom of the averaged failure specimen of Fig. 7-4(a) does not have the same porosity change during shear as the top. This phenomenon cannot be easily accounted for in physical terms, but seems to be associated with the fact that the bottom of the specimen is in the closest proximity to the volume change measuring burette. The sequence of water movements during and after a shear test is illustrated diagrammatically on Fig. 7-5. The soil dilates during shear drawing water from the outside burette mainly to the central region of the specimen. As mentioned in an earlier footnote (see page 45), the soil responds to the release of the deviator stress at the end of the test by expelling water. This will almost certainly come from the central failure zone and, as the burette at the base of the specimen remains open during the release of stresses, the water will pass through the bottom half of the specimen, Fig. 7-5(b). Finally, on the release of the cell pressure, the specimen takes back water from the burette due to the decrease of effective stress. Again, the bottom of the specimen receives the response to the pressure changes before the top half. A common characteristic to all the investigations of porosity changes during shear are the seemingly "false" increases of porosity towards the bottom of the specimen. It is particularly well illustrated on Fig. 7-4(b) in which the 38% porosity contour of the average of all the plane strain specimens dips towards the right at the bottom, reflecting the position of the burette connection to the apparatus (Fig. 4-1).

What causes non-uniform volume changes at failure? It is undoubtedly the result of the frictional forces between the soil and loading platens which inhibits, though it does not prevent, lateral displacements of the soil at these points.

The theoretical solution of the stress distribution resulting from friction on the loading platens of cylindrical specimens has been treated by Filon (1902) and more recently by Balla (1957). The author is not familiar with Filon's work but, according to Balla, the numerical results of the two analyses are in close agreement with each other. A typical analysis shows that the shearing stress is reasonably uniform over the central two-thirds height of the specimen. At the edges of each loading platen, where a discontinuity in the external shear stress condition occurs, high internal shear stresses are developed in the specimen. Immediately below the centre of the loading platens, the internal shear stresses are the lowest of any region in the specimen. In summary, the analyses of Filon and Balla give theoretical grounds to show that the distribution of shear stresses within the specimen deviate most from the non-uniform condition in the regions next to the loading platens.

Onset of dilation

Kirkpatrick (1954) observed that the minimum volume condition, or onset of dilation, occurred at a fairly constant value of principal stress ratio, irrespective of the initial density of the soil. Although there was a fair amount of scatter in his results, he concluded that dilation began when the "rubbing friction" (ultimate strength) of the soil had been mobilized.

Fraser (1957), in independent work, also found that the minimum volume condition of his sand occurred at a certain principal stress ratio. His tests on large, 4 inch diameter, triaxial specimens examined several loading paths to failure and

he concluded that the constant principal stress ratio was independent of the type of consolidation, magnitude of the stresses, initial porosity or stress history. Fraser did not continue his tests beyond the maximum deviator stress, but it is pertinent to mention here that tests by the present author on the same Brasted sand have shown that the principal stress ratio at the commencement of dilation quoted in Fraser's thesis is approximately equal to the principal stress ratio at the ultimate condition (see Fig. 8-22).

This minimum volume condition has been termed the point of dilation by Fraser and has been plotted for the plane strain and standard triaxial test results of this investigation on Fig. 8-13. For Series E, in which the cell pressure was held constant and the axial stress increased, the minimum volume occurred at a fairly constant value of principal stress ratio which was independent of the initial porosity. The result substantiates the previous work although it must be remarked that the stress ratio was changing rapidly when the minimum volume condition occurred and can only be determined with moderate accuracy. The average value of the ratio for Series E was 2.18, equivalent to an apparent angle of shearing resistance of $31.5^{\circ}$. This value corresponds closely with the ultimate strength of saturated Brasted sand and bears out Kirkpatrick's observation that dilation commences when the ultimate shearing resistance or "rubbing" friction is first mobilised.

In Series F, however, the principal stress ratio at minimum volume did not remain constant, but decreased with increasing density until the denser specimens dilated from the start of shear. This condition was brought about by the decreasing stresses on the specimen, and it is clear that the rate of dilation did not reach

an appreciable amount until the principal stress ratio had surpassed the value at which Series E began to dilate (Fig.8-14).

It seems possible that Kirkpatrick's observation about dilation may be true. Here, the volume change concepts of Eldin (1951) are useful. At the start of the shear stage, the increases in effective stress and the change in soil structure produced by grain shear movements combine in consolidating the specimen at a decreasing rate. Dilation volume changes begin when the ultimate principal stress ratio has been mobilized. However, friction at the ends of the specimen produce non-uniform shear stress conditions with corresponding non-uniform volume changes such that only parts of the specimen dilate. For example, there seem to be "dead" zones immediately under the centre of the loading platens which do not dilate during shear. This is consistent with the Filon and Balla analyses of shear stress distribution. The shear stresses beneath the centre of the loading platens are so low that the ultimate principal stress ratio is never mobilized during the shear test.

Although the whole specimen does not dilate during shear, dilation is likely to commence at the edges of the loading platens before the ratio of the applied external stresses have reached the ultimate principal stress ratio. Dilation commences in these regions first because (i) the shear stresses are higher due to end friction and (ii) the placement density at the ends of the specimen are higher; hence, less movement is required to mobilize a given amount of frictional resistance. Therefore, in Series E, it is fortuitous that the dilation volume changes in the overstressed regions near the edges of the loading platens nullify the consolidating volume changes in the rest of the specimen (i.e. minimum volume or <u>apparent</u> point of dilation) when the measured average stresses have just reached the ultimate principal stress ratio.

The characteristic barrel shape of the standard triaxial compression test (e.g. Plate 8-2) is the result of end friction between the loading platens and the specimen. It has two components, namely: (i) frictional deformation (Balla, 1957) and (ii) non-uniform dilatancy volume changes which are greater at the mid-height than at the ends of the specimen.

Uniformity of volume changes in plane strain

So far, the discussion on volume changes during shear has been concentrated on the standard triaxial compression tests as a convenient means of introducing the concepts of non-uniform volume changes. The volume changes during the shear stage of the plane strain tests suggest that the consolidation volume changes comprise a much greater part of the total volume changes than is the case in the standard triaxial tests, i.e. the dilating zone is less extensive than in the standard triaxial test.

The volume changes at the failure and ultimate conditions show a much smaller net increase in volume yet the soil in the failure zone was in a very loose condition. For example, Plate 8-1 is a photograph of the densely compacted plane strain specimen P-5, after shearing to the ultimate condition (Fig.A10-1). The membrane was carefully removed at the end of the test without collapsing the sand structure. A slight pressure was then applied to the upper platen and the specimen separated into two wedges of soil along the failure zone. The sand structure within each wedge was not disturbed, illustrating beyond doubt that the sand on the failure zone is in a much looser state than within the rest of the specimen. However, the net volume change at the ultimate condition was only +1% compared with +4 to +5% in a corresponding standard triaxial specimen.

The volume change curves of the individual test results (Fig. A10-1 to 25) show that appreciable consolidating volume changes take place during shear in all specimens. For example, examining the medium dense porosity of 38%, we note that specimens C-33 (Fig. A10-38) and C-36 (Fig. A10-39) have a negative volume change at the minimum volume condition of approximately 0.05% or 0.8 cc, compared with the average values of plane strain specimens P-19 (Fig. A10-13) and P-24 (Fig. A10-18) of 0.14% or 3.4 cc. The differences are admittedly small, but it is unlikely that they can be accounted for in terms of the higher average principal stress in the plane strain specimens at the minimum volume condition. Finally, in some of the looser specimens, the maximum rate of dilation takes place not at, but immediately after, the maximum deviator stress condition. Despite the precaution of using a slow machine rate-of-strain, this probably represents a slight time lag between the response of the specimen to changes in the external stresses. Two typical examples are given on Figs. A10-4 and A10-14.

It is not surprising, therefore, that the principal stress ratio for the minimum volume condition in plane strain specimens (Fig. 8-13) did not occur at a constant value. In Series A and C, the value increased with increasing density and was always greater than the fairly constant value for the standard triaxial Series E. On the other hand, the principal stress ratio at the commencement of dilation decreased with increasing density for test Series B, in which the average principal stress was decreased to failure. For the loosest specimen of Series B, the stress ratio was similar to those of the loose specimens in Series A & C. The medium and dense specimens dilated from the start of the shearing phase, but it is clear from Fig. 8-14 that the increases of volume in the early stages of the test were comparatively small and are probably caused by the reduction in effective stresses.

If it is agreed that consolidating volume changes from the non-dilating regions influence the net volume change characteristics, the plot of Fig. 8-14 suggests that the behaviour of the specimens in plane strain is not inconsistent with the view that dilation begins when the principal stress ratio corresponding to the ultimate condition is first mobilized.

The reason for the lower dilatancy volume changes in plane strain is difficult to substantiate further without an internal stress analysis similar to those put forward by Filon and Balla for the cylindrical compression test. Nevertheless, indirect evidence from the strength of other materials indicates that the slip zones are less widely distributed under plane strain conditions. Nadai (1950) gives a detailed discussion of the behaviour of materials, mainly metals, subjected to axial compression (see Chapter 20, Nadai). He also carried out a series of tests on specimens of dark-coloured paraffin wax in which regions subjected to excessive distortion - lines of slip - became lighter in colour and could be easily picked out. Compression tests with rough loading plates on long prismatic specimens and cylindrical specimens were included in his investigation. In the plane perpendicular to the direction of compression, a long prismatic specimen showed considerable distortion on the diagonals extending from the corners of the specimen, and little or no distortion elsewhere. The cylindrical specimens behaved in a similar fashion except that the distortion was more widespread, but less severe, in the regions between the diagonals and vertical walls of the specimen (cf Fig.20-19 and 20-12, Nadai).

Bridgmann (1946) observed a similar pattern of slip lines in a steel test specimen subjected to two-dimensional compression. He commented that these tests, approximating to plane strain, were much more "sensitive" than the cylindrical shape of specimen to the large shear distortions at the edges of the specimen initiated by boundary friction. Both Bridgmann and

If it is agreed that consolidating volume changes from the non-dilating regions influence the net volume change characteristics, the plot of Fig. 8-14 suggests that the behaviour of the specimens in plane strain is not inconsistent with the view that dilation begins when the principal stress ratio corresponding to the ultimate condition is first mobilized.

The reason for the lower dilatancy volume changes in plane strain is difficult to substantiate further without an internal stress analysis similar to those put forward by Filon and Balla for the cylindrical compression test. Nevertheless, indirect evidence from the strength of other materials indicates that the slip zones are less widely distributed under plane strain conditions. Nadai (1950) gives a detailed discussion of the behaviour of materials, mainly metals, subjected to axial compression (see Chapter 20, Nadai). He also carried out a series of tests on specimens of dark-coloured paraffin wax in which regions subjected to excessive distortion - lines of slip - became lighter in colour and could be easily picked out. Compression tests with rough loading plates on long prismatic specimens and cylindrical specimens were included in his investigation. In the plane perpendicular to the direction of compression, a long prismatic specimen showed considerable distortion on the diagonals extending from the corners of the specimen, and little or no distortion elsewhere. The cylindrical specimens behaved in a similar fashion except that the distortion was more widespread, but less severe, in the regions between the diagonals and vertical walls of the specimen (cf Fig.20-19 and 20-12, Nadai).

Bridgmann (1946) observed a similar pattern of slip lines in a steel test specimen subjected to two-dimensional compression. He commented that these tests, approximating to plane strain, were much more "sensitive" than the cylindrical shape of specimen to the large shear distortions at the edges of the specimen initiated by boundary friction. Both Bridgmann and

Nadai are firmly of the opinion, based on theoretical and experimental evidence, that failure in metals begins in these regions. Slip gets started with great ease at the edges and propagates to the central portion of the specimen under increasing compressive stress. Sliding fractures in metals usually pass through an edge between specimen and loading platen, in a similar way to the shear failures of Brasted sand.

A summary of the author's present views on this topic are as follows :- The distribution of the applied deviator stress within a test specimen is non-uniform, resulting from boundary friction between the specimen and loading platens. The singularity in the stress field at the upper and lower edges of the specimen set up large distortions in these regions and cause failure to begin in these parts at an earlier stage than in the rest of the soil. Failure in plane strain is characterised by a pair of conjugate shearing zones emanating diagonally across the plane of the intermediate principal stress. In the standard triaxial compression test the dilatancy is more widespread but less severe than in the cone-shaped region extending from the edge of the loading area. The cylindrical specimen is more subject to cross-slips from multiple conjugate planes, such that <u>any</u> point on the cylindrical wall is part of a potential slip zone passing through an edge between the specimen and loading platen. Multiple conjugate planes are a result of the equal principal stresses in the horizontal plane. This concept of the dilating zones at failure in the two cases is illustrated diagrammatically on Fig. 8-15.

Progressive failure

It is probable that failure in Brasted sand commences in the regions of high shear stress and progresses diagonally across the specimen. If failure is progressive to an appreciable extent, the maximum deviator stress measured in the tests will be less than the maximum deviator stress developed by the soil under uniform stress and strain conditions. When the apparent maximum deviator stress is reached, soil in different parts of the failure zone will be at different points on the "true" stress-strain curve. It follows that soils with a pronounced peak in the stress-strain curve will be most affected by progressive failure.

Taylor (1941) conducted a series of standard triaxial compression tests on sand using end caps which were capable of expanding laterally with the soil specimen during a shear test. He was able to obtain uniform lateral strain up to failure but not at strains beyond failure. The strengths measured in these tests gave close agreement with corresponding tests on the same soil using rigid end caps.

Another possible factor affecting the shear stress distribution within the specimen is the tilting of the top loading platen, which can produce eccentric loading. Penman (1953) devised a composite loading cap consisting of two parallel plates separated by ball bearings. When this arrangement was used in triaxial tests, the top cap remained horizontal but the measured strength was the same as the corresponding tests using the conventional loading cap. To sum up, progressive failure is not considered to have any appreciable influence on the strengths measured in standard triaxial tests.

The stress-strain curves of the dense plane strain specimens have such a pronounced peak that it is difficult to imagine that they can be seriously affected by progressive failure. However, the slight curvature and occasional shallow S-shape of the failure zone at the ends of the specimens are similar to the qualitative slip line characteristics suggested by Prandtl (1925) for compression tests between rough loading plates. Only plane strain tests without boundary friction can provide the final answer to this point. Since the completion of this research work, Blight (1961) has carried out undrained tests in which end friction has been practically eliminated by inserting circular pieces of rubber membrane coated with silicone grease between the specimen ends and loading platens. The distribution of pore pressures, analogous to volume changes in drained tests, were much more uniform than in conventional tests permitting end friction to be developed.

Volume changes & ultimate strength

Volume changes in the dilating regions are complete at the ultimate condition, at which the test specimen is separated into two soil wedges by the failure zone. The two wedges of soil deform as rigid bodies and additional axial strains are taken up by relative displacements between the two wedges via the failure zone. The total concentration of shear strain in the failure zone probably occurs at the first appearance of the zone and it is associated with a rapid drop in the rate of volume increase (e.g. Fig. A10-40). A glance through the literature will reveal that such "work softening" is a common characteristic of dilatant soils in shear. Various types of failed specimens are illustrated on Fig. 8-17 and, in each case, the soil is finally shearing within a narrow zone of the material.

The sand grains in the failure zone at the ultimate condition are probably in the loosest possible* intergranular packing for that particular shear stress or, perhaps, average principal stress. Therefore, at the ultimate condition, the porosity in the narrow zone is probably constant, irrespective of the initial packing. The original structure in this zone has been completely destroyed by the shearing process. The approximate value of the ultimate porosity in tests at a cell pressure of 40 lb/sq.in. can be deduced from Fig. 8-20 as 42.2%. The extent of the shearing zone at the ultimate condition can be determined from the width and depth of the membrane discolourations at the ends of plane strain specimens. Computations show that the volume of water accepted by a specimen from failure to the ultimate condition is sufficient to enable the porosity of the sand in the failure zone to change to 42.2%. Typical calculations are cited below :-

| | Loose | Medium | Dense |
|---|---|---|---|
| Specimen No. | P-20 | P-18 | P-16 |
| Measured width of membrane discolouration (cm) | 0.3 | 0.35 | 0.175 |
| Depth of membrane discolouration (cm) | 11.18 | 11.99 | 13.19 |
| Volume of ultimate failure zone (c.c) | 136.8 | 171.3 | 94.3 |
| Volume of voids-ultimate ($n$ = 42.2%) (c.c) | 57.6 | 72.3 | 39.8 |
| Porosity at failure - measured (%) | 40.57 | 38.80 | 35.35 |
| Volume of voids - failure (c.c) | 53.9 | 63.0 | 29.8 |
| Calculated required volume change, failure to ultimate (c.c) | 3.7 | 9.3 | 10.0 |
| Measured burette volume change, failure to ultimate (c.c) | 3.7 | 10.0 | 14.0 |

The calculated volume change is a maximum amount. At failure, soil in the eventual failure zone is probably looser than the calculated average porosity of the whole specimen.

## V. Standard Triaxial Extension Tests

The author has purposely chosen to present these results at a later stage of the text because the results cannot be determined with comparable accuracy to the compression test data and it is difficult to know how much credence to place on them.

The six axial extension test results are given on Fig. A10-46, 47, 48; the failure characteristics are summarised on Fig. 8-21 and the curves of the axial compression tests are drawn on the same graphs. The two densest specimens each have a strength slightly above the standard triaxial compression curve and well below the plane strain curve. The other four test results lie slightly below the standard triaxial curve, although the strength of specimen C-43 would probably have been slightly greater than the plotted value, which represents the strength at an axial strain well beyond the failure point (see Chapter 6, page 54). The problem of measuring strength in extension tests has already been mentioned in Chapters 2 and 6, and it must be admitted that six results are not really sufficient* to permit a dogmatic interpretation of the results. Bearing this in mind, it can be stated that, on balance, the data is in good agreement with the conclusions of Bishop & Eldin (1953) and Kirkpatrick (1957), i.e. the angle of shearing resistance is approximately equal in standard triaxial compression and extension tests at the same initial density.

---

* the number of tests was limited by the time available to the author.

In the extension tests, the failure zone is localised with more than two-thirds the total height of the specimen being outside a potential failure plane inclined at $(45 + \frac{1}{2}\phi)$ degrees to the vertical. The porosity variations within the specimen after compaction cannot be overlooked in extension tests. If variations of 2 - 3% in porosity can occur within the same specimen, as stated in Chapter 7, it seems likely that failure will take place in the loosest part. Hence, the initial density in the part of the specimen which fails will be less dense than the average initial density of the whole specimen, thus displacing the plotted strength values to the right on the graph, Fig. 8-21.

Specimens were compacted by the identical compaction techniques of shear test specimens C-46, 47 & 48 so that a comparison could be made between the initial and final porosities within the specimens (Fig. 7-5). Accepting the measured initial porosities of the compacted twin specimens at their face value, the position of the failure zone appears to be influenced by both the porosity variations and the shear stress distribution; for example, specimen C-46 failed at the top of the specimen, despite the soil being initially denser at this location. The initial diameter of this specimen was 0.007 in. less at the top than at the mid-height, which increases the deviator stress by only 0.35%, a negligible amount. This suggests that failure was mainly due to the stress distribution set up by friction between the specimen and top cap, an affect already discussed several times in the preceding text. The influence of the end friction on a specimen tends to counteract the influence of porosity variations. In these circumstances, it would be unreasonable to assume that failure occurs in the loosest part of the specimen. On the other hand, the average initial porosities should not be accepted without some idea of the porosity in the part of the specimen which actually fails. For simplicity, the average initial porosity in the failure zone has been calculated from the porosities measured on the compaction specimens. The effect of this correction to the test results is

shown by the open-centred circles on Fig. 8-21. The alterations do not materially affect the conclusion that the strengths measured in the standard triaxial extension tests are similar to the corresponding compression tests.

The porosity variations again illustrate that failure is accompanied by a migration of water to the failure zone (Fig.7-5). Specimen C-46 is a particularly good example because failure occurred away from the influence of the end-of-test water movements. However, the other specimens also lend support to the earlier discussion on water migration during shear.

## VI. Strength and Strain Conditions during Shear

The average ultimate strength measured in the plane strain tests was $32.3^{\circ}$ and in the standard triaxial compression tests was $33.0^{\circ}$. Relative to the accuracy of measurement, these results are considered to be sufficiently close to merit the conclusion that the ultimate strength of the Brasted sand is the same in both types of test; that is, independent of the intermediate principal stress.

The average of the two ultimate strength values, $32.6^{\circ}$, is slightly less than the failure shear strength measured on the loosest plane strain and standard triaxial specimens, both of which dilated slightly before reaching the ultimate condition. Furthermore, it is clear from the stress-strain and volume change curves that the greater is the difference between the peak and ultimate strengths, the greater is the maximum rate of dilation. Therefore, the rates of dilation $\rightarrow 0$ as the peak strength $\rightarrow$ ultimate strength. Now, all the test specimens mobilized a greater principal stress ratio than the ultimate and all the specimens dilated in doing so. The author believes that, had

it been possible to set up a test specimen slightly looser than these, the soil would have sheared directly to the ultimate strength without a peak in the stress-strain curve and without dilating. Furthermore, the strength would have been the same under both plane strain and standard triaxial shear conditions. The shear test characteristics of such a specimen are illustrated on Fig. 8-18; the point of dilation, failure strength and ultimate strength merge into one unique principal stress ratio. In other words, the strength-density curves for plane strain and standard triaxial compression tests meet at an initial porosity slightly looser than the loosest test specimens, and at a strength equal to the ultimate strength.

There are several methods of estimating the initial porosity at which the two strength envelopes meet. One method is to plot the maximum rate of dilation against the placement density, Fig. 8-12, and make a short extrapolation to zero rate of dilation. The extrapolation can be carried out with some degree of confidence, as the plotted points form a shallow curve. The extrapolated initial porosity for a specimen which does not dilate at failure is 44.1% from the plane strain curve and 44.3% from the standard triaxial curve. A second method of obtaining this result is to calculate the change in volumetric strain from the point of failure to the ultimate condition. The initial porosity at which these two conditions occur simultaneously is determined by extrapolation. This second method is probably less accurate than the first method - there are fewer results - but it is obvious from Fig. 8-12(c) that the extrapolated porosity is in good agreement with the other two values. Other methods include (iii) plotting the difference in strength between plane strain and standard triaxial specimens against placement density

(Fig. 8-9) and extrapolate to zero difference, and (iv) plotting the ratio of peak : ultimate strength in both types of test and extrapolating the curve to a ratio of 1.0.

What is the shear strength for specimens initially looser than the porosity at which the two strength-density curves meet? The Norwegian Geotechnical Institute (Bjerrum, Kringstad & Kummeneje, 1959) has provided part of the answer by using an experimental technique of placing the sand in a very loose condition. They allowed a sample of fine sand to "bulk" by mixing it up to a moisture content of 11%. The capillary forces created at this moisture content produce a honeycomb structure and the triaxial specimens made with the sand had initial porosities of up to 75%. Water was then passed slowly up through the soil. The structure was allowed to collapse but the soil remained in a very loose condition with a final "collapsed" porosity of 46 to 48%. These porosities were greater than the measured maximum porosity of 46.2%, as defined by Kolbuszewski (1948). In subsequent drained shear tests, the soil failed at very low strengths. It is thought that these tests may help to explain the flow slides which take place in Scandinavian countries.

The very loose test specimens fail at a very low strength, probably because the arched structure cannot sustain shearing loads. The author believes that the meeting point of the two strength-density curves is of fundamental importance in marking the transition point between an intergranular stable structure and a honeycombed unstable structure which collapses under the action of shearing loads. Therefore, the porosity has been termed the "minimum stable (initial) density". At looser densities, the test specimen will quickly collapse, but if it is capable of being supported (by, for example, the walls of a shear box), it

would eventually form a denser packing and shear at the ultimate strength. On the other hand, the Norwegian Geotechnical Institute's technique of passing water slowly up through a specimen of damp sand will destroy most, but not all, of the arches in the sand. The test specimen is looser than the minimum stable density, but it is not fully saturated. If saturation is then completed by the application of high back (pore-water) pressures, the specimen will consolidate to the minimum stable density, or slightly denser, thus forming a specimen with a very loose intergranular structure.

Since completing the research on Brasted sand, the author has proved the latter point experimentally on another sand. Large (4" diameter) standard triaxial specimens of loose sand were prepared using the Norwegian placement technique. After allowing water to seep up through the soil in the mould, the specimens were fully saturated by the application of back pressures and they reduced in volume to a porosity slightly lower than the minimum stable density. The stress-strain and volume change curves were similar to Fig. 8-18, there being zero rate of dilation at failure. The volume change and axial strain at failure were approximately -6% and 25% respectively for specimens consolidated to an all-round effective stress of 20 - 60 lb/sq.in.

The porosity of 44.2% and the strength angle of $32.8^{\circ}$ have been adopted to represent the meeting point of the two strength-density curves. The strength was determined from Fig. 8-19 and is $0.2^{\circ}$ higher than the average measured ultimate strength.

To repeat briefly, the main facts in the strength comparisons are :-

(a) the shear strength of the sand in the plane strain compression tests is always greater than the shear strength in the standard triaxial tests at corresponding placement densities over the test range. The difference in strength increases progressively from $\frac{1}{2}^{\circ}$ for the loosest specimens to $4^{\circ}$ in the densest specimens.

(b) the shear strength of the sand in the standard triaxial compression and extension tests are approximately equal at corresponding placement densities over the density range of the test series.

(c) the strength-density curves for plane strain and standard triaxial tests have a similar shape.

(d) the ultimate strength in the plane strain and standard triaxial compression tests are approximately equal and constant, independent of the placement density or the value of the intermediate principal stress. The ultimate strength is slightly lower than the shear strength at failure of the loosest test specimens.

(e) all the test specimens, plane strain or standard triaxial, dilated before the ultimate strength was attained.

Development of shear strength in intergranular structure

What causes the difference in strength between the two strength-density curves and what is the influence of the intermediate principal stress on strength? The author has postulated that there is a unique initial porosity, just beyond the test range, from which the soil will shear to the constant ultimate strength without dilating. This porosity, termed the minimum stable (initial) density is the meeting point of the two strength-density envelopes and probably represents a change-point between two structural conditions in the sand.

Dilatancy is a process of structural loosening in the zone of yield. Soil which is placed denser than the minimum stable (initial) density exhibits the property of dilatancy and is looser at the ultimate condition than at failure; such a soil has a structure with the grains in intimate contact with each other so that the movement of any individual grain is influenced by the

position of adjacent grains. The ultimate condition is attained when the sand grains can displace each other under the applied stresses without any net loosening of the soil in the failure zone. Before reaching the ultimate condition, dilatant soils must loosen* in the failure zone. Work is done against the stresses external to the failure zone, but in shearing, the soil will try to keep the external work to a minimum by the soil grains choosing the direction of least resistance to sliding.

Consider a specimen of sand in a shear test. At any stage in the test, the mass of sand is in equilibrium with the external forces acting on its surfaces. The frictional forces at point-to-point contacts between adjacent grains will vary from zero to the limiting value. A change in the external stresses will now alter the equilibrium condition such that some grains, which were at the limiting value previously, slide into a new position of equilibrium along a line offering the least resistance to shear.

The sand grains move because one or more neighbouring grains push them, the whole process of movement in the aggregate being a chain reaction in three dimensions. Therefore, shearing cannot be envisaged as merely a classical friction system in which rigid bodies move relative to each other in one direction, because displacement of both grains is a related and interdependent process. The "limiting value" of each contact depends on the normal forces between the two grains in the direction in which the grain moves, i.e. the choice of sliding direction to the individual grains is related to the frictional resistance which they are capable of developing.

At the start of shear, some grains will be pushed into new positions with little difficulty. The normal stresses acting in the direction of movement will be small but the grain will eventually take up a position which will make further sliding more

---

* i.e. at failure, although the net volume change of the specimen during shear need not be dilatant.

difficult. On the other hand, some grains will be in an arrangement with surrounding grains such that it is difficult, or impossible, for them to slide but are pushed bodily without sliding to new positions. Frictional resistance in the former grain is built up as the grain becomes impeded in its progress after some movement, whereas in the latter grain, resistance can be acquired immediately. Therefore, frictional resistance in the aggregate is built up gradually and consists of setting up normal stresses in the grain structure as the grains push or slide along. At the same time, sliding allows the grain structure to loosen in dilatant soils which has the effect of reducing the normal stresses. The maximum shearing resistance is a function of these two factors; the more sliding required to mobilize shearing resistance, the less resistance can be mobilized.

The choice of sliding direction will be governed by two factors :-

(i) the structural packing of the grains

(ii) the external stress conditions, particularly the intermediate principal stress.

In a statistically large assembly of grains, the structural packing of the grains will be approximately the same for the same initial density of specimen. Therefore, factor (i) is the same for all types of test at the same placement density.

Factor (ii) is really a strain condition and not a stress condition. A common characteristic of the standard triaxial compression and extension tests, which approximately agree to a common strength-placement density curve, is that two of the three principal stresses are equal in magnitude and sign. In the horizontal plane of the test specimens, there is a symmetry

of stress conditions such that the aggregate of soil grains strain equally in the direction of equal stresses. Now, an individual grain of sand will pick its line of movement through adjacent grains without regard to the aggregate movement. It will follow the direction offering the least resistance and clearly, for symmetric strain conditions, the direction could be anywhere in the horizontal plane for factor (ii). The actual direction it would take is governed by the relative positions of neighbouring grains.

When there is no symmetry of external stresses, the movements of individual sand grains become more restricted; then, the most favourable direction from the granular packing viewpoint may be nullified by the greater effort required to push an interfering grain in the direction of a higher external stress. The direction of sliding no longer depends solely on the geometry of neighbouring grains, but is modified by the external stress relationship. The extent of the restrictions can be judged from the external strain conditions.

In plane strain, the sand grains are least free to move in a random direction in the horizontal plane. Individual grains will not deviate much from a vertical path in the plane of the intermediate principal stress. A soil grain obstructed by an adjacent grain in the line of shear will develop a considerably higher normal stress in moving around it, at or near to failure, than a grain in a corresponding structural arrangement but subjected to less stringent strain conditions. It is also obvious that the maximum frictional resistance of the aggregate will be mobilized with less grain movements in plane strain. Hence, for a given structural packing (i.e. placement density), the plane strain condition will mobilize the maximum shearing resistance in the

sand, and symmetric strain conditions will mobilize the minimum. The influence of the intermediate principal stress on strength is to control the external strain conditions acting on the soil, which in turn modify the internal shearing movements of the sand grains. The strain mechanism is, therefore, a major factor influencing the shear strength of dilatant soils.

The stress value of the intermediate principal stress has no importance on strength. This conclusion is based on the following results :-

(i) within the limits of experimental error, the standard triaxial compression and extension tests agree to a common strength-placement density curve. For the same shear stress or principal stress ratio, the average principal stress in the extension test is 45 - 55% higher than in the compression test, over the test range.

(ii) the ultimate strength is approximately the same in the plane strain and standard triaxial compression tests, yet the average principal stress is 8% higher in plane strain. It may be argued that, beyond failure, the intermediate principal stress in the zone of failure is indeterminate, i.e. the ultimate condition in the standard triaxial tests approximate to shear in plane strain. However, some of the triaxial tests were sufficiently close to the minimum stable density condition that the change in strength from peak to ultimate was very small, amounting to a 1% change in the average principal stress. Therefore, it is unlikely that the ultimate strength is affected by the strain mechanism.

The strength under different strain conditions can be related through either the major or minor principal stresses, the author having chosen the latter.

The strength of the sand in the plane strain and triaxial compression tests has been plotted against the average porosity at failure in Fig. 8-16(b). The two curves are closer together than the corresponding curves of strength against placement density (Fig. 8-16a). The two curves may move closer together, or coincide, on tests performed under uniform strain conditions. If they did coincide, the result would bear out Hvorslev's view that the frictional resistance in soils is a function of the mean normal stress on the plane of failure and the voids ratio in the zone of failure. One would certainly expect the triaxial and plane strain curves to move toward each other because the more direct route to failure imposed by plane strain does not permit the soil to loosen as much as in the corresponding symmetric strain tests.

## VII. Theoretical Solutions

The relationship between strength and dilatancy has interested Dr. A. W. Bishop for many years and the results of the present investigation will now be examined with regard to two of his theoretical solutions.

### A. Energy Term Hypothesis

An energy concept (Bishop, 1954) can be applied to the compressive strength measured in drained shear tests to separate out (i) the internal work done in overcoming friction from (ii) the external work done by the specimen against the fluid pressure surrounding the soil. In saturated, dilatant sands, the specimen is expanding at the maximum deviator stress condition and the energy term reduces the measured deviator stress.

The volume change-axial strain curve for a saturated, dilatant sand is shown on Fig. 8-24.

Consider an increment of volume change, $\delta V$, corresponding to an increment of axial strain, $\delta \epsilon_1$, at failure in a drained test.

Then, if $(\sigma_1 - \sigma_3)_t$ represents the measured maximum deviator stress, the energy equation is

$$(\sigma_1 - \sigma_3)_t . A_f . l_c . \delta \epsilon_1 = (\sigma_1 - \sigma_3)_f . A_f . l_c . \delta \epsilon_1 + \sigma_3 . \delta V$$

where $A_f$ = horizontal cross-sectional area of specimen at failure

$l_c$ = length of specimen prior to shear

Then the corrected deviator stress $(\sigma_1 - \sigma_3)_f$ is given by:-

$$(\sigma_1 - \sigma_3)_f = (\sigma_1 - \sigma_3)_t - \sigma_3 . \left\{ \frac{\frac{\delta V}{V_c}}{\delta \epsilon_1} \right\} . \frac{A_c}{A_f} \quad *$$

The term $\left\{ \frac{\frac{\delta V}{V_c}}{\delta \epsilon_1} \right\}$ is the slope of the volume change-axial strain curve. The slope reaches its maximum positive value at the maximum deviator stress condition.

It can be shown that the energy term for the plane strain tests, and the standard triaxial compression and extension tests is given by the general form :-

$$\sigma \left\{ \frac{\frac{\delta V}{V}}{\delta \epsilon} \right\} \frac{A_c}{A_f}$$

where $\sigma$ = effective cell pressure

$\epsilon$ = axial strain

and the term is always subtracted from the total deviator stress.

Test results

The effect of subtracting the energy term from the standard triaxial and plane strain compression tests is shown at the end of Chapter 9 on Figs. 9-1 and 2. In both cases, the corrected strengths increase with increasing placement density. The standard triaxial compression curve, Fig. 9-2, increases from a

---

* this form differs from the original Bishop (1954) term by and was derived by Dr. I. Donald. In practice, the error in the original form is negligible.

corrected angle of approximately 32½°, at the loosest initial densities, to 38° for the densest specimens. The corresponding values in plane strain are 34° to 43° (Fig. 9-1). The corrected strength-density curve for plane strain lies above the total strength-density curve for the standard triaxial tests.

The corrected deviator stress in the extension test is subtracted from the cell pressure to give the corrected minor principal stress. The corrected angle, $\phi_r$, decreases rapidly with increasing placement density (Table 8-3). Also, the corrected principal stress ratio is decreasing at the maximum principal stress ratio of the applied stresses in all the specimens.

One further experimental point needs to be mentioned concerning extension tests. The axial strain in the region of failure, where necking occurs, is probably greater than the measured average change in axial strain of the whole specimen. If this is correct, the slope of the volume change-axial strain curve over-estimates the true slope pertaining to the failure region, and, hence, the correction to the measured strength is also over-estimated. However, it must also be borne in mind that the volume changes at failure are local to the failure region and may not be representative of a more uniformly dilating specimen.

B. Simple Shear Failure Zone Hypothesis (Bishop, unpublished)

Assume that at failure, when both $\tau$ and $\sigma_n$ are constant, strain and volume change are confined to a thin zone or series of zones, and that $\frac{\tau}{\sigma_n} = \phi_d$ max. (see Fig. 8-25). $\phi_d$ is the effective angle of shearing resistance in the drained tests.

Since there is zero strain normal to the direction of the simple shear zone, the volume changes at failure are represented by increases in thickness $\delta y$ of a zone of thickness $y$, consequent to a movement $\delta x$ in the direction of the zone.

Hence, dilatancy is represented by $\alpha$

where $\tan \alpha = \frac{\delta y}{\delta x}$ .....(1) (Fig.8-25a)

Compression tests ($\epsilon$ positive in compression)

Let $h_c$ be the consolidated height and $A_c$ be the consolidated cross-sectional area of a specimen, and let A be the average cross-sectional area at the strain at which slip occurs.

Let $\Theta$ be the angle between the slip zone and the plane of the major principal stress (Fig. 8-25b).

Assume that, in any given zone, strain in the plane of slip at right angles to the direction of slip is negligible. Then, for a change in axial strain $\delta\epsilon_1$ the specimen height changes by $-\delta h$

where $-\frac{\delta h}{h_c} = \delta\epsilon_1$ .....(2)

Hence $-\delta h = \delta x . \sin\Theta - \delta y . \cos\Theta$ .....(3)

Now area of slip zone $= A . \sec\Theta$ .....(4)

$\therefore$ volume change $\delta V = A . \sec\Theta . \delta y$ .....(5)

Required :- Relationship between $\frac{\frac{\delta V}{V_c}}{\delta\epsilon_1}$, $\Theta$ and $\alpha$

$$h_c \delta\epsilon_1 = \delta x . \sin\Theta - \delta y . \cos\Theta \quad \text{.....(6)}$$

From (1) $$= \delta y . (\cot\alpha . \sin\Theta - \cos\Theta) \quad \text{....(7)}$$

From (5) $$= \frac{\delta V}{A \sec\Theta} (\cot\alpha . \sin\Theta - \cos\Theta) \quad \text{....(8)}$$

Now $$V_c = A_c h_c \quad \text{.....(9)}$$

$$\therefore \frac{V_c}{A_c} \cdot \delta\epsilon_1 = \frac{\delta V}{A \sec\Theta} (\cot\alpha . \sin\Theta - \cos\Theta)$$

$$\sec\Theta . \delta\epsilon_1 = \frac{\delta V}{V_c} \cdot \frac{A_c}{A} (\cot\alpha . \sin\Theta - \cos\Theta)$$

$$\text{i.e. } \sec\Theta = \frac{\frac{\delta V}{V_c}}{\delta\epsilon_1} \cdot \frac{A_c}{A} (\cot\alpha . \sin\Theta - \cos\Theta) \quad \text{..(10)}$$

Let $m = \frac{\delta v}{v_c} \Big/ \delta\epsilon_1$, the slope of the volume change - axial strain curve at failure.

$$\sec\Theta = m.\frac{A_c}{A}\left(\cot\alpha.\sin\Theta - \cos\Theta\right) \quad \ldots\ldots\ldots(11)$$

$$\sec\Theta.\frac{A_c}{A} + m.\cos\Theta = m.\cot\alpha.\sin\Theta$$

$$\text{i.e.} \quad \tan\alpha = \frac{m.\sin\Theta}{m.\cos\Theta + \frac{A}{A_c}.\sec\Theta}$$

$$\text{or} \quad \tan\alpha = \frac{m.\tan\Theta}{m + \frac{A}{A_c}\sec^2\Theta} \quad \ldots\ldots\ldots\ldots\ldots(12)$$

Now it can be shown that the most critical line of slip for a frictional material is given by angle $\Theta = 45^\circ + \frac{1}{2}(\phi + \alpha)$

$$\text{i.e.} \quad \frac{\sigma_1}{\sigma_3} = \tan^2\Theta_{\text{critical}}$$

As $\sec^2\Theta = 1 + \tan^2\Theta$, the relationship between angle $\alpha$ and the principal stresses is given by

$$\tan\alpha = \frac{m.\sqrt{\frac{\sigma_1}{\sigma_3}}}{m + \left(1 + \frac{\sigma_1}{\sigma_3}\right)\frac{A}{A_c}} \quad \ldots\ldots\ldots\ldots\ldots\ldots\ldots(13)$$

From the Mohr diagram,

$$\tan(\phi + \alpha) = \frac{\frac{(\sigma_1 - \sigma_3)}{2}}{\sqrt{\frac{(\sigma_1 + \sigma_3)}{2} - \frac{(\sigma_1 - \sigma_3)}{2}}}$$

$$\text{i.e.} \quad \tan(\phi + \alpha) = \frac{\left(\frac{\sigma_1}{\sigma_3} - 1\right)}{2\sqrt{\frac{\sigma_1}{\sigma_3}}} \quad \ldots\ldots\ldots\ldots\ldots\ldots\ldots(14)$$

$$\tan\phi = \tan\left\{(\phi + \alpha) - \alpha\right\} \quad \ldots\ldots\ldots\ldots\ldots\ldots\ldots(15)$$

$$= \frac{\tan(\phi + \alpha) - \tan\alpha}{1 + \tan(\phi + \alpha)\tan\alpha} \quad \ldots\ldots\ldots\ldots\ldots\ldots\ldots(16)$$

$$= \frac{\frac{\left(\frac{\sigma_1}{\sigma_3} - 1\right)}{2\sqrt{\frac{\sigma_1}{\sigma_3}}} - \frac{m\sqrt{\frac{\sigma_1}{\sigma_3}}}{m + \left(1 + \frac{\sigma_1}{\sigma_3}\right)\frac{A}{A_c}}}{1 + \frac{\left(\frac{\sigma_1}{\sigma_3} - 1\right)}{2\sqrt{\frac{\sigma_1}{\sigma_3}}}.\frac{m.\sqrt{\frac{\sigma_1}{\sigma_3}}}{m + \left(1 + \frac{\sigma_1}{\sigma_3}\right)\frac{A}{A_c}}}$$

$$= \frac{\left(\frac{\sigma_1}{\sigma_3} - 1\right)\left\{m + \left(1 + \frac{\sigma_1}{\sigma_3}\right)\frac{A}{A_c}\right\} - 2m.\frac{\sigma_1}{\sigma_3}}{\frac{\sigma_1}{\sigma_3}\left\{2m + 2\left(1 + \frac{\sigma_1}{\sigma_3}\right)\frac{A}{A_c} + m\left(\frac{\sigma_1}{\sigma_3} - 1\right)\right\}}$$

$$= \frac{\frac{\sigma_1}{\sigma_3}m + \frac{\sigma_1}{\sigma_3}\frac{A}{A_c} + \left(\frac{\sigma_1}{\sigma_3}\right)^2\frac{A}{A_c} - m - \frac{A}{A_c} - \frac{\sigma_1}{\sigma_3}\frac{A}{A_c} - 2m.\frac{\sigma_1}{\sigma_3}}{\sqrt{\frac{\sigma_1}{\sigma_3}}\left\{2m + 2\frac{A}{A_c} + 2\cdot\frac{\sigma_1}{\sigma_3}\cdot\frac{A}{A_c} + m.\frac{\sigma_1}{\sigma_3} - m\right\}}$$

$$= \frac{\frac{A}{A_c}\left\{\left(\frac{\sigma_1}{\sigma_3}\right)^2 - 1\right\} - m\left(1 + \frac{\sigma_1}{\sigma_3}\right)}{\frac{\sigma_1}{\sigma_3}\left\{m\left(1 + \frac{\sigma_1}{\sigma_3}\right) + 2\cdot\frac{A}{A_c}\left(1 + \frac{\sigma_1}{\sigma_3}\right)\right\}}$$

$$\therefore \tan\phi = \frac{\frac{A}{A_c}\left\{\frac{\sigma_1}{\sigma_3} - 1\right\} - m}{\frac{\sigma_1}{\sigma_3}\left\{m + 2\cdot\frac{A}{A_c}\right\}} \qquad \ldots\ldots\ldots\ldots\ldots\ldots(17)$$

The angle $\phi$ is the value mobilized in opposition to sliding in the direction $\delta s$

Extension tests

$\epsilon_3$ is negative in extension tests.

As before, put $m$ = slope of volume change - axial strain curve

$$\text{i.e. } m = \frac{\frac{\delta V}{V_c}}{-\delta\epsilon_3} \qquad \ldots\ldots\ldots\ldots\ldots\ldots(18)$$

from sign conventions adopted, $+\frac{\delta h}{h_c} = -\delta\epsilon_3$

From the geometry of Fig. 8-26(c), and substituting (5) for $\delta y$

$$-h_c\,\delta\epsilon_3 = \frac{\delta V}{A\sec\Theta}\left(\cot\alpha.\sin\Theta + \cos\Theta\right) \qquad \ldots\ldots\ldots(19)$$

Substitute (19) for $h_c$ and re-arranging the equation we obtain

$$\tan\alpha = \frac{m\tan\Theta}{\frac{A}{A_c}\cdot\left(1 + \tan^2\Theta\right) - m} \qquad \ldots\ldots\ldots\ldots(20)$$

From the Mohr diagram,

$$\left(\frac{\sigma_1}{\sigma_3}\right) = \tan^2\left\{45° + \frac{(\phi+\alpha)}{2}\right\}$$

$$= \cot^2\left\{45° - \frac{(\phi+\alpha)}{2}\right\}$$

$$\text{or } \sqrt{\left(\frac{\sigma_3}{\sigma_1}\right)} = \tan\left\{45° - \frac{(\phi+\alpha)}{2}\right\} = \tan\Theta_{critical}$$

Substitute (21) in (20) to give

$$\tan\alpha = \frac{m\sqrt{\frac{\sigma_3}{\sigma_1}}}{\frac{A}{A_c}\left(1+\frac{\sigma_3}{\sigma_1}\right) - m}$$

Again, equation (16) is

$$\tan\phi = \frac{\tan(\phi+\alpha) - \tan\alpha}{1 + \tan(\phi+\alpha)\tan\alpha}$$

$$= \frac{\frac{\left(\frac{\sigma_1}{\sigma_3}-1\right)}{2\sqrt{\frac{\sigma_1}{\sigma_3}}} - \frac{m\sqrt{\frac{\sigma_3}{\sigma_1}}}{\left\{\frac{A}{A_c}\left(1+\frac{\sigma_3}{\sigma_1}\right)-m\right\}}}{1 + \frac{\left(\frac{\sigma_1}{\sigma_3}-1\right)}{2\sqrt{\frac{\sigma_1}{\sigma_3}}} \cdot \frac{m\sqrt{\frac{\sigma_3}{\sigma_1}}}{\left\{\frac{A}{A_c}\left(1+\frac{\sigma_3}{\sigma_1}\right)-m\right\}}}$$

$$= \frac{\left(\frac{\sigma_1}{\sigma_3}-1\right)\left\{\frac{A}{A_c}\left(1+\frac{\sigma_3}{\sigma_1}\right)-m\right\} - 2m}{2\sqrt{\frac{\sigma_1}{\sigma_3}}\left\{\frac{A}{A_c}\left(1+\frac{\sigma_3}{\sigma_1}\right)-m\right\} + \left(\frac{\sigma_1}{\sigma_3}-1\right)m\sqrt{\frac{\sigma_3}{\sigma_1}}}$$

Multiplying out and sorting the terms gives

$$= \frac{\frac{1}{\sigma_1\sigma_3}\left\{\frac{A}{A_c}\cdot\sigma_1^2 - m\,\sigma_1^2 - \frac{A}{A_c}\cdot\sigma_3^2 - m.\sigma_1\sigma_3\right\}}{\sqrt{\frac{\sigma_1}{\sigma_3}}\left\{2\cdot\frac{A}{A_c} - m\right\} + \sqrt{\frac{\sigma_3}{\sigma_1}}\left\{2\cdot\frac{A}{A_c} - m\right\}}$$

Now $$\sqrt{\frac{\sigma_1}{\sigma_3}} = \frac{\sigma_1}{\sigma_3}\sqrt{\frac{\sigma_3}{\sigma_1}} \qquad \ldots\ldots\ldots\ldots\ldots\ldots\ldots\ldots\ldots\ldots(23)$$

$$\therefore \tan\phi = \frac{\frac{A}{A_c}\left\{\frac{\sigma_1^2-\sigma_3^2}{\sigma_1\sigma_3}\right\} - m\frac{(\sigma_1+\sigma_3)}{\sigma_3}}{\sqrt{\frac{\sigma_3}{\sigma_1}}\left\{2.\frac{\sigma_1}{\sigma_3}.\frac{A}{A_c} - m.\frac{\sigma_1}{\sigma_3} + 2\cdot\frac{A}{A_c} - m\right\}}$$

$$\tan\phi = \frac{\left(\frac{\sigma_1 + \sigma_3}{\sigma_3}\right)\left\{\frac{A}{A_c}\,\frac{(\sigma_1 - \sigma_3)}{\sigma_1} - m\right\}}{\sqrt{\frac{\sigma_3}{\sigma_1}}\left\{2\,\frac{A}{A_c} - m\right\}\left(1 + \frac{\sigma_1}{\sigma_3}\right)}$$

$$\tan\phi = \frac{\frac{A}{A_c}\left(1 - \frac{\sigma_3}{\sigma_1}\right) - m}{\sqrt{\frac{\sigma_3}{\sigma_1}}\cdot\left(2\,\frac{A}{A_c} - m\right)} \qquad \text{.....(24)}$$

Slip on a number of parallel planes involves rotation. A general shear failure must, therefore, involve conjugate planes or cones in an axially symmetrical test. Assuming a conical failure surface for a cylindrical specimen, the area of a slip zone is again $A.\sec\Theta$ where $A$ is the horizontal cross-sectional area of the specimen and $\Theta$ is the angle of inclination of the slip zone to the horizontal.

The angle $\phi$ is the value mobilized in opposition to sliding in the direction of $\delta s$. The angle $\phi$ is independent of the thickness of the failure zone or the number of zones (or conjugate zones) formed at failure. The reason is that the maximum slope of the volume change-axial strain curve is independent of the zone thickness. Hence, the method is also applicable to test specimens subjected to non-uniform internal shear stresses, provided the initial assumptions are satisfied and the interference from cross-slips, such as conjugate planes, is small.

Test results

The results for the plane strain compression and standard triaxial compression and extension tests are given on Fig. 8-26(a), (b) & (c) respectively. The angle $\phi$ in plane strain remains approximately constant at all porosities, although there is a

slight tendency for the angle to decrease with increasing placement density. ~~The average angle for the 22 tests is 32.~~ $^{\circ}$. The calculations of angle $\alpha$ were based on the dilatancy slope at failure and not the maximum rate, which occurred shortly after failure in some of the looser specimens.

The angle $\phi$ in the standard triaxial compression tests decreased appreciably with increasing placement density, the curves of $\phi$ and $(\phi + \alpha)$ converging at the minimum stable density Fig. 8-26(b). At the dense end of the curve, the angle $\phi$ is approximately 27½$^{\circ}$, a drop of 5$^{\circ}$ over the test range of porosities ( $n_o$ = 34.2 - 44.2%).

The angle $\phi$ in the triaxial extension tests is approximately constant at all densities, the average angle being 30.8$^{\circ}$. As mentioned under Hypothesis A, the measured maximum slope of the volume change-axial strain curve may be over-estimated slightly in the extension tests. The specimen undergoes a slight amount of necking by the time failure is reached, and the changes in axial strain occurring in the failure region are probably greater than the measured average changes of the whole specimen.

The angles $\alpha$ in all the tests are plotted against placement density on Fig. 8-27. The small shear box tests (Appendix 7) are also included for completeness. All the results lie within a moderately broad band; the extension test results tend to lie slightly below the other types of test and the plane strain values reflect the small rates of dilatancy at failure in the looser specimens.

Interpretation of dilatancy terms

This thesis contains test data on the same sample of Brasted sand under four types of test conditions - plane strain, shear box (approximating to plane strain), triaxial compression and triaxial extension (both axially symmetric strain tests). When the measured angle of shearing resistance, $\phi_d$, is corrected for a dilatancy term, there does not appear to be a simple explanation for linking the different types of test. Therefore, the interpretation one gives to dilatancy terms is necessarily a personal one. The two main categories of interpretation are :-

(i) the dilatancy term should account for all the strength mobilised in excess of the ultimate strength, i.e. the increase in strength with increasing placement density. This is the approach most favoured by the author and several reasons have been compiled in Appendix 9.

(ii) the dilatancy term is calculated from the test measurements and a rational explanation of the corrected strength should be sought for each type of test.

Interpretation (i) is stating the required result and any anomalies have to be explained. Logical reasons are not difficult to suggest in most cases, but such explanations are never a satisfactory substitute for direct evidence from experiment. Therefore, this approach must be a cautious one, and form the basis for a future research programme to verify or reject the explanations of the observed anomalies.

Interpretation (ii) is the more objective approach, but it also has drawbacks. It takes for granted the assumptions on which the Hypothesis is based and it relies heavily on the correctness of the experimental data, both of which may be questioned to some extent in interpretation (i).

Dr. Bishop's present views on his energy concept (Hypothesis A) have been stated in the following way :- The energy concept separates out the component of axial compressive or shear stress which is used to provide the energy for dilating against the normal stress. What is left to combat internal friction will depend on the relationship between vertical and horizontal strains and is not the same in the dilating and non-dilating cases. Therefore, the dilatancy term calculated in Hypothesis A does not lead to the "constant volume" friction angle.

This point can be clarified by considering the analogous situation of a block on a rough inclined plane. The friction between the block and plane represents the "constant volume" friction and the inclination of the plane represents the dilatancy. Then, from consideration of the statics of the problem, it can be shown that the friction between block and plane can be obtained by differentiating frictional work with respect to movement in the direction of the frictional force (i.e. along the plane) and dividing by the force normal to this direction. Therefore, to correctly use the energy concept, the angle $\alpha$ must be known.

The shear box test, for example, is analogous to applying a horizontal force to the block on the inclined plane. Dividing the dilatancy work by the horizontal movement of the box does not lead directly to the "constant volume" friction angle between the block and inclined plane. However, $\alpha$ is the dilatancy angle whose tangent is the ratio of the vertical to horizontal movements of the box at failure. The "constant volume" angle $\phi$ is then obtained by subtracting $\alpha$ from the total angle $(\phi + \alpha)$.

The significance of Hypothesis B is still under active consideration. It would be inappropriate to discuss it further in this Thesis.

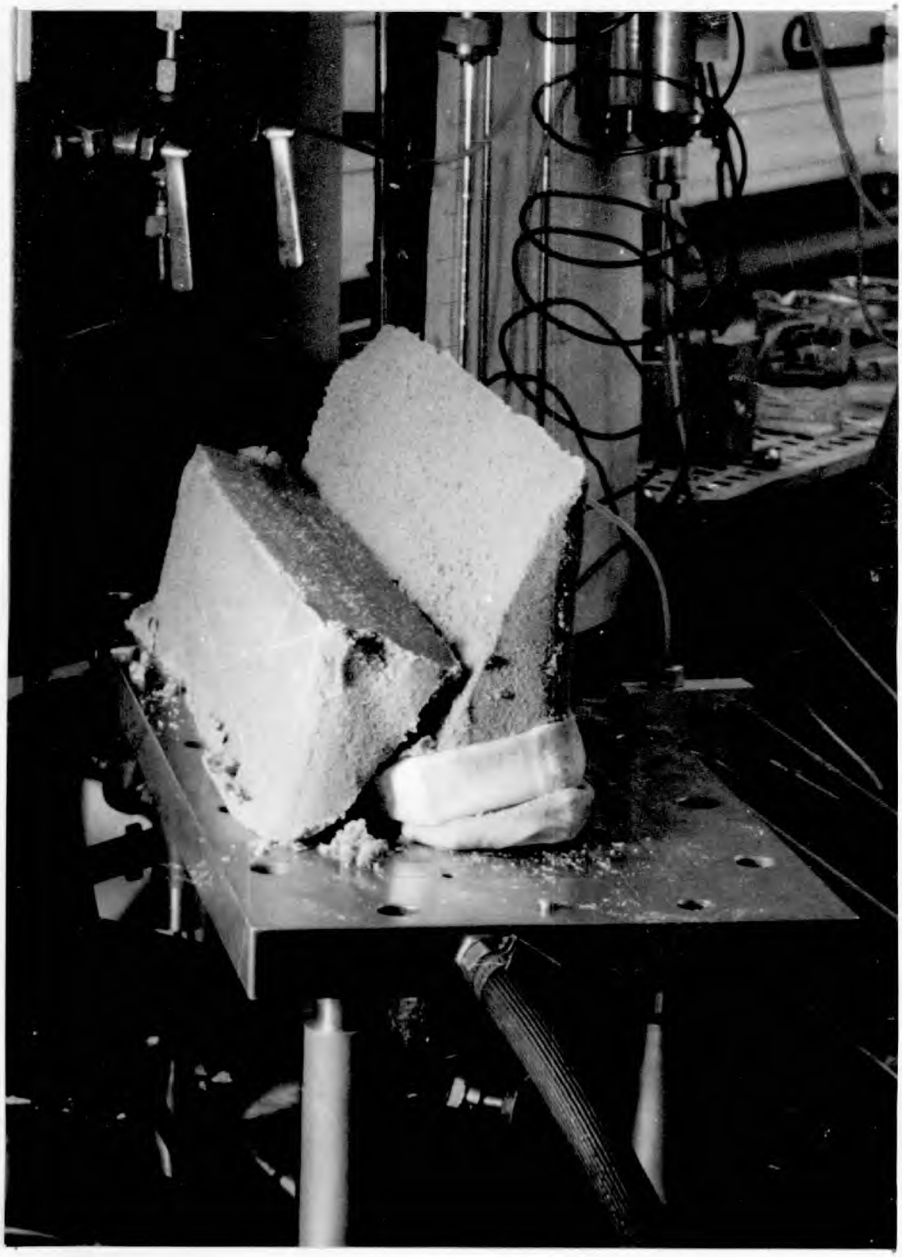


PLATE 8-1 DENSE SAND SHEARED TO FAILURE

UNDER PLANE STRAIN CONDITIONS (P-5)



PLATE 8-2

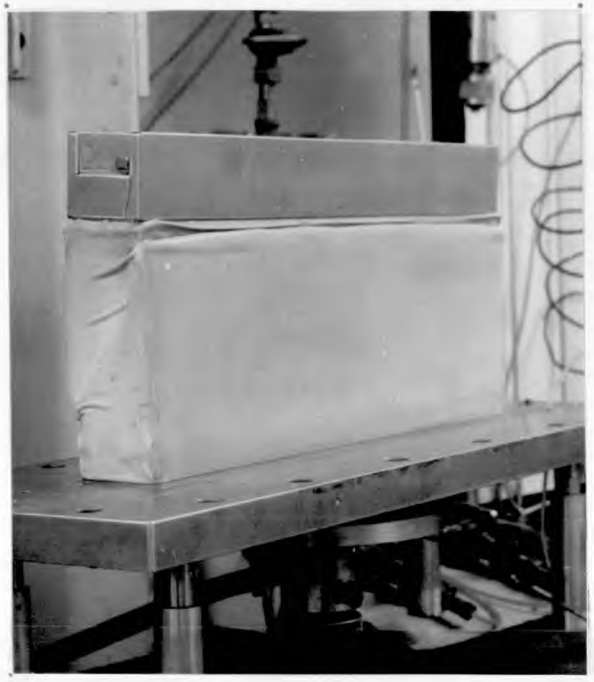


PLATE 8-3

SHEAR FAILURES (see also PLATE 8-1)

PLATE 8-2 Triaxial Compression. C-22, loose $n_o$ = 42.5% consolidated-undrained test stopped at axial strain of 16%.

PLATE 8-3 Plane Strain Compression. P-12, dense $n_o$ = 35.6% drained test without plane strain end clamp, stopped at axial strain of 15%.

| Figure Number | Test Number | Porosities % | | | | $K_o$ | Failure Stresses lb./sq.in | | | | Deviator Stress Ratio $\frac{\sigma_1-\sigma_3}{\sigma_3}$ | | | Deviator Stress Ratio $\frac{\sigma_2-\sigma_3}{\sigma_3}$ | | Axial Strain % | Volumetric Strain % | | Ratio $\partial(\frac{\Delta V}{V_c})/\partial(\epsilon_1)$ | | Angle of Shear Resist. | | Ratio $\frac{\sigma_2}{\sigma_1+\sigma_3}$ |
|---|---|---|---|---|---|---|---|---|---|---|---|---|---|---|---|---|---|---|---|---|---|---|
| A10- | | Initial | Consol. | Failure | Ultimate | Consol. | $\sigma_1-\sigma_3$ | $\sigma_3$ | $\sigma_1$ | $\sigma_2$ | Dilat? | Failure | Ultimate | Failure | Ultimate | Failure | Failure | Ultimate | Failure | Maximum | $\phi_d$ ° | Hyp. A, $\phi_r$ / Hyp. B, $\phi$ | Failure |
| Series A - cell pressure constant, axial stress increased to failure | | | | | | | | | | | | | | | | | | | | | | |
| 1 | P-5 | 35·26 | 35·0 | 35·2 | 35·7 | 0·355 | 184·7 | 40·0 | 224·7 | 71·5 | 3·10 | 4·62 | 2·24 | 0·79 | 0·35 | 1·60 | +0·27 | +1·05 | 0·540 | 0·540 | 44·25 | 42·2 / 34·3 | 0·270 |
| 2 | P-6 | 41·79 | 40·7 | 40·6 | 40·8 | 0·451 | 115·6 | 40·0 | 155·6 | 65·0 | 2·79 | 2·89 | 2·29 | 0·63 | 0·46 | 2·77 | -0·25 | +0·03 | 0·124 | 0·142 | 36·20 | 35·5 / 33·5 | 0·333 |
| 3 | P-8 | 40·28 | 39·4 | 39·4 | 39·7 | 0·431 | 134·0 | 40·0 | 174·0 | 69·5 | 2·81 | 3·35 | 2·34 | 0·74 | 0·45 | 2·10 | -0·02 | +0·45 | 0·265 | 0·304 | 38·75 | 37·4 / 33·3 | 0·325 |
| 4 | P-9 | 42·47 | 41·4 | 41·1 | 41·2 | 0·479 | 102·4 | 40·0 | 142·4 | 64·1 | 2·56 | 2·56 | 2·33 | 0·60 | 0·47 | 2·35 | -0·46 | -0·34 | 0·000 | 0·070 | 34·15 | 34·2 / 34·2 | 0·351 |
| 5 | P-10 | 42·99 | 42·1 | 41·8 | 41·9 | 0·444 | 107·4 | 40·0 | 147·4 | 74·3 | 2·66 | 2·69 | 2·25 | 0·86 | 0·78 | 3·90 | -0·55 | -0·38 | 0·048 | 0·068 | 34·95 | 34·7 / 33·9 | 0·397 |
| 10 | P-16 | 35·62 | 35·1 | 35·3 | 35·7 | 0·356 | 174·8 | 40·0 | 214·8 | 68·8 | 2·68 | 4·37 | 2·25 | 0·72 | 0·53 | 1·34 | +0·33 | +0·93 | 0·670 | 0·670 | 43·30 | 40·5 / 31·1 | 0·270 |
| 11 | P-17 | 34·42 | 34·0 | 34·2 | 34·6 | 0·343 | 195·6 | 40·0 | 235·6 | 80·4 | 3·22 | 4·89 | 2·39 | 1·01 | 0·41 | 1·36 | +0·30 | +0·95 | 0·740 | 0·740 | 45·20 | 42·5 / 32·1 | 0·292 |
| 12 | P-18 | 39·40 | 38·8 | 38·8 | 39·1 | 0·436 | 127·9 | 40·0 | 167·9 | 71·7 | 2·74 | 3·20 | 2·38 | 0·79 | 0·46 | 2·12 | -0·03 | +0·46 | 0·310 | 0·310 | 37·95 | 36·3 / 31·5 | 0·345 |
| 13 | P-19 | 38·07 | 37·6 | 37·6 | 37·9 | 0·420 | 140·9 | 40·0 | 180·9 | 68·0 | 2·75 | 3·52 | 2·35 | 0·70 | 0·37 | 1·83 | +0·05 | +0·51 | 0·350 | 0·350 | 39·60 | 37·9 / 32·5 | 0·308 |
| 14 | P-20 | 41·92 | 40·9 | 40·6 | 40·7 | 0·451 | 105·3 | 40·0 | 145·3 | 62·8 | 2·63 | 2·63 | 2·20 | 0·57 | 0·40 | 3·20 | -0·58 | -0·43 | 0·000 | 0·079 | 34·65 | 34·7 / 32·9 | 0·339 |
| 15 | P-21 | 41·68 | 40·9 | 40·6 | 40·8 | 0·454 | 111·9 | 40·0 | 151·9 | 66·7 | 2·76 | 2·80 | 2·25 | 0·67 | 0·51 | 3·00 | -0·48 | -0·20 | 0·029 | 0·135 | 35·65 | 35·5 / 35·0 | 0·348 |
| 17 | P-23 | 36·40 | 35·9 | 36·0 | 36·5 | 0·380 | 177·6 | 40·0 | 217·6 | 73·0 | 3·07 | 4·44 | 2·40 | 0·83 | 0·35 | 1·47 | +0·20 | +0·84 | 0·570 | 0·570 | 43·60 | 41·3 / 33·0 | 0·284 |
| 18 | P-24 | 38·81 | 38·2 | 38·1 | | 0·430 | 131·3 | 40·0 | 171·3 | 66·3 | 2·73 | 3·28 | | 0·66 | | 1·95 | -0·03 | | 0·350 | 0·350 | 38·40 | 36·5 / 31·2 | 0·314 |
| Series B - axial stress constant, cell pressure decreased to failure. | | | | | | | | | | | | | | | | | | | | | | |
| 16 | P-22 | 42·70 | 41·5 | 41·3 | 41·4 | 0·455 | 104·7 | 40·3 | 145·0 | 66·5 | 2·59 | 2·60 | 2·25 | 0·65 | 0·51 | 2·80 | -0·24 | -0·10 | 0·049 | 0·092 | 34·40 | 34·1 / 33·3 | 0·359 |
| 16 | P-25 | 40·24 | 39·3 | 39·3 | | 0·441 | 122·4 | 41·5 | 163·9 | 71·9 | 2·31 | 2·95 | | 0·73 | | 2·27 | +0·02 | | 0·180 | 0·180 | 36·55 | 35·5 / 32·7 | 0·350 |
| 19 | P-26 | 38·08 | 37·3 | 37·5 | | 0·429 | 144·7 | 41·0 | 185·7 | 74·3 | 1·33 immediately | 3·53 | | 0·81 | | 1·36 | +0·28 | | 0·370 | 0·370 | 39·65 | 37·8 / 32·2 | 0·328 |
| 19 | P-27 | 36·29 | 35·5 | 35·8 | | 0·384 | 174·6 | 40·0 | 214·6 | 76·8 | 1·60 immediately | 4·37 | | 0·92 | | 1·04 | +0·45 | | 0·630 | 0·630 | 43·30 | 40·7 / 31·7 | 0·302 |
| Series C - similar to Series A except that plane strain end clamp was omitted. | | | | | | | | | | | | | | | | | | | | | | |
| 6 | P-11 | 38·31 | 37·7 | 37·8 | | 0·354 | 137·8 | 40·0 | 177·8 | | 2·75 | 3·45 | | | | 1·88 | +0·20 | | 0·338 | 0·338 | 39·25 | 37·5 / 32·4 | |
| 7 | P-12 | 35·64 | 35·1 | 35·3 | 35·9 | 0·350 | 187·0 | 40·0 | 227·8 | | 3·28 | 4·68 | 2·25 | | | 1·73 | +0·33 | +1·30 | 0·630 | 0·630 | 44·45 | 42·1 / 33·1 | |
| 6 | P-13 | 39·72 | 39·0 | 39·0 | | 0·431 | 124·2 | 40·0 | 164·2 | | 2·67 | 3·11 | | | | 2·56 | +0·01 | | 0·263 | 0·263 | 37·45 | 36·0 / 32·2 | |
| 8 | P-14 | 42·27 | 41·5 | 41·2 | 41·3 | 0·448 | 106·0 | 40·0 | 146·0 | | 2·64 | 2·65 | | | | 3·90 | -0·49 | | 0·038 | 0·074 | 34·75 | 34·5 / 33·9 | |
| 9 | P-15 | 36·61 | 36·1 | 36·2 | 36·9 | 0·377 | 160·8 | 40·0 | 200·8 | | 2·90 | 4·02 | 2·21 | | | 1·32 | +0·20 | +1·32 | 0·632 | 0·632 | 41·90 | 39·0 / 30·0 | |
| | | | | | | | | | | | | | | | | | | | | | | - | |

DRAINED COMPRESSION TESTS (PLANE STRAIN)

TABLE 8-1

| Figure Number | Test Number | Porosities % | | | | $K_o$ | Failure Stresses lb./sq.in | | | Deviator Stress Ratio $\frac{\sigma_1 - \sigma_3}{\sigma_3}$ | | | Axial Strain % | Volumetric Strain % | | Ratio $\partial(\frac{\Delta v}{v_c})/\partial(\epsilon_1)$ | Angle of Shear Resist. | |
|---|---|---|---|---|---|---|---|---|---|---|---|---|---|---|---|---|---|---|
| A10 - | | Initial | Consol. | Failure | Ultimate | Consol. | $\sigma_1 - \sigma_3$ | $\sigma_3 = \sigma_2$ | $\sigma_1$ | Dilat ? | Failure | Ultimate | Failure | Failure | Ultimate | Failure | $\phi_d$ ° | Hyp. A, $\phi_r$ / Hyp. B, $\phi$ |
| Series E - cell pressure constant at 60 lb./sq.in., axial stress increased to failure. | | | | | | | | | | | | | | | | | | |
| 26 | C-7 | 36.00 | 35.4 | 36.6 | | 0.341 | 206.8 | 60.0 | 266.8 | 2.21 | 3.45 | | 4.8 | +1.80 | | 0.495 | 39.25 | 36.8 / 29.9 |
| 26 | C-8 | 40.31 | 39.6 | 40.1 | | 0.438 | 160.6 | 60.0 | 220.6 | 2.10 | 2.68 | | 7.0 | +0.78 | | 0.213 | 34.90 | 33.6 / 30.5 |
| 27 | C-9 | 35.43 | 35.0 | 36.3 | | 0.350 | 223.0 | 60.0 | 283.0 | 2.32 | 3.72 | | 3.8 | +2.01 | | 0.646 | 40.55 | 37.5 / 28.8 |
| 27 | C-10 | 41.14 | 40.3 | 40.6 | | 0.442 | 155.9 | 60.0 | 215.9 | 2.21 | 2.60 | | 5.1 | +0.45 | | 0.198 | 34.40 | 33.1 / 30.2 |
| 28 | C-12 | 43.29 | 42.3 | 41.9 | | 0.446 | 145.3 | 60.0 | 205.3 | 2.31 | 2.42 | | 12.0 | -0.61 | | 0.049 | 33.20 | 32.9 / 32.2 |
| 29 | C-13 | 38.53 | 37.8 | 38.5 | | 0.419 | 176.2 | 60.0 | 236.2 | 2.16 | 2.94 | | 6.4 | +1.24 | | 0.293 | 36.50 | 34.8 / 30.6 |
| 30 | C-15 | 37.70 | 37.2 | 38.2 | | 0.384 | 187.5 | 60.0 | 247.5 | 2.19 | 3.12 | | 4.8 | +1.61 | | 0.410 | 37.55 | 35.3 / 29.5 |
| 29 | C-16 | 35.44 | 35.0 | 36.2 | | 0.350 | 213.0 | 60.0 | 273.0 | 2.28 | 3.55 | | 3.8 | +1.90 | | 0.605 | 39.75 | 36.8 / 28.5 |
| Series E - cell pressure constant at 40 lb./sq.in., axial stress increased to failure. | | | | | | | | | | | | | | | | | | |
| 31 | C-21 | 42.95 | 42.0 | 41.8 | 42.1 | 0.452 | 96.9 | 40.0 | 136.9 | 2.23 | 2.42 | 2.36 | 11.8 | -0.30 | +0.18 | 0.068 | 33.20 | 32.8 / 31.8 |
| 34 | C-25 | 39.86 | 39.3 | 40.1 | 41.3 | 0.448 | 111.3 | 40.0 | 151.4 | 2.07 | 2.78 | 2.31 | 7.4 | +1.28 | +3.39 | 0.250 | 35.55 | 34.2 / 30.5 |
| 36 | C-27 | 37.09 | 36.6 | 37.8 | 39.4 | 0.414 | 130.2 | 40.0 | 170.2 | 2.08 | 3.25 | 2.45 | 4.4 | +1.93 | +4.54 | 0.523 | 38.25 | 35.5 / 28.3 |
| 38 | C-29 | 34.65 | 34.2 | 35.3 | | 0.351 | 155.7 | 40.0 | 195.7 | 2.35 | 3.89 | | 3.4 | +1.79 | | 0.734 | 41.35 | 38.0 / 28.2 |
| 40 | C-32 | 36.74 | 36.3 | 37.5 | 39.2 | 0.378 | 137.6 | 40.0 | 177.6 | 2.19 | 3.44 | 2.58 | 3.7 | +1.86 | +4.65 | 0.570 | 39.20 | 36.3 / 28.4 |
| 38 | C-33 | 38.19 | 37.8 | 38.7 | | 0.430 | 122.4 | 40.0 | 162.4 | 2.04 | 3.06 | | 4.8 | +1.58 | | 0.396 | 37.20 | 35.0 / 29.4 |
| 41 | C-34 | 36.30 | 35.9 | 37.0 | 38.2 | 0.379 | 136.0 | 40.0 | 176.0 | 2.20 | 3.40 | 2.45 | 3.8 | +1.79 | +3.62 | 0.585 | 39.00 | 36.0 / 28.0 |
| 39 | C-36 | 37.95 | 37.5 | 38.6 | | 0.424 | 121.0 | 40.0 | 161.0 | 2.00 | 3.03 | | 5.6 | +1.72 | | 0.436 | 37.00 | 34.6 / 28.5 |
| Series F - axial stress constant, cell pressure decreased to failure. | | | | | | | | | | | | | | | | | | |
| 33 | C-23 | 43.04 | 42.0 | 42.0 | | 0.453 | 98.5 | 41.0 | 139.5 | 2.14 | 2.40 | | 11.2 | -0.01 | | 0.069 | 33.10 | 32.5 / 31.2 |
| 35 | C-26 | 39.50 | 38.7 | 39.6 | 40.4 | 0.444 | 112.1 | 40.0 | 152.1 | 1.85 | 2.80 | 2.29 | 7.5 | +1.47 | +2.82 | 0.246 | 35.70 | 34.3 / 30.7 |
| 37 | C-28 | 37.37 | 36.8 | 38.1 | 39.7 | 0.416 | 128.4 | 38.5 | 166.9 | immediately 1.41 | 3.33 | 2.42 | 3.8 | +2.01 | +4.86 | 0.566 | 38.70 | 35.7 / 28.0 |
| 39 | C-31 | 34.47 | 33.9 | 35.3 | | 0.349 | 158.3 | 40.5 | 198.8 | immediately 1.87 | 3.91 | | 3.0 | +2.21 | | 0.810 | 41.40 | 37.6 / 27.1 |
| 45 | C-40 | 37.62 | 37.1 | 38.2 | 39.3 | 0.420 | 124.6 | 39.8 | 164.4 | immediately 1.41 | 3.13 | 2.34 | 4.4 | +1.93 | +3.61 | 0.477 | 37.60 | 35.0 / 28.4 |

DRAINED COMPRESSION TESTS (STANDARD TRIAXIAL)

TABLE 8-2

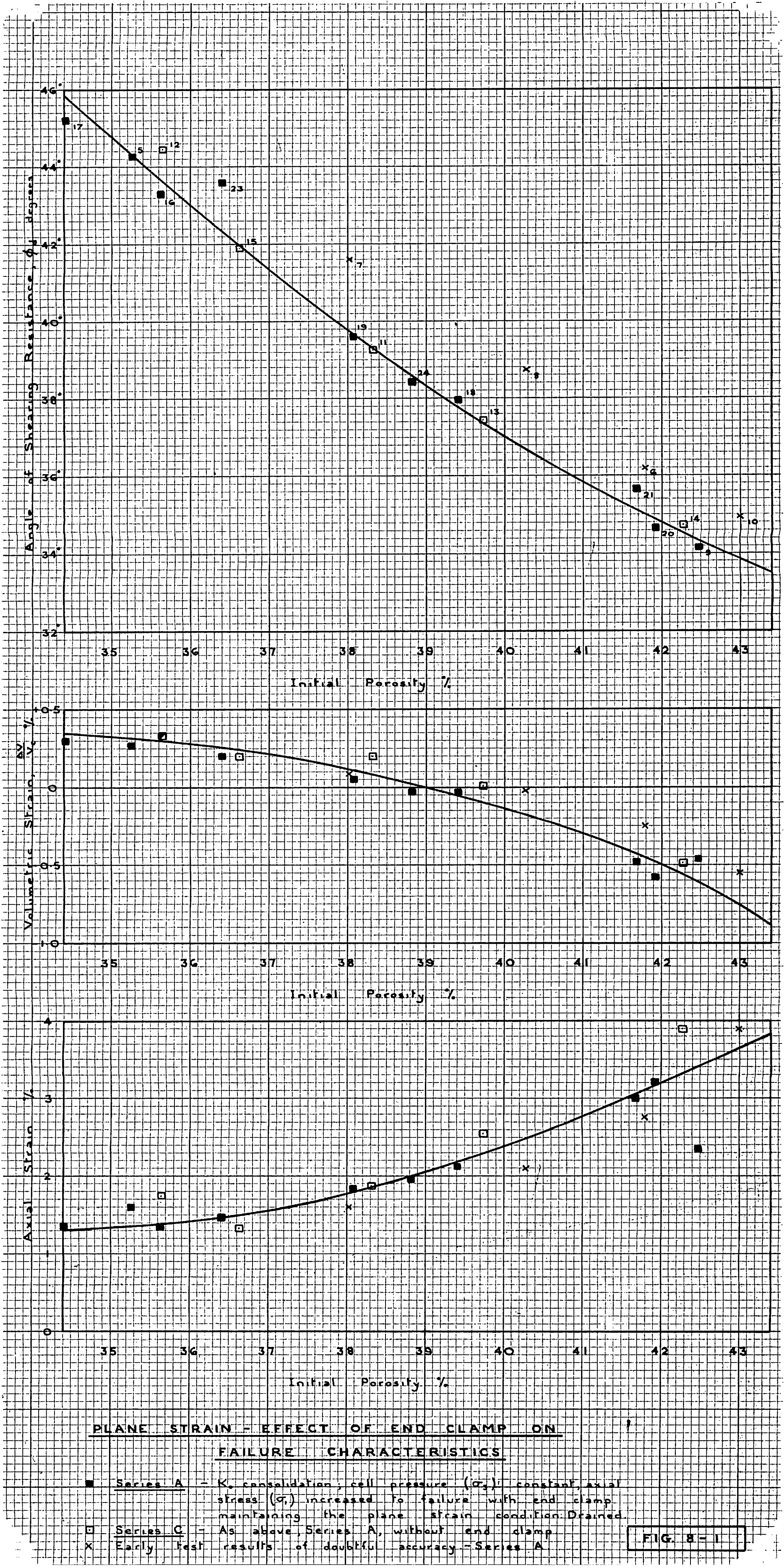
| Figure Number | Test Number | Porosities % | | | | $(K_o)_c$ | Failure Stresses lb./sq.in | | | Deviator Stress Ratio $\frac{\sigma_1 - \sigma_3}{\sigma_3}$ | | Axial Strain | Volume Strain | Ratio $\partial(\frac{\Delta V}{V_c})/\partial(\epsilon_3)$ | Angle of Shearing Res. | |
|---|---|---|---|---|---|---|---|---|---|---|---|---|---|---|---|---|
| A10- | | Initial | Consol. | Failure | Ultimate | Consol. | $\sigma_1 - \sigma_3$ | $\sigma_3$ | $\sigma_1 = \sigma_2$ | Dilat? | Failure | Failure | Failure | Failure | $\phi_d$° | Hyp. A, $\phi_r$<br>Hyp. B, $\phi$ |
| Series G - cell pressure constant, axial stress decreased to failure. | | | | | | | | | | | | | | | | |
| 46 | C-43 | 42·15 | 40·7 | 39·7 | | 0·457 | 92·30 | 37·70 | 130·0 | 2·04 | 2·45 | -9·0 | -1·60 | 0·095 | 33·40 | 26·4<br>30·7 |
| 47 | C-44 | 35·95 | 35·3 | 35·8 | | 0·350 | 101·81 | 28·19 | 130·0 | 1·75 | 3·61 | -4·6 | +0·82 | 0·307 | 40·05 | 18·2<br>30·8 |
| 47 | C-45 | 40·10 | 39·3 | 39·3 | | 0·436 | 94·00 | 36·00 | 130·0 | 1·91 | 2·61 | -7·0 | -0·09 | 0·137 | 34·50 | 24·5<br>30·6 |
| 48 | C-46 | 38·14 | 37·4 | 37·4 | | 0·436 | 96·97 | 33·03 | 130·0 | 1·94 | 2·94 | -4·0 | -0·03 | 0·170 | 36·50 | 23·9<br>31·8 |
| 48 | C-47 | 35·67 | 35·1 | 35·7 | | 0·360 | 102·78 | 27·32 | 130·1 | 1·25 | 3·76 | -4·2 | +0·94 | 0·335 | 40·75 | 17·1<br>30·4 |
| 48 | C-48 | 37·40 | 36·7 | 37·1 | | 0·384 | 105·15 | 34·65 | 139·8 | 1·73 | 3·04 | -4·7 | +0·63 | 0·231 | 37·10 | 20·7<br>30·3 |

## DRAINED EXTENSION TESTS (STANDARD TRIAXIAL)

| Figure Number | Test Number | Porosities % | | | $(K_o)_c$ | Cell Pressure lb./sq.in | Pore Water Pressure lb./sq.in | | | Deviator Stress Ratio $\frac{\sigma_1' - \sigma_3'}{\sigma_3'}$ | | | Deviator Stress Ratio $\frac{\sigma_3' - \sigma_3'}{\sigma_3'}$ | | Axial Strain | Angle of Shear Resist$^e$ deg. | | Ratio $\frac{\sigma_3'}{\sigma_1' + \sigma_3'}$ |
|---|---|---|---|---|---|---|---|---|---|---|---|---|---|---|---|---|---|---|
| A10- | | Initial | Consol. | Failure | Consol. | Shear | Consol. | Max. $\sigma_3'/\sigma_3'$ | Max. $\sigma_1' - \sigma_3'$ | Max. $\sigma_3'/\sigma_3'$ | Ult. $\sigma_3'/\sigma_3'$ | Max. $\sigma_1' - \sigma_3'$ | Max. $\sigma_3'/\sigma_3'$ | Ult. $\sigma_3'/\sigma_3'$ | Max. $\sigma_3'/\sigma_3'$ | Max. $\sigma_3'/\sigma_3'$ | Max. $\sigma_1' - \sigma_3'$ | Max. $\sigma_3'/\sigma_1' + \sigma_3'$ |
| Series D - cell pressure constant, axial stress increased (plane strain undrained) | | | | | | | | | | | | | | | | | | |
| 20 | P-28 | 41·69 | 40·4 | 0·447 | 60·0 | 60·0 | 0 | +28·8 | | 2·73 | | | 0·67 | | 2·50 | 35·25 | | 0·352 |
| 20 | P-29 | 39·94 | 39·0 | 0·442 | 50·0 | 50·0 | 0 | + 6·0 | | 3·07 | | | 0·72 | | 2·70 | 37·25 | | 0·339 |
| 21 | P-30 | 38·41 | 37·9 | 0·428 | 35·0 | 58·0 | +22·9 | +10·4 | | 3·39 | | | 0·72 | | 2·20 | 38·95 | | 0·312 |
| 21 | P-31 | 34·99 | 34·6 | 0·402 | 15·0 | 60·0 | +42·0 | +22·1 | | 4·27 | | | 0·74 | | 1·70 | 42·95 | | 0·271 |
| 22 | P-32 | 39·46 | 39·2 | 0·440 | 4·0 | 60·1 | +56·0 | +52·1 | +29·7 | 3·26 | 2·24 | 2·32 | 0·75 | 0·31 | 1·75 | 38·25 | 32·45 | 0·333 |
| 23 | P-33 | 41·91 | 40·9 | 0·448 | 50·1 | 50·1 | +0·4 | +27·0 | +17·9 | 2·82 | 2·34 | 2·53 | 0·69 | 0·55 | 3·00 | 35·85 | 34·10 | 0·347 |
| 24 | P-34 | 38·07 | 37·8 | 0·430 | 4·0 | 60·1 | +52·9 | +42·9 | - 7·0? | 3·62 | | 2·58? | 0·81 | | 2·00 | 40·10 | 34·7? | 0·320 |
| 25 | P-35 | 35·48 | 35·2 | 0·400 | 15·0 | 60·0 | +41·4 | +15·9 | | 4·36 | | | 0·84 | | 1·60 | 43·30 | | 0·287 |
| Series H - cell pressure constant, axial stress increased (standard triaxial undrained) | | | | | | | | | | | | | | | | | | |
| 32 | C-22 | 42·54 | 41·5 | 0·453 | 60·0 | 60·0 | 0 | +13·2 | | 2·38 | | | | | 9·7 | 32·90 | | |
| 42 | C-37 | 38·83 | 38·7 | 0·448 | 4·0 | 64·0 | +59·9 | +45·5 | | 2·68 | | | | | 1·75 | 34·90 | | |
| 43 | C-38 | 38·15 | 38·1 | 0·500 | 2·0 | 139·9 | +137·3 | +120·4 | | 2·74 | | | | | 1·6 | 35·30 | | |
| 44 | C-39 | 40·56 | 40·0 | 0·440 | 24·5 | 60·0 | +35·4 | + 7·2 | | 2·44 | | | | | 6·8 | 33·35 | | |
| Series J - cell pressure constant, axial stress decreased (standard triaxial undrained) | | | | | | | | | | | | | | | | | | |
| 49 | C-49 | 42·81 | 41·2 | 0·455 | 130·0 | 130·0 | 0 | +121·8 | +63·1 | ≐2·62 | ≐2·35 | ≐0·49 | | | -6·1 | ≐34½ | ≐ 11 | |
| 50 | C-50 | 39·15 | 38·3 | 0·443 | 130·0 | 130·0 | 0 | + 4·3 | | 2·39 | | | | | -4·5 | 33·00 | | |

## UNDRAINED TESTS

TABLE 8-3




PLANE STRAIN - EFFECT OF END CLAMP ON FAILURE CHARACTERISTICS

■ Series A – $K_o$ consolidation; cell pressure ($\sigma_3$) constant, axial stress ($\sigma_1$) increased to failure with end clamp maintaining the plane strain condition. Drained.

□ Series C – As above, Series A, without end clamp.

× Early test results of doubtful accuracy - Series A

FIG. 8 - 1

PLANE STRAIN - EFFECT OF STRESS HISTORY ON FAILURE CHARACTERISTICS

■ Series A - K₀ consolidation; cell pressure constant = 40 lb/sq.in., axial stress increased to failure. Drained.

Series B - K₀ consolidation; axial stress constant, cell pressure decreased to failure at approx. 40 lb./sq.in. Drained.

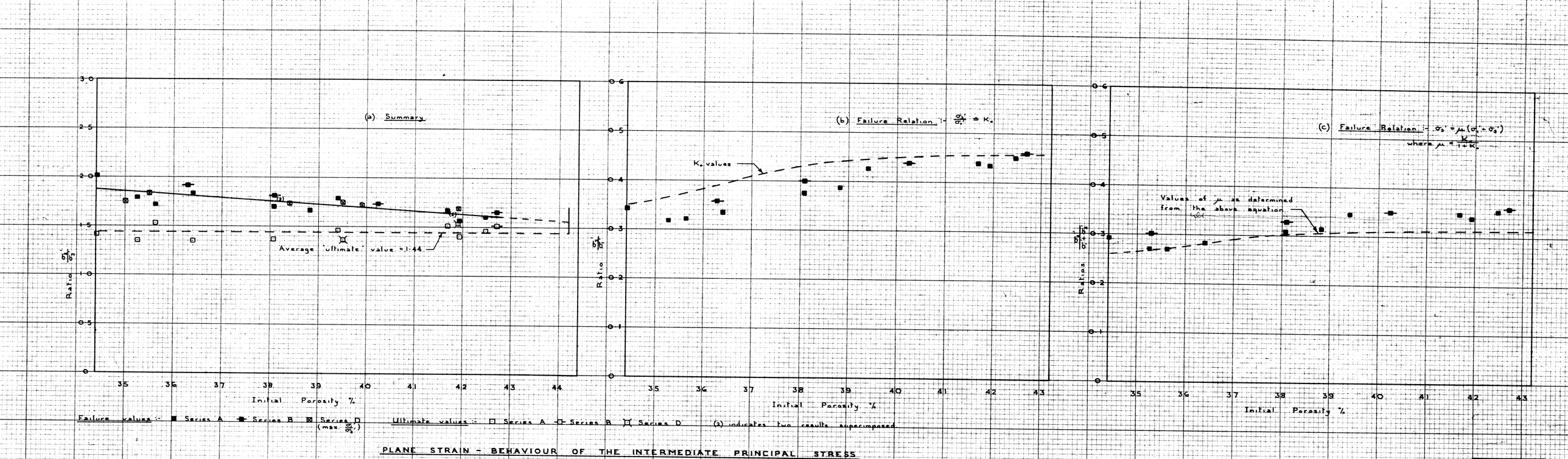
FIG. 8-2

PLANE STRAIN – ULTIMATE STRENGTHS

■ Series A ✚ Series B ⊡ Series C ⊠ Series D × Series A – doubtful

The Standard Triaxial ultimate strength results are plotted on Fig. 8-7.

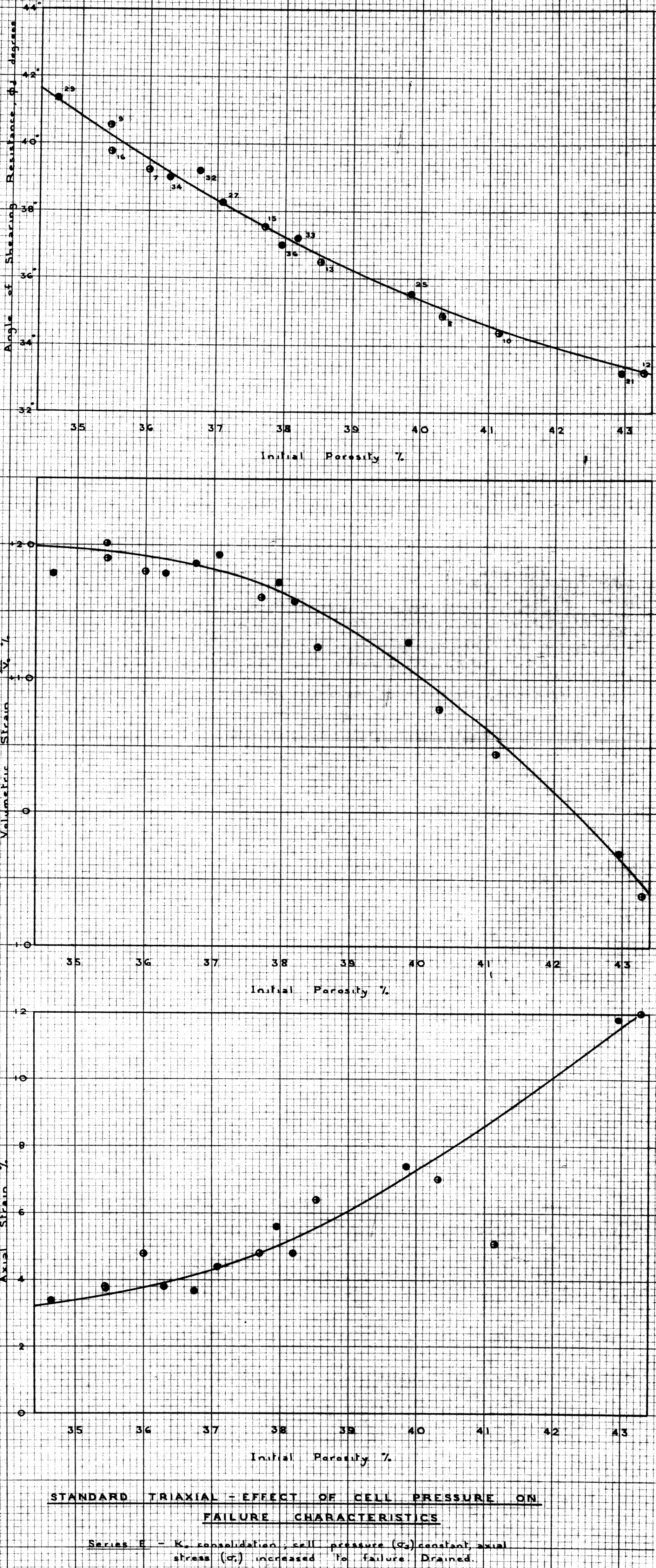
FIG. 8-3




Failure values :- ■ Series A ● Series B ⊠ Series D (max. $\frac{\sigma_2'}{\sigma_1'}$)  Ultimate values :- □ Series A ⊡ Series B ⊡ Series D  (2) indicates two results superimposed

PLANE STRAIN - BEHAVIOUR OF THE INTERMEDIATE PRINCIPAL STRESS

FIG. 8-4

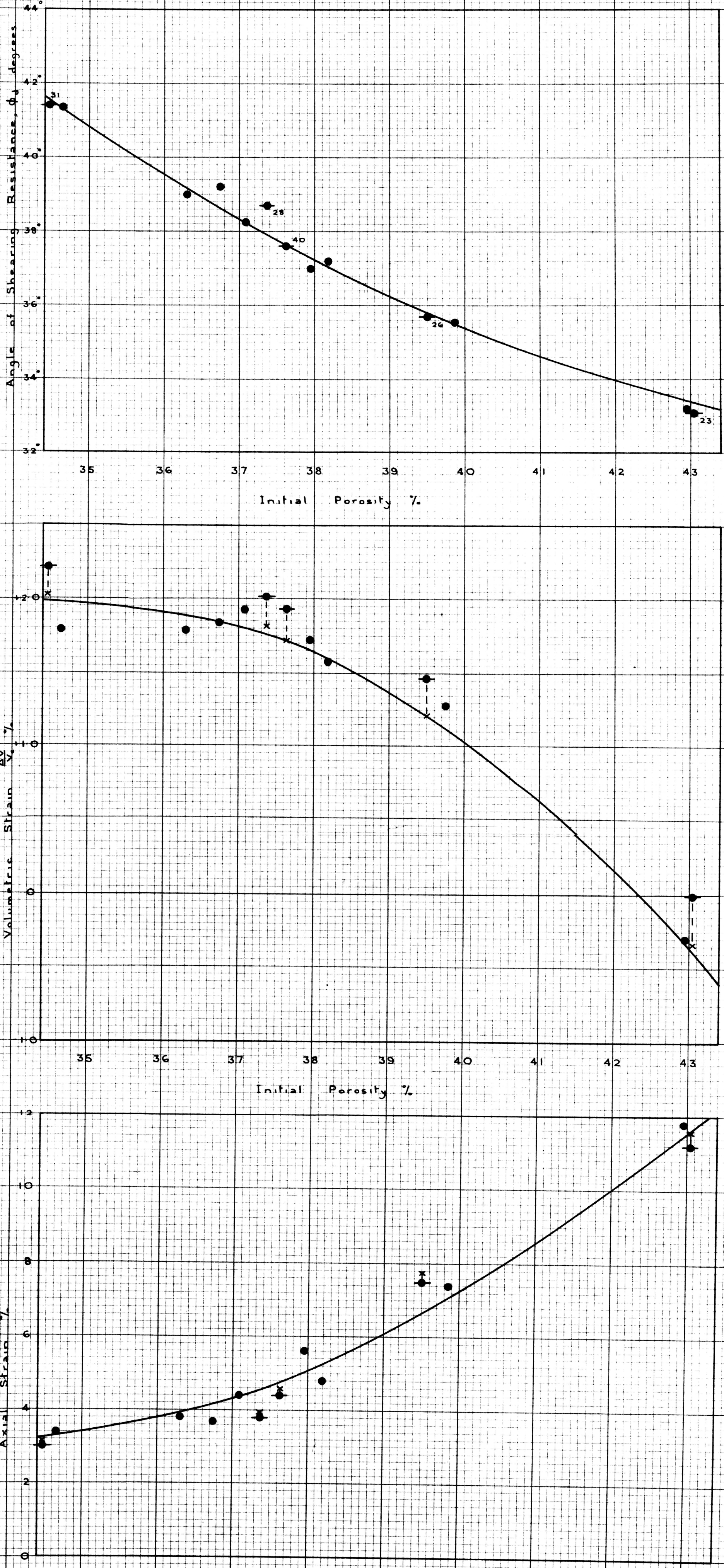



STANDARD TRIAXIAL - EFFECT OF CELL PRESSURE ON FAILURE CHARACTERISTICS

Series E - $K_o$ consolidation; cell pressure ($\sigma_3$) constant, axial stress ($\sigma_1$) increased to failure. Drained.

● cell pressure = 40 lb/sq.in.
⊕ cell pressure = 60 lb/sq.in.

FIG. 8 - 5

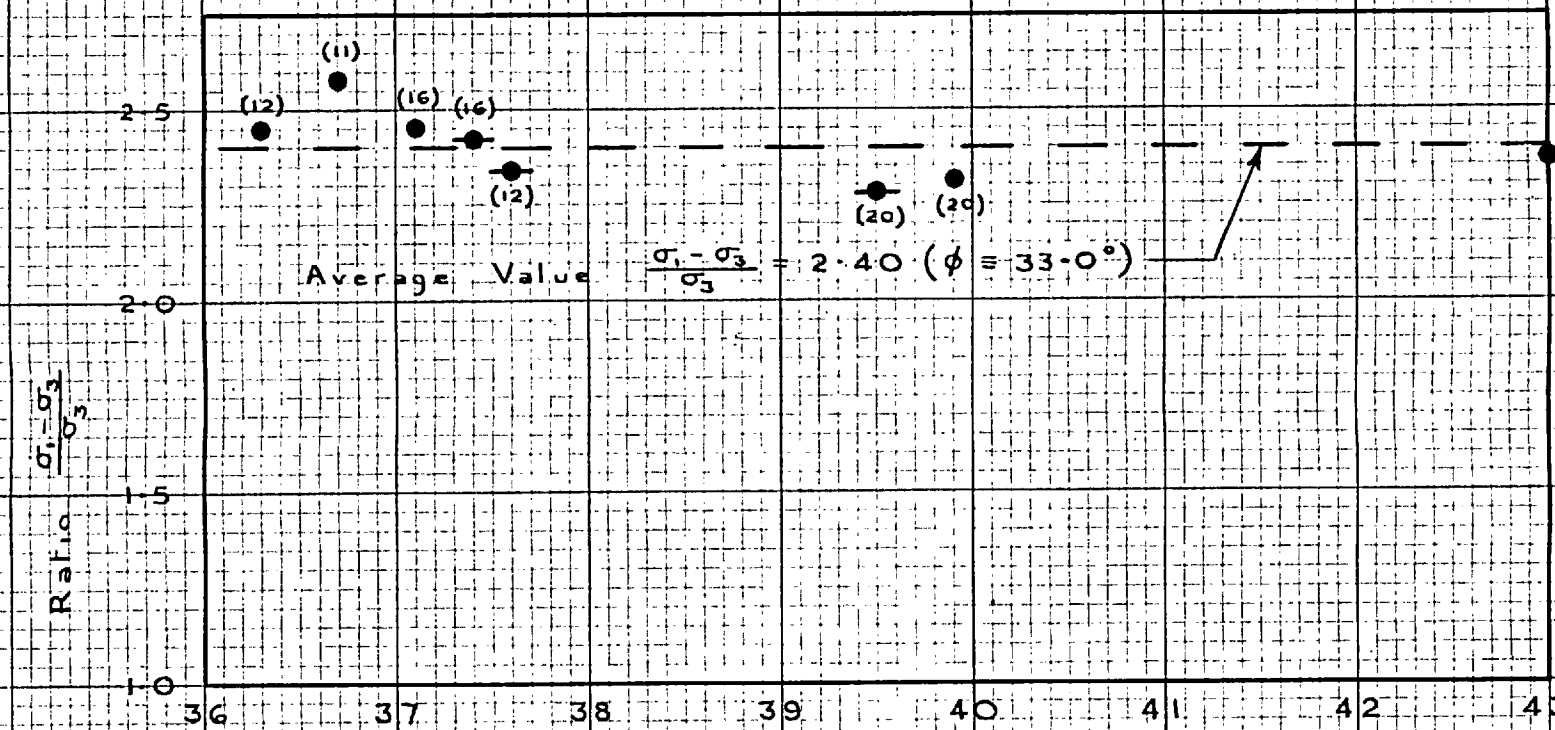



STANDARD TRIAXIAL - EFFECT OF STRESS HISTORY ON FAILURE CHARACTERISTICS

Series E - $K_o$ consolidation; cell pressure constant = 40 lb/sq.in., axial stress increased to failure. Drained.

Series F - $K_o$ consolidation; axial stress constant, cell pressure decreased to failure (at approx. 40 lb./sq.in.). Drained.

FIG. 8 - 6

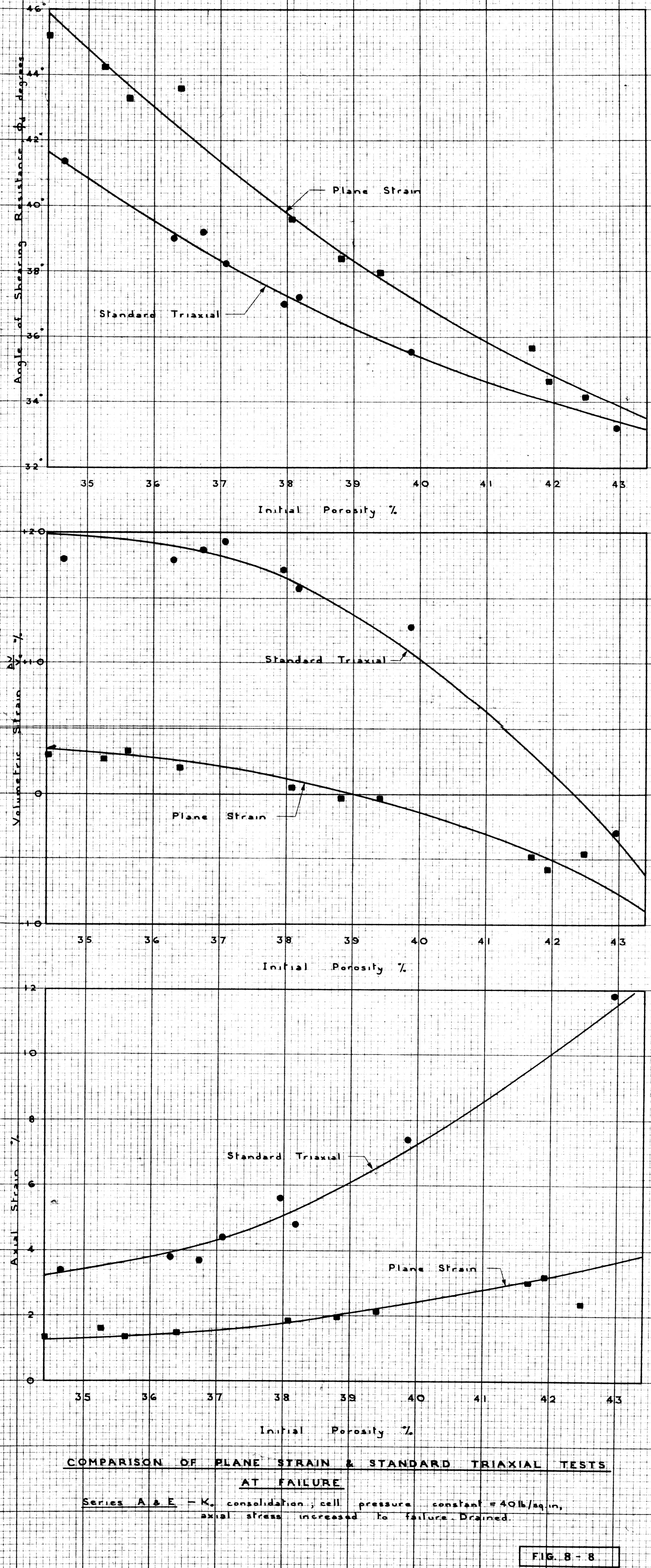



STANDARD TRIAXIAL - ULTIMATE STRENGTHS

● Series E —●— Series F

The Eldin (1951) area corrections are:- the measured strength, based on the assumption that the specimen retains the shape of a right cylinder during shear, under-estimates the true strength by a negligible amount at up to 6% axial strain, by 1½% at 11% axial strain and by 3% at 20% axial strain. As the ultimate strength varies slightly with the strain at which the calculation is made (see text), the strain is shown in brackets on the graph.

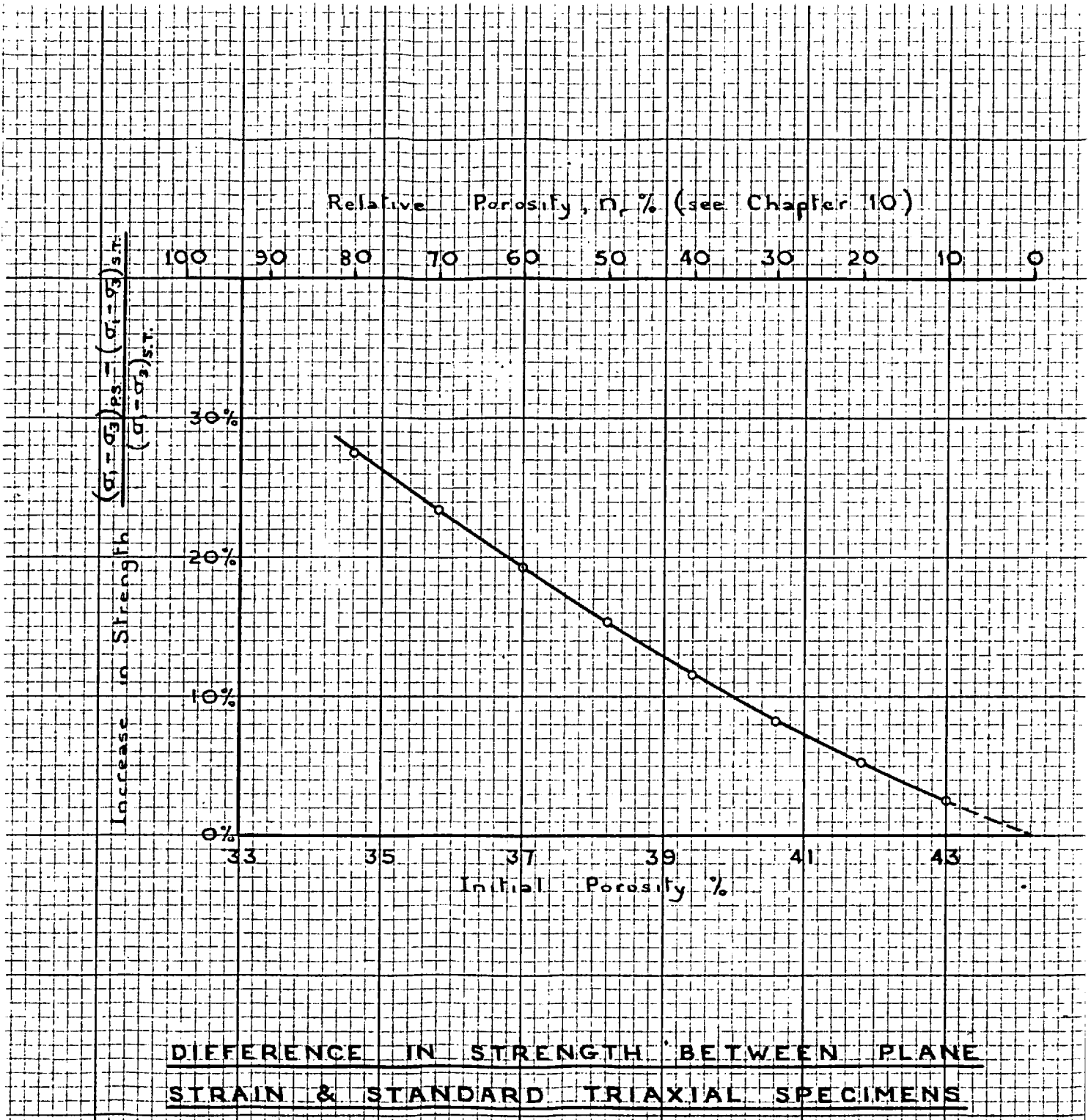
FIG. 8 - 7




COMPARISON OF PLANE STRAIN & STANDARD TRIAXIAL TESTS AT FAILURE

Series A & E – $K_o$ consolidation ; cell pressure constant = 40 lb/sq in, axial stress increased to failure. Drained.

FIG. 8 - 8

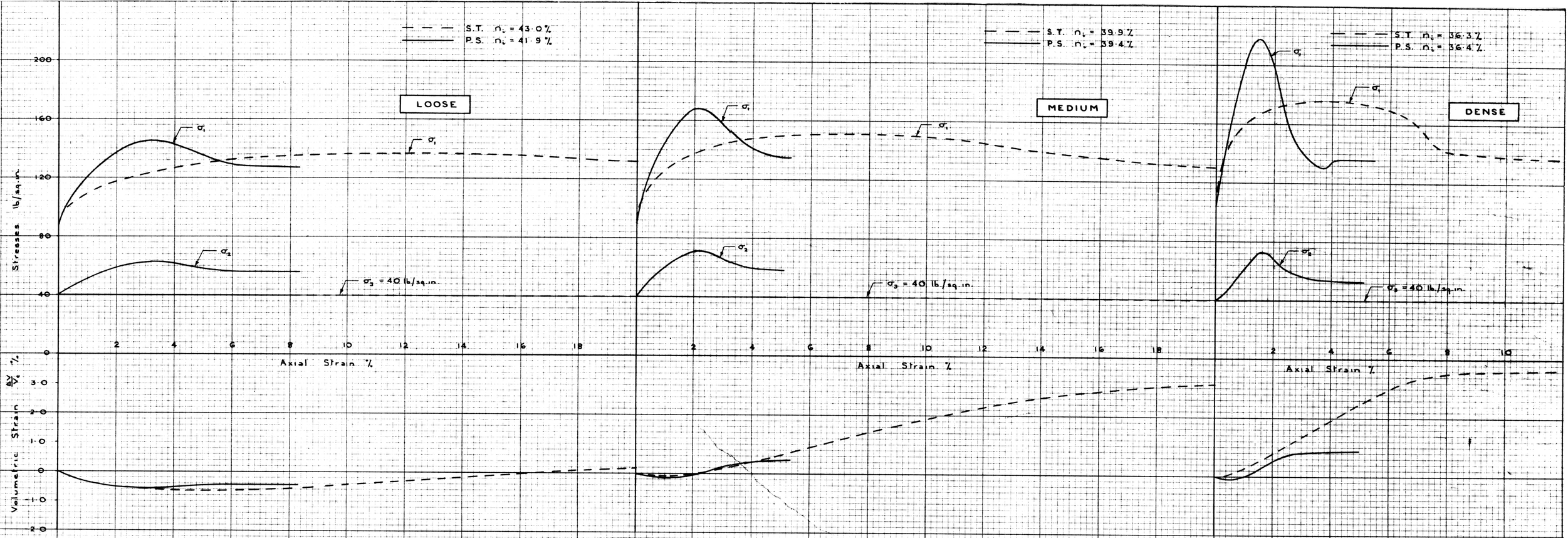



DIEFERENCE IN STRENGTH BETWEEN PLANE STRAIN & STANDARD TRIAXIAL SPECIMENS

$K_o$ = consolidated, drained compression tests.
Cell pressure = 40 lb/sq in.
Comparison at peak deviator stress.

Note:- $$\frac{(\sigma_1-\sigma_3)_{P.S.}-(\sigma_1-\sigma_3)_{S.T.}}{(\sigma_1-\sigma_3)_{S.T.}} = \frac{R_p - R_s}{R_s}$$ (see Chapter 10)

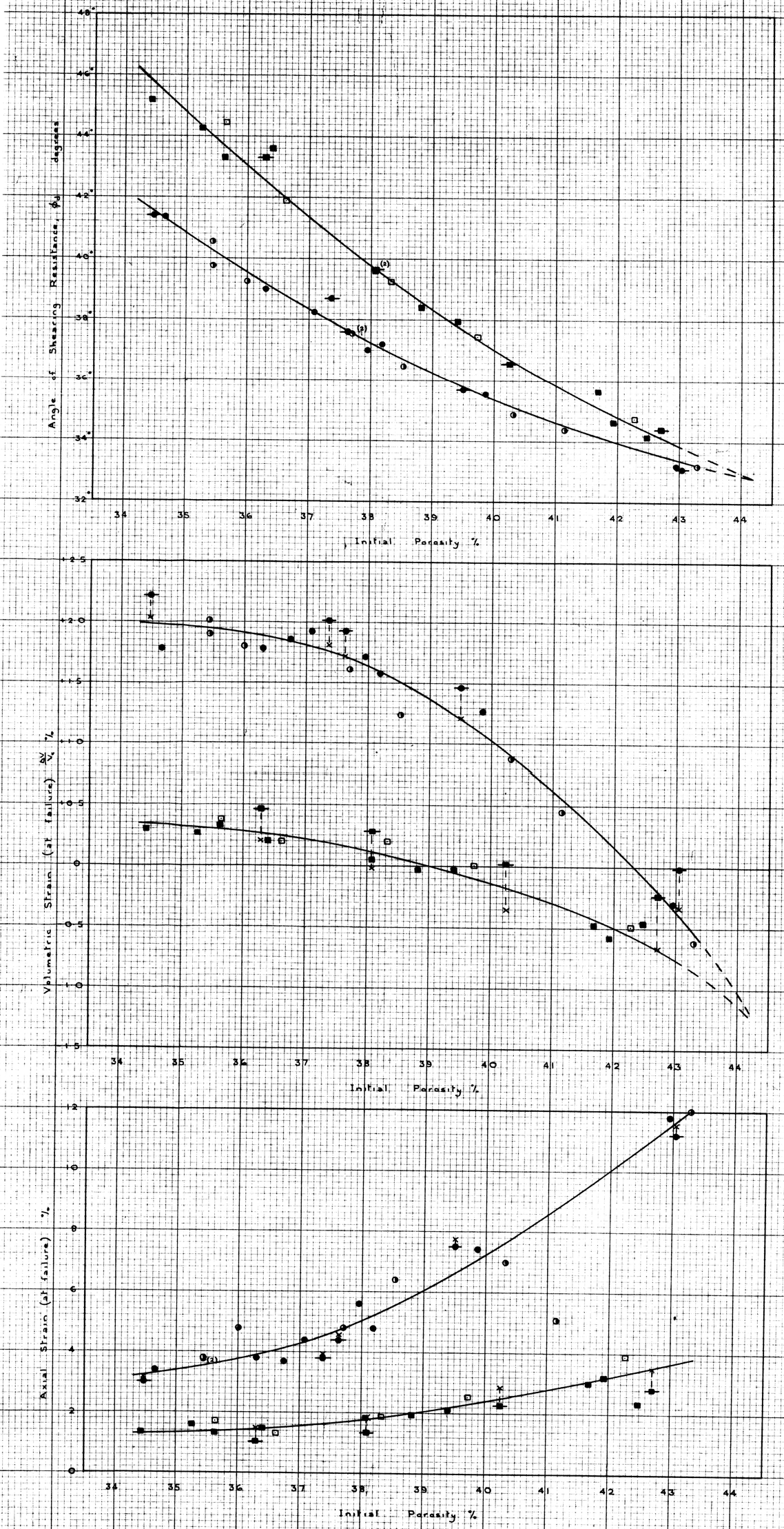
FIG. 8-9




COMPARISON OF PLANE STRAIN AND STANDARD TRIAXIAL TESTS AT THREE DIFFERENT DENSITIES

$K_o$ consolidation ; Cell pressure constant, axial stress increased under drained conditions to failure.

FIG. 8 - 10









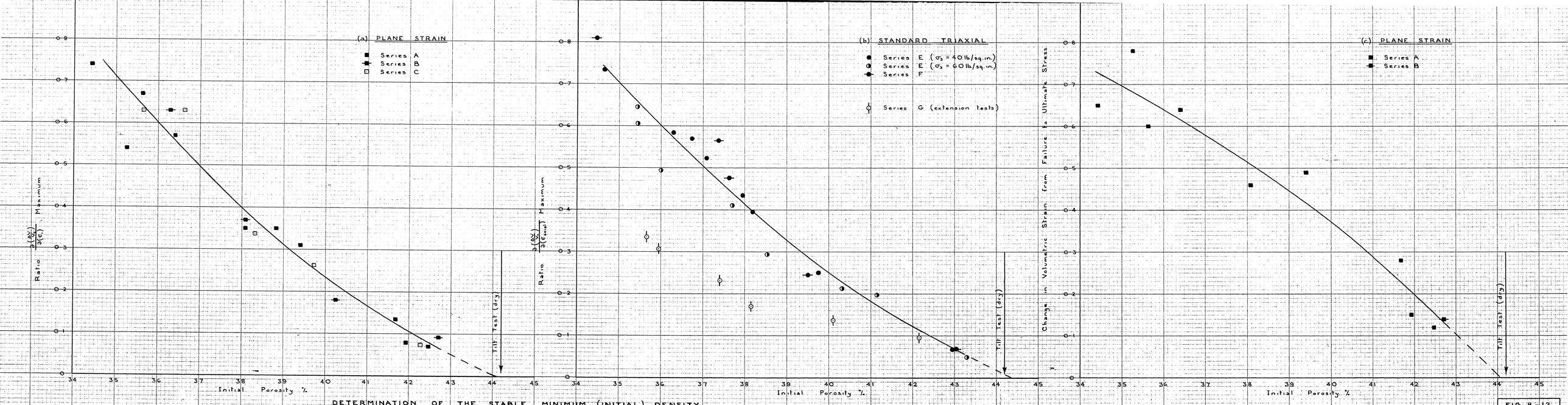

COMPRESSION TESTS - SUMMARY CURVES (DRAINED)

Plane Strain :-
- Series A
- Series B
- Series C

Standard Triaxial :-
- Series E ($\sigma_3$ = 40 lb/sq.in.)
- Series E ($\sigma_3$ = 60 lb/sq.in.)
- Series F

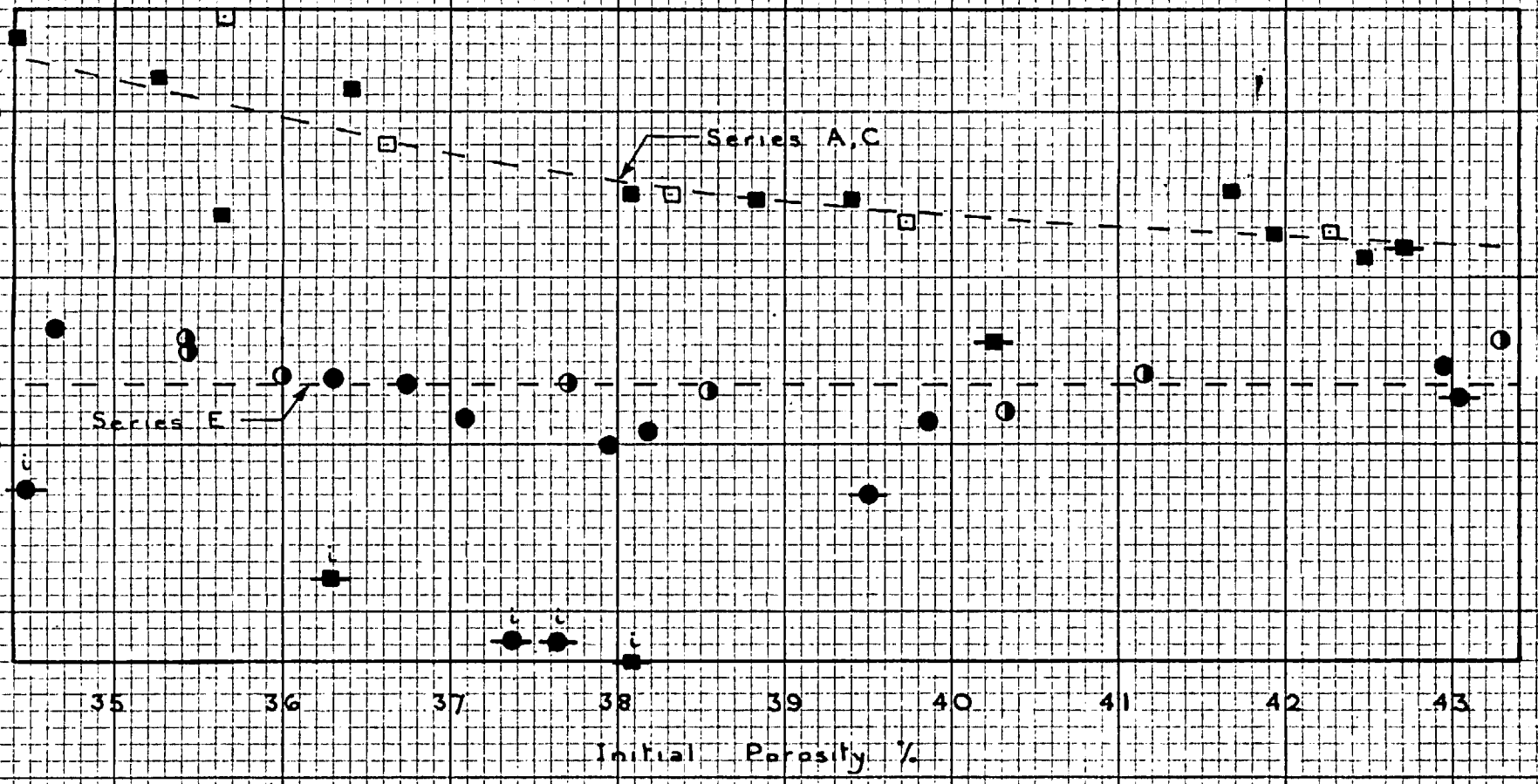
The behaviour of the intermediate principal stress at failure is summarized on Fig. 8 - 4.

FIG. 8 - 11




DETERMINATION OF THE STABLE MINIMUM (INITIAL) DENSITY

FIG. 8-12




PLANE STRAIN & STANDARD TRIAXIAL - STRESS RATIOS AT MINIMUM VOLUME

Plane Strain :-

- ■ Series A
- ■ Series B
- ⊡ Series C

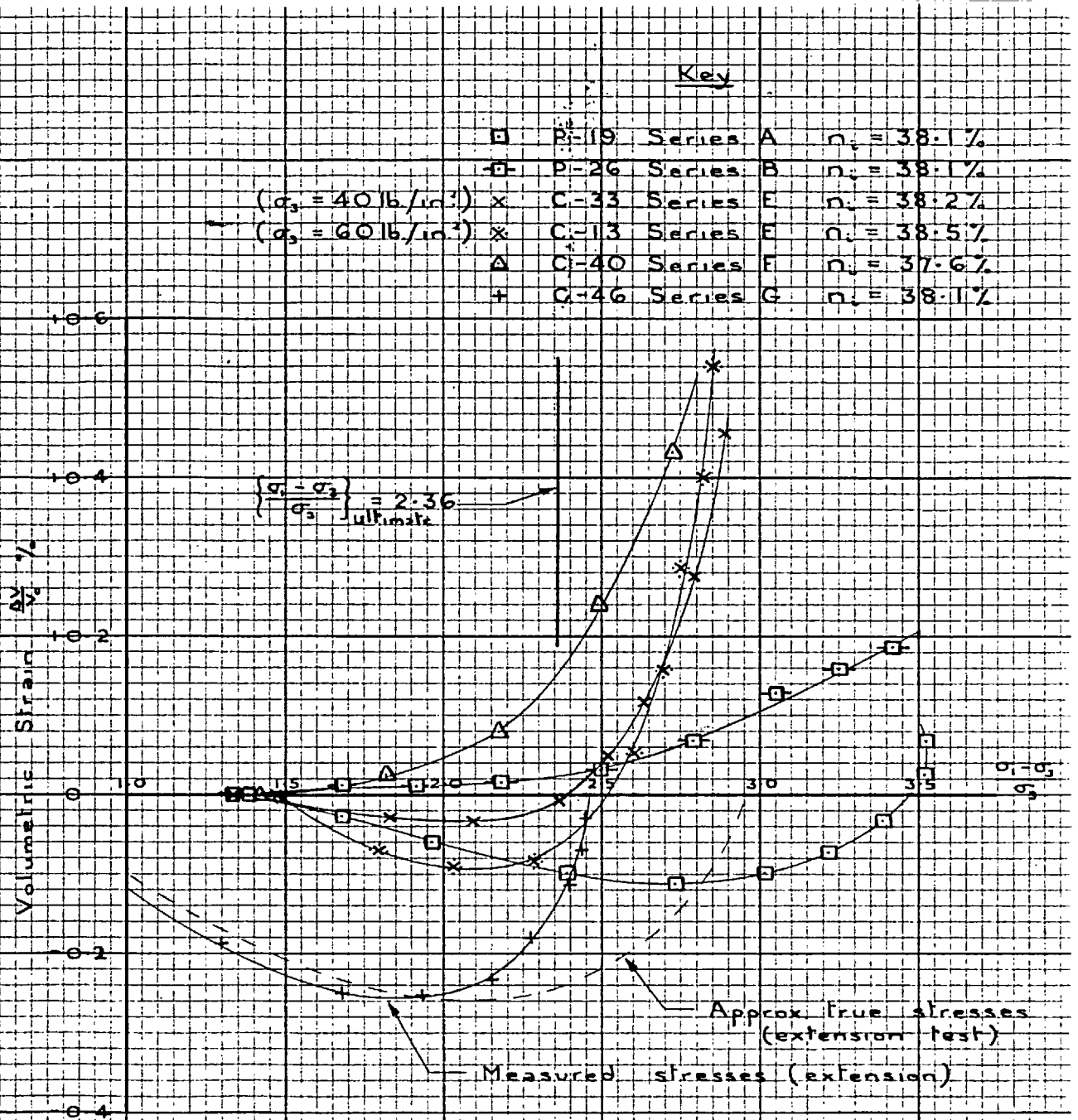
Standard Triaxial :-

- ● Series E ($\sigma_3$ constant = 40 lb/sq.in.)
- ◑ Series E ($\sigma_3$ constant = 60 lb/sq.in.)
- ⊖ Series F

i denotes immediate dilatation at the commencement of shear phase.

Average value of ratio $\frac{\sigma_1 - \sigma_3}{\sigma_3}$ for series E = 2·18 i.e. $\phi$ = 31·5°

FIG. 8 - 13



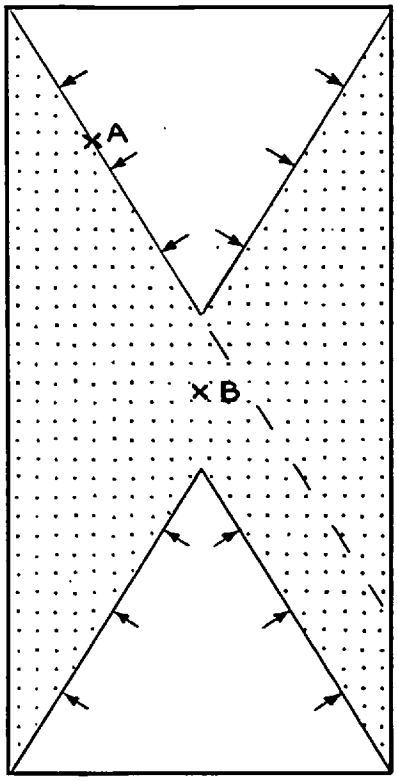

## RELATION BETWEEN VOLUME CHANGES & PRINCIPAL STRESS RATIO

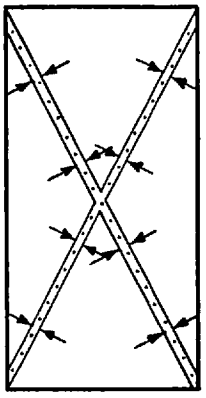
(Medium dense specimens)

Note Standard Triaxial specimens at $n_i$ = 38·0% have the following failure characteristics:-

$\left\{\frac{\sigma_1-\sigma_3}{\sigma_3}\right\}$ = 3·06 $\frac{\Delta V}{V_c}$ = +1·65

FIG. 8-14



Standard Triaxial

Plane Strain

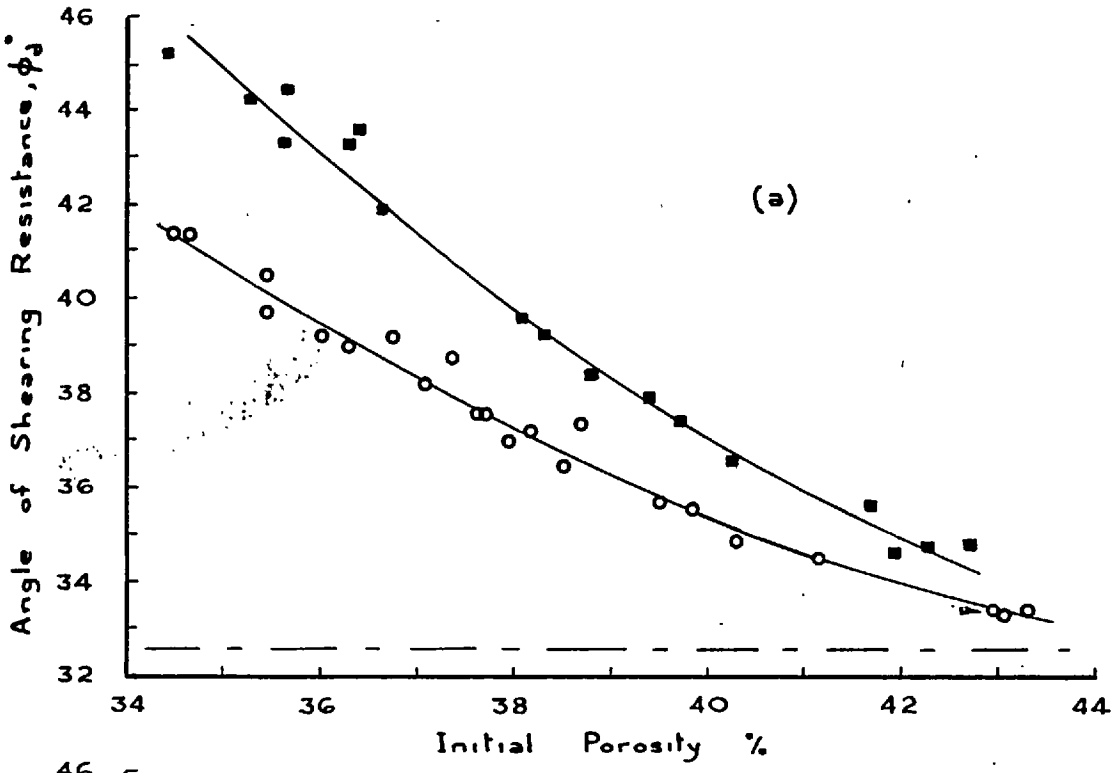
Dilating zone

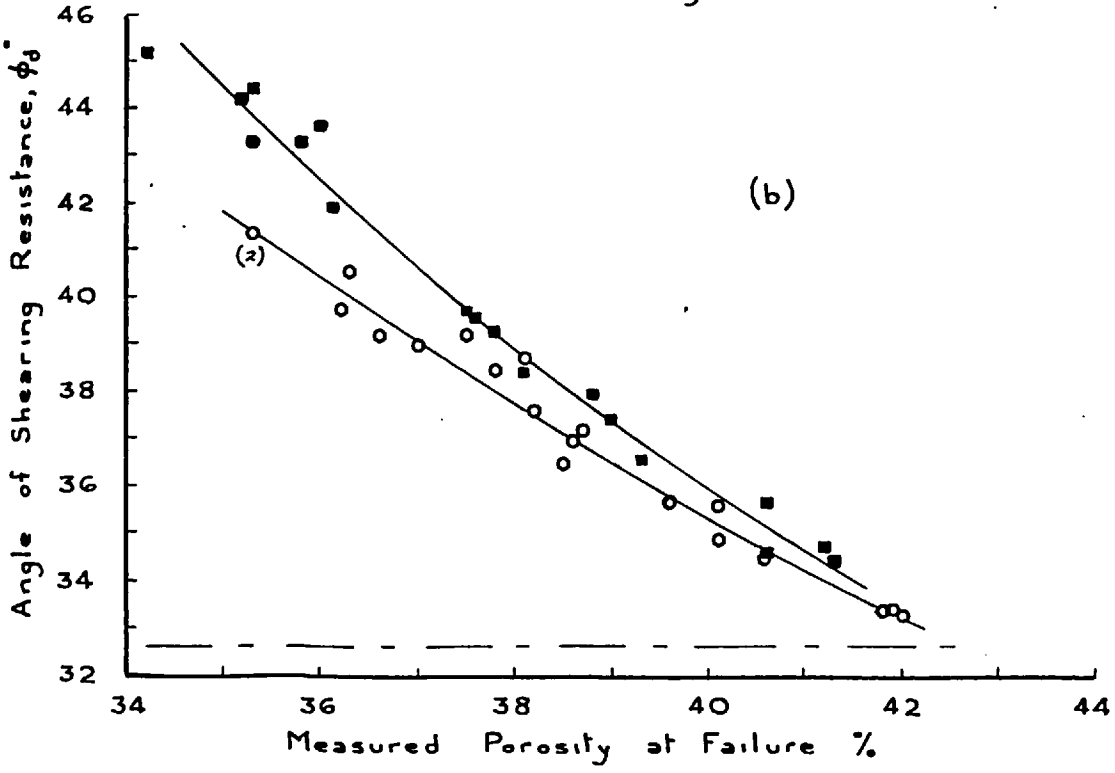
Non-dilating zone

PROBABLE DILATING ZONES

(Half Scale)

FIG. 8-15

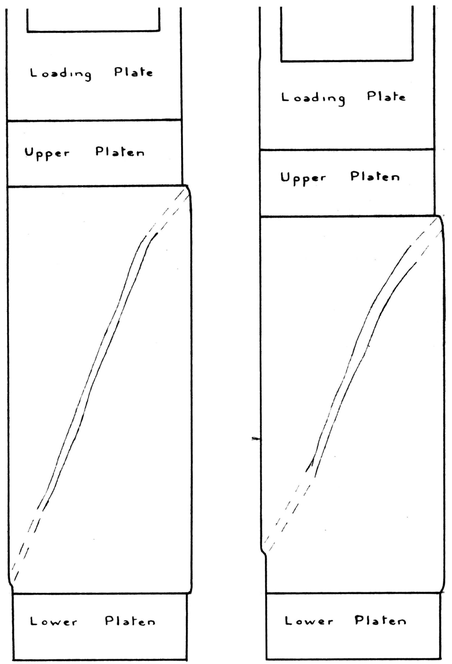



**STRENGTH - DENSITY RELATIONSHIPS :-**
**COMPARISON OF INITIAL & FAILURE POROSITIES**

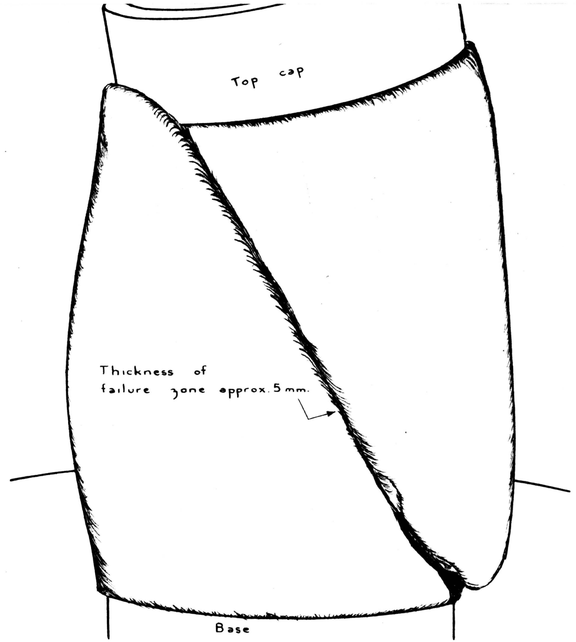
FIG. 8 - 16

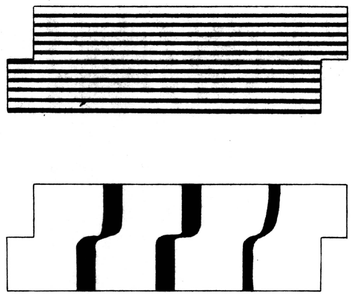
KEY :- ■ Plane strain drained tests
o Standard triaxial drained (compression) tests
—— - —— - Ultimate strength (average)

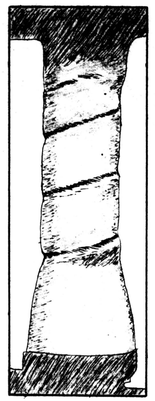


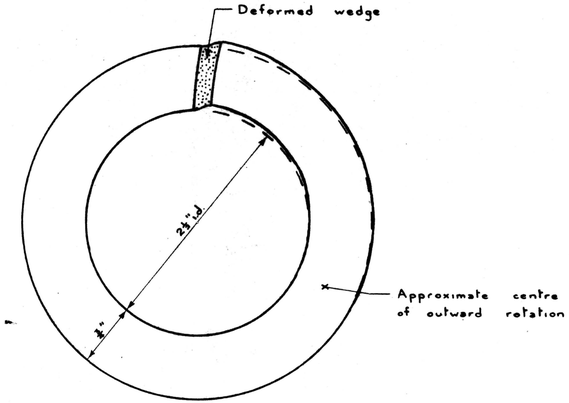











Type of Test :- PLANE STRAIN

Source :- Cornforth

Description :- Left: P-17, $n_i$ = 34·4 % very dense. Right: P-18, $n_i$ = 39·4 % medium density. Both drawings approx. full scale

Type of Test :- STANDARD TRIAXIAL

Source :- Cornforth

Description :- C-26, $n_i$ = 39·5 %, medium density. Free-hand sketch at axial strain of 26 %. Approx. full scale drawing.

Type of Test :- SHEAR BOX

Source :- Hafiz (1950)

Description :- 12 in. square × 4 in. deep box. Layers of dyed sand. Drawn from photographs.

Type of Test :- TORSION

Source :- Habib (1953)

Description :- Loose sand, spiral failure. Sketched from a photograph.

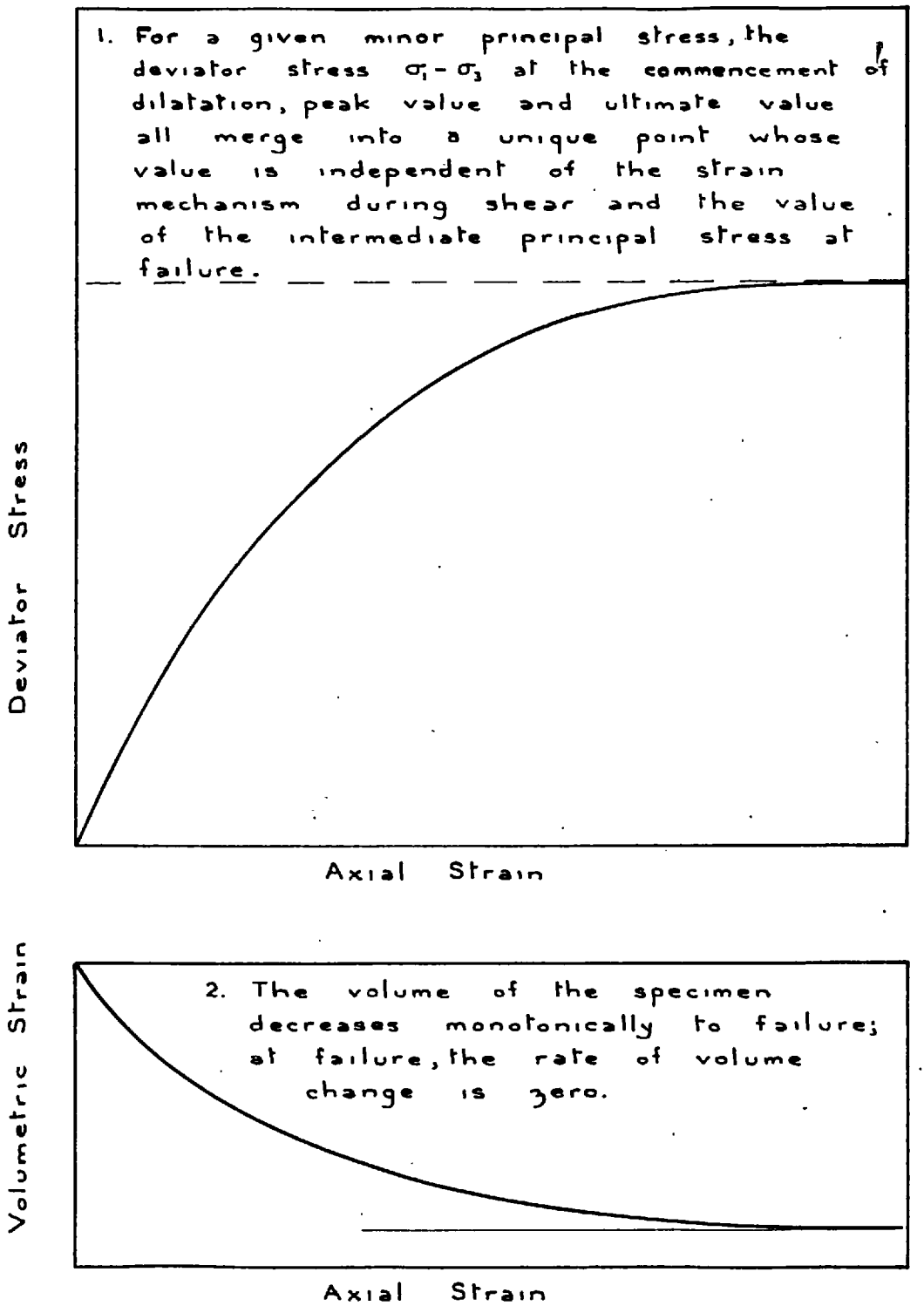
Type of Test :- THICK CYLINDER

Source :- Kirkpatrick (1954)

Description :- Dense sand, failure occurs by outward movement of one wall of the vertical crack. Approx. full scale.

## EXAMPLES OF FAILURES WITHIN A NARROW ZONE

FIG. 8 - 17




## CONDITIONS AT THE MINIMUM STABLE DENSITY

FIG. 8 - 18

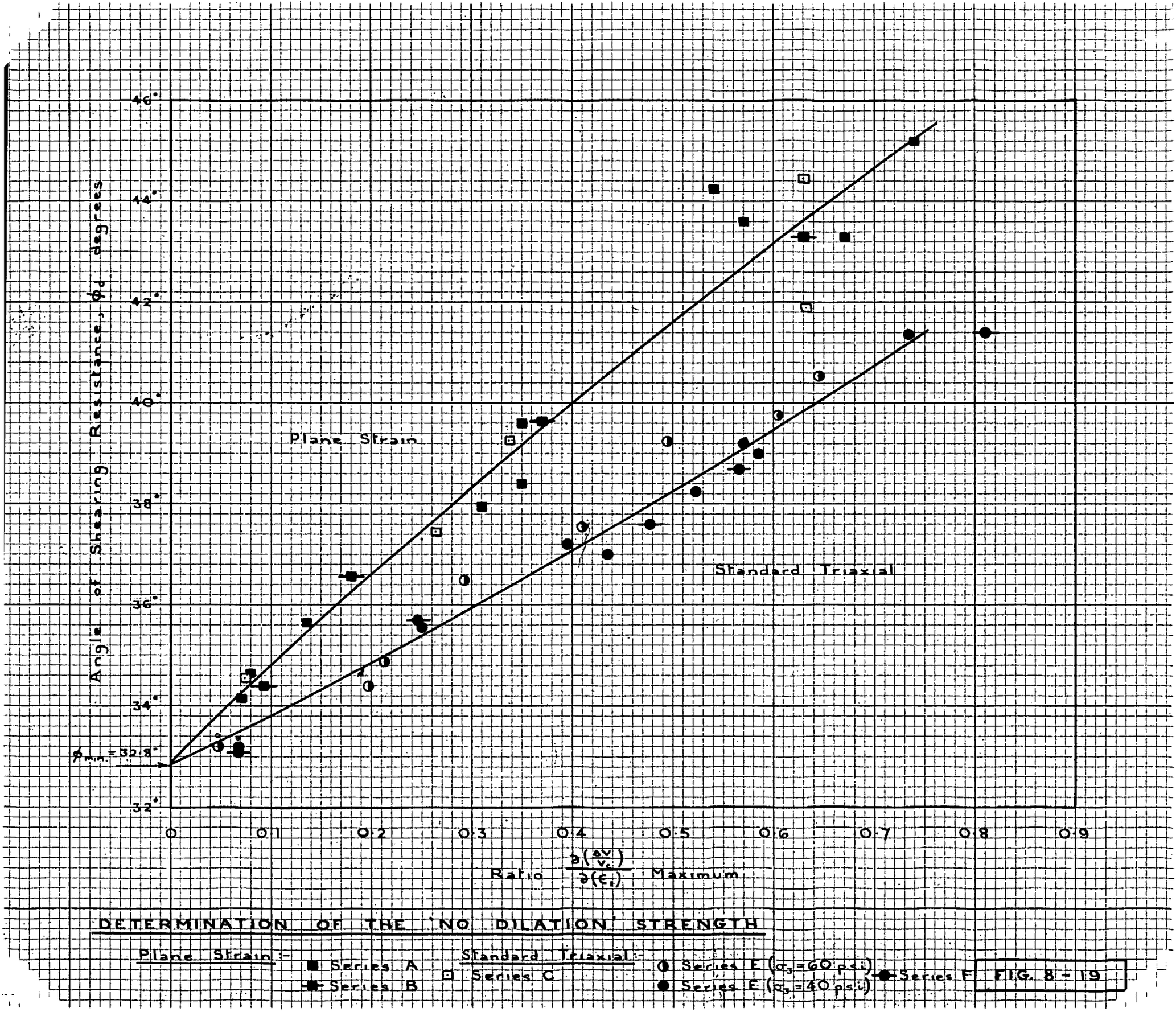

Angle of Shearing Resistance, $\phi_d$ degrees
46°
44°
42°
40°
38°
36°
34°
32°
$\phi_{min.} = 32.8°$
Plane Strain
Standard Triaxial
0
0·1
0·2
0·3
0·4
0·5
0·6
0·7
0·8
0·9
Ratio $\frac{\partial(\frac{\Delta V}{V_c})}{\partial(\epsilon_1)}$ Maximum
DETERMINATION OF THE 'NO DILATION' STRENGTH
Plane Strain :- Series A, Series B
Standard Triaxial :- Series C, Series E ($\sigma_3$=60 p.s.i.), Series E ($\sigma_3$=40 p.s.i.), Series F

FIG. 8 - 19

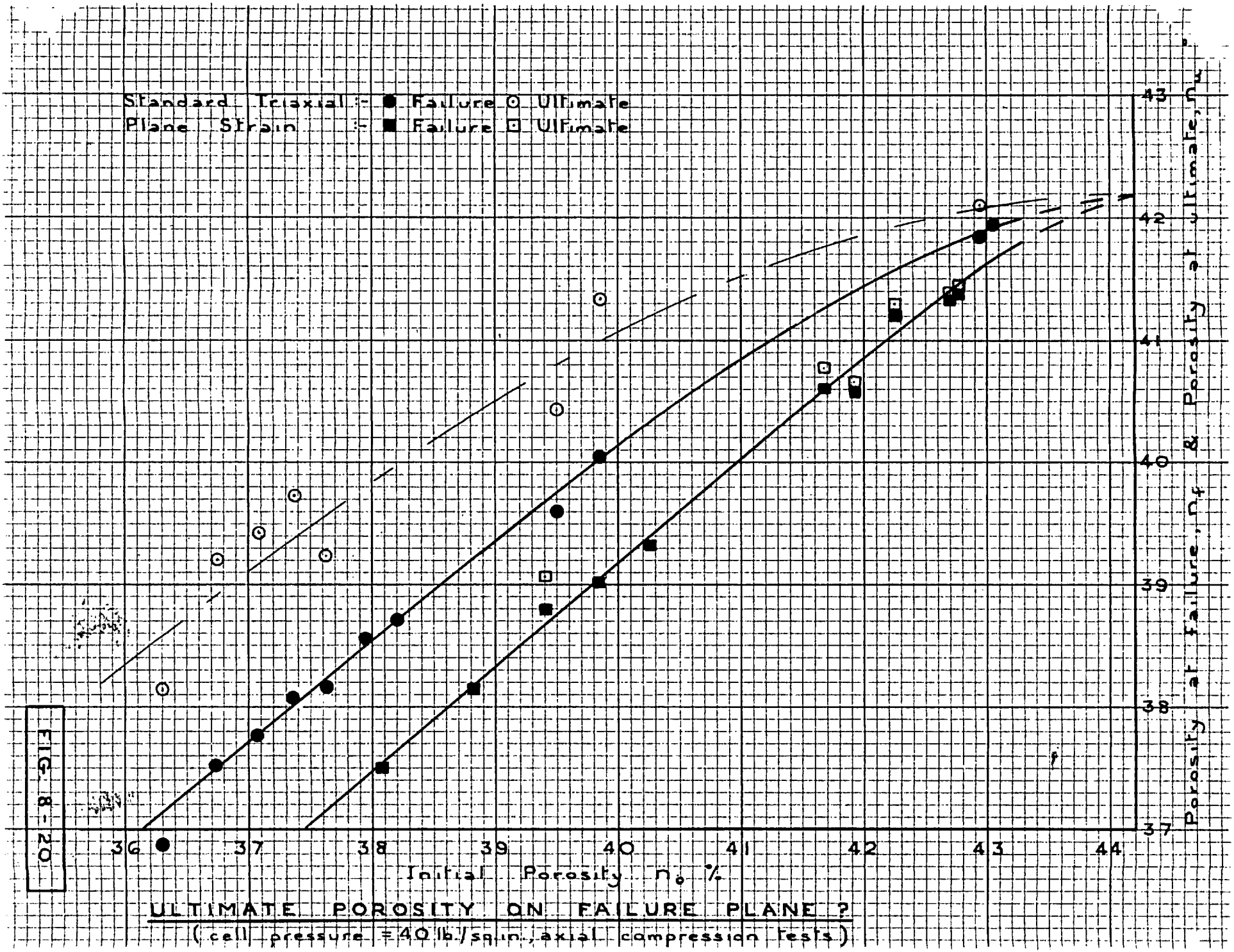
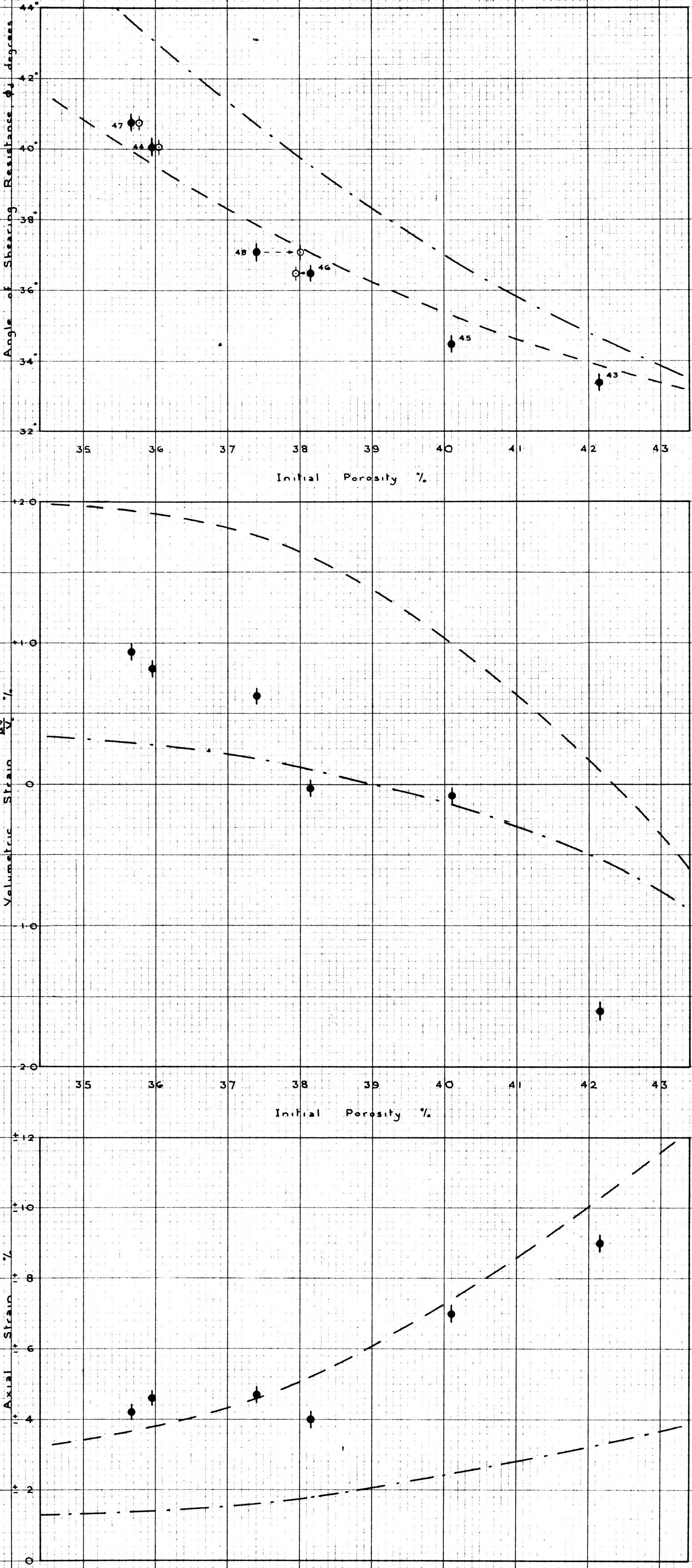



FIG. 8-20

ULTIMATE POROSITY ON FAILURE PLANE ?

(cell pressure = 40 lb/sq.in., axial compression tests)




STANDARD TRIAXIAL EXTENSION TESTS

● Series G – $K_o$ consolidation; cell pressure ($\sigma_1$) constant, axial stress ($\sigma_3$) decreased to failure. Drained.

— — — Standard triaxial compression curves abstracted from summary curves Fig. 8 - 11

—— · —— Plane strain compression curves abstracted from summary curves Fig. 8 - 11

FIG. 8 - 21

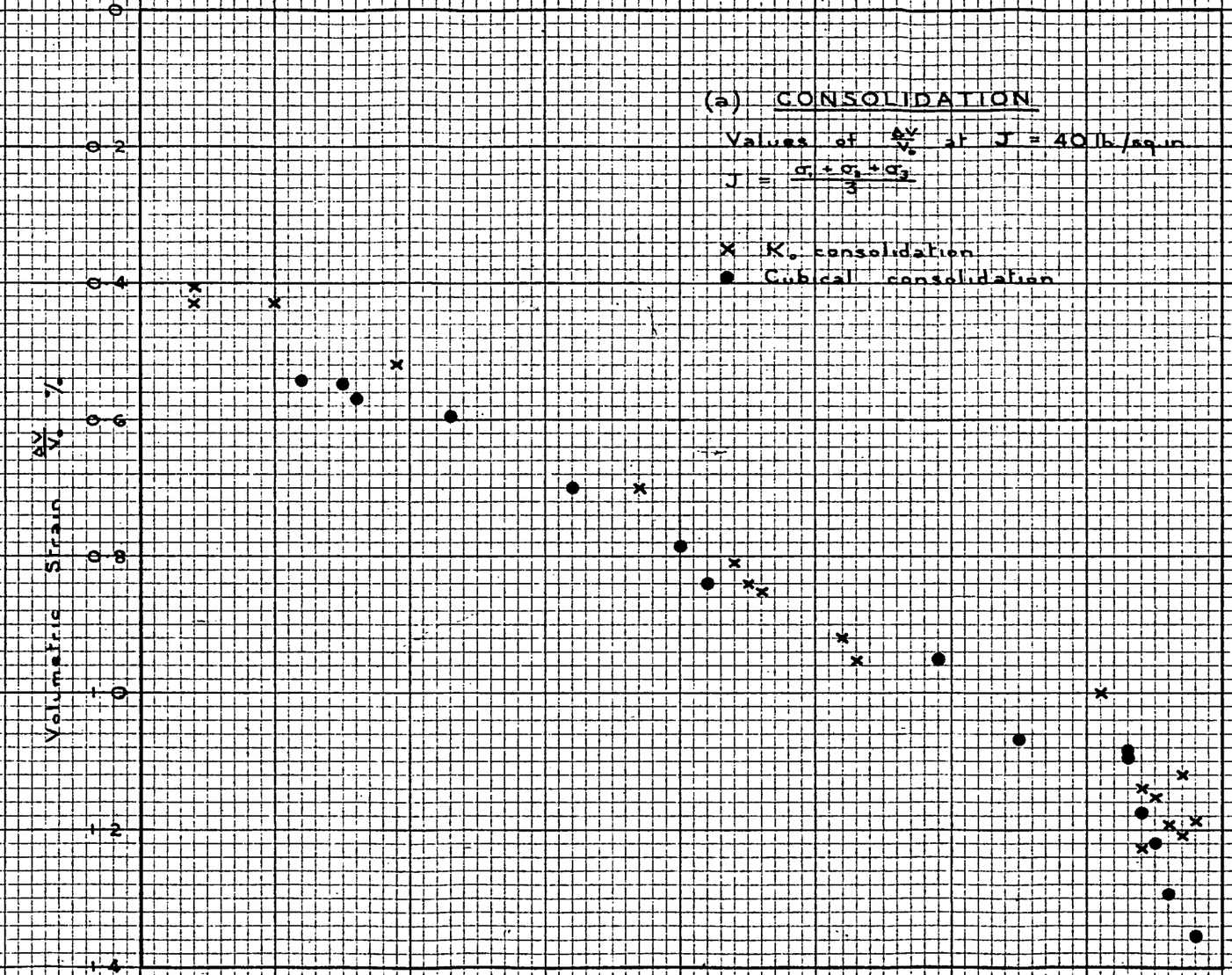
(a) CONSOLIDATION

Values of $\frac{\Delta V}{V_0}$ at $J$ = 40 lb/sq in

$J = \frac{\sigma_1 + \sigma_2 + \sigma_3}{3}$

× $K_o$ consolidation

● Cubical consolidation




(b) J = constant TESTS

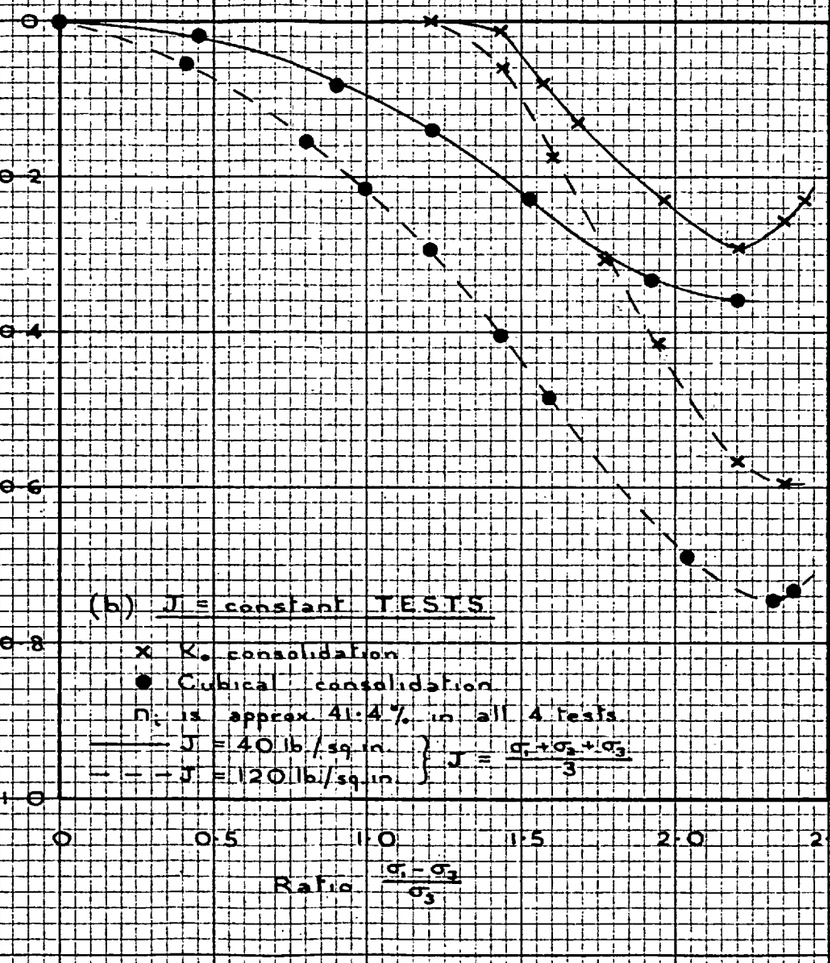
× $K_o$ consolidation

● Cubical consolidation

$D_r$ is approx. 41·4 % in all 4 tests.

——— J = 40 lb/sq in. } $J = \frac{\sigma_1 + \sigma_2 + \sigma_3}{3}$

– – – J = 120 lb/sq in. }



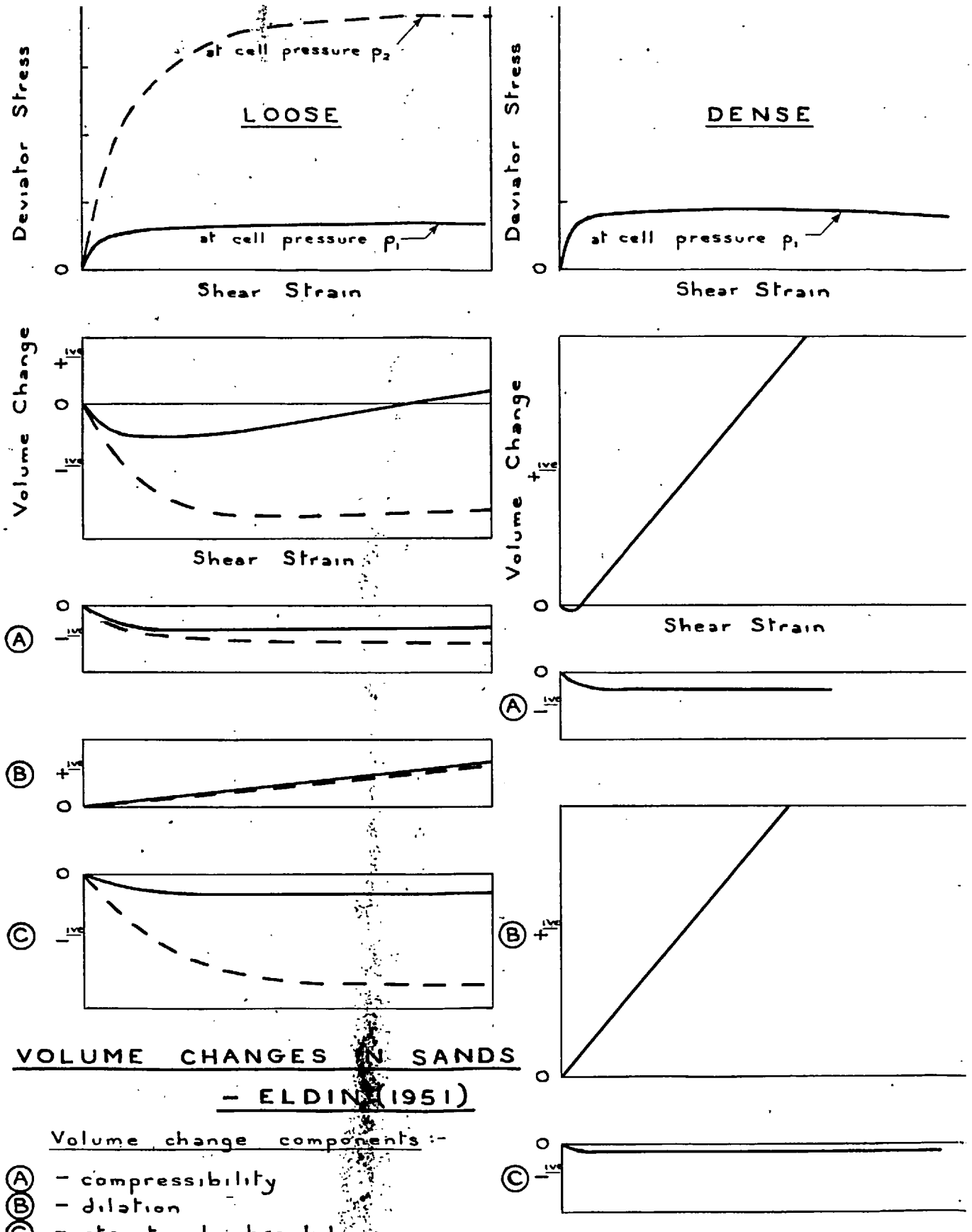

## VOLUME CHANGES IN SANDS – FRASER (1957)

Conclusions :-

(a) For the same $J$, volume changes under cubical and $K_o$ consolidation are approx. equal at all porosities.

(b) During shear, volume changes take place due to changes in principal stress ratio, even though $J$ remains constant. When dilatation occurs, the volume changes are approx. equal for the same $J$.

FIG. 8 – 22



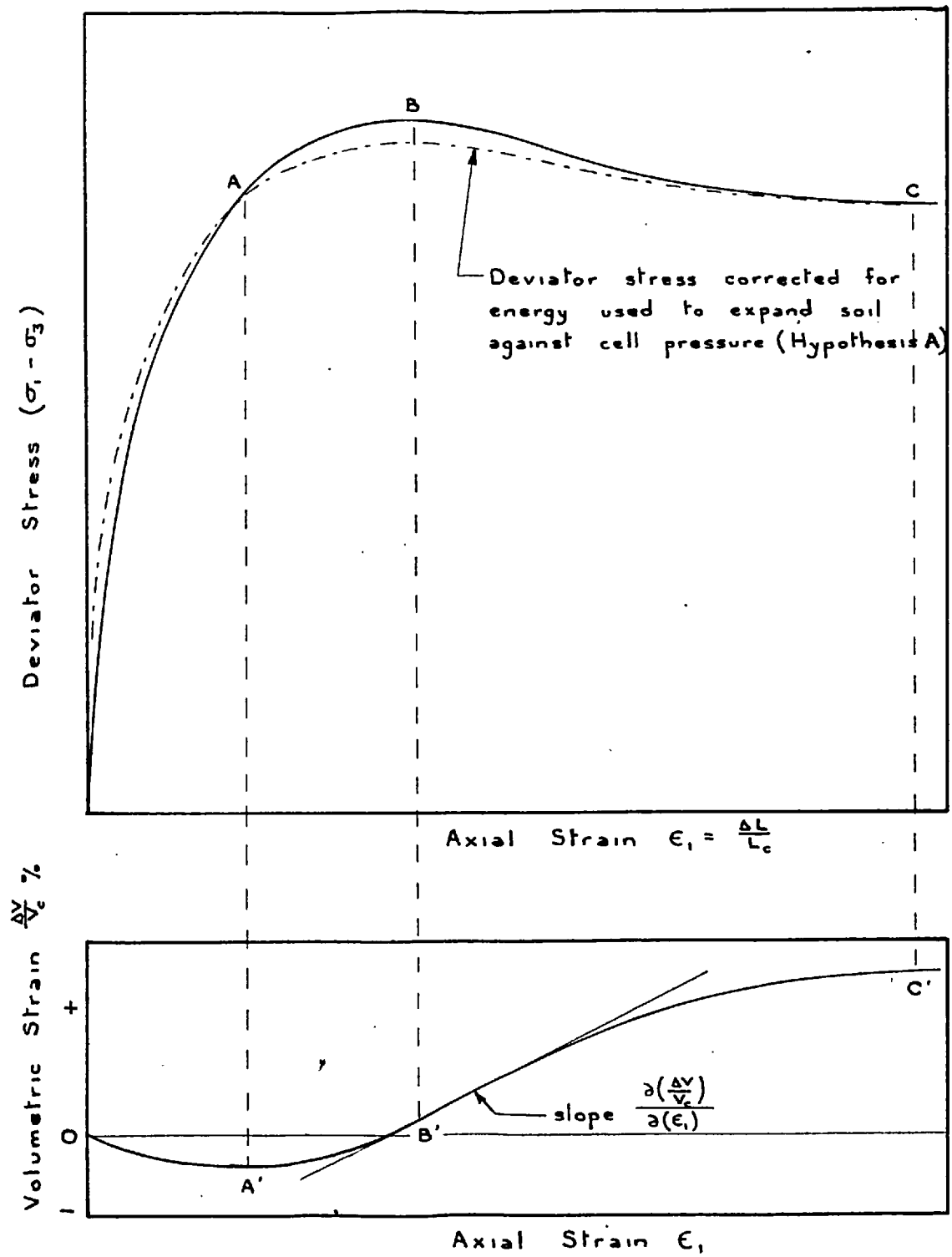

## VOLUME CHANGES IN SANDS

## - ELDIN (1951)

Volume change components :-

(A) - compressibility
(B) - dilation
(C) - structural breakdown

FIG. 8 - 23

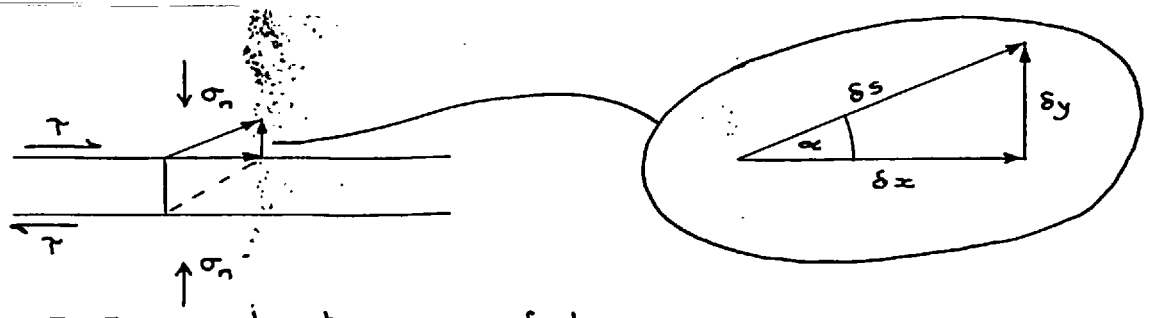



**TYPICAL DRAINED TRIAXIAL COMPRESSION TEST**

(All-round cell pressure constant, axial stress increased to failure)

Points A - A' Apparent point of dilation.
B - B' Peak or maximum deviator stress
C - C' 'Ultimate' shear stress (constant volume)

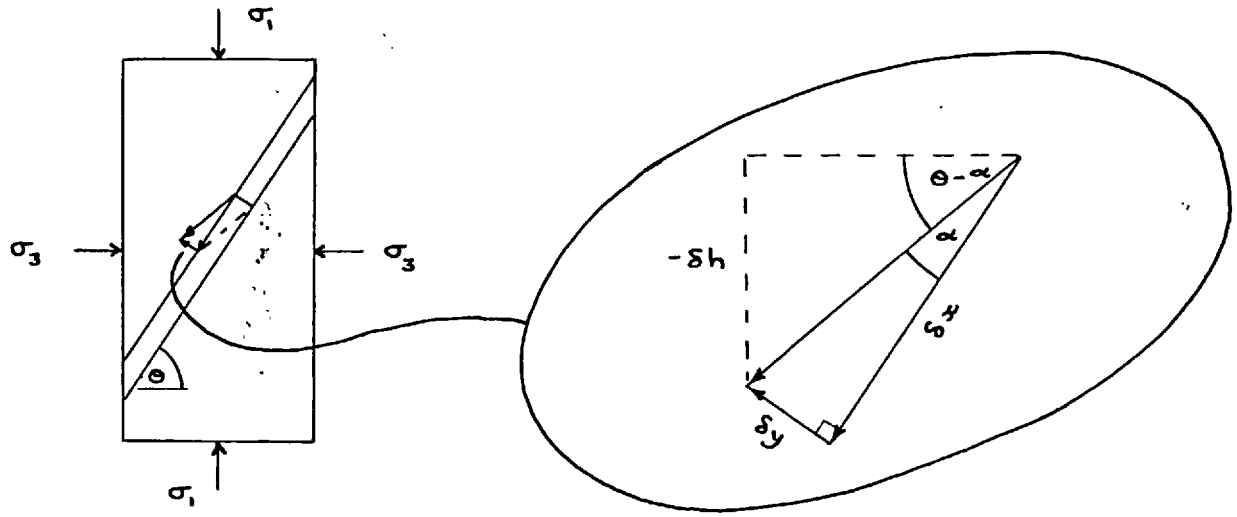
FIG. 8 - 24



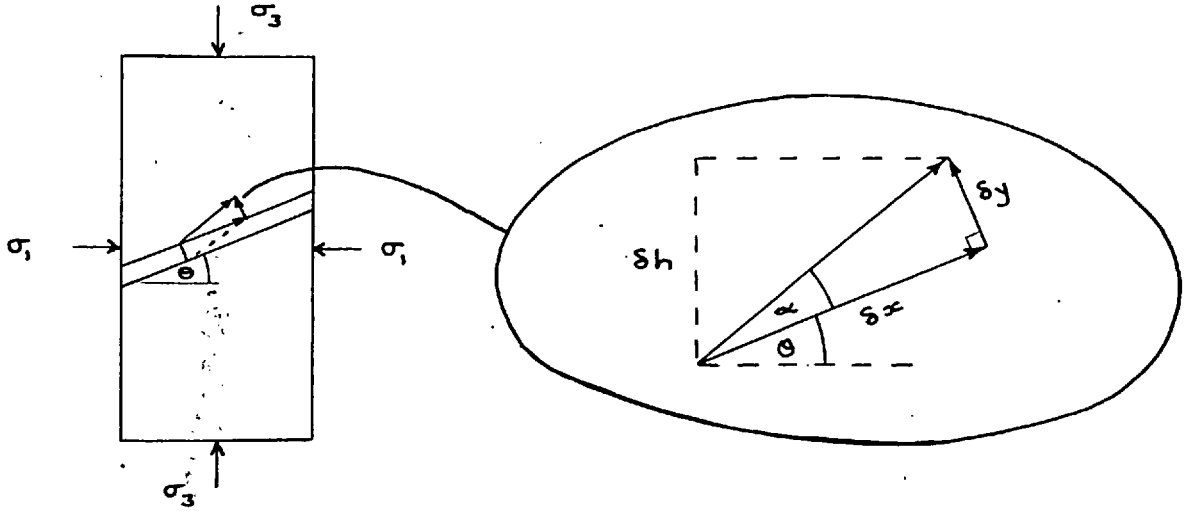

$\sigma_n$ = normal stress on failure zone

$\tau$ = shear stress on failure zone

(a) the $\alpha$ concept of dilatancy




(b) deformation in compression test




(c) deformation in extension test

## Hypothesis B. FAILURE ZONE IN SIMPLE SHEAR

FIG. 8-25

(a) PLANE STRAIN COMPRESSION

(b) STANDARD TRIAXIAL COMPRESSION

(c) STANDARD TRIAXIAL EXTENSION

(d) SHEAR BOX

Friction Angles $\phi_d$ & $\phi$

Minimum Porosity

Maximum Porosity

Initial Porosity, $n_o$ %

45° 40° 35° 30° 25°

33 34 35 36 37 38 39 40 41 42 43 44

50° 45° 40° 35° 30° 25°

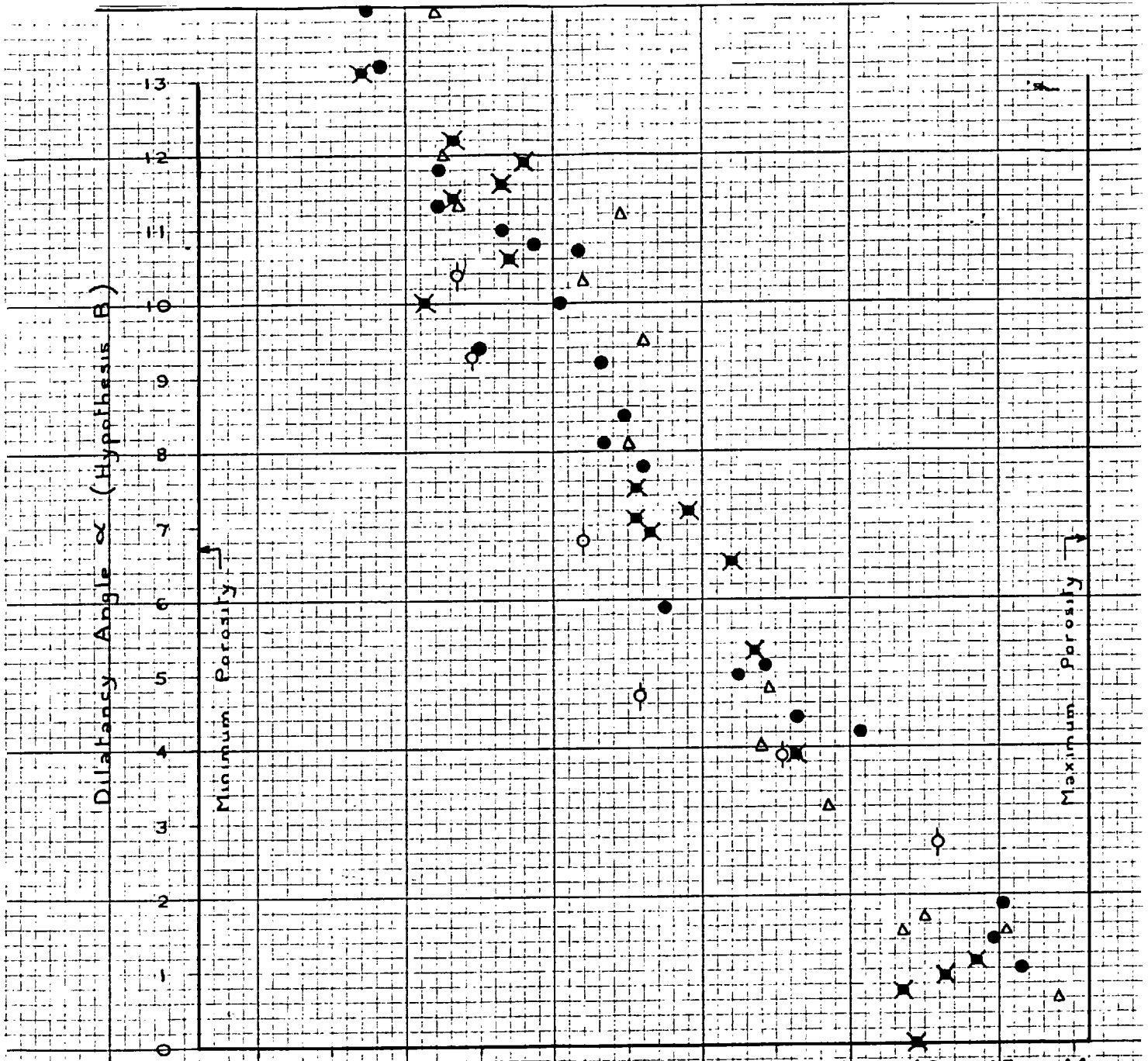
**SIMPLE SHEAR FAILURE ZONE HYPOTHESIS**

**– ANALYSIS OF TEST DATA**

Key :-

⊙ $\phi_d$ values (= $\phi$ + ∝)  × $\phi$ values

FIG 8-26




## RELATIONSHIP BETWEEN ANGLE ∝ AND DENSITY – ALL TYPES OF TEST

Key :-

- Plane Strain Compression (at failure, not max. dilatancy)
- Standard Triaxial Compression
- Standard Triaxial Extension
- Standard Shear Box

FIG. 8 – 27

## Chapter 9 UNDRAINED TEST RESULTS AND DISCUSSION

The previous information available on the undrained shear strength of cohesionless materials has been limited by the dilation of the soil, which produces large negative pore-water pressures during shear (see Chapter 5, page 37). The comparatively small net increase in volume of the drained plane strain tests at failure suggested that a much wider range of densities could be tested undrained in this apparatus and it proved to be the case. Consequently, the plane strain test results, obtained over a wide range of placement densities, give a greater insight into the behaviour of dilatant cohesionless soils under undrained conditions than has hitherto been possible. The undrained test results will be analysed using the concepts of the preceding chapter as a basis. It will be seen that some commonly held opinions on the undrained test are fallacious.

### I. Plane Strain Tests

#### Stress-strain curve

The results of a typical consolidated-undrained plane strain test (P-32) on a medium dense sand are plotted on Figure A10-22. The specimen was first consolidated under a cell pressure of 4 lb/sq.in. and then the cell pressure was increased to 60 lb/sq.in. under undrained conditions. This placed a positive pore-water pressure of 56 lb/sq.in. on the specimen prior to shear and ensured that the pore pressures remained positive throughout the test. In the shear test, the pore pressure increased slightly in the early stages and later decreased until a fairly constant value was reached. The deviator stress, $(\sigma_1 - \sigma_3)$, rose rapidly at first and then continued to rise until it reached a peak value at an axial strain of 5.6%.

Below the stress curves are plotted the effective deviator stress ratios, $(\sigma_1' - \sigma_3') / \sigma_3'$ and $(\sigma_3' - \sigma_3') / \sigma_3'$. Both of the deviator stress ratios rise to a peak value at an axial strain of approximately 1.75%, long before the maximum deviator stress is

is attained. Furthermore, the levelling off in the pore pressure curve is associated with the two deviator stress ratios reaching approximately constant residual values. The two curves immediately suggest a similarity with the fully drained tests where the corresponding curves rise to a peak and then decrease to the ultimate condition.

This similarity in the characteristics of the drained and undrained tests was recognised early in the investigation and the programme of undrained tests was devised with two separate objectives in mind, as follows :-

(i) to shear the soil so that the minor principal stress was approximately 40 lb/sq.in. when the maximum principal stress ratios were reached (Specimens P-28, P-29, P-30, P-31, P-35).

(ii) to shear the soil so that the maximum deviator stress would be reached before cavitation of the pore water occurred (Specimens P-32, P-33, P-34). These tests were consolidated under a lower effective cell pressure than for objective (i).

The common objective of the undrained test series was to take advantage of the less dilatant characteristics of the sand in plane strain to investigate undrained strengths over a wide range of densities; in particular, to shed some light on the behaviour of the soil at the maximum principal stress ratio and the maximum deviator stress in the undrained test. The reader is reminded that these two conditions are coincidental in all fully drained tests.

Strength at maximum principal stress ratio

The comparison between the drained and undrained tests at the maximum principal stress ratio condition is given on Fig. 9-1. The undrained shear strength values are in excellent agreement with the drained test strength-density curve except, perhaps, for the two tests at the dense end of the curve. However, the end-of-test moisture content determinations on

specimen P-31 (Table 7-1) suggest that the soil was probably looser than the measured porosity so this result is of questionable accuracy. The test was repeated by compacting and shearing a second specimen, P-35, in an identical manner. The second result gives much better agreement with the drained envelope. The three specimens (P-32, P-33 & P-34) tested for objective (ii) have lower minor principal stresses at the maximum principal stress ratio condition (approx. 20 lb/sq.in. or less) and lie slightly above the drained test curve. The two results of the residual principal stress ratio in the undrained tests are in excellent agreement with the constant ultimate principal stress ratio line of the drained tests (Fig. 8-3, Series D).

The ratio of the effective intermediate to the effective minor principal stress (at the maximum principal stress ratio) shows excellent agreement with the corresponding drained curve (Fig. 9-1). The ratio decreases with decreasing placement density. The two results of the ultimate ratio of these two principal stresses agree reasonably well with the constant average value obtained in the drained tests (Fig. 8-4a, Series D).

There are other important similarities to be noted from Fig. 9-1. The pore-water pressure change curve for the maximum principal stress ratio condition is, in general, similar to the volume change curve in the drained tests i.e. the pore-water pressure is negative when the net volume of the specimen is increased, and positive when the corresponding drained specimen decreases in volume at failure. The two curves cross the zero line at approximately the same initial porosity.

In the presentation of the drained plane strain results, it was pointed out that the stress-strain conditions at failure were unique, provided that the stress paths were not too divergent before failure was attained. This uniqueness cannot be applied to the undrained tests because the condition of zero volume change is maintained at all densities. Therefore, it is not expected

that the axial strain at the maximum principal stress ratio should be the same as the axial strain in the drained tests, but it is interesting to note that the strains approximately do coincide for drained specimens which have zero over-all volume change at failure. Where the volume changes in the drained tests are positive at failure, the axial strain at maximum principal stress ratio in the undrained test is slightly greater, and where the volume changes at failure in the drained test are negative, the axial strain in the undrained test is slightly less.

Two further points are worth mentioning at this stage. Undrained tests which were stopped at the maximum principal stress ratio had no visible failure plane, similar to drained tests at failure. Undrained tests continued to the ultimate condition, or thereabouts, did exhibit a failure plane. What is particularly interesting is that specimen P-34 (Fig. A10-24) had a failure plane, but it had not quite reached the maximum deviator stress condition when the test was stopped. The deviator stress ratio curves for this test show that the run-down (after the peak values) had occurred and this agrees with the earlier discussions concerning the first appearance of failure planes*. The second point is that the ratio of the effective intermediate to the sum of the other two effective principal stresses remained approximately constant throughout a test, similar to the drained tests.

Strength at maximum deviator stress

Turning to the maximum deviator stress condition, the results are few but indisputable. Two of the three results ** on Fig.9-1 lie well below both the drained strength-density curve and the

---

* since completing the present research, the author has many times observed the appearance of a failure plane in dilatant soils before the maximum deviator stress was reached (undrained tests).

** specimen P-34 was on the point of reaching the maximum deviator stress when the test was stopped. This result has, therefore, been extrapolated to the likely failure conditions; any error can only be of negligible importance to the position of the point on Fig. 9-1.

second curve representing the drained test results corrected for energy used to expand the specimen against the cell pressure at failure. The axial strains at the maximum deviator stress condition are much greater than the failure strains in the corresponding drained tests. In all cases, the maximum deviator stress occurs when the ultimate condition is being approached i.e. when the rate of pressure decrease in the pore water starts to slow down.

Another interesting event occurred in the two loosest undrained tests, specimens P-28 (Fig. A10-20) and P-33 (Fig. A10-23). The deviator stress, $(\sigma_1 - \sigma_3)$, rose rapidly to a maximum value at an axial strain of 0.1%, decreased to a minimum and then increased again, surpassing the earlier peak value. The test on specimen P-28 was stopped at this stage but specimen P-33 was continued until a second peak occurred. If we accept the maximum deviator stress as being the criterion of failure, it would have been legitimate to have stopped these tests when the deviator stress was decreasing at, say, 1% axial strain, and argue that the specimen had failed. In other words, a duality of results can be obtained in the undrained test from the maximum deviator stress criterion of failure. Yet, if the undrained results are viewed from an effective stress analysis, the effective deviator stress ratio curves are consistent in shape, and the peak and ultimate values correspond with drained tests at the same placement density.

Explanation of undrained strength

Why is the maximum deviator stress failure criterion favoured in place of the maximum principal stress ratio? The main body of opinion suggests that the engineer is primarily interested in the maximum stress which the soil can withstand under a given set of conditions. Hence, the $\frac{c_u}{p}$ ratio* is of greater importance than the maximum obliquity condition. However, the failure envelope

---

* $p$ is the effective consolidation pressure, $c_u$ is $\frac{1}{2}(\sigma_1' - \sigma_3')_f$

obtained from the maximum deviator stress condition is lower than the maximum obliquity envelope. Therefore, the stress conditions before failure are capable of crossing the failure envelope of the Mohr diagram, an extraordinary contradiction in terms. For conventional laboratory undrained tests, the author believes that the maximum deviator stress criterion is fallacious because it disregards the fundamental reasons for the increase of the deviator stress beyond the maximum principal stress ratio condition in the undrained test. We will now return to some of the concepts put forward in the last chapter.

The first point to be made concerns all shear test specimens placed denser than the minimum stable density i.e. the test specimens in the present investigations. Volume changes in the drained shear test are non-uniform within the specimen. The non-uniformity is thought to be the result of non-uniform stress conditions induced by frictional forces between specimen and loading plates. Understressed parts of the test specimen become non-dilating zones and do not participate in failure. They are mainly situated immediately adjacent to the loading plates (Balla 1957). As friction between the specimen and loading plates is common to both drained and undrained shear tests, the latter are also subjected to non-uniform volume changes within the specimen except that there are no net volume changes. In the undrained test, the non-dilating zones must supply the dilating zones with the water they require to loosen and yield. This is achieved by the negative pore pressures set up by dilation; they increase the effective stresses on the soil and consolidate the non-dilating zones, the expelled water then moving to the dilatant failure zone. Hence, although the test specimen remains at the same average density throughout the test, the density in different parts of the specimen will change continually during a test. The soil in the failure zone is expanding at failure irrespective of whether the imposed test conditions are drained or undrained.

This migration of water to the failure zone in undrained tests has been ascertained by the technique of taking moisture content determinations at different parts of a sheared specimen. A duplicate specimen is made up by the same compaction technique and corresponding moisture contents are obtained from the compacted specimen as a comparison. As it is almost impossible to achieve exactly the same density twice, the results are reduced to a common average density before the comparison is made. Specimens P-35 and P-36 are compared on Fig. 7-6b. The soil was placed in a dense state and the shear test on specimen P-35 was stopped shortly after the maximum principal stress ratio had been reached (Fig. A10-25). The moisture contents were taken at carefully measured intervals on both specimens and the average porosities were reduced to 35.0%. The results are remarkably consistent and clearly show a larger number of porosity contour lines on the sheared soil. In the bottom right-hand corner of Fig. 7-6b, the net change in porosity at different parts of the specimen has been indicated by a line representing zero change. The mid-height of the specimen has increased in porosity and the zones adjacent to the top caps have shown a decrease*. Although this represents only one result, the migration of water to the failure zone has been further substantiated by the standard triaxial undrained tests. Hence, the density on the failure plane does not remain constant throughout an undrained shear test.

Referring again to the typical shear test on specimen P-32 (Fig. A10-22), the behaviour of the soil is controlled by the volume change requirements of the failure zone. At low external shear stresses, the soil attempts to expel water in a similar manner to the drained test and a positive change in pore-water pressure

---

* the net increase in porosity at the bottom right-hand side of the specimen is attributed to the position of the drainage burette added prior to the release of stresses from the shear test specimen.

takes place. When the soil starts to dilate, the pore-water pressure starts to decrease, and when the specimen is dilating at its maximum rate, at failure, the pore-water pressure is dropping rapidly*. The decrease in pore-water pressure results in an increase in the effective stresses on the soil, thus producing the water which the failure zone requires from the non-dilating zones in the specimen. This water would normally be taken from the burette at atmospheric pressure in a drained compression test. Therefore, the effective normal stress on the failure plane, which becomes constant in the drained test at failure, is increasing rapidly in the undrained test when the maximum principal stress ratio is reached, and the deviator stress continues to rise. When the ultimate condition is approached, shear is concentrated in the failure zone. The failure zone stops expanding, as no further water is required for it to shear; the pore-water pressure levels off to an almost constant value, and the deviator stress reaches a peak.

In summary, the writer suggests that soil, in the failure zone of a dilatant test specimen, loosens in shearing to failure. Under the action of external shearing strains, the soil mobilizes shearing resistance, represented by the effective principal stress ratio; it appears to depend on (i) the effective stresses on the soil (ii) the external strain mechanism (iii) the placement density or packing of the sand grains.

The variable external stresses acting on the soil at any stage of the undrained shear test - in particular, the deviator stress, $(\sigma_1 - \sigma_3)$, - are controlled by a combination of (i) the mobilized shearing resistance, and (ii) the pore-water pressure. The mobilized shearing resistance is independent of the pore-water pressure but the converse is not true since the pore-water pressures depend on the shear stress distribution within the soil.

---

* though not constantly, as the compressibility of the soil decreases with increasing average effective stress.

The non-uniform shear stress distribution produces dilating and non-dilating zones and the resultant pore-water pressure gradients set up in an undrained test are not independent of the specimen geometry. Hence, the maximum deviator stress condition in the normal laboratory undrained test is a meaningless parameter in dilatant soils.

There is a second factor influencing the maximum deviator stress and it is the rate-of-strain. The undrained test is usually run at a slow rate so that the pore-water pressures will equalise throughout the specimen. The slow rate means, in fact, that the water movements in the soil will have sufficient time to adjust to the shear stress distribution within the specimen. In other words, the dilatant soil in the failure zone is able to draw all the water available throughout the whole specimen at that particular set of external stress conditions. Suppose that further tests are carried out at progressively faster rates-of-strain. The pore-water pressure characteristics will remain essentially unchanged until a speed is reached, depending on the coefficient of consolidation, when a uniform pore-water pressure will be incapable of supplying the water to the failure zone at a sufficient rate to keep pace with the applied shear rate* i.e. water can no longer be drawn from the longest drainage paths to the failure zone in time. The result is that pore-water pressure gradients are set up to obtain the necessary water from non-dilating zones with a shorter drainage path to the failure zone. In this case, the maximum deviator stress which the soil can withstand increases due to the higher effective normal stress on the failure plane. This state of affairs has been measured by La Rochelle (1960) on dilatant London Clay. Therefore, to obtain reasonable uniformity of pore pressures within the conventional undrained test, the test would have to be carried out at the same rate-of-strain as in the corresponding drained test.

---

* the water required by the failure zone is controlled by the mobilization of shearing resistance.

We must distinguish between two components of pore water movements within the soil specimen, namely :-

(i) movements resulting from a non-uniform distribution of the shear stresses within the specimen.

(ii) movements resulting from a shear rate which is too great for the specimen to maintain uniformity of pore pressure within its geometry.

Although they are two separate components which make up the actual movement of pore water in an undrained test on a saturated dilatant soil, they are both a result of the same phenomenon - frictional forces at the upper and lower boundaries of the specimen. Running undrained tests at slow rates-of-strain only eliminates the second component.

Returning to the discussion of the plane strain results, one final point can be added to complete the analysis. On Fig.9-1, the pore-water pressures at the maximum principal stress ratio condition are positive when the volume changes in the drained test are negative, and vice versa. This suggests that the work done by the soil in expanding against the cell pressure in the drained test can be equated to the internal work done by the soil to consolidate the non-dilating zones in the undrained test at the maximum principal stress ratio. This point can be illustrated quantitatively. In the last chapter, the volume change characteristics at failure in the standard triaxial drained compression test Series E, at cell pressures of 40 lb/sq.in. and 60 lb/sq.in., were practically identical. Suppose then, as a first approximation, that the net volume change - initial porosity graphs for plane strain specimens are also independent of the consolidation cell pressure. For test specimen P-30 (Fig. A10-21), having an initial porosity of 38.4%, the consolidated cell pressure was 35.0 lb/sq.in. and when the maximum principal stress ratio was attained in the undrained shear test, the effective cell pressure was 47.5 lb/sq.in. Now, in

consolidating a test specimen, having the same initial porosity as test specimen P-30, from a cell pressure of 35.0 to 47.5 lb/sq.in. a volume change $\frac{\Delta V}{V_c}$ of +0.12% would take place*. This value is of the same order as a volume change in a drained plane strain test of +0.07% for a specimen having the same initial porosity. The results of all the undrained plane strain tests which had a negative pore pressure change at the maximum principal stress ratio are given on Table 9-1. The corresponding volume changes which take place in a $K_o$ consolidation test when the effective cell pressure changes by this amount under drained conditions (red crosses on Fig. 9-1) are compared with the volume changes measured in the drained shear tests. It is seen that there is an excellent general agreement except for the two undrained tests which were consolidated under an effective cell pressure of only 4 lb/sq.in. (ringed on Fig. 9-1). It is likely that the first approximation mentioned earlier in this paragraph no longer holds good for these two tests.

No attempt has been made to relate the equivalent volume changes for the undrained tests in which the pore pressure was positive at the maximum principal stress ratio, as no volume change curves are available for decreasing effective stresses. However, the general result that undrained tests having a positive pore pressure at the maximum principal stress ratio correspond with drained tests having negative volume changes is clearly indicated on Fig. 9-1.

The migration of water to the failure zone in drained tests has been known for some time (Taylor 1951), but there has been little comment on its effect in the undrained test up to the time at which the present results and conclusions were drawn (1959). In earlier published work on the undrained test, there have been three common fallacies, namely :-

---

* the volume change curves are not published, so these figures must be accepted in good faith.

(i) that the soil is sheared at constant voids ratio, tacitly interpreted as the soil on the failure plane.

(ii) that the maximum deviator stress is a product of the test drainage conditions.

(iii) that discrepancies between the strengths measured at the maximum deviator stress condition in the drained and undrained tests can be explained in terms of the external work done by the drained tests in expanding the soil against the confining pressure.

Fallacy (iii) is suggested by the comprehensive evidence obtained from the plane strain apparatus, in which tests were carried out over a wide range of placement densities. As will be seen in the next pages, this apparent fallacy is not inconsistent with the results of standard triaxial undrained tests.

## II. Standard Triaxial Tests

The characteristics of the standard triaxial compression undrained tests at the maximum principal stress ratio are shown on Fig. 9-2. All the four results lie below the strength-density envelope representing the drained tests but are in good agreement with the envelope representing the drained tests corrected for the energy used to expand the specimens against the cell pressure.

The two looser specimens, C-22 (Fig. A10-32) and C-39 (Fig. A10-44), each had a peak value in the deviator stress-strain curve at an axial strain of 0.1%. The mobilized friction at this stage was equivalent to an apparent angle of shearing resistance of $26^{\circ}$. The deviator stress then decreased to a minimum and increased again, surpassing the earlier peak, and was approaching a second peak when the test was stopped.

The principal stress ratios behaved consistently except that, like all the undrained tests, the friction was mobilized much quicker than in drained tests at the same placement density, i.e. the effective deviator stress ratio curves $(\sigma_1' - \sigma_3')/\sigma_3'$ had a much flatter peak. When the pore-water pressures dropped towards zero in a shear test, the cell pressure was raised to increase the pore-water pressure. There was no apparent change in the effective principal stress ratio curves as a result of these changes in cell pressure.

Explanation of undrained strength

It is clear that the undrained tests are limited to the looser densities because of the greater dilatancy of the sand in the standard triaxial apparatus. Furthermore, the axial strain and negative pore-water pressures at the maximum principal stress ratio in the two denser specimens, C-37 (Fig. A10-42) and C-38 (Fig. A10-43) are less than one might have expected if the sand behaved in a similar fashion to the plane strain specimens. One possible explanation of the discrepancies between the drained and undrained standard triaxial tests at the maximum effective principal stress ratio may be as follows :-

The major part of the standard triaxial specimen is dilating at the maximum principal stress ratio and the main source of water supplying the dilating parts comes from the non-dilating zones at the ends of the specimen. The more dense the specimen, the greater are the water requirements during shear. The soil closest to the non-dilating zones will be the first to receive water from these zones. Hence, the structure in the dilating areas next to the non-dilating zones will loosen first and will subsequently act as drainage paths for the water supplied to areas further from the non-dilating zones. In other words, the non-uniformity of strain (or progressive shear failure)

experienced in the drained test will become more exaggerated in undrained conditions such that areas close to the non-dilating zones (e.g. point A, Fig. 8-15) will have reached the ultimate shearing resistance when the maximum shearing resistance is being mobilised at the point on the failure plane at the greatest distance from the non-dilating zones (point B).

This may well account for the much flatter stress-strain curves measured in undrained conditions and the reason for the occurrence of an apparent peak stress at a small axial strain on the two denser specimens, C-37 (Fig. A10-42) and C-38 (Fig. A10-43). Both specimens showed appreciable bulging near the top, a phenomenon which was not observed on any of the drained tests.

Porosity changes during shear, based on comparison moisture content determinations, lend further support to the suggestion of a more progressive failure in the undrained test. The upper tables on Fig. 7-6 show a considerable reduction in the density of the soil adjacent to the end caps on specimen C-38. The same is probably true for specimen C-39. As there was no twin specimen compacted by the identical compaction technique, the changes can be estimated by adding 1% to all the initial porosities of specimen C-35. On these sheared specimens, the greater density increases occur at the quarter heights immediately adjacent to the top cap, at the point where the maximum bulging was observed.

A slight lack of vertical symmetry also can be seen in the lateral strains of specimen C-22 (Plate 8-2), but it is less noticeable on this specimen than on the denser specimens.

A second explanation may be that the standard triaxial specimens are closer to the "true" undrained conditions than the plane strain specimens. Suppose that the distribution of the shear stresses within the plane strain specimen is less uniform than in the triaxial specimen. In the triaxial specimen, the principal zones which are not participating in failure are situated at the ends of the specimen and this may allow part of the soil, near the ends, to develop a partial "drained" strength. Hence, there is a slight peak in the stress-strain curve and noticeable bulging near the ends. For plane strain undrained tests, there may be sufficient available water at all levels in the specimen to allow soil on the narrow failure zone to expand and do sufficient internal work so that the drained frictional resistance is attained. In the corresponding drained test itself, the non-dilating zones remain fairly passive and water is drawn in from the drainage burette.

The two explanations lead to quite different conclusions. The first explanation is suggesting that the standard triaxial specimen has a lower maximum principal stress ratio than the corresponding drained test because progressive failure is more pronounced in the undrained test. The second explanation suggests that a uniformly stressed undrained specimen, shearing at constant voids ratio, mobilizes a different frictional resistance than a corresponding drained specimen.

To complete this section, two occurrences in the author's more recent experience will be mentioned. Both concern standard triaxial compression undrained tests. In the first case, a failure plane was observed in a saturated silt long before the maximum deviator stress was reached. Observations on the Brasted sand drained tests showed that failure planes do not develop until after the run-down of deviator stress following failure, and this point has also been confirmed on other soils.

Hence, the silt must have been approaching the ultimate principal stress ratio when the maximum deviator stress was recorded in the undrained test. In the second case, a silt was re-compacted and saturated prior to shear. It was sheared in an undrained test with pore-water pressure measurements. It failed by uniform bulging, the top cap remaining horizontal and central throughout the test. The deviator stress was still increasing rapidly at an axial strain of 35%, due to a continued drop in the pore-water pressure. The point behind this test is that if the failure zone continues to dilate without forming a failure plane, the pore-water pressure will continue to drop and the deviator stress increases. On the other hand, if the specimen is loaded eccentrically or by a tilted top cap, the maximum deviator stress will be attained much more quickly.

The undrained standard triaxial extension tests do not provide any more evidence on the points which have been discussed in this chapter. Both of the specimens C-49 (Fig. A10-49) and C-50 (Fig. A10-50) have a premature peak in the deviator stress-strain curve equivalent to an apparent angle of shearing resistance of $11^{\circ}$ (C-49) and $23^{\circ}$ (C-50).

The effective deviator stress ratio curves are consistent in both tests. The scatter of the experimental points on the curve for specimen C-49 is due to the very low stresses which were measured as the peak conditions were approached, but the peak value is in good agreement with the anticipated strength of soil subjected to symmetric strain conditions at this density. The density changes within specimen C-50 are summarised on Fig. 7-6. They again illustrate the migration of water to the failure zone in the undrained test.

## III. Undrained Conditions in the Laboratory and Field

The conventional laboratory undrained test seems to have little practical value. End bearing frictional forces produce a movement of pore water towards the failure zone and the soil in the failure zone does not remain at a constant voids ratio. These movements can only be averted by having uniform stress and strain conditions within the specimen. This could be achieved by (i) use of membrane discs coated with silicone grease at the ends of the specimen (Blight, 1961); consolidation could be via leads passing through sealed joints in the vertical membrane, or (ii) a simple shear apparatus, similar in principle to the Roscoe (1953) apparatus, but modified to accept ambient cell pressures.

This Chapter has been primarily concerned with the mobilization of shearing resistance in the undrained test. However, loose sands may fail before the maximum principal stress ratio is attained as, for example, the undrained extension test specimen C-49 (Fig. A10-49). The maximum deviator stress in these cases needs to be examined under uniform stress conditions. The result probably also depends upon the type of consolidation and stress history during shear, since these factors affect the volume changes in drained tests.

In practical engineering, any form of undrained shear condition is a dynamic problem - dynamic in the sense that it involves the passage of time between the application of new stress conditions and the final equilibrium conditions. The pore pressures are not in a steady state and there is usually a non-uniform distribution of shearing stresses. Therefore, in dilatant soils*, the conditions on the failure zone differ from the surrounding

---

* normally consolidated clays are exempt from this category - hence, the successful application of the "$\phi = 0$" analysis.

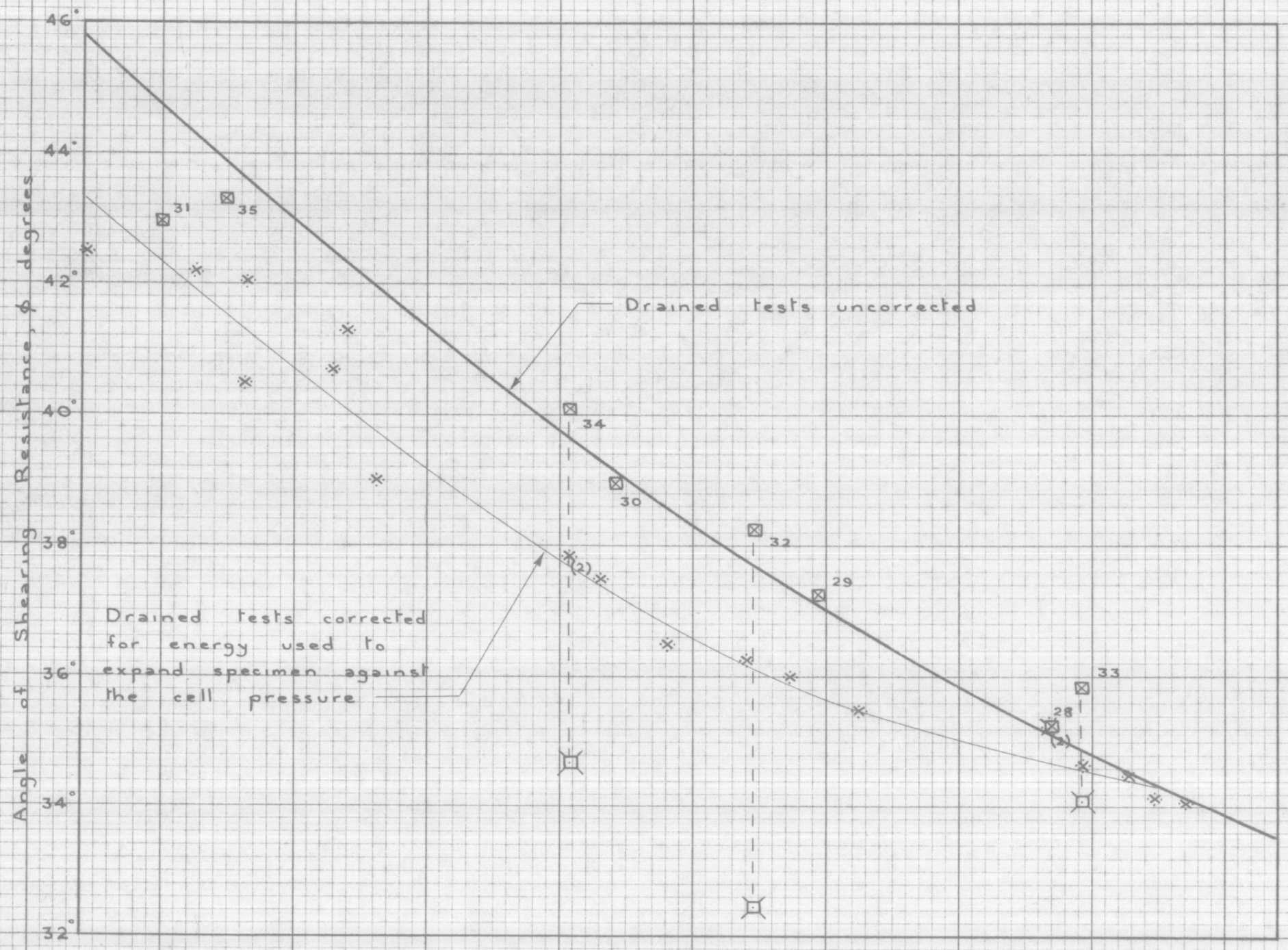
soil, but in a different manner to the conventional laboratory undrained test. The time element, eliminated from the conventional undrained test and non-existent in a uniformly constant voids ratio test, is an essential consideration in many soil problems. (e.g. La Rochelle, 1960). The maximum deviator stress in an undrained test can be correctly measured by either (i) a conventional triaxial test at a fast rate-of-strain which will not permit water migration or (ii) producing uniform stress and strain conditions within the test specimen by eliminating end loading restraints. The second method is more desirable because it permits uniform pore-water pressures to be measured but in some practical problems on dilatant soils, the result can only be used in an empirical role.

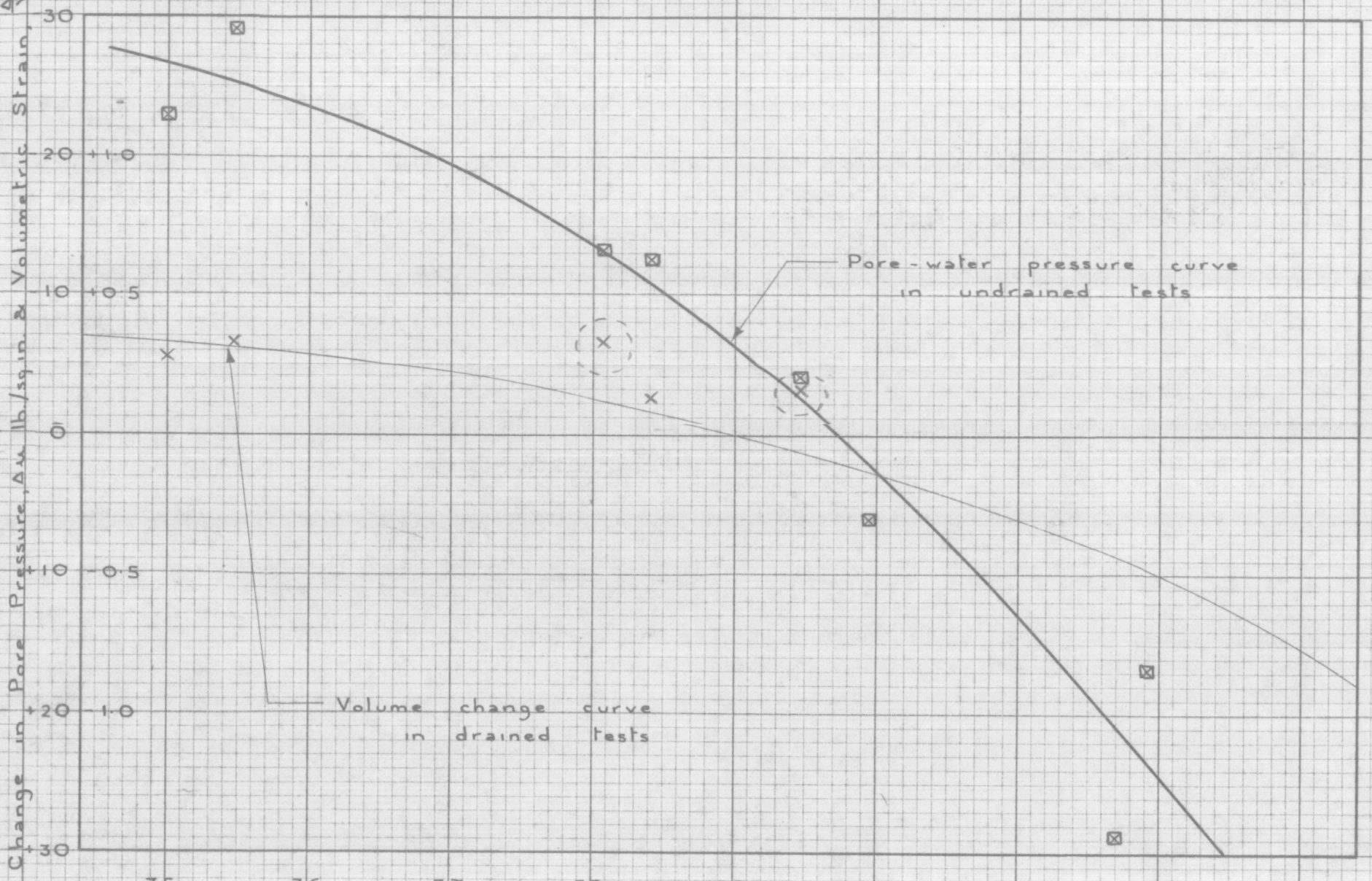
Table 9-1 Equivalent Volume Changes in Undrained Tests (Plane Strain)

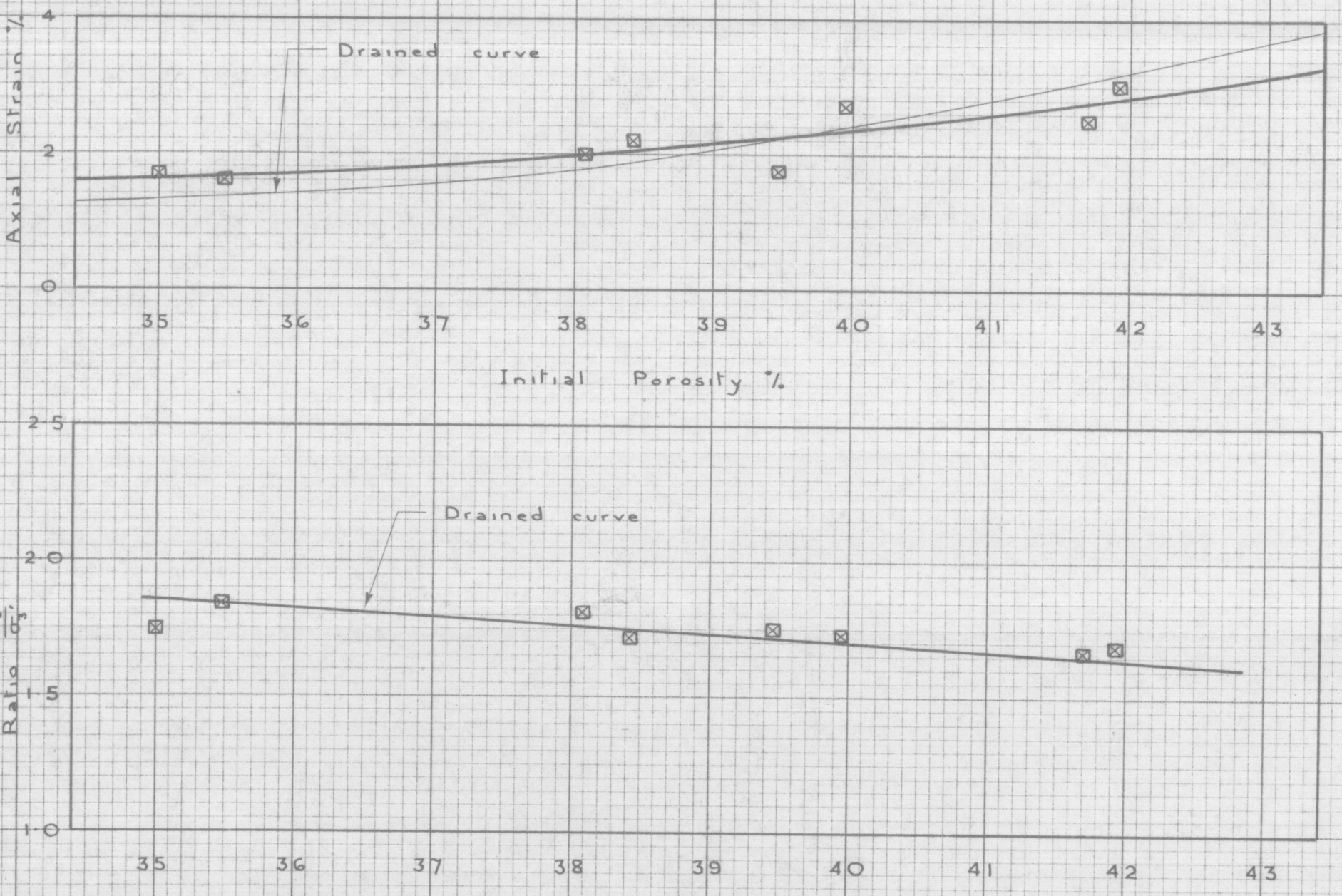
| Test No. | Initial Porosity % | Consol. Cell Pressure $\sigma_{3c}'$ lb/sq.in. | $\sigma_3'$ at $\left(\frac{\sigma_1'}{\sigma_3'}\right)_{max.}$ lb/sq.in. | A Equiv. Volume Change % | B Drained Volume Change % |
|---|---|---|---|---|---|
| P-30 | 38.4 | 35.0 | 47.5 | + 0.12 | + 0.07 |
| P-31 | 35.0 | 15.0 | 37.9 | + 0.28 | + 0.33 |
| P-32 | 39.5 | 4.0 | 7.9 | + 0.15 | - 0.06 |
| P-34 | 38.1 | 4.0 | 17.5 | + 0.33 | + 0.11 |
| P-35 | 35.5 | 15.0 | 43.3 | + 0.33 | + 0.32 |

Column A The equivalent consolidation volume change which would take place in a specimen having the same initial porosity if it was to consolidate from a cell pressure of $\sigma_{3c}'$ (consolidation) to the $\sigma_3'$ (at maximum principal stress ratio).

Column B The volume change at failure in a drained test having the same initial porosity. (The values are abstracted from the drained tests summary curve.)



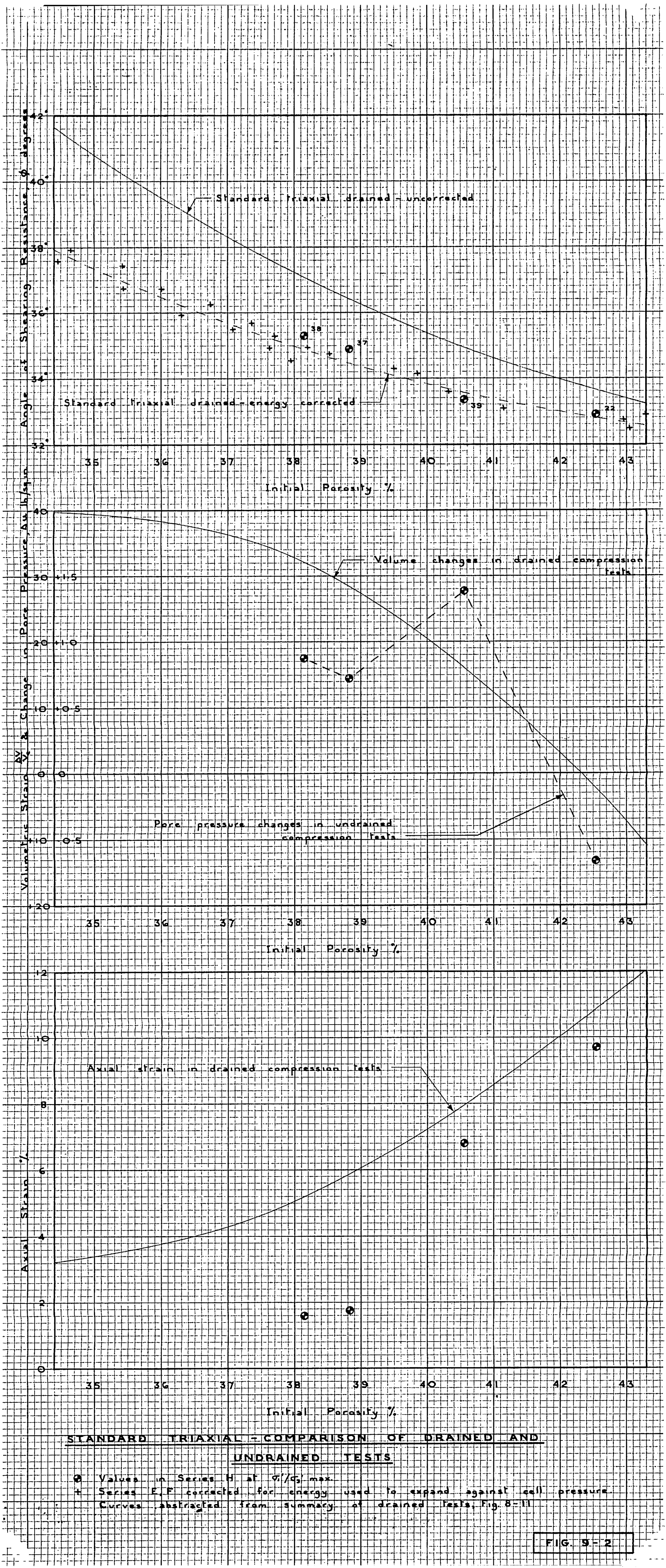

PLANE STRAIN - COMPARISON OF DRAINED AND UNDRAINED TESTS

⊠ Series D at $\sigma_1'/\sigma_3'$ max. (2) indicates two results superimposed.

⊡ Series D at $(\sigma_1' - \sigma_3')$ max.

※ Series A, B, C at $\sigma_1'/\sigma_3'$ & $(\sigma_1' - \sigma_3')$ max. corrected for the energy used to expand against the cell pressure.

FIG. 9 - 1




STANDARD TRIAXIAL - COMPARISON OF DRAINED AND UNDRAINED TESTS

● Values in Series H at $\sigma_1'/\sigma_3'$ max.
+ Series E, F corrected for energy used to expand against cell pressure.
Curves abstracted from summary of drained tests, Fig. 8-11

FIG. 9-2

## Chapter 10 A PRACTICAL METHOD OF ESTIMATING THE STRENGTH OF SANDS UNDER PLANE AND SYMMETRIC STRAIN CONDITIONS

### Introduction

In Chapter 8, it has been shown experimentally in the shear test series that Brasted sand has always a greater strength under plane strain conditions than under symmetric strain conditions, for a given placement density. The denser the soil, the greater is the difference in strength. The limiting loose density condition for this effect is when the sand is placed sufficiently loose that it no longer dilates during shear i.e. at the minimum stable density. The strength of the sand is then constant, equal to the ultimate strength in denser soil, and is independent of the strain mechanism. The author considers this condition to be linked with a change in the structure of the sand grains and the initial density has been chosen as the parameter. There is no evidence in the standard triaxial compression tests at cell pressures of 40 lb/sq.in. and 60 lb/sq.in. to dispute this choice.

The external strain conditions have an important influence in modifying the paths chosen by the individual sand grains before the soil yields. In the symmetric strain tests, the movement of the grains in the plane of equal stresses depends only on the structural arrangement of the adjacent grains, but, in plane strain, the choice of path is governed both by the structural arrangement and the unequal stress conditions. The mean statistical grain of sand in plane strain moves along a line in the plane of the intermediate principal stress. Hence, for a given initial density, plane strain probably represents the greatest restriction in grain movements during the loosening of the soil by shear forces; symmetric strain conditions represent the least restriction in following the path of least resistance to failure. Comparing the two types of test at the same placement density, greater axial strains are required to mobilize the full shearing resistance in the symmetric strain tests and the strength of the sand is lower.

If the above concepts are correct, they will be applicable to all granular soils. Therefore, the shear parameters of standard triaxial tests are conservative when applied to two-dimensional stability problems involving dilatant granular soils. It is useful for the designer to have some idea of the likely strength of the soil under these conditions. If the difference in strength is large, a suitable compromise can be made which may result in a substantial economy in the earthworks. For important projects, there is no satisfactory substitute for actually testing the soil under the appropriate strain conditions. However, no plane strain apparatus of the type described in this thesis is commercially available.

To what extent can the results of the present investigation be applied to other sands? To proceed further, the suitability of existing general theories on soil strength must be considered, as follows :-

Theoretical solutions

Most theoretical solutions for stress-strain conditions in a material are based on the concepts of elasticity and plasticity. The author has not attempted a mathematical treatment but such an analysis must take account of the earlier discussions. Two major points to bear in mind are that non-uniformities in strains and volume changes do not seem to have an appreciable effect on the measured strength, and the structural loosening of the grains in the zone of failure play an important role in the development of strength and cannot be ignored (Chapter 8). A common analogy in theoretical considerations is to compare the behaviour of soils with that of equal diameter frictional spheres arranged in a known packing. However, solutions to this problem do not involve the statistical movement of the spheres similar to the concept of shear envisaged in the discussions of Chapter 8.

Empirical solutions

Hafiz (1950) attempted to correlate the strength-density curves measured in a large shear box on five granular soils (Fig. 10-1). The limiting densities of the soils were determined by the suggested standard methods of Kolbuszewski (1948). The relative porosities gave a fairly good correlation but the five curves reduced to an almost unique curve when the strength of each soil in its loosest state was subtracted from the strength at other values of relative porosity. It has been known for many years (Skempton, 1945) that the strength of loose sand is approximately equal to the angle of repose of a heap of loose sand. Hafiz verified this to be correct for the five granular soils. It will be seen that the method proposed later in this chapter is similar to the Hafiz correlation.

Kirkpatrick, 1957 (see Chapter 2). The presentation of the test results on a right section to the space diagonal $\sigma_1 = \sigma_2 = \sigma_3$ has been rejected as a method of relating the plane strain and standard triaxial tests. The main reason is that the right section is a plane of equal average principal stress. This is not suitable for bringing out various points of the hypothesis put forward in the preceding discussions. The surface of yield is not symmetrical about the space diagonal and hence it is not obvious from such a diagram that the strength of the sand at a given initial density is approximately equal at the limiting values of the intermediate principal stress. This conclusion is fundamental to the explanation of the differences in strength measured in the symmetric strain and plane strain tests. Secondly, the author prefers to relate the strengths through the minor principal stress as it has been suggested that when the sand is set up at the minimum stable density it will have a strength which is equal under any strain condition and which is independent of the intermediate

principal stress. This important point would be "hidden" on a yield surface representing the minimum stable density. Finally, a yield surface would only represent one initial density of the soil and a series of such surfaces would have to be drawn to obtain a general picture of the soil's shear strength behaviour*.

The Roscoe, Schofield & Wroth Hypothesis (see Chapter 2) is not a suitable method for relating the results of the Brasted sand investigation in a general stress-strain system. Their Hypothesis can only be applied to tests under uniform strain conditions. Also, the average principal stress, p, is not considered to be a suitable parameter for relating the shear strength of sands under different strain conditions.

Method for relating plane & symmetric strain tests

The author believes that the factors governing the strength of dilatant soils have been sufficiently established to justify an empirical solution based on a single set of test results. In essence, the solution is an adaptation of the work by Bishop & Hafiz (Hafiz, 1950) and Skempton (1945) with several minor, though important, differences. The main point to be gained from the Hafiz correlation is that five cohesionless soils of widely different grain characteristics were satisfactorily correlated in terms of their relative porosity. On this basis, the author believes that the test results on Brasted sand, which define more accurately the shape of the strength and density relationship, can be applied to a wide range of cohesionless soils.

The method is essentially practical and it is intended as a first approximation for design purposes. It is hoped that later work on Dr. Bishop's plane strain apparatus will support the

---

* one solution to the last objection would be to make the right section into a dimensionless parameter by, for example, dividing all the distances from the space diagonal to the yield surface perimeter by the average principal stress of the section. An overall picture of the yield condition could then be obtained by replacing the space diagonal with a third dimension representing the soil density.

validity of the design method. However, the fact that it is based on only one set of plane strain test results must be remembered when following the suggested procedure.

Consider the fully drained strength of a dilatant cohesionless soil to be influenced by factors having primary or secondary importance. The primary factors will be those which have a fundamental effect on the strength. From the evidence put forward in the preceding chapters, they are:-

(i) the soil material, consisting of the soil mineralogy, grading, grain shape and surface roughness.

(ii) the packing of the soil grains.

(iii) the strain conditions during shear.

(iv) the effective cell pressure or, alternatively, the effective normal stress on the zone of rupture.

Factors will be classed as secondary where the factor is thought to have an insignificant influence on the strength from a practical viewpoint or where the influence of the factor has not been adequately evaluated in laboratory tests. Some of the more important factors in this group are :-

(i) cohesion intercept.

(ii) degree of saturation.

(iii) rate of strain, provided that the fully drained condition is maintained during shear.

(iv) stress history.

(v) type of consolidation.

(vi) non-uniform strain within the specimen during shear.

(vii) progressive failure in the failure zone.

(viii) non-uniform initial density within the specimen.

The design method to be presented deals only with the primary factors. The limitations imposed by the assumption that the secondary factors have no influence on strength have been discussed in earlier chapters.

If the possible existence of a cohesion intercept in sands is ignored, the effect of cell pressure can be easily dealt with by either using the angle of shearing resistance, $\phi_d$, from the Mohr envelope of stress or, alternatively, by dividing the compressive stress $(\sigma_1 - \sigma_3)$ by the cell pressure $\sigma_3$. As the angle of shearing resistance is a geometrical parameter, the non-dimensional deviator stress ratio is probably more fundamental and has been adopted for the present treatment. It uniquely defines the position of the effective stress circle on the Mohr diagram and can be readily converted into an angle of shearing resistance (Table 10-1).

For a Mohr envelope passing through the origin, the relationships are :-

$$\frac{(\sigma_1 - \sigma_3)}{\sigma_3} = \frac{2 \sin \phi}{(1 - \sin \phi)} \qquad \text{.....(1)}$$

$$\sin \phi = \frac{\frac{(\sigma_1 - \sigma_3)}{\sigma_3}}{\left\{2 + \frac{(\sigma_1 - \sigma_3)}{\sigma_3}\right\}} \qquad \text{.....(2)}$$

The relationship between strength and the other three primary factors - soil material, packing of the soil grains and the strain condition - is complex, but use of the relative porosity (Hafiz 1950) is an obvious starting point for simplifying the relationships. It positions the condition of granular packing in the soil between arbitrary limits of placement density.

The relative porosity, $n_r$ is defined by :-

$$n_r = \frac{n_{max.} - n}{n_{max.} - n_{min.}} \quad \ldots\ldots\ldots\ldots\ldots\ldots\ldots\ldots(3)$$

where $n_{max.}, n_{min.}$ are the porosities of the sand at the limiting densities and n is the porosity of the sand in its natural state.

At maximum density, $n_r = 1$ (or 100%)
At minimum density, $n_r = 0$

The concept of relative porosity is only applicable to sand denser than the minimum stable density. Therefore, although it is possible to place sand in a looser condition, the porosity at the minimum stable density will be adopted as zero relative porosity instead of the arbitrary loose limit suggested by Kolbuszewski (1948). (The plane strain and symmetric strain curves meet at the minimum stable density.)

An investigation was carried out (see Appendix 8) to obtain a simple laboratory procedure which would give a sound estimate of the minimum stable density. The rapid tilt test on dry sand (Kolbuszewski, 1948) was found to be the most suitable technique. This test gave an initial porosity of 44.2% for Brasted sand which is in good agreement with the estimated values of the minimum stable density in the plane strain and standard triaxial tests (Figure 8-12). The probable reason for the loose porosity measured in this test, as suggested by Kolbuszewski, is that the sand grains landing on the heap of deposited sand are "locked" in an open structure by the high intensity of deposition. It should be added to this explanation that the high velocity of fall prevents the formation of large void spaces or honeycomb structure. The latter produce an inherently unstable structure which will collapse under shearing loads.

The strength of the sand at this unique initial porosity is a property of the soil material, and the various elements of mineralogy, grading, grain shape and surface roughness will, in a comprehensive manner, determine this strength. Obviously, these properties of the sand grains will also influence the strength of the sand at other densities. However, density can be considered as a factor independent of the sand grain properties by determining the increase in strength from the minimum strength measured at zero relative porosity (i.e. minimum stable density). The two strength-density envelopes for Brasted sand have been determined with a good degree of accuracy and may be estimated for other granular soils by the use of a dimensionless "strength ratio" parameter, R, defined by :-

$$R = \frac{\left\{\frac{\sigma_1 - \sigma_3}{\sigma_3}\right\}}{\left\{\frac{\sigma_1 - \sigma_3}{\sigma_3}\right\}_{min.}} \qquad (R > 1, \text{ always}) \ldots\ldots\ldots\ldots (4)$$

where $\left\{\frac{\sigma_1 - \sigma_3}{\sigma_3}\right\}$ = major deviator stress ratio at any density

$\left\{\frac{\sigma_1 - \sigma_3}{\sigma_3}\right\}_{min.}$ = major deviator stress ratio at the minimum stable density

For a cohesion intercept of zero, the term $\left\{\frac{\sigma_1 - \sigma_3}{\sigma_3}\right\}_{min.}$ is constant for a particular sand.

The strain conditions during shear will be represented by two lines, $R_p$ and $R_s$ defined by :-

$R_p$ = parameter R under plane strain conditions

$R_s$ = parameter R under symmetric strain conditions

The author believes that the $R_p$ and $R_s$ lines represent the maximum and minimum strength curves of the soil but further research work is required to confirm this view.

First, the shear strength of the soil at zero relative porosity must be determined. From the observations of Skempton (1945), the simplest procedure is to determine the angle of repose for the sand. Angle of repose tests were

carried out on Brasted sand, the author being assisted by two other graduates to prevent bias in the test results. The average slope of the heap was measured as $32.5^{\circ}$, which agrees favourably with the estimated angle of shearing resistance of $32.8^{\circ}$ at zero relative porosity.

The final parameter to be decided is the initial porosity at the dense end of the strength-density curve. It should be the densest possible, though consistent with the requirement of a comparatively simple method of determination. The greater is the porosity range between the limits, the less important become any errors in the determination of either limit. Kolbuszewski's technique of vibrating saturated sand by a Kango hammer has been adopted as the dense limit of porosity. For the Brasted sand used in the present investigation, the dense porosity was 32.2% (Fig. 10-2c). Although it is probably the minimum porosity which can be achieved in the laboratory, the author has recently measured relative porosities of approximately 125% on uncemented "sandstones" at the Soil Mechanics Ltd. laboratory*. Hence, the limit is unlikely to represent the actual minimum initial porosity of the sand. The two limits will be termed "laboratory density limits" and will be estimated to the nearest 0.1% in porosity.

The four requirements in estimating the strength envelope of a cohesionless soil for design purposes are (i) zero relative porosity (ii) 100% relative porosity (iii) minimum strength at zero relative porosity (iv) the curves of parameter, R, and relative porosity, $n_r$. A detailed account of their determination follows :-

---

* these soils had curved (convex upwards) Mohr envelopes.

(i) Zero relative porosity

1000 gm. of dry sand are weighed out and placed in a 1000 ml. glass measuring cylinder. The cylinder should be graduated at 10 ml. intervals and should preferably not have a pouring lip. A piece of rubber membrane is stretched over the top of the cylinder and is sealed by a rubber O-ring. The cylinder is inverted, and then returned to its original upright position in a movement taking 4 to 8 seconds. The volume occupied by the sand is noted and the test is repeated several times (e.g. 20) until a consistent value has been obtained. The sand does not, in general, form a level horizontal stratum when it returns to the bottom of the cylinder. Experience has shown, however, that slight additional tilting of the cylinder to level the sand can be carried out without affecting the measured volume.

(ii) 100% relative porosity

The sand (approx. 750 to 3000 gm. dry weight) is saturated by pouring into boiling water, boiling for 10 minutes, and then allowing to cool to room temperature. The compaction mould recommended by the author, Fig. 10-2(b) can be cut from an old standard Proctor mould. The depth of the mould is reduced to 1.457 inches, giving a capacity of 300 ml.* The mould and base are weighed to the nearest gramme. The Proctor collar is put on the mould and sand is placed inside the assembly to a depth of approximately 2 inches. A Kango vibratory hammer (type F, with end piece consisting of a circular steel disc of slightly less diameter than the mould) is applied to the surface of the sand for a vibration time of 2 minutes. The hammer is slowly removed, care being taken to prevent suction on the soil. The collar is removed, the soil levelled to the top of the mould,

* ideally, the mould should be fixed to the base and not detachable; if detachable, place the apparatus in a flat-bottomed container and fill the container with water to the same depth as the sand i.e. 2 inches.

and the outside of the mould is dried. The mould and contents are weighed and the sand is oven-dried.

The porosity is calculated from (i) the weight of dry sand occupying the known volume of the mould, and (ii) the moisture content of the sand, assuming complete saturation. The results should agree to within 0.2% in porosity, if the volume of the mould is carefully measured. The test should be repeated several times until the result has been consistently established.

(iii) Minimum strength (angle of repose)

A large flat glass plate is carefully levelled by a spirit level. Dry sand is deposited through a funnel into a conical heap approximately 3 inches high (Plate 10-1). The heap is under-cut by scraping away sand grains from the bottom of the heap until the higher sand grains start to roll down the side. The equilibrium slope of the heap is then measured by some means e.g. using pieces of stiff cardboard cut to different angles, the angles differing by $1^{\circ}$ (Plate 10-1). The sand grains tend to move in waves, and the slope must be measured along the last completed wave. The test is repeated at least 10 times and the average value is adopted as the angle of repose (estimated to $0.1^{\circ}$).

(iv) Relationship between R and relative porosity, $n_r$

The strength-density curves were initially drawn by freehand and the strength at porosity intervals of 1% were abstracted from them. These strength values were subtracted from the minimum strength common to both envelopes at zero relative porosity, and the author was astonished to discover that the ratio of the differences in strength, at a given porosity, was approximately constant over the whole range of densities. For the central part of the curve (covering 4% in porosity), the plane strain increase in strength was exactly 70% greater than the standard triaxial increase in strength. The ratio was slightly greater

at the loose and dense ends of the envelopes, but the loose end is obviously less sensitive to such a ratio measurement and there was considerable scatter in the dense plane strain specimens. Hence, it was decided to adjust the curves slightly to make the ratio constant at 1.70 over the complete density range. At the dense end of the curve, the standard triaxial envelope was assumed to be correctly aligned in its original position and the plane strain envelope was altered accordingly. Hence, the increase in strength as a fraction of the minimum stable density strength is (R-1). The relationship between $R_p$ and $R_s$ is :-

$$\frac{R_p - 1}{R_s - 1} = 1.70 \qquad \ldots\ldots\ldots\ldots\ldots\ldots\ldots\ldots (5)$$

or $$R_p = 1.00 + 1.70\,(R_s - 1) \qquad \ldots\ldots\ldots\ldots (6)$$

This relationship between the two strength-density curves has been unchanged on all the curves preceding this chapter and it is clear that they satisfactorily fit the test results. A large copy of the results, including all the drained tests, is given on Fig. 10-3. The original strength calculations were based on the average cross-sectional area of the test specimens. However, Eldin (1951) measured up standard triaxial specimens after failure. He concluded that calculations of deviator stress using the average cross-sectional area of the specimen may under-estimate the strength of the soil. For compression tests, the error is negligible at 6% axial strain, 1½% at 11% axial strain and 3% at 20% axial strain. The small circles on Fig. 10-3, immediately above the large circles on the looser triaxial specimens, represent corrected strengths using Eldin's values. No corrections have been applied to the plane strain results, all of which failed at axial strains of less than 4%.

The relationship between the dimensionless parameter, R, and the relative porosity, $n_r$, is given on Figs. 10-4 and 5(b). For different angles of repose, the relationship between angle of shearing resistance, $\phi_s$, and relative porosity can be calculated. Fig. 10-6 gives these relationships under plane and symmetric strain conditions for a typical range of repose angles encountered in cohesionless soils. At the same relative porosity, the difference between the total angle and the corresponding angle of repose is remarkably constant over the range quoted on Fig. 10-6.

Example of design method

The author has taken the opportunity of applying the design method to drained triaxial compression test results obtained under the author's supervision in the laboratory at Soil Mechanics Limited. So far, three experimental strength-density curves have been defined and they, together with individual results at a specified relative porosity (sets of three tests), have shown good agreement with the design method outlined earlier in the Chapter.

As an illustration, the first of the three strength-density curves concerned 4 inch diameter specimens of "Ile de Sable" sand from Guinea, West Africa. The grey-brown medium sand contained numerous small shells and the particle size distribution is shown on Fig. 10-5(a). The laboratory density limits and minimum strength are :-

| | | |
|---|---|---|
| 100% relative porosity | - | 34.0% (3 compaction tests) |
| 0% relative porosity | - | 47.4% (10 rapid tilt tests) |
| Minimum strength | - | $33.3^{\circ}$ (10 angle of repose tests) |

The sand is, therefore, quite different from Brasted sand.

The calculations are given on Fig. 10-5(b) and the estimated strength-density envelope is compared with the measured envelope on Fig. 10-5(c). The estimated curve is above all but one of the test results. However, the maximum deviation from the measured envelope is only $\frac{3}{4}^{\circ}$ of which $0{\cdot}3^{\circ}$ represents an over-estimate of the minimum strength by the angle of repose tests. The author considers that the comparison is a favourable indication that the design method will provide a suitable means of estimating the shear strength of sands under any strain condition.

Uses of the design method

The value of such a correlation between different sands is fairly obvious. It is a well-known fact that it is extremely difficult to take undisturbed samples of sand in the field. The Bishop sand sampler (Bishop, 1948) was developed for this purpose and has been used with success on several projects (e.g. Nixon, 1950), but it is an expensive technique and many samples may be required to obtain a relative porosity profile. More recently, attention has been concentrated on penetrometers, which have the advantage of giving a general picture of a sand stratum from continuous readings. At least 12 Papers in the 1957 International Conference were concerned with penetrometers, and they are becoming increasingly reliable in their measurements. For example, the nucleonic penetrometer developed by Soil Mechanics Ltd. is capable of measuring bulk densities in sand to an accuracy of $\pm$ 1 lb/cu.ft. i.e. $\pm$ 5% relative porosity in Brasted sand. Disturbed samples of sand can be easily obtained and the strength-density curve at different depths can be estimated at a cost of approximately £6 per sample compared to approximately £180 for 15 large diameter triaxial shear tests; the time required to obtain the strength-density curve is reduced from 2 - 4 weeks to 1 day.

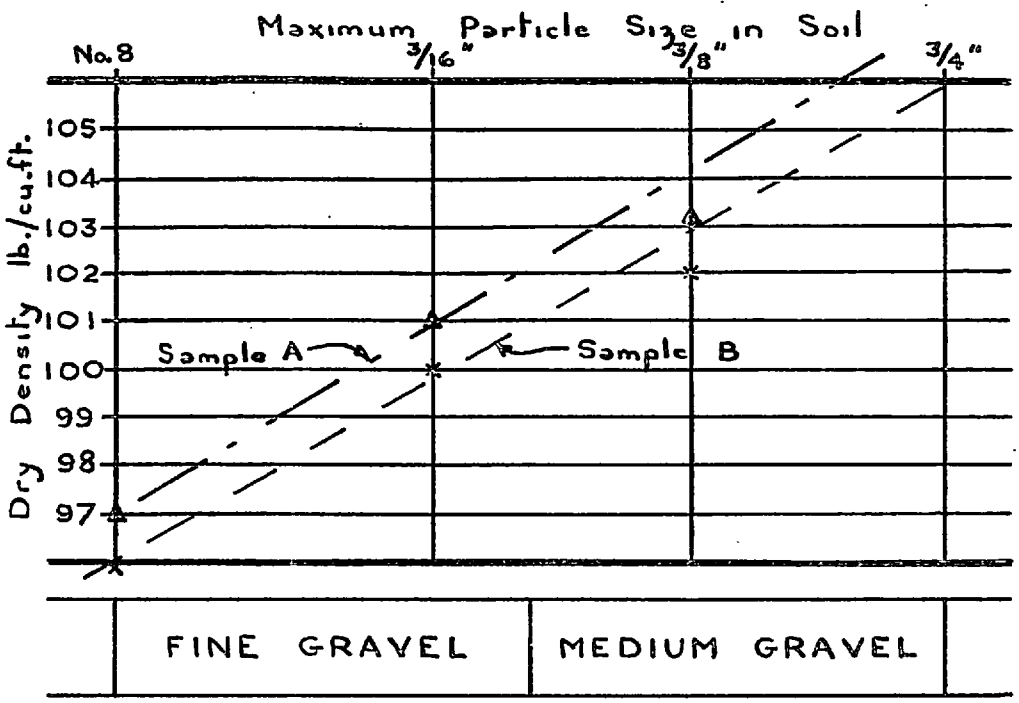
The design method can also be used to estimate the strength of sands in plane strain, as mentioned previously. The reasons for requiring knowledge about the plane strain condition were treated in Chapter 1.

Extension of the correlation to other soil types

The proposed design method has the disadvantage that it is only applicable to sands and coarse silts.

Density limits on gravels are difficult to determine with accuracy due to unnaturally high void ratios which occur between the soil and walls of the measuring vessel. Well-graded sandy gravels can be treated by slight changes in technique, as follows :-

Zero relative porosity. Dry soil is passed through a No. 8 B.S. sieve and rapid tilt tests are carried out on the finer fraction. Particle sizes up to $\frac{3}{16}$" and, later, $\frac{3}{8}$" are added to the tested material and the tilt tests are repeated. When particle sizes up to $\frac{3}{8}$" are included in the soil it is clearly seen that there are unnaturally high void spaces between the soil and glass measuring cylinder. With each successive increase in the maximum particle size, the dry density of the soil increases, probably as a result of the better grading. The results are then plotted on a semi-logarithmic grading curve representing dry density v. maximum particle size and a straight line extrapolation is made to the maximum particle size of the sandy gravel. For laboratory tests on 4 in. diameter test specimens, the maximum particle sizes are usually limited to $\frac{3}{4}$". A typical result, on the next page, shows the line passing above the dry density measured for material finer than $\frac{3}{8}$". A well-graded gravel has a dry density range of approximately 25 lb/cu.ft. so the above technique should be a satisfactory method of measuring zero relative porosity for practical purposes.




100% relative porosity. Exclude particle sizes larger than $\frac{3}{4}$" and vibrate the saturated soil in a Proctor mould using a Kango hammer. Vibration time :- 2 minutes. Repeat the test until consistent results have been obtained. To determine 100% relative porosity for well-graded materials containing particle sizes larger than $\frac{3}{4}$", an extrapolation method can be adopted on the same principles as the method outlined for zero relative porosity.

One possible means of relating the plane and symmetric strain conditions in clays may be through the equation (5), page 146 linking the two dimensionless parameters R. To determine $R_s$, standard triaxial compression tests should be continued to the ultimate condition. $R_s$ is then the ratio of the peak:ultimate strengths.

Normally consolidated clays do not dilate during shear but have characteristics similar to Fig. 8-18. The Mohr envelope usually passes through the origin and equation (5) suggests that the angle of shearing resistance will always be the same in these clays, irrespective

of the external strain condition.

The results of drained triaxial tests on undisturbed, heavily overconsolidated fissured clays are not as consistent, in general, as normally consolidated clays. On the limited evidence available to the author, it appears that the ratio $R_s$ ( peak : ultimate ) of well-defined Mohr envelopes is surprisingly constant at all effective consolidation pressures in the usual laboratory pressure range. e.g. London Clay. Hence, an estimate of the plane strain Mohr envelope for the peak strength, calculated from the equation (5) suggests that both the cohesion intercept and angle of shearing resistance will be greater in plane strain than under symmetric strain conditions. It will be interesting to see whether these relationships for clays are borne out by later experiments on Dr. Bishop's plane strain apparatus.

Relative porosity, relative density & relative dry density

Burmister (1939, 1948) first suggested methods of determining the limiting densities of a sand in the laboratory. He related the natural density of the soil with the limiting densities through the relative density, $D_r$ , defined by:-

$$D_r = \frac{e_{max.} - e}{e_{max.} - e_{min.}}$$

where $e_{max.}$, $e_{min.}$ are the voids ratios of the sand at the limiting densities and $e$ is the voids ratio of the soil in its natural state.

At maximum density, $D_r = 1$ (or 100%)
At minimum density, $D_r = 0$

Therefore, at the laboratory density limits, relative porosity and relative density are numerically equal. At intermediate densities, the relative density is always higher than the relative porosity. It is unfortunate that the two definitions should have arisen. The author adopted the relative porosity term because it has been used in British research work for several years. However, in putting forward a practical method, it is important to consider the differences between the two definitions as the relative density is sometimes used to predict the likely behaviour of sand deposits in the field (Terzaghi & Peck, 1948; Menzenbach, 1958). It will be shown that, for practical purposes, they can be regarded as interchangeable and the foundation engineering criteria for relative density are equally valid for relative porosity values.

$$n_r = \frac{(n_{max.} - n)}{(n_{max.} - n_{min.})}$$

$$= \frac{\dfrac{e_{max.}}{(1 + e_{max.})} - \dfrac{e}{(1 + e)}}{\dfrac{e_{max.}}{(1 + e_{max.})} - \dfrac{e_{min.}}{(1 + e_{min.})}}$$

$$= \frac{\dfrac{e_{max.}(1 + e) - e(1 + e_{max.})}{(1 + e_{max.})(1 + e)}}{\dfrac{e_{max.}(1 + e_{min.}) - e_{min.}(1 + e_{max.})}{(1 + e_{max.})(1 + e_{min.})}}$$

$$= \frac{\dfrac{e_{max.} + e\cancel{.e_{max.}} - e - e\cancel{.e_{max.}}}{(1 + e_{max.})(1 + e)}}{\dfrac{e_{max.} + e\cancel{_{max.}.e_{min.}} - e_{min.} - e\cancel{_{max.}.e_{min.}}}{(1 + e_{max.})(1 + e_{min.})}}$$

$$= \left\{\frac{(e_{max} - e)}{(e_{max.} - e_{min.})}\right\}\left\{\frac{(1 + e_{max.})(1 + e_{min.})}{(1 + e_{max.})(1 + e)}\right\}$$

$$\text{i.e. } n_r = D_r \cdot \frac{(1 + e_{min.})}{(1 + e)} \qquad \ldots\ldots\ldots\ldots\ldots\ldots\ldots\ldots\ldots\ldots\ldots\ldots(8)$$

$D_r \geqslant n_r$. The difference is greatest when $\frac{d(D_r - n_r)}{d(e)} = 0$

$$\frac{d}{d(e)}(D_r - n_r) = \frac{d}{d(e)}\left\{\frac{(e_{max.} - e)}{(e_{max.} - e_{min.})}\right\}\left\{\frac{(e - e_{min.})}{(1 + e)}\right\}$$

$$= \frac{(e - e_{min.})}{(1 + e)} \cdot \frac{(-1)}{(e_{max.} - e_{min.})} + \frac{(e_{max.} - e)}{(e_{max.} - e_{min.})} \cdot \left\{\frac{(1 + e) - (e - e_{min.})}{(1 + e)^2}\right\}$$

$$= \frac{-(e - e_{min.})(1 + e) + (e_{max} - e)(1 + e_{min.})}{(1 + e)^2(e_{max.} - e_{min.})}$$

Numerator = 0 when

$$(1 + e)(e - e_{min.}) = (1 + e_{min.})(e_{max.} - e)$$

$$\text{i.e.} \qquad e^2 + 2e - (e_{max.} + e_{min.} + e_{min.} e_{max.}) = 0$$

$$e > 0, \qquad \therefore \; e = -1 + \sqrt{(1 + e_{min.} + e_{max.} + e_{min.} \cdot e_{max.})} \qquad ..(9)$$

e.g. Brasted sand $n_{max.} = 44.2\%$ $e_{max.} = 0.792$

$n_{min.} = 32.2\%$ $e_{min.} = 0.475$

Maximum difference between $n_r$ and $D_r$ occurs when

$$e = -1 + \sqrt{(1 + 1{\cdot}267 + 0{\cdot}376)}$$

$$= 0{\cdot}626$$

For this value of $e$, $D_r = 52{\cdot}0\%$, $n_r = 47{\cdot}2\%$.

Therefore, the difference between the relative porosity and relative density is always less than 5%, the maximum difference occurring at a density approximately half-way between the limits.

The relative porosity and relative density are not particularly apt definitions for practical work. The two expressions are slightly confusing in that a minimum density is given by a maximum voids ratio or porosity, and vice versa. Secondly, both expressions require the measurement of the specific gravity of the soil particles and yet, by the very use of relative terms, the absolute value of the voids ratio or porosity is discounted. A more convenient practical form would be a term such as a relative dry density, defined by :-

$$\gamma_r = \frac{\gamma_d - \gamma_{d(min.)}}{\gamma_{d(max.)} - \gamma_{d(min.)}} \qquad \text{.....(10)}$$

where $\gamma_{d(min.)}$, $\gamma_{d(max.)}$ are the dry densities of the sand at the limiting densities and $\gamma_d$ is the dry density of the sand in its natural state.

At maximum density, $\gamma_r = 1$ (or 100%)

At minimum density, $\gamma_r = 0$

$$\gamma_r = \frac{\frac{1}{(1+e)} - \frac{1}{(1+e_{max.})}}{\frac{1}{(1+e_{min.})} - \frac{1}{(1+e_{max.})}}$$

$$= \frac{\frac{(1+e_{max.}) - (1+e)}{(1+e)(1+e_{max.})}}{\frac{(1+e_{max.}) - (1+e_{min.})}{(1+e_{min.})(1+e_{max.})}}$$

$$= \left\{\frac{(e_{max.} - e)}{(e_{max.} - e_{min.})}\right\}\left\{\frac{(1+e_{min.})(1+e_{max.})}{(1+e)(1+e_{max.})}\right\}$$

$$\therefore \gamma_r = D_r \cdot \left\{\frac{(1+e_{min.})}{(1+e)}\right\} \qquad \text{.....(11)}$$

The surprising fact emerges that the relative dry density is numerically equal to the relative porosity. It has advantages over the latter term in that it is more readily understood and can be more quickly evaluated in practice. The author would like to see equation (10) given international recognition as the definition of "relative density", replacing the relative porosity and the existing definition of relative density. This should not be difficult because the three terms are, for practical purposes, interchangeable.



PLATE 10-1 MEASUREMENT OF THE ANGLE OF REPOSE

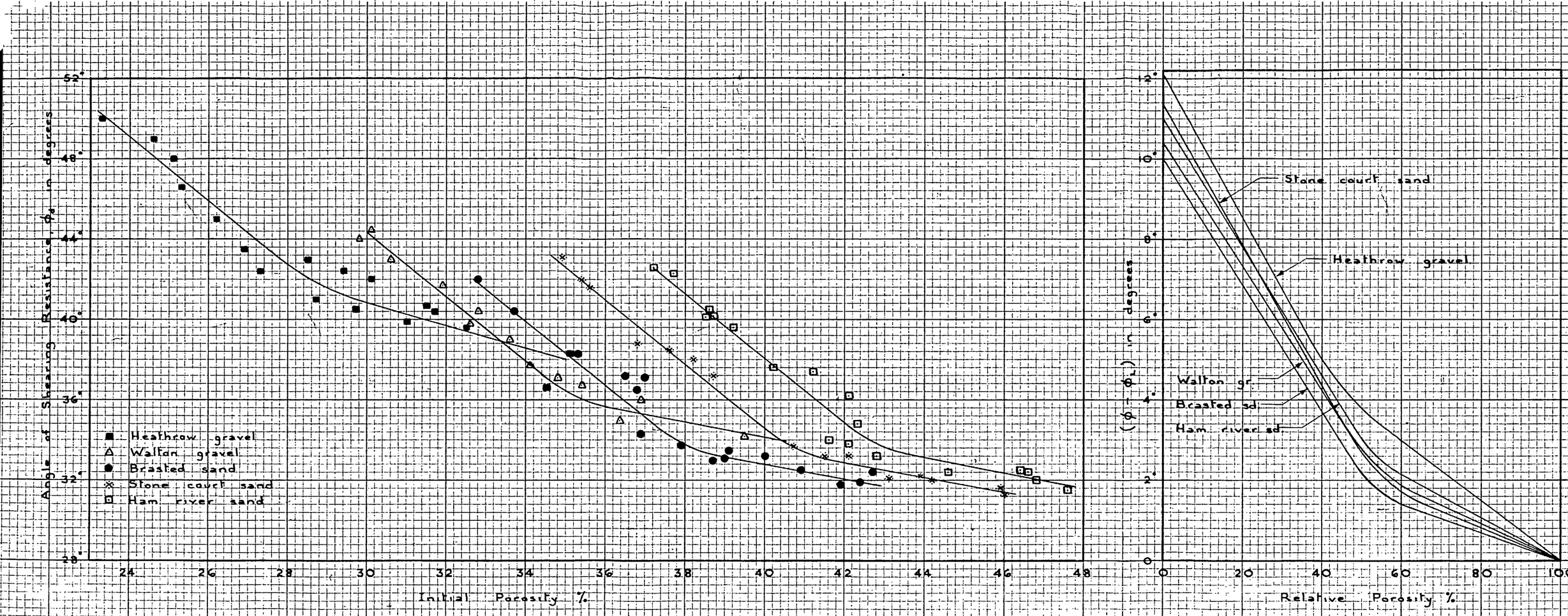
**Table 10-1** **Relation between $\phi'$ and $\frac{(\sigma_1' - \sigma_3')}{\sigma_3'}$**

(for an effective stress envelope passing through the origin of the Mohr diagram)

| $\phi'$ | $\frac{(\sigma_1' - \sigma_3')}{\sigma_3'}$ | Diff. |
|---|---|---|
| 18° | 0.894 | 71 |
| 19° | 0.965 | 75 |
| 20° | 1.040 | 77 |
| 21° | 1.117 | 81 |
| 22° | 1.198 | 84 |
| 23° | 1.282 | 89 |
| 24° | 1.371 | 93 |
| 25° | 1.464 | 97 |
| 26° | 1.561 | 102 |
| 27° | 1.663 | 107 |
| 28° | 1.770 | 112 |
| 29° | 1.882 | 118 |
| 30° | 2.000 | 124 |
| 31° | 2.125 | 130 |
| 32° | 2.255 | 137 |
| 33° | 2.392 | 145 |
| 34° | 2.537 | 153 |
| 35° | 2.690 | 162 |

| $\phi'$ | $\frac{(\sigma_1' - \sigma_3')}{\sigma_3'}$ | Diff. |
|---|---|---|
| 36° | 2.852 | 171 |
| 37° | 3.023 | 181 |
| 38° | 3.204 | 191 |
| 39° | 3.395 | 204 |
| 40° | 3.599 | 216 |
| 41° | 3.815 | 230 |
| 42° | 4.045 | 244 |
| 43° | 4.289 | 261 |
| 44° | 4.550 | 279 |
| 45° | 4.829 | 30 |
| 46° | 5.13 | 32 |
| 47° | 5.45 | 34 |
| 48° | 5.79 | 36 |
| 49° | 6.15 | 40 |
| 50° | 6.55 | 42 |
| 51° | 6.97 | 46 |
| 52° | 7.43 | |

Fractions of a degree may be estimated by linear interpolation.







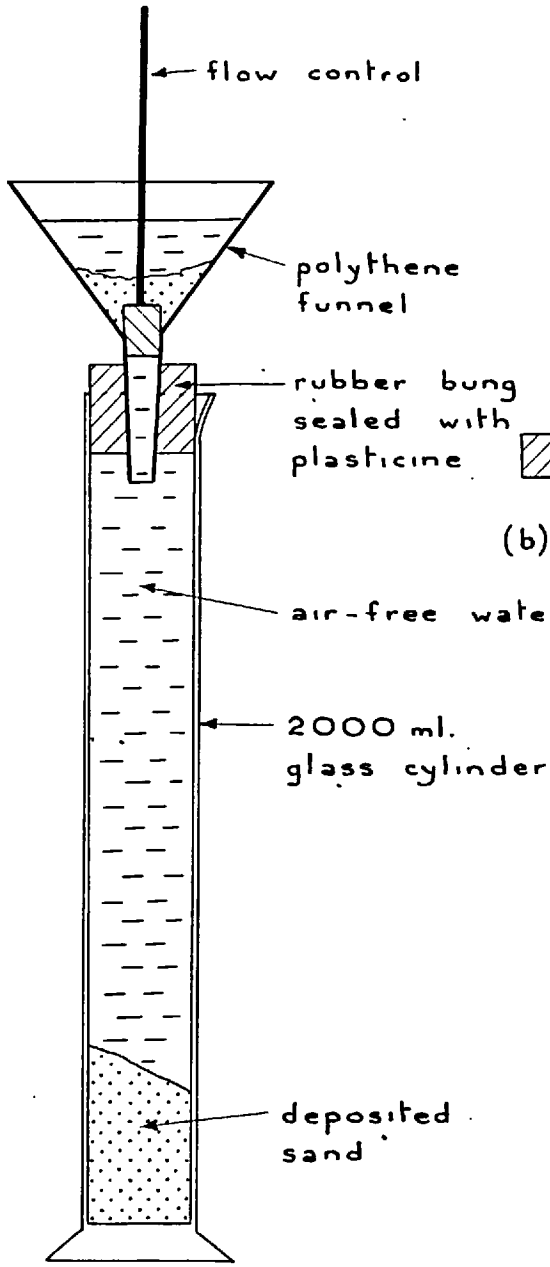
## CORRELATION BETWEEN STRENGTH AND POROSITY FOR FIVE GRANULAR SOILS

### BY HAFIZ (1950)

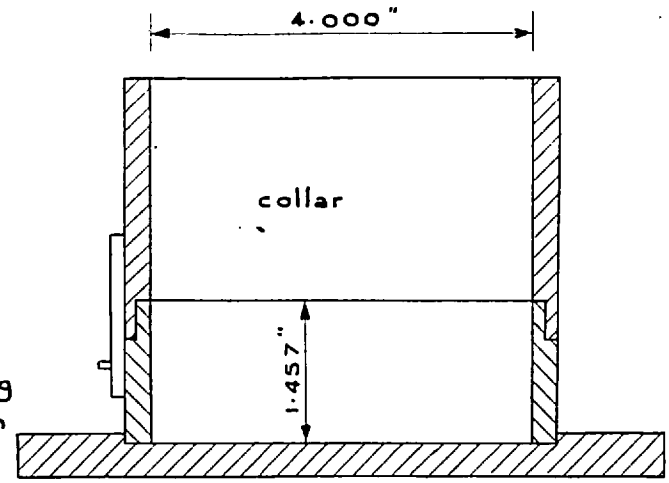
Large shear box (12 in square); Normal pressure 2·00 ton/sq.ft.
Limiting initial densities obtained by methods of Kolbuszewski (1948)

| Angles of Repose (degrees) | $\phi_L$ |
|---|---|
| Heathrow gravel – 36·9° | – 37·8° |
| Walton gravel – 34·8° | – 34·2° |
| Brasted sand – 32·2° | – 31·8° |
| Stone court sand – 31·8° | – 31·4° |
| Ham river sand – 32·0° | – 31·7° |

FIG. 10-1

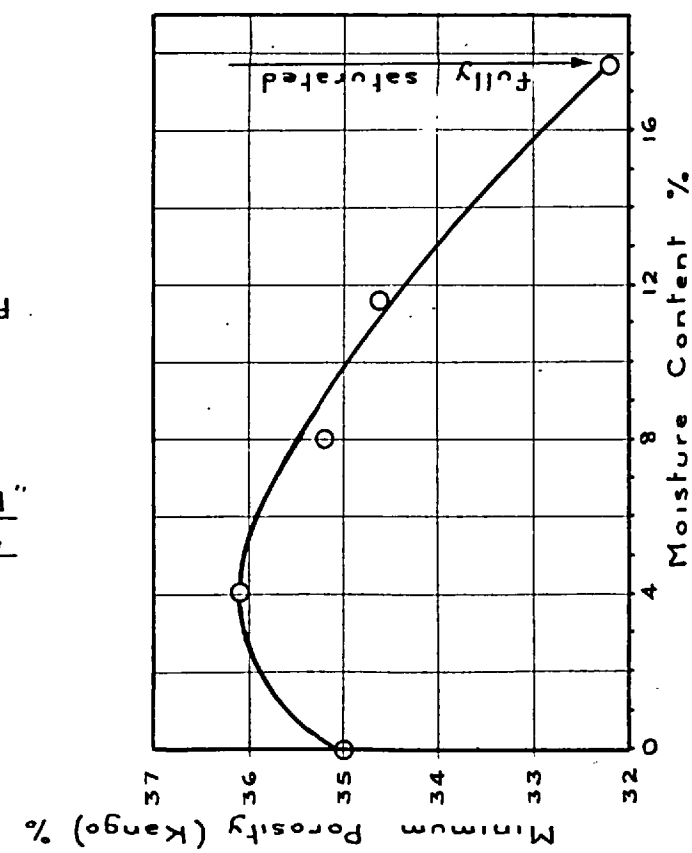



(a) Kolbuszewski's "Standard" Technique – Max. Porosity




(b) Apparatus for Measuring Minimum Porosity Limit

Proctor mould reduced to 300 ml. capacity.
Weight of soil required to fill mould = 550 - 600 gm.




(c) Relation between Min. Porosity & Moisture Content using Kango Hammer & Apparatus (b)

## LIMIT DENSITIES

FIG. 10-2

Relative Porosity, $n_r$ %

80 70 60 50 40 30 20 10 0

## SHEAR STRENGTH PARAMETERS – DRAINED COMPRESSION TESTS

□ Plane strain
○ Standard triaxial

(2)

$R = \left[\frac{\sigma_1 - \sigma_3}{\sigma_3}\right]_{min.}$ & $\left[\frac{\sigma_1 - \sigma_3}{\sigma_3}\right]_{min.}$ Ratios

$\left[\frac{\sigma_1 - \sigma_3}{\sigma_3}\right]_{min.} = 2.36 \quad (\phi = 32.8°)$

Angle of Repose = 32.5°

Angle of Shearing Resistance, $\phi_d$

Tilt test n = 44.2%

Initial Porosity %

FIG. 10 - 3

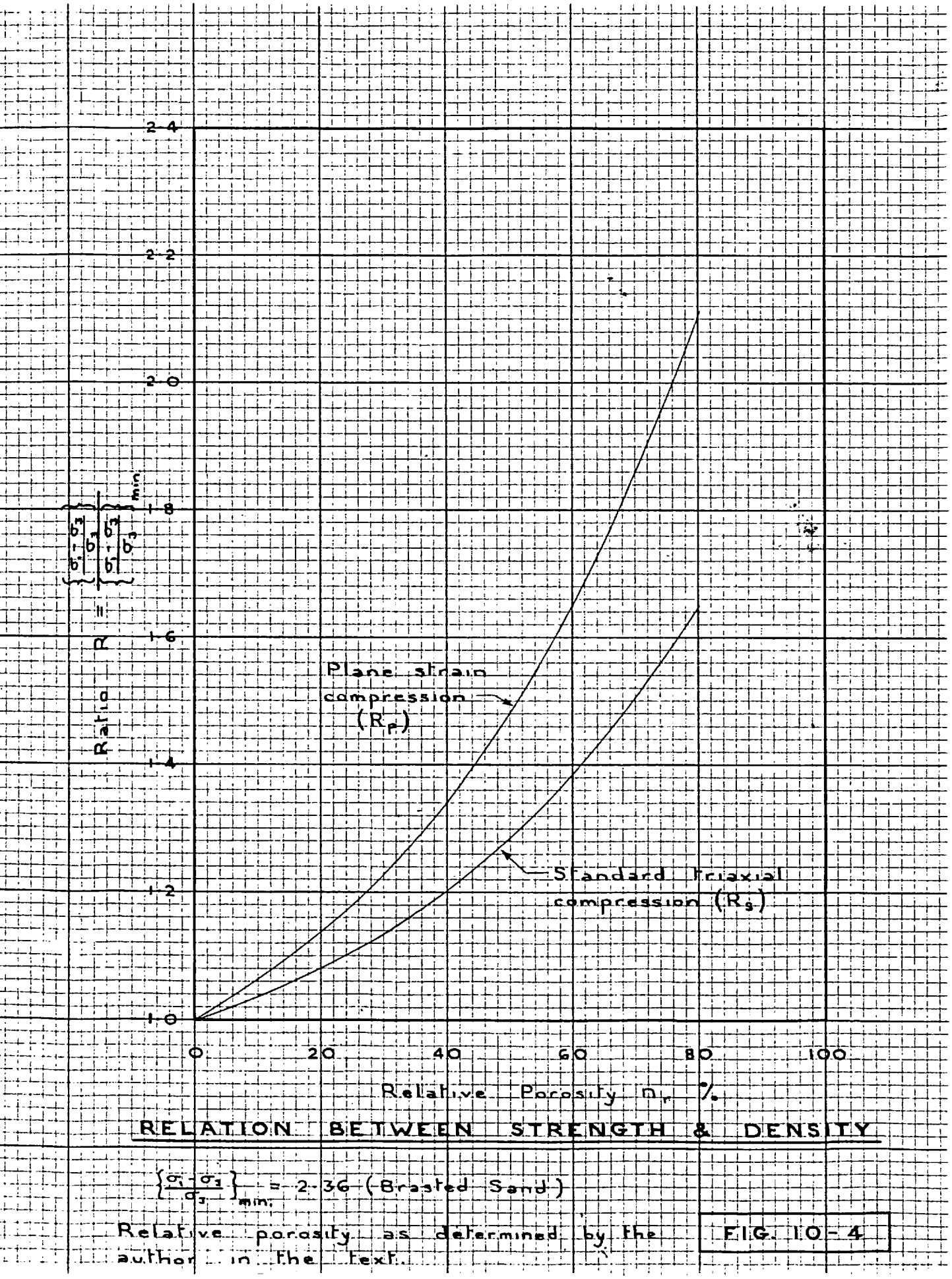
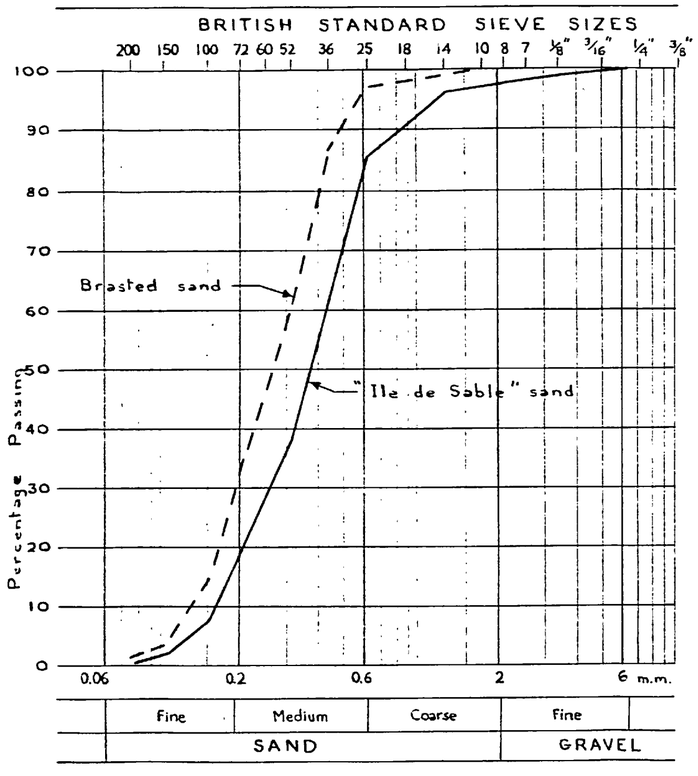
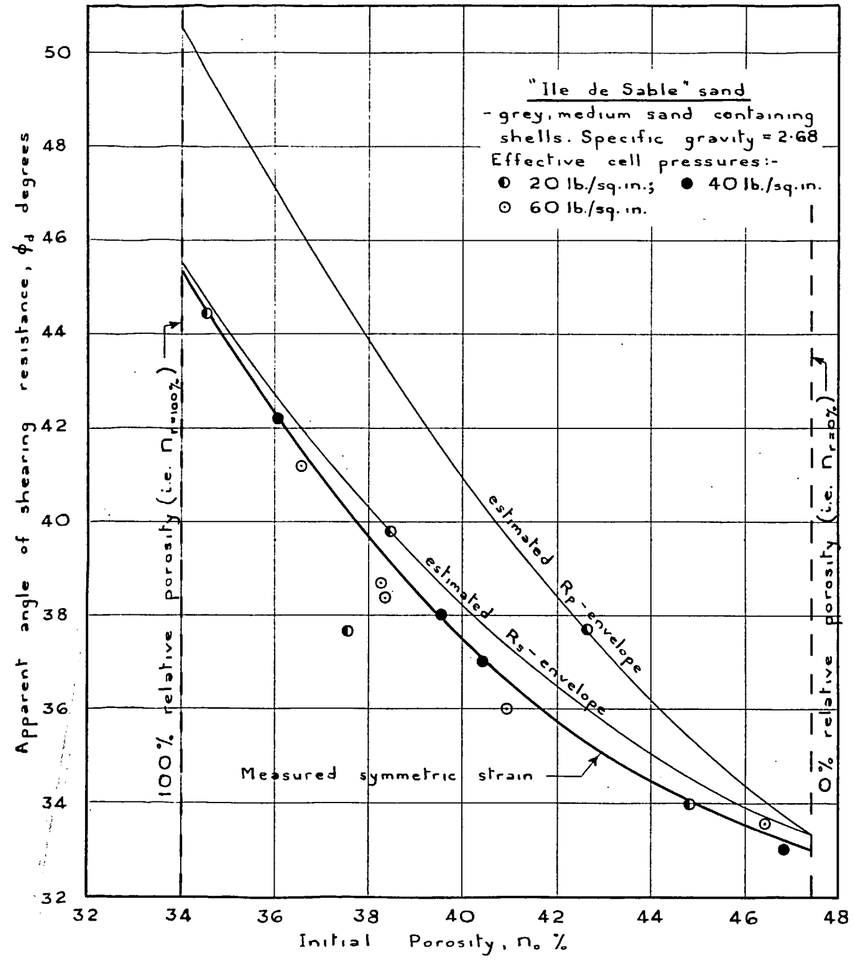

2·4
2·2
2·0
1·8
1·6
1·4
1·2
1·0
Ratio R
Plane strain compression ($R_p$)
Standard triaxial compression ($R_s$)
0
20
40
60
80
100
Relative Porosity $n_r$ %
RELATION BETWEEN STRENGTH & DENSITY
$\left\{\frac{\sigma_1-\sigma_3}{\sigma_3}\right\}_{min.}$ = 2·36 (Brasted Sand)
Relative porosity as determined by the author in the text.

FIG. 10-4




(a) Grading curves




(b) Drained standard triaxial shear tests on saturated sand
(4-inch diameter specimens compacted by tamping)

| Relative Porosity $n_r$ % | SYMMETRIC STRAIN $R_s$ | $\left\{\frac{\sigma_1-\sigma_3}{\sigma_3}\right\}_s$ | $\{\phi_d\}_s$ degrees | PLANE STRAIN $R_P$ | $\left\{\frac{\sigma_1-\sigma_3}{\sigma_3}\right\}_P$ | $\{\phi_d\}_P$ degrees | Initial Porosity $n_o$ % |
|---|---|---|---|---|---|---|---|
| 0 | 1·000 | 2·435 | 33·3 | 1·000 | 2·435 | 33·3 | 47·40 |
| 10 | 1·038 | 2·527 | 33·95 | 1·065 | 2·593 | 34·35 | 46·06 |
| 20 | 1·081 | 2·632 | 34·6 | 1·139 | 2·774 | 35·5 | 44·72 |
| 30 | 1·134 | 2·761 | 35·45 | 1·228 | 2·990 | 36·8 | 43·38 |
| 40 | 1·200 | 2·922 | 36·4 | 1·341 | 3·265 | 38·3 | 42·04 |
| 50 | 1·282 | 3·122 | 37·55 | 1·478 | 3·599 | 40·0 | 40·70 |
| 60 | 1·381 | 3·362 | 38·85 | 1·648 | 4·013 | 41·85 | 39·36 |
| 70 | 1·505 | 3·666 | 40·3 | 1·859 | 4·527 | 43·9 | 38·02 |
| 80 | 1·650 | 4·019 | 41·9 | 2·104 | 5·123 | 46·0 | 36·68 |
| 90 | (1·82) | 4·43 | 43·55 | (2·40) | 5·85 | 48·15 | 35·34 |
| 100 | (2·05) | 4·99 | 45·55 | (2·78) | 6·77 | 50·5 | 34·00 |

Initial Porosity, $n_o\% = (n)_{r=0\%} - \left\{\frac{(n)_{r=0\%} - (n)_{r=100\%}}{100}\right\} n_r$

(c) Table of calculations for estimated strength-density envelopes

PRACTICAL DESIGN METHOD; WORKED EXAMPLE, ILLUSTRATING A COMPARISON BETWEEN THE MEASURED & ESTIMATED STRENGTH-DENSITY ENVELOPES FOR SYMMETRIC STRAIN CONDITIONS

FIG. 10-5

Angle of Shearing Resistance, $\phi_d$ degrees

54° 53° 52° 51° 50° 49° 48° 47° 46° 45° 44° 43° 42° 41° 40° 39° 38° 37° 36° 35° 34° 33° 32° 31° 30° 29° 28°

100 90 80 70 60 50 40 30 20 10 0

Relative Porosity %

Angle of Repose values

# STRENGTH OF COHESIONLESS SOILS IN PLANE & SYMMETRIC STRAIN FOR COMMON REPOSE ANGLES

plane strain — symmetric strain

FIG. 10-6

## LIST OF REFERENCES


ARMSTRONG, E.C. (1945) "Progress report on testing apparatus installations. Anderson Ranch Dam, Idaho" U.S. Bureau of Reclamation.

BALLA, A. (1957) "Stress conditions in the triaxial compression test." Proc. 4th Int. Conf. Soil Mech. I.pp. 140-143.

BISHOP, A.W. (1954) Letter to Geotechnique Géotechnique Vol. IV, pp 43-45

BISHOP, A.W. (1955) "The use of the slip circle in the stability of slopes." Géotechnique V; pp 7-17.

BISHOP, A.W. (1958) "Test requirements for measuring the coefficient of earth pressure at rest." Proc. European Conf. on Earth Pressures Vol. 1. (Brussels).

BISHOP, A.W. & EIDIN, A.K.G. (1950) "Undrained triaxial tests on saturated sands and their significance in the general theory of shear strength." Géotechnique Vol. II; pp 13-32.

BISHOP, A.W. & EIDIN, A.K.G. (1953) "The effect of stress history on the relation between $\phi$ and porosity in sand." Proc. 3rd Int. Conf. Soil Mech. I pp 100-105.

BISHOP, A.W. & HENKEL, D.J. (1957) "The measurement of soil properties in the triaxial test." Edward Arnold, London, 190 pp.

BJERRUM, L. (1954) "Theoretical and experimental investigations on the shear strength of soils." Norges Geotekniske Institutt Publication No.5 112 pp.

BJERRUM, L., KRINGSTAD, S. & KUMMENEJE, O. (1959) "The shear strength of a fine loose sand." Norwegian Geotechnical Institute Internal Report (unpublished)

BLIGHT, G.E. (1961) "Strength and consolidation characteristics of compacted soils." Ph.D.Thesis, University of London.

BRIDGMANN, P.W. (1946) "Studies of plastic flow, especially in two-dimensional compression." Journal of App. Physics. Vol.17 p.225.

BURMISTER, D.M. (1948) "The importance and practical use of relative density in soil mechanics." Vol. 48, Proc. A.S.T.M. pp. 1249-1269.

CASAGRANDE, A. & SHANNON, W.L. (1948) "Stress-deformation and strength characteristics of soils under dynamic loads." Proc. 2nd. Int. Conf. on Soil Mechanics. Vol. V, p.29.

DANIEL, A.W.T. (1954) "A study of the stress-strain characteristics of granular materials." Ph.D. Thesis, University of London.

DE JOSSELIN DE JONG, G. (1959) "Statics and kinematics in the failable zone of a granular material." Uitgeverij Waltman (Delft).

ELDIN, A.K.G. (1951) "Some fundamental factors controlling the shear properties of sand." Ph. D. Thesis, University of London.

FILON, L.N.G. (1902) "On the elastic equilibrium of circular cylinders under certain practical systems of load." Phil. Trans. A, 198, p. 147.

FOURTH INTERNATIONAL CONFERENCE (1958) Discussion on "Soil Properties and their Measurement". Vol. III, 4th Int. Conf. on Soil Mech, London.

FRASER, A.M. (1957) "The influence of stress ratio on compressibility and pore pressure coefficients in compacted soils" (2 volumes) Ph.D. Thesis, Univ. of London .

HABIB, P. (1953) "Influence de la variation de la contrainte principale moyenne sur la résistance au cisaillement des sols." Proc. 3rd. Int. Conf. Soil Mech. I. pp. 131-6.

HAFIZ, M.A.A. (1950) "Strength characteristics of sands and gravels in direct shear." Ph.D. Thesis, University of London.

HENKEL, D.J. (1959) "The relationships between the strength, pore-water pressure, and volume-change characteristics of saturated clays." Geotechnique IX. P.119.

HILL, R. (1950) "The mathematical theory of plasticity." Oxford University Press.

HIRSCHFELD, R.C. (1958) "Factors influencing the constant volume strength of clays." Ph.D. Thesis, Harvard University, Cambridge, Mass.

HOLTZ, W.G. (1947) "The use of the maximum principal stress ratio as the failure criterion in evaluating triaxial shear tests on earth materials." Proc. Amer. Soc. Test. Mater. Vol. 47.

JAKOBSON, B. (1957) "Some fundamental properties of sand." Proc. 4th Int. Conf. Soil Mech.I pp167-171.

KIRKPATRICK, W.M. (1954) "The behaviour of sands under three dimensional stress systems." Ph.D. Thesis, University of Glasgow.

KIRKPATRICK, W.M. (1957) "The condition of failure for sands." Proc. 4th Int. Conf. Soil Mech.I pp 172-178

KJELLMAN, W. (1936) "Report on an apparatus for consummate investigation of the mechanical properties of soils." Proc. Int. Conf. Soil Mech. I. 2:16-20.

KOLBUSZEWSKI, J.J. (1948a) "An experimental study of the maximum and minimum porosities of sands." Proc.2nd Int. Conf. Soil Mech. I. pp 158-165.

KOLBUSZEWSKI, J.J. (1948b) "General investigation of the fundamental factors controlling loose packing of sands." Proc. 2nd Int. Conf. Soil Mech. VII, pp. 47-49.

KUMMENEJE, O. (1957) "'To-dimensjonale' vakuum-triaxialforsök på törr sand." Norwegian Geotechnical Institute Internal Report F.80 (unpublished).

LA ROCHELLE, P. (1960) "The short-term stability of slopes in London Clay." Ph.D. Thesis, University of London.

LITTLE, A.L. & PRICE, V.E. (1958) "The use of an electric computer for slope stability analysis." Géotechnique Vol. VIII. p.113.

LODE, W. (1926) "Versuche über den einfluss der mittleren hauptspannung auf der fliesen der metalle eisen, kupfer und nickel." Zeitschrift für Physik bd.36, p.913.

MENZENBACH, E. (1958) "The use of penetrometers in site investigations." Dissertation for D.I.C., University of London.

MOGAMI, T. & KUBO, K. (1953) "The behaviour of soil during vibration." Proc. 3rd. Int. Conf. Soil Mech. I. pp 152-155.

NADAI, A. (1950) "Theory of flow and fracture of solids." Vol.I. McGraw-Hill, New York.

NASH, J.K.T.L. (1953) "The shearing resistance of a fine closely graded sand." Proc. 3rd Int. Conf. Soil Mech. I, pp.160-164.

PELTIER, M.R. (1957) "Recherches expérimentales sur la courbe intrinsèque de rupture des sols pulvérulents." Proc. 4th Int. Conf. Soil Mech.I pp179-182.

PENMAN, A.D.M. (1953) "Shear characteristics of a saturated silt, measured in triaxial compression." Géotechnique Vol. III. pp. 312-328.

PENMAN, A.D.M. (1956) "A field piezometer apparatus." Géotechnique VI; pp. 57-65.

PRANDTL, L. (1925) "Spannungsverteilung in plastischen Koerpern." Proc. 1st. Int. Congress App. Mech. Delft, Holland.

ROSCOE, K.H. (1953) "An apparatus for the application of simple shear to soil samples." Proc. 3rd. Int. Conf. Soil Mech. I. pp.186-191.

ROSCOE, K.H. SCHOFIELD, A.N. & WROTH, C.P. (1958) "On the yielding of soils." Géotechnique Vol. VIII. pp. 22-53.

SHOCKLEY, W.G. (1953) Discussion. Proc. 3rd. Int. Conf. Soil Mech. III. p.122.

SKEMPTON, A.W. (1946) "Earth pressure and the stability of slopes." Institution of Civil Engineers - The Principles and Applications of Soil Mechanics. pp 31-61.

SKEMPTON, A.W. (1960) "Effective stress in soils, concrete and rocks."
Opening address, Conf. on Pore Pressure and Suction in Soils. Butterworths, London.

SKEMPTON, A.W. & BISHOP, A.W. (1954) "Soils".
Chapter X of "Building Materials, their elasticity and inelasticity"; edited by M. Reiner. North-Holland (Amsterdam).

TAYLOR, D.W. (1941) "Cylindrical compression research program on stress-deformation and strength characteristics of soils."
7th Progress Report U.S. Army Engineers, Cambridge, Mass.

TAYLOR, D.W. (1948) "Fundamentals of soil mechanics."
John Wiley, New York.

TAYLOR, D.W. (1951) "Research on shearing resistance of clay."
Report to U.S. Army Engineers. Waterways Expt. Station. Corps of Engineers, Vicksburg, Miss.

TERZAGHI, K. & PECK, R.B. (1948) "Soil mechanics in engineering practice."
Wiley & Sons, New York.

TRIAXIAL SHEAR REPORT (1947) P.C. Rutledge. Waterways Expt. Stn. Vicksburg, Miss.

TSCHEBOTARIOFF, G.P. & WELCH, J.D. (1948) "Lateral earth pressures and friction between soil minerals."
Proc. 2nd Int. Conf. Soil Mech. VII, p.135.

WOOD, C.C. (1958) "Shear strength and volume change characteristics of compacted soil under conditions of plane strain."
Ph.D. Thesis, University of London.

WROTH, C.P. (1958) "The behaviour of soils and other granular media when subjected to shear."
Ph.D. Thesis, University of Cambridge, 244 pp.

## Appendix 1 CALIBRATION OF MEASURING DEVICES

### (a) Proving rings

The proving rings were calibrated for loads up to 400 lb. by loading with weights hanging from a loading frame. As a check on their relative calibration values, the two rings were placed one on top of the other and re-loaded in the frame. Despite these procedures, the calibration values are not very reliable in this range of loading.

The maximum working load of each ring was 3000 lb. The two rings were calibrated for the heavier loads by two testing machines - the Buckton machine of the Civil Engineering Department and the Lochenhausenwerk hydraulic testing machine of the Aeronautical Engineering Department. Ball bearings were interposed between the rings and machines during the tests to simulate the actual shear test conditions. Figure A1-1 shows the calibration curves obtained and it is seen that both machines show a similar trend i.e. that ring 332 has a slightly higher load factor than ring 133. The absolute values of the load factors differ slightly between the two machines and it was decided to adopt the values obtained from the Lochenhausenwerk machine which has been installed fairly recently and is reputed by the makers to be accurate within $\pm$ 1%. Surprisingly enough, use of the Buckton calibration values would only alter the measured angles of shearing resistance in the drained compression tests by less than $0.1^{\circ}$

### (b) Manometers and pressure gauges

The triaxial cell fitted with a rotating bush was connected to the manometers and pressure gauges. The cell was filled with water and castor oil was added to prevent excessive leakage between the piston and bushing. The piston was loaded with weights hanging from a loading frame and after each weight increment, the pressure required to "float" the piston (at a predetermined level) was added to the cell from a screw ram. The pressure was calculated from the total weight on the piston divided by the piston cross-sectional area.

The pressure measuring devices were also calibrated directly by

measuring the difference between the mercury levels applying the pressure. The formula used to compute the pressure is given in Bishop & Henkel (1957). It is thought that the triaxial cell method gives the most accurate values of pressure.

(c) Plane strain end clamp

In the shearing stage of a plane strain test, the water in the diaphragm of the end clamp is at a higher pressure than the cell pressure and a certain amount of expansion takes place in the rubber annulus, nylon tubing and other component parts of the apparatus. If the plane strain condition is to be maintained, allowance must be made for these expansions and the mercury level in the null indicator raised progressively as the lateral deviator stress increases. A dummy sample made of steel is used to calibrate the end clamp, the pressure in the null indicator system being raised in increments by the hand operated screw ram, and noting the corresponding rise in the level of the mercury in the null indicator. A rise of 0.1 inches for every 60 lb./sq.in. pressure is allowed for the elastic compression of the dummy sample. The calibration of the end clamp was checked at intervals over the plane strain test programme, the time taken for each calibration being approximately equal to the time taken for a shear test. For future long-term tests, however, allowance will have to be made for creep and loss of water through the walls of the nylon tubing.

The second part of the calibration is to measure experimentally the effective area of the end clamp loading diaphragm. Loads are applied from a small loading frame via a proving ring to the rigid disc at the centre of the diaphragm. The height of the mercury thread in the null indicator is kept at the appropriate reference mark by adjusting either the manual screw ram of the intermediate principal stress measuring system, or a screw jack in the loading frame.

This part of the calibration was not carried out in the present investigation; instead, it was erroneously assumed that the area of the rigid disc represented the effective area of the diaphragm. From the calibration quoted by Wood (1958), this error is comparatively small and is discussed in Appendix 4.

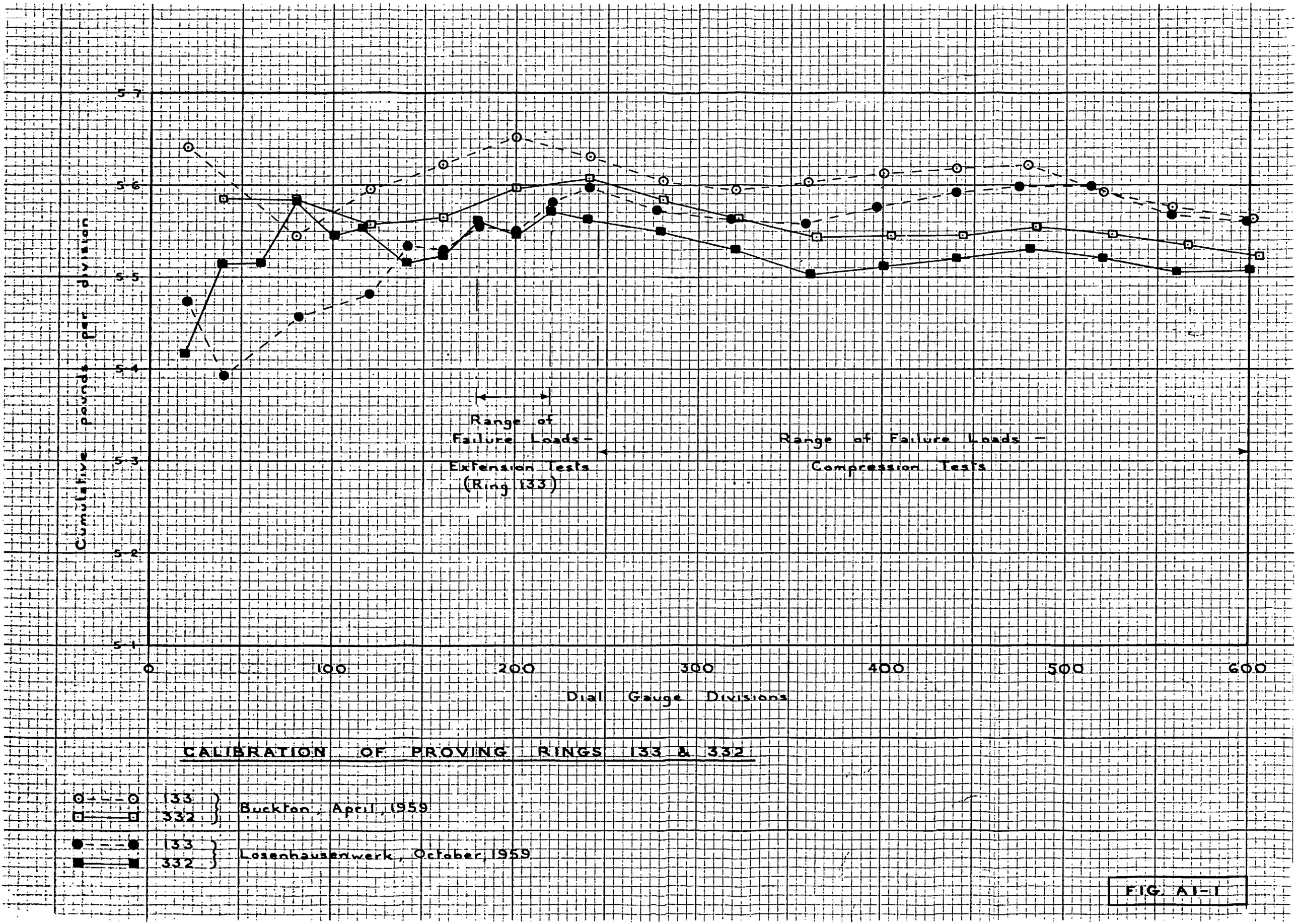

5·7
5·6
5·5
5·4
5·3
5·2
5·1
Cumulative pounds per division
0
100
200
300
400
500
600
Dial Gauge Divisions
Range of Failure Loads — Extension Tests (Ring 133)
Range of Failure Loads — Compression Tests
CALIBRATION OF PROVING RINGS 133 & 332
133
332
Buckton, April, 1959
133
332
Losenhausenwerk, October, 1959

FIG. A1-1

## Appendix 2 METHOD OF MAKING RUBBER MEMBRANES

The membranes used in the plane strain tests were made in the laboratory by coating a solid perspex former with an emulsion of latex and allowing it to dry. Dipping was repeated until the desired thickness of membrane had been obtained. After drying, the membrane was removed from the former with the aid of French chalk. By using two formers, a continuous supply of membranes was obtained, each membrane being used for one test only. Suppliers of Revultex and coagulant are Revertex, Ltd., 51-55 Strand, London, W.C.2.

Procedure The technique adopted to make a membrane differed from the two-stage method described by Wood (1958). The former was thoroughly cleaned and dried. It was then immersed in the latex dipping tank and partially withdrawn so that the upper edge of the former was level with the surface of the emulsion. The former was held in this position for approximately 1 minute until the surplus latex had run down the 1 in 4 slope of the upper surface and back into the tank. The former was slowly withdrawn and hung up by the handle to dry for approximately 1 hour. After drying, the former was inverted and the cycle of dipping repeated 4 times to produce a membrane 0.012 to 0.016 inches thick, which is the minimum thickness recommended for tests on sand. The latex covered the flat surfaces of the perspex more thickly than the edges. Alcohol coagulant was coated onto the edges of the former before the 4th dipping cycle to thicken the membrane at these points.

The dried membrane surface was dusted with French chalk. The upper and lower surfaces of the membrane were cut to the shape required for the upper and lower platens of the testing machine. The membrane was carefully stripped from the former, applying French chalk to each part of the inner surface of the membrane as it became free. It was unnecessary to wash the membrane afterwards.

## Appendix 3 RUBBER MEMBRANE CORRECTIONS

Following the methods outlined by Henkel & Gilbert (1952) and Wood (1958), the membrane corrections were computed as follows:-

### Plane Strain

$$\text{Membrane correction} = \frac{2(b+t)M\epsilon}{A_\epsilon}$$

where $M$ = extension modulus of membrane

$2(b+t)$ = initial perimeter of sample

$\epsilon$ = axial strain

$A_\epsilon$ = actual cross-sectional area of sample

Tests have shown that $M \triangleq 175\,T$, where $T$ is the thickness of membrane in inches and $M$ is in lb./in.

To simplify the above expression:-

$2(b+t)$ = 36 inches nominally

$A$ = 32 sq.in. nominally

$$\text{Correction (P.S.)} \triangleq 200\,T\epsilon \text{ lb./sq.in.}$$

Example:- Test P-19 (medium dense)

At failure, $\epsilon$ = 1.8% = 0.018

$T$ = 0.019 in.

$\therefore$ Membrane correction = 0.07 lb./sq.in.

Measured failure stress = 141.0 lb./sq.in.

$\therefore$ Membrane correction = 0.05% of deviator stress at failure

### Standard Triaxial

$$\text{Membrane correction} = \frac{\pi DM\epsilon}{A_\epsilon}$$

where $D$ = original diameter of sample.

$M, \epsilon, A_\epsilon$ are as defined above

Simplifying the above expression by substituting the nominal dimensions of the sample:-

$$\text{Correction (S.T)} \triangleq 175\,T\epsilon \text{ lb./sq.in.}$$

Example:- Test C-33 (medium dense)

At failure, $\epsilon$ = 4.8% = 0.048

$T$ = 0.011 in.

$\therefore$ Membrane correction = 0.09 lb./sq.in.

Measured failure stress = 122.6 lb./sq.in.

$\therefore$ Membrane correction = 0.07% of deviator stress at failure

## Appendix 4 EFFECT OF ERRORS IN MEASUREMENTS

It would be difficult to estimate, in a comprehensive manner, the likely order of errors in the measured porosities and strengths of the shear tests, since both sets of measurements are subject to many individual sources of error. Nevertheless, it is useful to have some idea of the relative effects of individual errors when other sources of error are neglected. A brief list follows:-

### Plane Strain

Average test specimen (P-11 to P-35). Initial values:- height = 4.435 in., width = 2.061 in., length = 16.063 in.; total volume = 2406.0 cc.; volume of solids = 1470.7 cc.; volume of voids = 935.3 cc.; porosity = 38.87%; average dry weight of sand in a specimen = 3947 gm. The drained strength of such an average specimen would be approximately

$$\frac{(\sigma_1' - \sigma_3')}{\sigma_3'} = 3.30 \quad (\phi = 38.6°)$$

### A. errors in porosity

(i) width - extremely consistent from specimen to specimen due to the use of a sand former. Maximum error probably $\pm$ 0.002 in. $\equiv$ $\pm$ 0.05% porosity.

(ii) length - error probably negligible unless some of the looser specimens decreased in length on application of the initial negative pressure. From the check measurements (to 0.01 in.) this did not seem to have occurred. If error is $\pm$ 0.01 in., error in porosity is $\pm$ 0.03%.

(iii) height - of the three linear dimensions, the height is most susceptible to unreliable measurement. The likely error is difficult to estimate but it will probably not be more than $\pm$ 0.04 cm. $\equiv$ $\pm$ 0.22% porosity.

(iv) the maximum error in the estimate of the "lost" volume at the rounded ends of the specimen is probably $\pm$ 2 cc. $\equiv$ $\pm$ 0.05% porosity.

(v) the effect of an incorrect measurement of the sands dry weight of $\pm$ 3 gm. would be $\pm$ 0.02% porosity.

B. errors in strength

(i) assumed $K_o$ value in gross error.

Average consolidation volume change = 26.3 cc.

Volumetric strain = 1.093%

If all-round pressure ($K_o$ = 1) was used instead of the true $K_o$ value, the area and hence, the strength, would be in error by 0.73% (0.13 degrees). Any errors in the $K_o$ value must be considerably less than this figure.

(ii) length and width having maximum error of same sign.

Change in cross-sectional area = change in strength = 0.15% (negligible).

(iii) effect of $\pm$ 2 cc. maximum error in the estimated "lost" volume at the rounded ends of the specimen on the calculation of the cross-sectional area. Error on average specimen = $\pm$ 0.08% in area and strength (negligible).

(iv) proving ring calibration in error by $\pm$ 1% at failure ($\pm$ 0.18 degrees).

C. errors in measurement of $\sigma_2$

Unfortunately, an error in the calculations of the intermediate principal stress has been pointed out to the Author at a late stage in the preparation of the Thesis. The area transmitting the water pressure inside the end clamp has been assumed to be the area of the rigid disc attached to the diaphragm whereas part of the load on the rubber annulus is also transmitted to the ends of the specimen i.e. the effective loading area is greater than the area of the rigid disc in the centre. If the rigid disc remains stationary during shear, the effective diameter of the diaphragm will be approximatley equal to the diameter of the rigid disc plus the width of the annulus. This effective area is 6.1% greater than the area of the rigid disc. However, for plane strain, the rigid disc moves outwards from the pressure cell to compensate for the extension of the tie bars under load. This movement will tend to distribute more of the annulus load to the outer retaining ring (Fig. 3-2). Direct calibration of the $\sigma_2$ pressure cell by Wood (1958)

gave an effective area for the diaphragm of 3.69 sq.in.,* an increase of 4.0% relative to the area of the rigid central disc (3.55 sq.in.)

There are several small compensating errors in the calculations of $\sigma_2$. Briefly, the errors which come to mind are:-

(i) errors in the calculated height after consolidation (see top of p.44). The vertical deformation during consolidation was over-estimated due to expansion of the cell under pressure. The "true" vertical deformation for each specimen has been calculated on the assumption that the extension test specimen volume changes most closely represent the correct consolidation properties of the sand (Fig. 7-7). These calculations show that the consolidated end area of the specimen was under-estimated by approximately 0.3 - 0.4% in the shear test calculations of $\sigma_2$. In some cases, the error was as high as 1%.

(ii) the gauge measuring the pressure in the diaphragm cell was not re-calibrated after the lead had been changed from small bore copper tubing to nylon tubing (see Appendix 6). The nylon tube expanded under pressure to a greater extent than the copper tubing with a consequent greater rise of mercury in the glass indicator tube to maintain the null condition of the specimen. The gauge has to support the mercury thread in the null indicator and a greater correction should be applied to the gauge readings as the mercury column rises under pressure. The error is likely to have been approximately 2 inches of mercury at failure or 1 lb./sq.in. on the gauge.

Summarising these points, the errors in the measured values of $\sigma_2$ are:-

| Cause of error | % error at failure |
|---|---|
| Incorrect effective area of diaphragm from Wood (1958) calibration | ± 4.0% |
| Consolidated height of specimen measured incorrectly due to cell expansion | + 0.4% |
| Pressure gauge not re-calibrated for more expansive nylon tubing | + 1.3% |

* this figure relates to the pressure range at failure in the present test series (drained tests).

The composite error of these 3 items is = 2.3%, and as $(\sigma_2' - \sigma_3')$ is typically $\frac{1}{4}$ of the effective cell pressure $(\sigma_3')$, the value of the intermediate principal stress has been under-estimated by 1% i.e. 0.7 lb./sq.in.

Although these errors in the calculations are regretted, they are probably well within the bounds of the total experimental error in the measurement of the intermediate principal stress. Correction of the test results by the composite error of 1.0% would alter the plotted points on Fig. 8- 4 by less than $\frac{1}{2}$ small square of the graphs. None of the graphs or tables quoting intermediate principal stress relationships have been corrected for the errors referred to in this Appendix.

Standard Triaxial Compression

Average test specimen (C-21 to C-40). Initial values:- diameter = 3.974 in.; height = 7.941 in.; total volume = 1614.1 cc.; volume of solids = 990.8 cc.; volume of voids = 623.3 cc.; porosity = 38.62%; average dry weight of sand in a specimen = 2659 gm.

The drained strength of such an average specimen would be approximately

$$\frac{(\sigma_1' - \sigma_3')}{\sigma_3'} = 2.95$$

A. errors in porosity

(i) width - maximum error probably $\pm$ 0.003 in. $\equiv$ $\pm$ 0.10% in porosity.

(ii) height - maximum error probably $\pm$ 0.03 cm. $\equiv$ $\pm$ 0.10% in porosity.

For brevity, other errors in the standard triaxial tests will be omitted, being similar in magnitude to the plane strain errors.

## Appendix 5 TYPICAL PLANE STRAIN TEST COMPUTATION

### Test No. BS-P-24

**Compaction:-** 4 layers, as follows:-
7 sec. x 3 layers, light vibration
No vibration on final layer.

**Width (inches)**

| Top | Middle | Bottom |
|---|---|---|
| 2.295 | 2.297 | 2.298 |
| .296 | .299 | .300 |
| .299 | .300 | .301 |
| .298 | .301 | .299 |
| .296 | .298 | .298 |
| .295 | .296 | .297 |

**Height (centimetres)**

| | Side no. 1 | Side no. 2 |
|---|---|---|
| L.H.S. | 20.51 | 20.42 |
| Middle | 20.43 | 20.36 |
| R.H.S. | 20.36 | 20.27 |

Average reading = 2.298 in.
Dial correction = - 0.198 in.
Membrane thickness (2 sides) = - 0.025 in.

∴ Width of specimen = 2.075 in.

Average reading = 20.39 cm.
Height of platens, top cap, membrane = - 9.34 cm.

∴ Height of specimen = 11.05 cm.
= 4.348 in.

Length of specimen and membrane = 16.100 in.
Thickness of 2 ends of membrane = - 0.028 in.
∴ Length of specimen = 16.072 in.

**Weight of sand**

Weight of sand boiled for test = 5000 gm.
Weight of sand not used in test = 1111 gm.
∴ Weight of sand before test = 3889 gm.
Final weight of sand after test = 3882 gm.
∴ Average weight of sand in test = 3885½ gm.
Weight of sand trapped between membrane and lower platen = 14 gm.
∴ Net weight of sand in specimen = 3871½ gm.

Computations

| | | |
|---|---|---|
| Cross-sectional area in the plane of the major principal stress | = 33.38 | sq.in. |
| Specimen volume | = 2367.9 | cc. |
| "Lost" volume due to rounded corners (estimate) | = - 9.0 | cc. |
| Volume change occurring between measurement and beginning of test | = - 1.8 | cc. |
| Initial cross-sectional area in the plane of the major principal stress, | = 33.23 | sq.in. |
| Cross-sectional area in the plane of the intermediate principal stress after consolidation, $A_E$ | = 8.92 | sq.in. |
| Net volume of specimen, $V_o$ | = 2357.1 | cc. |
| Volume occupied by the solids, $V_s$ | = 1442.4 | cc. |
| ∴ Volume occupied by the void space, $V_v$ | = 914.7 | cc. |
| ∴ Initial porosity of the specimen, $n_o$ | = 38.81% | |

Test details

$K_o$ = 0.436, Fraser (1957) for $n_o$ = 38.5%

$K_o$ stresses applied by hand loading

Specimen sheared at a constant rate-of-strain of 0.0012 inches/minute

Shear test - see test sheet overleaf.

Test comments

No failure plane visible at end of test.

Specimen moisture contents (end of test)

| | L.H.S. | Middle | R.H.S. |
|---|---|---|---|
| Top | 23138 | 23.76 | 23.74 |
| Middle | 23.73 | 23.61 | 23.86 |
| Bottom | 22.55 | 23.15 | 22.55 |

Average final moisture content = 23.37%

Average final porosity (for a fully saturated specimen) = 38.55%

Compare:-

final porosity, calculated from the initial weight-volume measurements and the volume changes occurring in the test = 38.53%

| Time | Cell Pressure gauge | Cell Pressure corr | Pore Water Pressure corr | Pore Water Pressure gauge | Axial Strain left dial | Axial Strain right dial | Axial Strain mean dial | Axial Strain ε mean | Load No.133 left | Load load | Load No.332 right | Load load | Load total load | Load corr. W=285 | Load net total | Area 1-ε | Area corr area | Intermediate Principal Stress gauge | Intermediate Principal Stress $\sigma_3$ + corr. | Intermediate Principal Stress net load | Intermediate Principal Stress $\sigma_3 - \sigma_0$ 0.445δ | gauge | dial | Volume burette corr. | Volume rams corr. | Volume cell + rams c. | Volume ΔV | ΔV corr. | net ΔV | $\frac{\Delta V}{V_0}$ | 100 × $\frac{\Delta V}{V_0}$ | $\sigma_1 - \sigma_3$ | $\sigma_3'$ | $\sigma_1'$ | $\frac{\sigma_3'}{\sigma_1'}$ | $\frac{\sigma_3}{\sigma_1'}$ | $\sigma_1' + \sigma_3'$ | $\frac{\sigma_1 - \sigma_3}{\sigma_1'}$ | φ' | $\sigma_2'$ | Miscellaneous Data Date | Rate of Strain | Temp. | $\frac{\Delta V}{V_0}(\sigma_3 \cdot 7.20)$ | J = $\frac{\sigma_1 - \sigma_3}{\sigma_1' + \sigma_3'}$ | $\frac{\sigma_2}{\sigma_1' + \sigma_3'}$ |
|---|---|---|---|---|---|---|---|---|---|---|---|---|---|---|---|---|---|---|---|---|---|---|---|---|---|---|---|---|---|---|---|---|---|---|---|---|---|---|---|---|---|---|---|---|---|---|---|---|---|---|
| hr. °C | lb/sq.in | lb/sq.in | lb/sq.in | lb/sq.in | | | | | | lb | | lb. | lb. | lb. | lb. | | sq.in. | lb/sq.in | lb/sq.in | lb/sq.in | lb/sq.in | | | c.c. | c.c. | c.c. | c.c. | c.c. | c.c. | | | lb/sq.in | lb/sq.in | lb/sq.in | | | | | | lb/sq.in | | day | in/min | °C | | | |
| | Zero | 0·05 | | | 100 | Zero | 100 | Zero | 1700 | Zero | 900 | | | | | | | 3·6 | | | | | | | | | | 57·40 | burette at sample | | | | | | | | | | | | | Mon. 11th May | | | | | |
| | | 0·00 | | | 0 | 0 | 0 | | | | | | | | | | | 3·6 | | | | | | | | | | 45·00 | under 24" negative | | | | | | | | | | | | | | | | | | |
| | | 1·00 | | | 2·1 | 1·4 | 1·7 | | | | | | | | | | | 4·7 | | | | | | | | | | 44·00 | < measure > | 44·00 | | | | | | | | | | | | | | | | | |
| | | 2·00 | | | 5·8 | 3·7 | 4·7 | | | | | (days) | 66·0 | +19·9 | 85·9 | | | 5·7 | | | | | | | | | | 44·30 | | | | | | | | | | | | | | | | | |
| | | 4·00 | | | 10·7 | 7·2 | 8·9 | | | | | ↓ | 154 | +18 | 172 | | | 7·8 → 7·9 | | | | | | | | | | 42·20 | 0 | 0 | | | | | | | | | | | | | | | | |
| | | 7·00 | | | 16·6 | 11·2 | 13·9 | | | | | 28 | 286 | +15 | 301 | | | 10·8 | | | | | | | | | | 39·65 | 2·55 | 0·108 | | | | | | | | | | | | | | | | |
| | | 10·00 | | | 19·8 | 13·3 | 16·5 | | 41 | | 39 = | 40 | 416 | +13 | 429 | | | 13·8 | | | | | | | | | | 37·20 | 5·00 | 0·212 | | | | | | | | | | | | | | | | |
| | | 15·00 | | | 24·4 | 16·8 | 20·6 | | | | | 59 | 635 | + 8 | 643 | | | 18·7 | | | | | | | | | | 33·75 | 8·45 | 0·358 | | | | | | | | | | | | | | | | |
| | 19·6 | 20·00 | | | 28·8 | 20·3 | 24·5 | | | | | 80 | 855 | + 4 | 859 | | | 23·5 | | | | | | | | | | 30·75 | 11·45 | 0·485 | | | | | | | | | | | | | | | | |
| | 24·8 | 25·00 | | | 33·0 | 23·7 | 28·3 | | 102 | | 98 = | 100 | 1063 | 0 | 1063 | | | 28·4 | | | | | | | | | | 29·00 | 13·30 | 0·559 | | | | | | | | | | | | | | | | |
| | 29·7 | 30·0 | | | 36·7 | 26·9 | 31·8 | | | | | 120·5 | 1295 | − 5 | 1290 | | | 33·5 | | | | | | | | | | 26·35 | 15·85 | 0·671 | | | | | | | | | | | | | | | | |
| 15:00 | 39·8 | 40·0 | reset 100→ | | 44·9 | 34·7 | 39·8 | 0·92 | 1857·5 | 872 | 1062·5 | (160) | 1759 | − 14 | 1745 | 100·0 | | 43·5 | 43·0 | 0·5 | 0·2 | | | | | | | 24·30 | 17·90 | 0·759 | | | | | | | | | | | | | | | | |
| | | | | | 4·4 | 4·2 | 4·3 | 0·10 | 1883 | 1016 | 1090 | 1055 | 2071 | | 2057 | 99·90 | | 44·8 | | 1·8 | 0·7 | | | | | | | 22·50 | 19·70 | 0·835 | | | | | | | | | | | | | | | | |
| | | | | | 11·3 | 10·3 | 10·8 | 0·25 | 1912 | 1181 | 1120 | 1225 | 2406 | | 2392 | 99·75 | | 47·0 | | 4·0 | 1·6 | | | | | | | 20·95 | 21·35 | 0·899 | | | | | | | | | | | | | | | | |
| | | | | | 22·7 | 20·5 | 21·6 | 0·50 | 1953 | 1414 | 1166 | 1477 | 2891 | | 2877 | 99·50 | | 53·9 | | 10·9 | 4·3 | | | | | | | 18·10 | 24·10 | 1·020 | 100·0 | | 58·51 | 40·0 | 92·5 | 0·432 | | 0·0012 | | 0·535 | 57·9 | 0·302 |
| | | | | | 33·9 | 30·9 | 32·4 | 0·75 | 1982 | 1626 | 1207 | 1700 | 3326 | | 3312 | 99·25 | | 65·5 | | 22·5 | 9·0 | | | | | | | 17·50 | − 0·60 | 0·026 | 99·974 | | 61·85 | | 101·9 | | 1·313 | | 40·2 | | ≡ | | 0·287 |
| | | | | | 45·1 | 41·1 | 43·1 | 1·00 | 2023 | 1739 | 1241 | 1881 | 3680 | | 3666 | 99·00 | | 75·9 | | 32·9 | 13·1 | | | | | | | 16·60 | − 1·50 | 0·064 | 99·936 | | 71·84 | | 111·8 | | 1·546 | | 40·7 | | 14% | | 0·274 |
| | | | | | 56·4 | 51·4 | 53·9 | 1·25 | 2050 | 1946 | 12695 | 2034 | 3950 | | 3946 | 98·75 | | 86·7 | | 43·7 | 17·4 | | | | | | | 15·55 | − 2·55 | 0·109 | 99·891 | | 86·24 | | 126·2 | | 1·796 | | 41·6 | | strain | | 0·274 |
| | | | | | 67·5 | 61·9 | 64·7 | 1·50 | 2072 | 2070 | 1292 | 2160 | 4230 | | 4216 | 98·50 | | 94·7 | | 51·7 | 20·6 | | | | | | | 14·80 | − 3·30 | 0·141 | 99·859 | | 98·05 | | 139·1 | | 2·156 | | 44·3 | | per | | 0·267 |
| | | | | | 78·3 | 72·7 | 75·5 | 1·75 | 2088 | 2160 | 1310·2 | 2261 | 4421 | | 4407 | 98·25 | | 101·4 | | 58·4 | 23·2 | | | | | | | 14·50 | − 3·60 | 0·154 | 99·846 | | 109·38 | | 149·4 | | 2·476 | | 45·0 | | hour | | 0·273 |
| | | | | | 84·7 | 78·9 | 81·8 | 1·90 | 2091·5 | 2182 | 1313·7 | 2281 | 4463 | | 4449 | 98·10 | | 105·1 | | 62·1 | 24·7 | | | | | | | 14·70 | − 3·40 | 0·145 | 99·855 | | 118·02 | | 158·0 | | 2·735 | | 53·1 | | | | 0·280 |
| | | | | | 90·6 | 84·9 | 87·75 | 2·03 | 2091·5 | 2182 | 1313·7 | 2281 | 4463 | | 4449 | 97·97 | | 106·7 | | 63·7 | 25·3 | | | | | | | 15·20 | − 2·90 | 0·124 | 99·876 | | 125·12 | | 165·1 | | 2·950 | | 57·4 | | | | 0·290 |
| | | | | | 95·0 | 90·5 | 92·75 | 2·15 | 2090 | 2173 | 1310 | 2260 | 4433 | | 4419 | 97·85 | | 108·5 | | 65·5 | 26·1 | | | | | | | 16·10 | − 2·00 | 0·086 | 99·914 | | 130·40 | | 170·4 | | 3·128 | | 60·6 | | | | 0·296 |
| | | | | | 101·0 | 97·0 | 99·0 | 2·29 | 2088 | 2162 | 1305 | 2232 | 4394 | | 4380 | 97·71 | | 109·2 | 43·0 | 66·2 | 26·3 | | | | | | | 16·95 | − 1·15 | 0·049 | 99·951 | | 131·36 | | 171·4 | | 3·260 | | 62·2 | | | | 0·301 |
| motor stopped; equilib[m] | | | | valves | 104·3 | 101·0 | | | 2080 | | 1294 | | | | | | | | | | | | | | | | | | 17·80 | − 0·30 | 0·013 | 99·987 | | 131·16 | | 171·2 | | 3·284 | 38·4 | 64·7 | | | | 0·307 |
| | | | | | | | | | 2000 | approx | 1200 | | release of deviator stress | | | | | | | | | | | | | | | | 18·80 | + 0·70 | 0·030 | 100·030 | | 130·15 | | 170·2 | | 3·275 | | 65·2 | | | | 0·309 |
| | | | | | 93·1 | 92·5 | | | 1900 | | 1100 | | | | | | | | | | | | | | | | | | 19·95 | + 1·85 | 0·079 | 100·079 | | 128·88 | | 168·9 | | 3·254 | | 64·1 | | | | 0·315 |
| | | | | | 80·3 | 80·8 | | | 1800 | | 1000 | | | | | | | | | | | | | | | | | | 20·70 | | | | | | | | | 3·222 | | 64·3 | | | | 0·317 |
| | | 40·0 | | | 58·9 | 69·3 | | | 1700 | 0 | 900 | 0 | | | | | | | | | | | | | | | | | 21·05 | | | | | | | | | | | | | | | |
| | | 0 | | | 152·3 | 160·8 | | | 1700 | 0 | 900 | 0 | release of cell pressure | | −14· | | | | | | | | | | | | | | 21·25 | | | | | | | | | | | | | | | |
| | | | | | | | | | | | | | | | | | | | | | | | | | | | | | 20·50 | | | | | | | | | | | | | | | |
| | | | | | | | | | | | | | | | | | | | | | | | | | | | | | 16·55 | water sucked out of burette to reading 80·30 c.c. | | | | | | | | | | | | | | |
| | | | | | | | | | | | | | | | | | | | | | | | | | | | | | 95·40 | under 29·5" negative head | | | | | | | | | | | | | | |

$$\frac{A}{A_0} = \frac{3{\cdot}55}{8{\cdot}93} = 0{\cdot}398$$

PLANE STRAIN TEST NO:- BS - P - 24

Date:- May, 1959 (mo: yr.)

Soil Type & Condition:- Saturated Brasted sand; medium dense; drained test Series A ($\sigma_c$ const., $\sigma_a$ incr.)

Nominal Size of Specimen :- l = 16 in. b = 2 in. h = 4 in.

Initial Volume, $V_0$ = 2357 c.c.

Cell Correction = , c.c./lb. per sq.in.

Consolidated Volume, $V_c$ = 2333 c.c.

Consolidated Length = 4·308 in.

Consolidated Area = 33·23 sq.in.

Observed Correction = $V_0\epsilon$ = c.c. ; Weight of top plates, rams, etc. W = 21·6 lb.

Intermediate Principal Stress Gauge :- Zero = 3·0 psi ; Clamped = 3·6 psi

$\sigma_2$ prestress = 0·398 × 0·6 = 0·24 psi

Membrane correction at failure = $\frac{200(0{\cdot}025)}{0{\cdot}10}(0{\cdot}019)$ lb/sq.in.

FIG. A 5-1

## Appendix 6 ALTERATIONS TO THE PLANE STRAIN APPARATUS

Several modifications were carried out on the plane strain apparatus to ease the operational procedure. Basic principles of the design remained unchanged. A brief list of alterations follows:-

### End clamp

1. The copper tubing connecting the pressure diaphragm with the null indicator was replaced by flexible nylon tubing. This abolished the necessity of breaking the joint between the top of the clamp and the tubing after each test.

2. An air release screw (Fig. 3-2) was added to the clamp at the lowest point of the water reservoir. To de-air the pressure measuring device, the clamp was inverted and de-aired water passed through the diaphragm cell and out through the air release screw.

3. A segment of 0.04 inches depth was removed from the inside face of each tie-bar to leave more space between the specimen and the tie-bars.

4. New springs were made to replace the original springs which support the end clamp and maintain the facing plates at the correct level mid-way between the upper and lower platens (the original springs were too soft).

5. At the start of the test series, it was found that the facing plates were not perfectly flat. They were made plane by filing, but this removed some of the anodised aluminium surfacing. A check test on the friction properties of the new surface using silicone grease has been carried out by Mr. N. Wade following the technique used by Wood (1958). His results show a coefficient of friction $\mu = 0.024$ compared with Wood's value of 0.018 at the same normal load of 150 lb. From a practical viewpoint, the layer of silicone grease between the end plates and the specimen effectively reduces the friction to a negligible amount.

### Loading head

6. New adjustable screws were made for the loading head to give greater head-room so that larger diameter proving rings could be used for the apparatus.

Cell base plate

7. The pore-water pressure/drainage connection was moved from the centre of the base platen to a position four inches from the centre. In its original condition, the copper tubing from the base platen was bent through a right angle before passing along a duct in the pedestal plate. At the end of the test, the copper tubing had to be straightened again to lift the platen from the cell base plate and the continual bending of the copper tube was a source of weakness and operational inconvenience.

8. Longer legs were fitted at the four corners of the cell base plate. This gave greater head-room for screwing the base platen to the cell base plate, fitting sealing joints for nylon and copper tubing etc.

Most of these alterations can be seen on Plate 3-1.

## Appendix 7. RESULTS AND DISCUSSION OF STANDARD SHEAR BOX TESTS

A series of standard shear box tests were carried out as a comparison with the results of the standard triaxial and plane strain tests. The shear box test specimens were nominally 6 cm. square and 2 cm. deep, the depths being measured at the four corners of the boxes by a dial gauge with a maximum travel of 2 inches. Constant rate-of-strain loading was employed such that failure was reached in ¾ to 1½ hours (0.004 in/min.). Full drainage was allowed and the normal stresses on the boxes varied from 41 to 44 lb/sq.in., thus giving slightly lower values of the minor principal stress at failure than in the plane strain and standard triaxial tests. These values of normal stress were necessary to prevent overstressing of the proving rings. The shear stress was calculated as the load on the horizontal proving ring divided by the original cross-sectional area of the specimen. The specimens were compacted in three layers by either tamping or by vibration but the results of the two techniques were so similar that they have not been differentiated on the strength-porosity plot (Fig. A7-1).

The failure characteristics of Brasted sand in the shear box are given on Fig. A7-1. As one would expect, there is a fair amount of scatter in the results and they cannot be regarded as being comparable in accuracy to the larger specimens in the plane strain and triaxial tests. However, sufficient tests were carried out to indicate the main trends. The comparison of friction angles in the shear box (Taylor interpretation) and standard triaxial tests are similar to the measurements of Nash (1953). At the higher porosities, the strengths of the sand in the shear box are lower than in the standard triaxial test. With increasing density, the two curves cross and, at the lowest porosities tested, the shear box tests give similar results to the plane strain tests.

The dilatancy terms of Chapter 8 for shear box tests are as follows :-

Hypothesis A (Chapter 8, page 106)

Dilatancy term = $\sigma_n \cdot \frac{\delta y}{\delta x}$

where $\sigma_n$ = normal stress

$\frac{\delta y}{\delta x}$ = slope of vertical:horizontal deformation curve

It is subtracted from the total deviator stress, and the corrected friction angles are plotted on Fig. A7-1 for the tests in which vertical movements were measured.

Hypothesis B (Chapter 8, page 108)

Dilatancy term represented by $\alpha$ which is subtracted from the total angle $(\phi + \alpha)$ to give the constant volume angle $\phi$

$$\tan \alpha = \frac{\delta y}{\delta x}$$

Angles $(\phi + \alpha)$ and $\phi$ are plotted on Fig. 8-26(d) and angles $\alpha$ are plotted on Fig. 8-27.

Two further points worth mentioning about the shear box results are :- (i) the Hill (1950) interpretation of the shear box test (Chapter 2, p.11 ) gives unrealistically high values of strength, ranging from friction angles of 38° in the loosest specimens to more than 70° in the densest specimens. Clearly, this interpretation bears no direct relationship with the strength of sand in plane strain.
(ii) the graph of $\frac{\delta y}{\delta x}$ v. initial porosity is consistent with the minimum stable density concept of Chapters 8 and 10. The term $\frac{\delta y}{\delta x} \rightarrow 0$ as $n_o \rightarrow 44.2\%$. However, the strength-density curve for the shear box suggests a slightly lower strength at this porosity than the ultimate strength measured in the plane strain and triaxial tests.

plane strain & std triaxial curves shown thus:- ——————

Angle of Shearing Resistance, $\phi^\circ$

48 47 46 45 44 43 42 41 40 39 38 37 36 35 34 33 32 31 30

Maximum Density

Minimum Density

32 33 34 35 36 37 38 39 40 41 42 43 44 45

Initial Porosity n. %

Slope $\frac{\delta y}{\delta x}$ = vertical deformation / horizontal deformation

3 2 1 0

32 34 36 38 40 42 44

Initial Porosity n. %

$\frac{\Delta h}{h_0}$ at Failure

+ 0 %

+ 0.5 %

0

34 36 38 42 44

Initial Porosity n. %

Vertical Strain

0.5%

1.0%

Horizontal Deform. at Failure $\Delta x$ inches.

1.5

1.0

0.5

0

32 34 36 38 40 42 44

Initial Porosity n. %

STANDARD SHEAR BOX - TEST

RESULTS ON BRASTED SAND

FIG. A7-1

## Appendix 8. SOME NOTES ON THE PACKING OF SANDS

Some excellent work has been carried out on density limits in granular soils by Professor Kolbuszewski at Imperial College and Birmingham University. However, the suggested 'standard' procedure of measuring the density limits are not known to correspond with any particular behaviour of the soil. In this respect, they are comparable with the Atterberg limits in clay soils.

The author investigated several testing techniques to obtain a loose packing of the sand grains. The object was not to measure the 'maximum' porosity but to decide upon a simple reliable procedure for measuring the minimum stable density of the soil (see Chapter 10). The author was assisted by Miss Jill Kinnerley, formerly assistant to Professor Kolbuszewski. The tests were :-

### 1. 'Standard' (Kolbuszewski) test for maximum porosity

Saturated sand (1000 gm.) was slowly sedimented through water in a 2000 ml. glass measuring cylinder with no air present (Fig. 10-2a). The volume occupied by the sediment was measured. Several tests gave a fairly wide scatter of results, the average measured porosity being 44.8%. Disadvantages of the technique are :-

(i) takes several hours to complete one test and sometimes needs considerable supervision to keep the flow rate steady.

(ii) top surface of sand often has considerable slope (e.g. 20° to horizontal) - difficult to read the volume accurately.

(iii) segregation of grain sizes is inevitable if silt is present.

### 2. 'Standard' test, followed by tilt test

At the end of tests 1, the polythene funnel was sealed by the flow control bung and the apparatus inverted until all the sand had reached the opposite end of the cylinder. It was returned to its original position and the sand was allowed to deposit.

This technique gave an even looser density than the method 1. Furthermore, the surface of the sand was almost horizontal, making possible an accurate reading without difficulty. Several tests showed that the porosity, which had an average value of 46.6%, was more reproducible than Kolbuszewski's 'standard' method. However, segregation of the grain sizes is inevitable.

3. Rapid tilt test on dry sand - chosen as method of determining minimum stable density (see Chapter 10). This is the 'field' method of Professor Kolbuszewski.

Summary

| Min. stable density :- | | Test techniques :- | |
|---|---|---|---|
| Standard triaxial, | n = 44.3% | 1. Deposit through water, | n = 44.8% |
| Plane strain, | n = 44.1% | 2. Water and tilt, | n = 46.6% |
| | 44.2% | 3. Rapid dry tilt, | n = 44.2% |

Comments on loose packing

The methods of depositing sand through water probably do not prevent arches from occurring and result in a structure which is inherently unstable. The difference in porosity between the dry tilt test of 44.2% and the saturated tilt test of 46.6% is too large to be dismissed as due merely to experimental errors. The fact that sand can be sedimented in an unstable structure may have some bearing on the phenomenon of flow slides in sand.

The porosity measured in the Kolbuszewski 'standard' method is lower than the method in which the Kolbuszewski method is followed by a rapid tilt test, the sand being saturated in both cases. The sloping surface formed in the first method is probably responsible for the difference. It is possible to watch the sand grains land on the slope and roll down into a position of denser packing. Hence, the observation by Professor Kolbuszewski that the 'standard' and 'field' methods give similar results is fortuitous; that the above loose porosity relationships on Brasted sand are typical of other sands has been proved in more recent tests.

Comments on dense sand techniques

1. 'Standard' Kolbuszewski method. He suggests that the maximum density can be obtained by vibrating fully saturated sand in a Proctor mould using a Kango hammer. The sand should be vibrated for 15 minutes on each of 3 equal layers.

A vibration time of 15 minutes seems to be unnecessary. The fine Brasted sand flows up through the clearance between the rammer head and sides of the compaction mould, and within a short time there is more sand over the rammer head than under it! There is also a danger that excessive vibration may fracture the sand grains. The second drawback of this test is that it requires a fairly large sample of sand - at least 2000 gm., allowing for a slight excess in the mould. This is more soil than is sometimes recovered from the Bishop sand sampler.

2. The author developed the shallower mould, Fig. 10-2(b).

Using the shallower mould, the following points were established :-

(i) the Proctor mould and shallower mould gave results in good agreement with each other.

(ii) the densest compaction was achieved on fully saturated soil - see Fig. 10-2(c). Two tests were carried out at each moisture content and 4 tests on soil in the saturated and dry states.

(iii) the densest state was reached in approximately 1 minute. After 2 minutes, further vibration had no effect on the density.

(iv) for the saturated state, the average porosity calculated from moisture content determinations was in excellent agreement with the average porosity calculated from weight-volume measurements.

## Appendix 9. FACTORS SUGGESTING THE SIGNIFICANCE OF THE ULTIMATE STRENGTH IN THE DILATANCY CONTRIBUTION TO SHEARING RESISTANCE

In Chapter 8, several paragraphs were devoted to a discussion on the significance of the dilatancy contribution to shear strength. One solution is to presume that the dilatancy term should account for all the shear strength in excess of the ultimate strength of the soil, and this view finds support in the following points :-

(i) the ultimate strength is the same in the plane strain and the standard triaxial compression tests, irrespective of the placement density. The specimens are then shearing at constant volume.

(ii) the increases in strength (R-1) with increasing placement density (Fig. 10-4) are curves of extraordinary similarity to the curves of maximum rates of dilatancy with increasing density (e.g. Fig. 8-12), for all types of test. It is clear that the greater is the difference between the peak and ultimate strengths, the greater is the maximum rate of dilation. Now, all the test specimens mobilized a greater principal stress ratio than the ultimate, and all specimens dilated in doing so. It is apparent that the rates of dilation $\rightarrow 0$ as the peak strength $\rightarrow$ ultimate strength. Also, it may be significant that the curves of (R-1) in symmetric and plane strain bear a constant relationship to each other at any placement density.

(iii) there are grounds for believing that dilation begins when the ultimate principal stress ratio is first mobilized, irrespective of the placement density.

(iv) there are theoretical grounds (Caquot, 1934) for believing that the constant volume strength of Brasted sand is approximately $32^{\circ}$, based on measurement of the coefficient of intergranular friction in quartz grains ($\phi_{\mu} \simeq 22^{\circ}$). This value is in excellent agreement with the measured ultimate strength of Brasted sand.

These points suggest that the peak strength mobilized, in excess of the ultimate strength, is a function of the soils dilatancy.

## Appendix 10.

## GRAPHICAL PRESENTATION OF SHEAR TEST RESULTS

**(excluding shear box tests)**

Stresses lb/sq.in

240
220
200
180
160
140
120
100
80
60
40
20
0

$\sigma_1$

$\sigma_2$

$\sigma_3 = 40.0$ lb/sq.in.

$\frac{\sigma_2}{\sigma_1+\sigma_3}$

Ratio $\frac{\sigma_1-\sigma_3}{\sigma_3}$: 5·0, 4·0, 3·0, 2·0

Ratio $\frac{\sigma_2}{\sigma_1+\sigma_3}$: 1·0, 0·3, 0·2, 0·1, 0

0 1 2 3 4 5 6 7 8

Axial Strain $\epsilon_1$ %

Volumetric Strain $\frac{\delta V}{V_c}$ %

+1·5
+1·0
+0·5
0
−0·5

Minimum

0 1 2 3 4 5 6 7 8

Axial Strain $\epsilon_1$ %

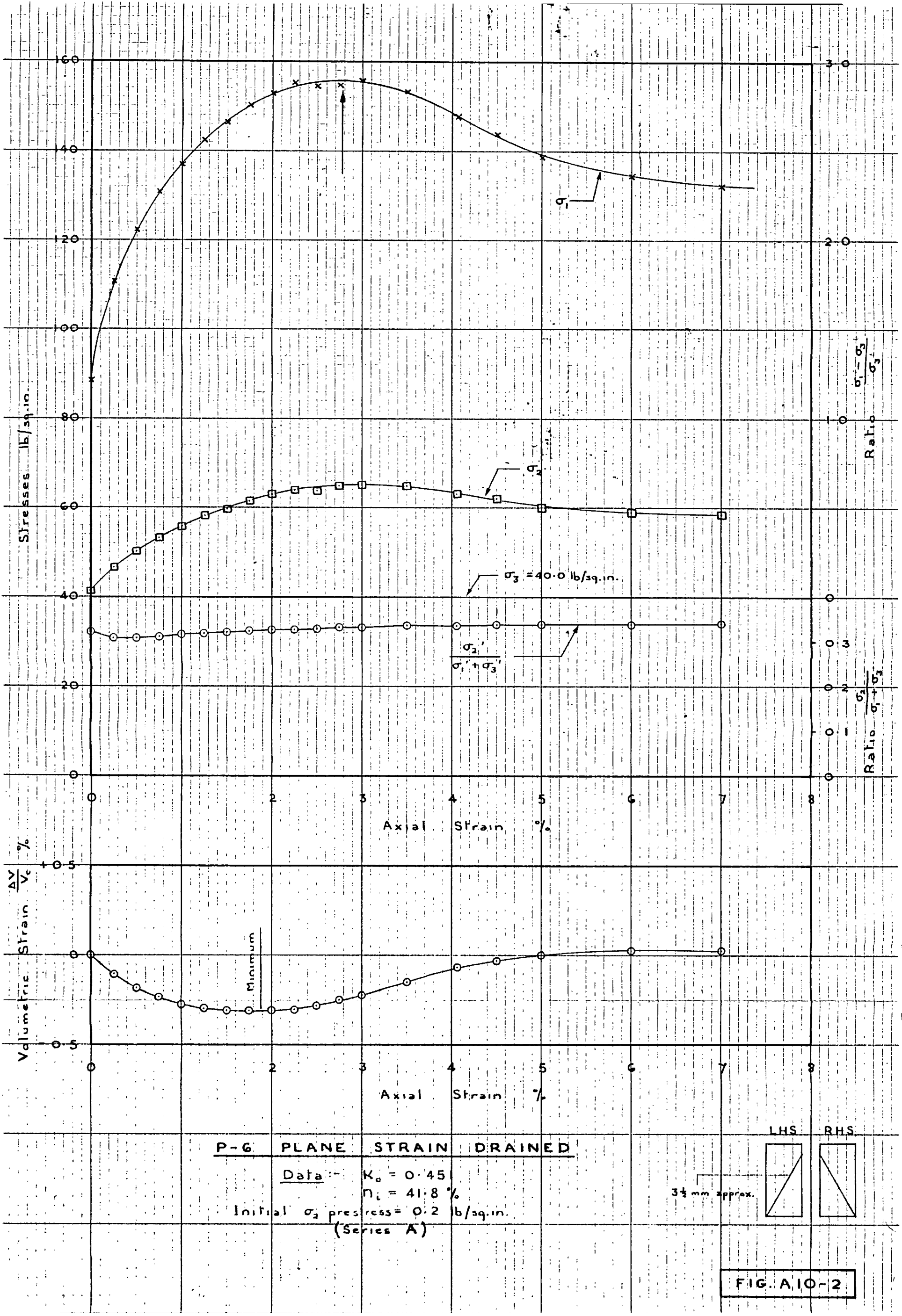
P-5 PLANE STRAIN DRAINED

Data :- $K_o = 0.355$
$n_c = 35.3\%$
Initial $\sigma_2$ prestress = 0·3 lb/sq.in
(Series A)

LHS RHS

5 mm

FIG. A 10-1




P-6 PLANE STRAIN DRAINED

Data :- $K_o$ = 0·45

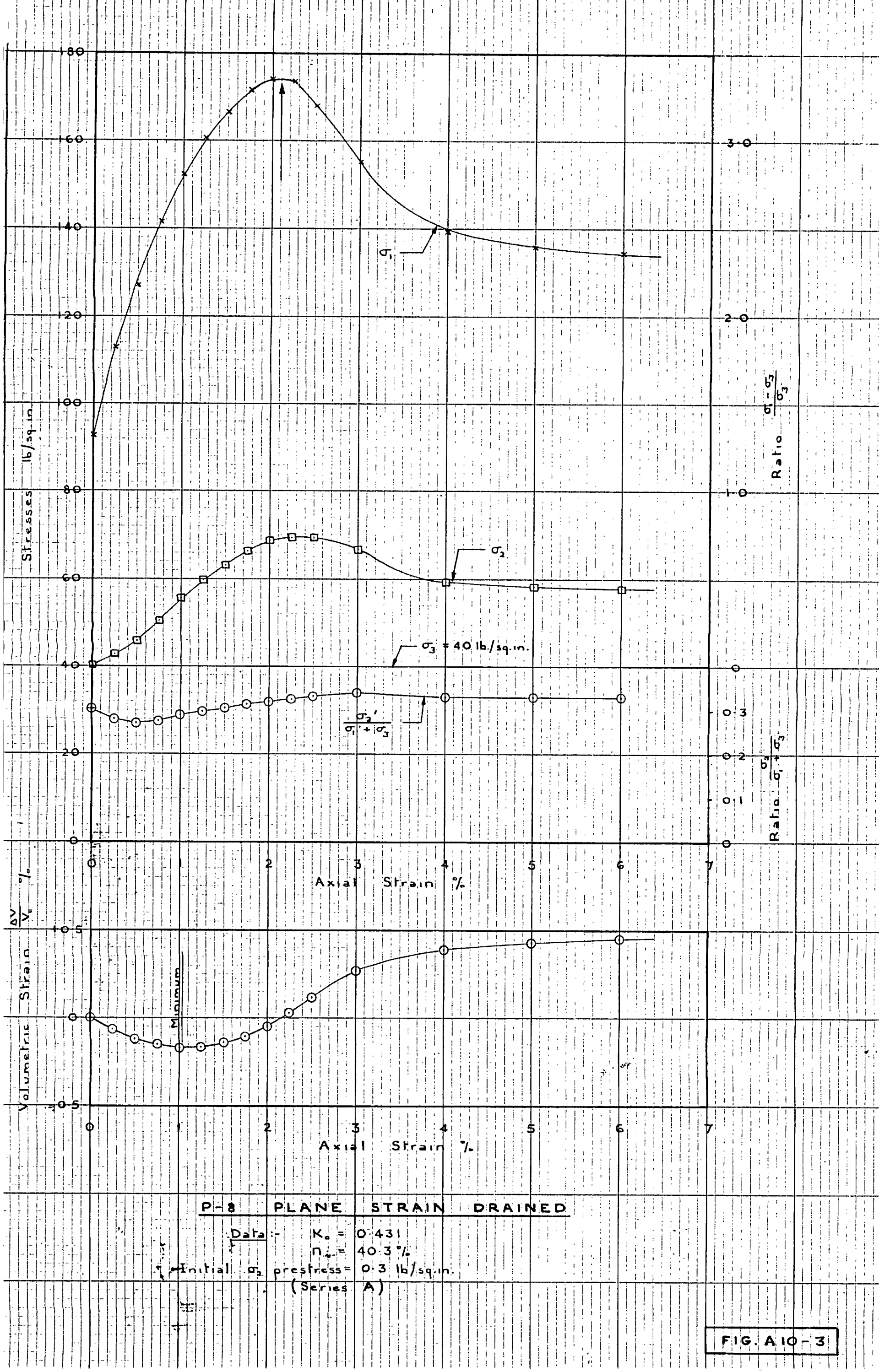
$n_i$ = 41·8 %

Initial $\sigma_3$ prestress = 0·2 lb/sq.in.

(Series A)



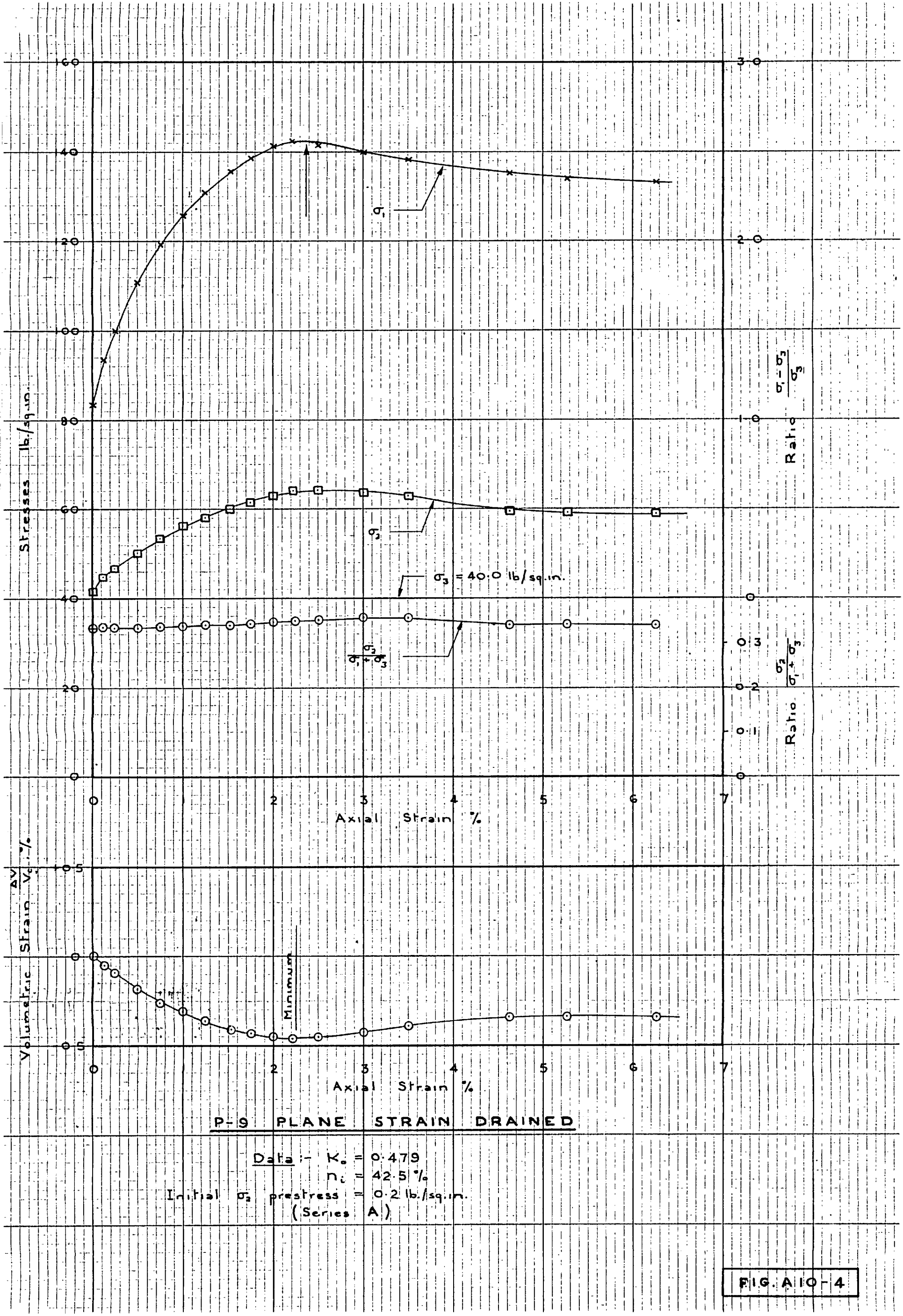

FIG. A10-2




**P-8 PLANE STRAIN DRAINED**

Data :- $K_o$ = 0·431
$n_{at}$ = 40·3 %
Initial $\sigma_3$ prestress = 0·3 lb/sq.in.
(Series A)

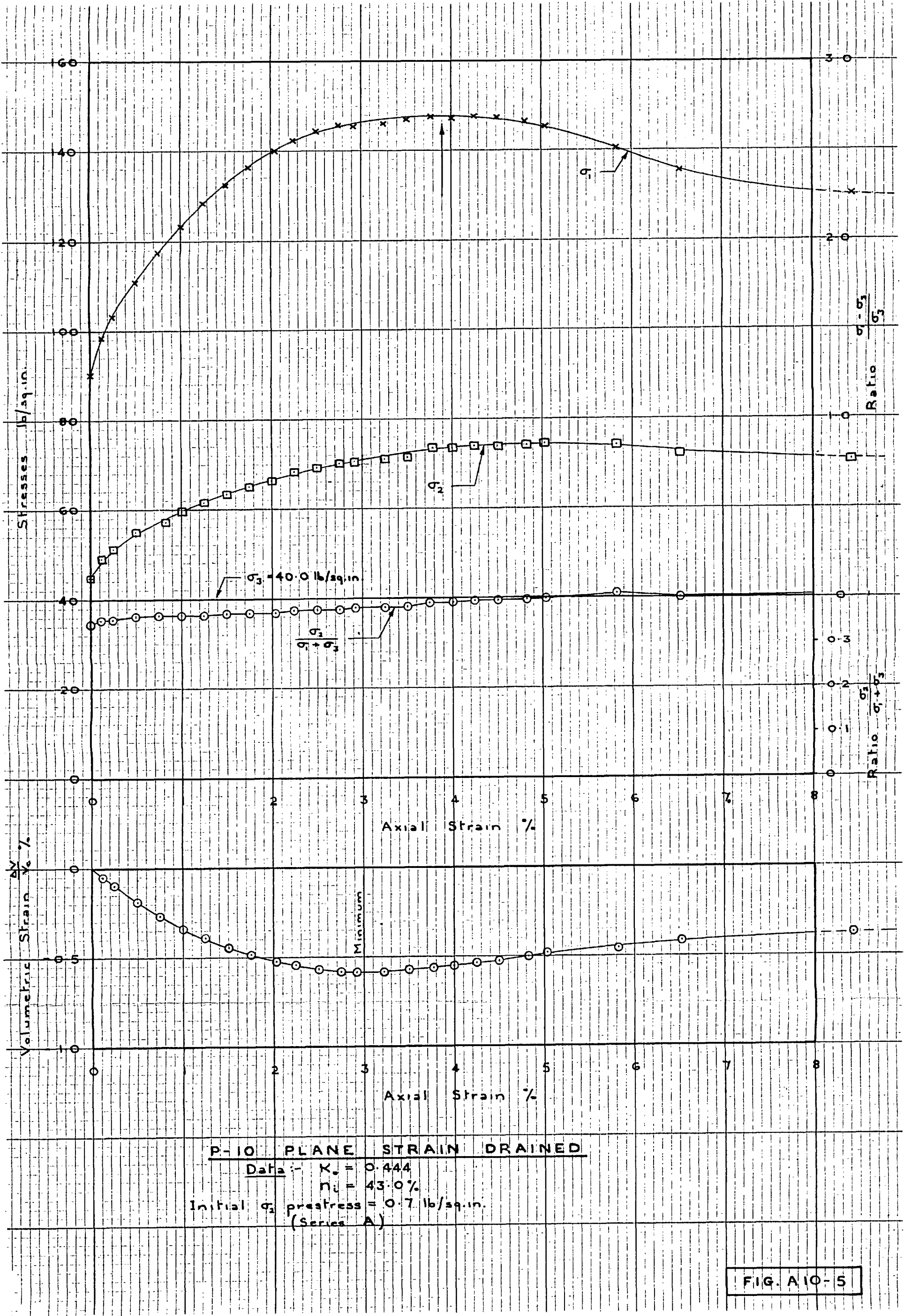
FIG. A10-3




P-9 PLANE STRAIN DRAINED

Data :- $K_o = 0.479$
$n_i = 42.5\%$
Initial $\sigma_3$ prestress = 0.2 lb./sq.in.
(Series A)

FIG. A10-4




P-10 PLANE STRAIN DRAINED

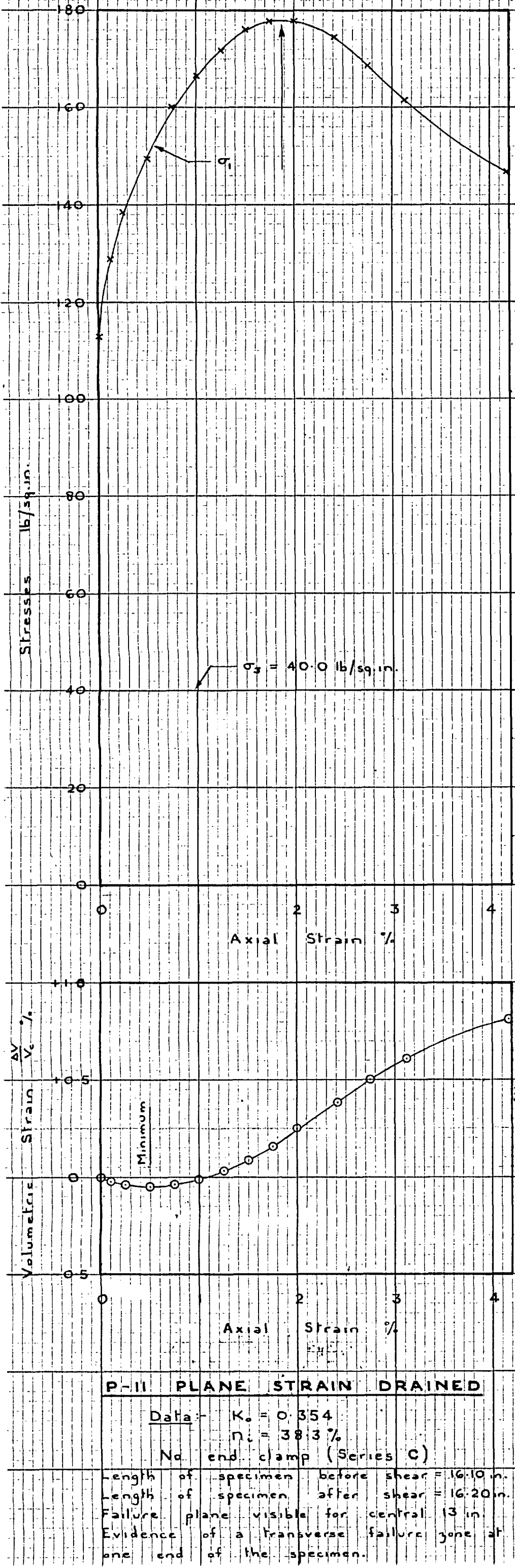
Data :- $K_o$ = 0·444

$n_i$ = 43·0 %

Initial $\sigma_3$ prestress = 0·7 lb/sq.in.

(Series A)

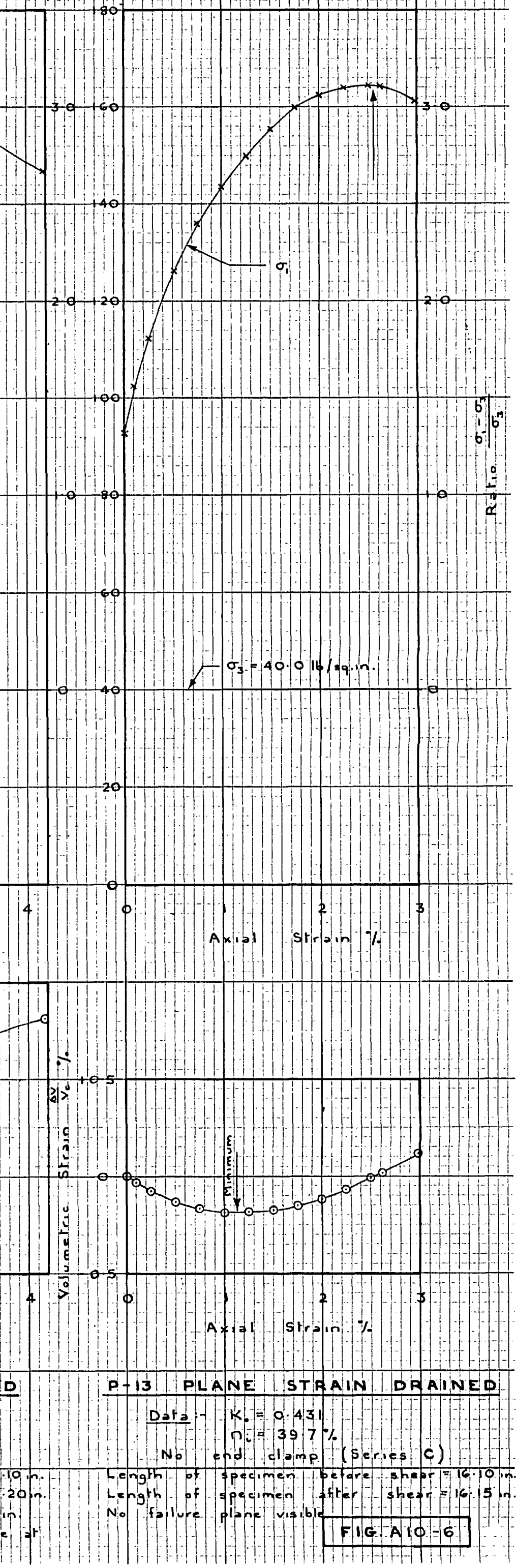
FIG. A10-5




P-11 PLANE STRAIN DRAINED

Data:- $K_o$ = 0·354
$n_c$ = 38·3 %
No end clamp (Series C)

Length of specimen before shear = 16·10 in.
Length of specimen after shear = 16·20 in.
Failure plane visible for central 13 in.
Evidence of a transverse failure zone at one end of the specimen.




P-13 PLANE STRAIN DRAINED

Data:- $K_o$ = 0·431
$n_c$ = 39·7 %
No end clamp (Series C)

Length of specimen before shear = 16·10 in.
Length of specimen after shear = 16·15 in.
No failure plane visible

FIG. A10-6

$\sigma_1$ ($\epsilon_1$ = 0 - 8 %)

$\sigma_1$ ($\epsilon_1$ = 8 - 16 %)

$\sigma_3$ = 40.0 lb/sq in.

Stresses lb/sq in

$\frac{\sigma_1 - \sigma_3}{\sigma_3}$ Ratio

Axial Strain %

$\frac{\Delta V}{V_0}$ ($\epsilon_1$ = 8 - 16 %)

$\frac{\Delta V}{V_0}$ ($\epsilon_1$ = 0 - 8 %)

Minimum

Volumetric Strain $\frac{\Delta V}{V_0}$ %

Axial Strain %

P-12 PLANE STRAIN DRAINED

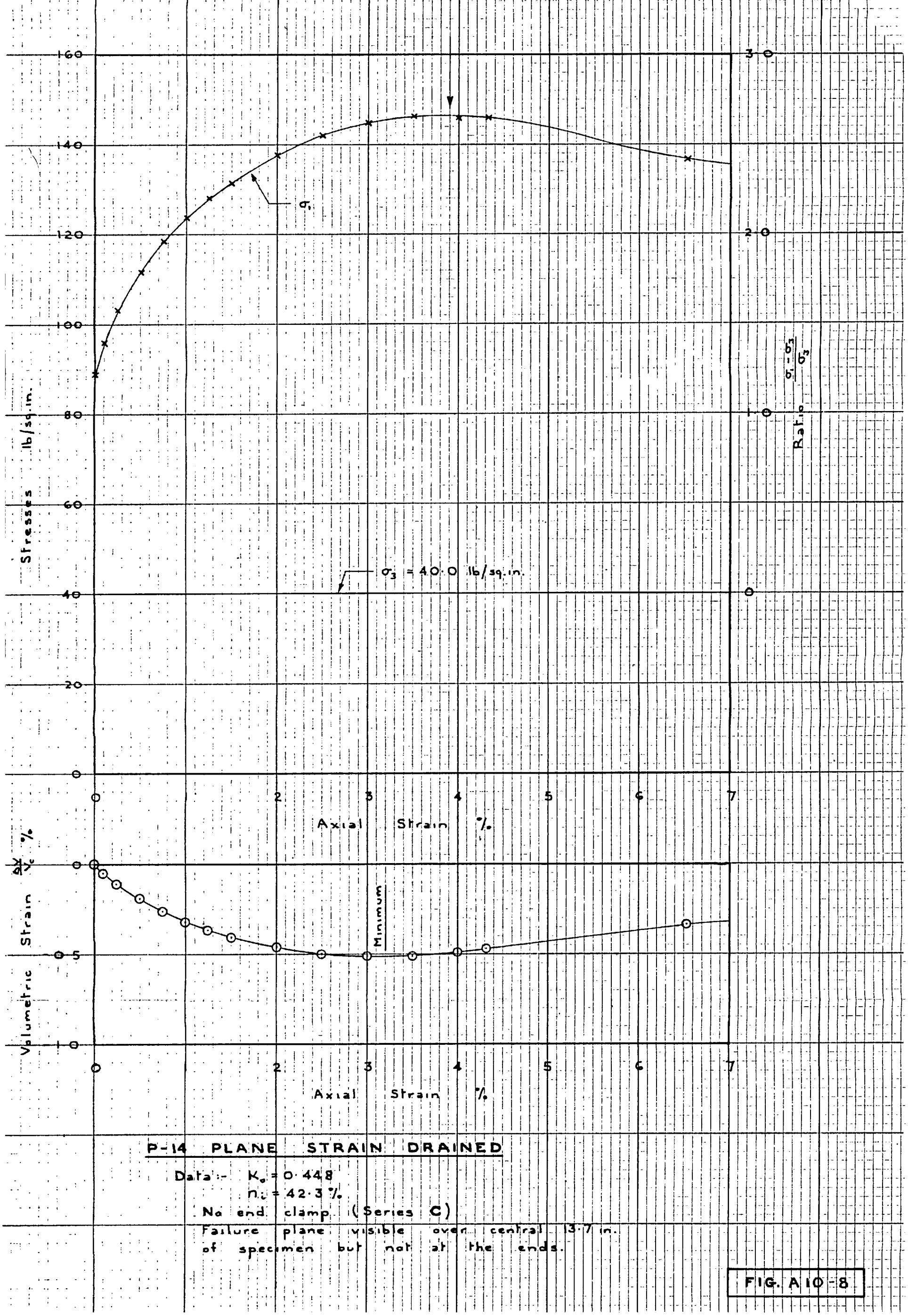
Data :- $K_0$ = 0.350

$n_i$ = 35.6 %

No end clamp (Series C)

LHS RHS

FIG. A 10-7




P-14 PLANE STRAIN DRAINED

Data :- $K_o = 0 \cdot 448$
$n_i = 42 \cdot 3\ \%$
No end clamp (Series C)
Failure plane visible over central 13·7 in. of specimen but not at the ends.

FIG. A10-8

Stresses lb/sq.in

200
180
160
140
120
100
80
60
40
20
0

4·0
3·0
2·0
1·0
0
Ratio $\frac{\sigma_1}{\sigma_3}$

$\sigma_1$

$\sigma_3$ = 40·0 lb/sq.in.

0 1 2 3 4 5 6 7 8

Axial Strain %

$\frac{\Delta V}{V_0}$ %

1·5
1·0
0·5
0
0·5

Minimum

0 1 2 3 4 5 6 7 8

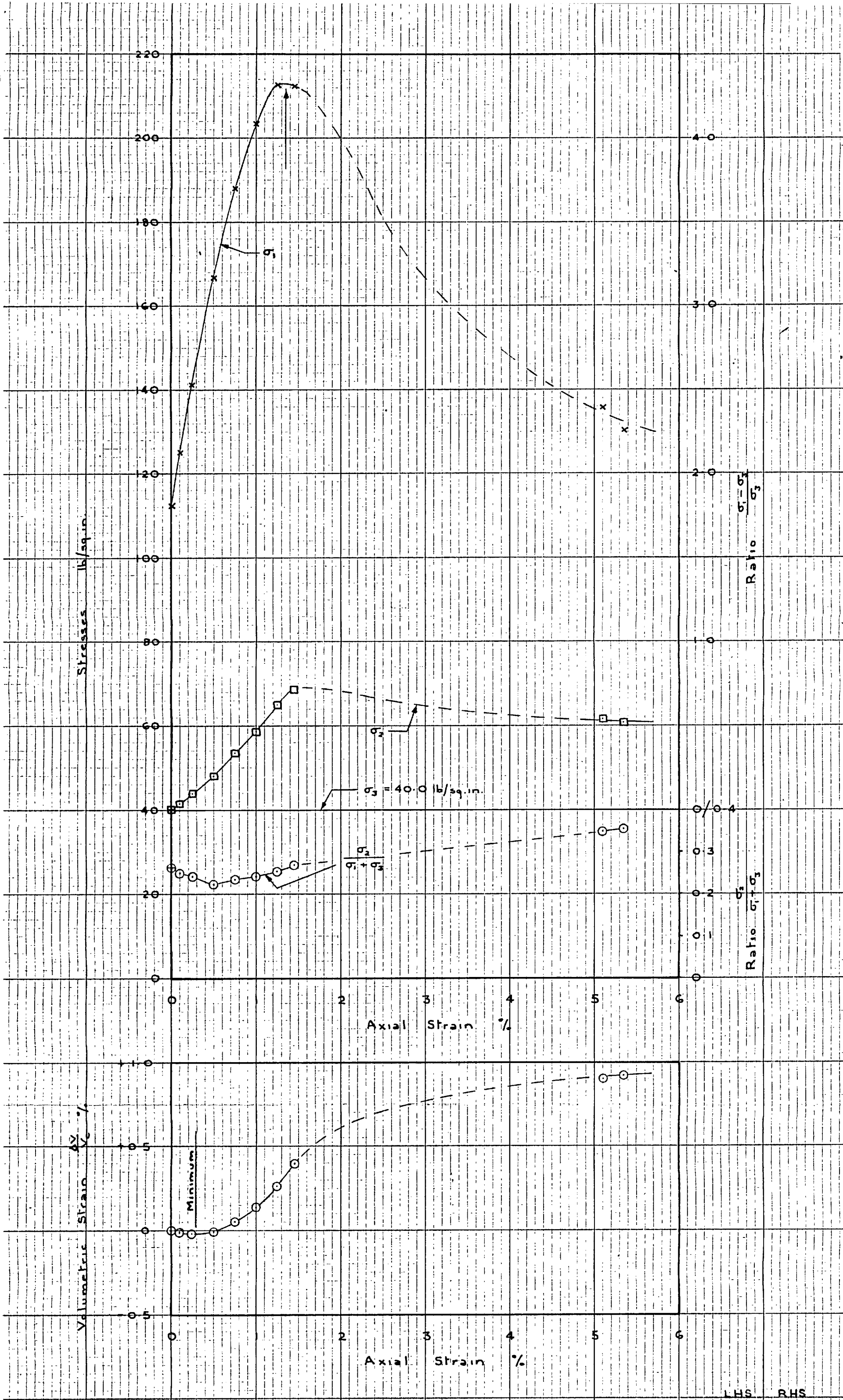
Axial Strain %

LHS RHS

**P-15 PLANE STRAIN DRAINED**

Data:- $K_0$ = 0·377
$\eta_i$ = 36·6 %
No end clamp (Series C)
Length of specimen before shear = 16·10 in.
Length of specimen after shear = 16·11 in. (top)
= 16·25 in (middle)

FIG. A 10-9




P-16 PLANE STRAIN DRAINED

Data :- $K_o = 0.356$
$n_i = 35.6$ %
Initial $\sigma_2$ prestress = 0.2 lb/sq.in.

(Series A)

FIG. A 10-10

Stresses lb/sq.in.

Axial Strain %

$\sigma_1$

$\sigma_2$

$\sigma_3$ = 40.0 lb/sq.in.

$\frac{\sigma_2}{\sigma_1+\sigma_3}$

Ratio $\frac{\sigma_1}{\sigma_3}$

Ratio $\frac{\sigma_2}{\sigma_1+\sigma_3}$

$\frac{\Delta V}{V_c}$ %

Volumetric Strain

Minimum

Axial Strain %

P-17 PLANE STRAIN DRAINED

Data :- $K_o$ = 0.343

$n_i$ = 34.4 %

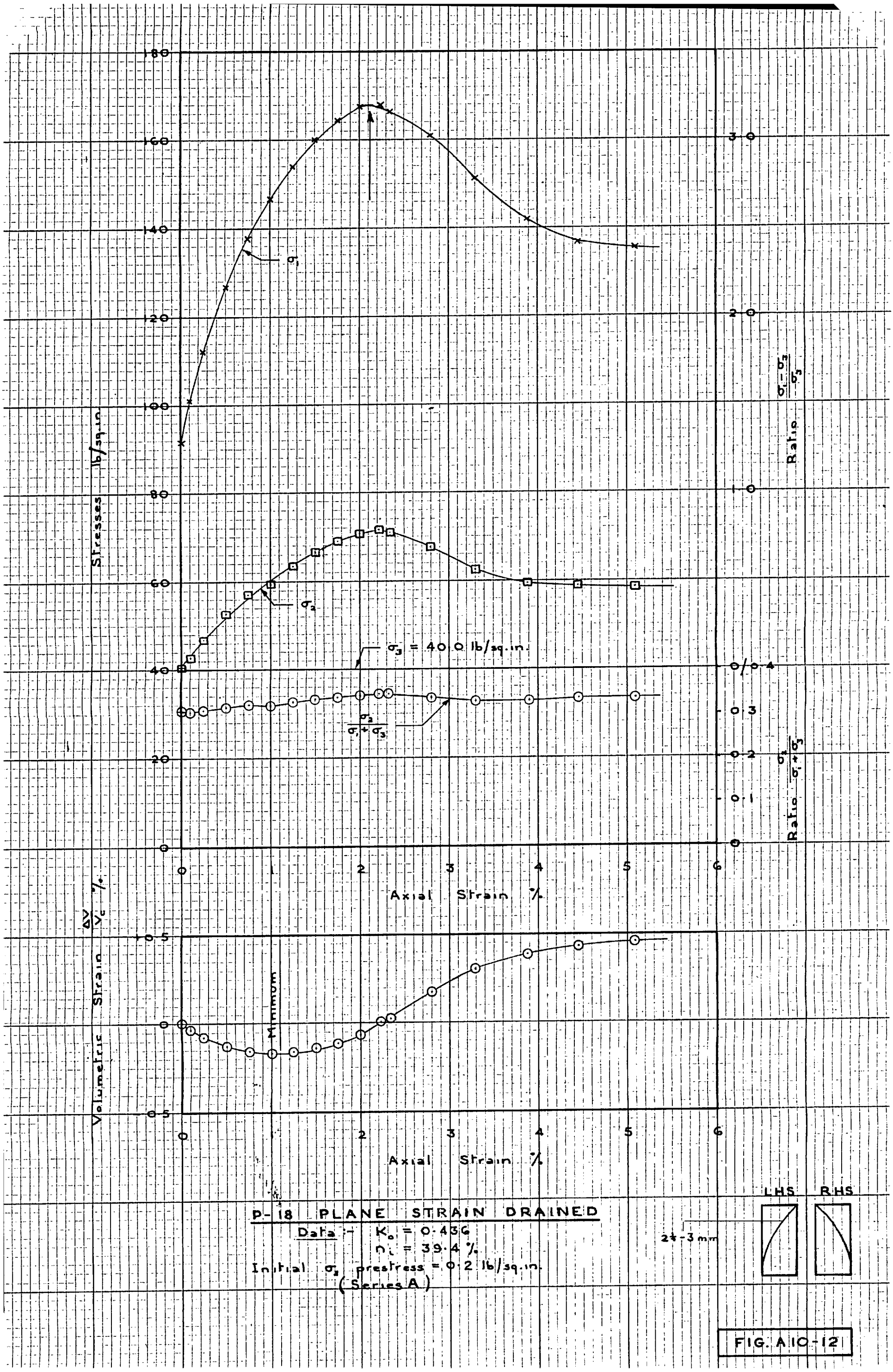
Initial $\sigma_3$ prestress = 0.4 lb/sq.in

(Series A)

LHS RHS

2¼ - 2¾ mm

FIG. A10-11




P-18 PLANE STRAIN DRAINED

Data :- $K_o$ = 0.436

$n_i$ = 39.4 %

Initial $\sigma_3$ prestress = 0.2 lb/sq.in.

(Series A)

FIG. A 10-12

P-19 PLANE STRAIN DRAINED

Data:- $K_o$ = 0.420
$n_i$ = 38.1 %
Initial $\sigma_3$ prestress = 0.3 lb/sq.in.
(Series A)

Volumetric Strain $\frac{\Delta V}{V_o}$ %

Axial Strain %

Minimum

Stresses lb/sq.in.

$\sigma_1$

$\sigma_2$

$\sigma_3$ = 40.0 lb/sq.in.

$\frac{\sigma_1 + \sigma_3}{2}$

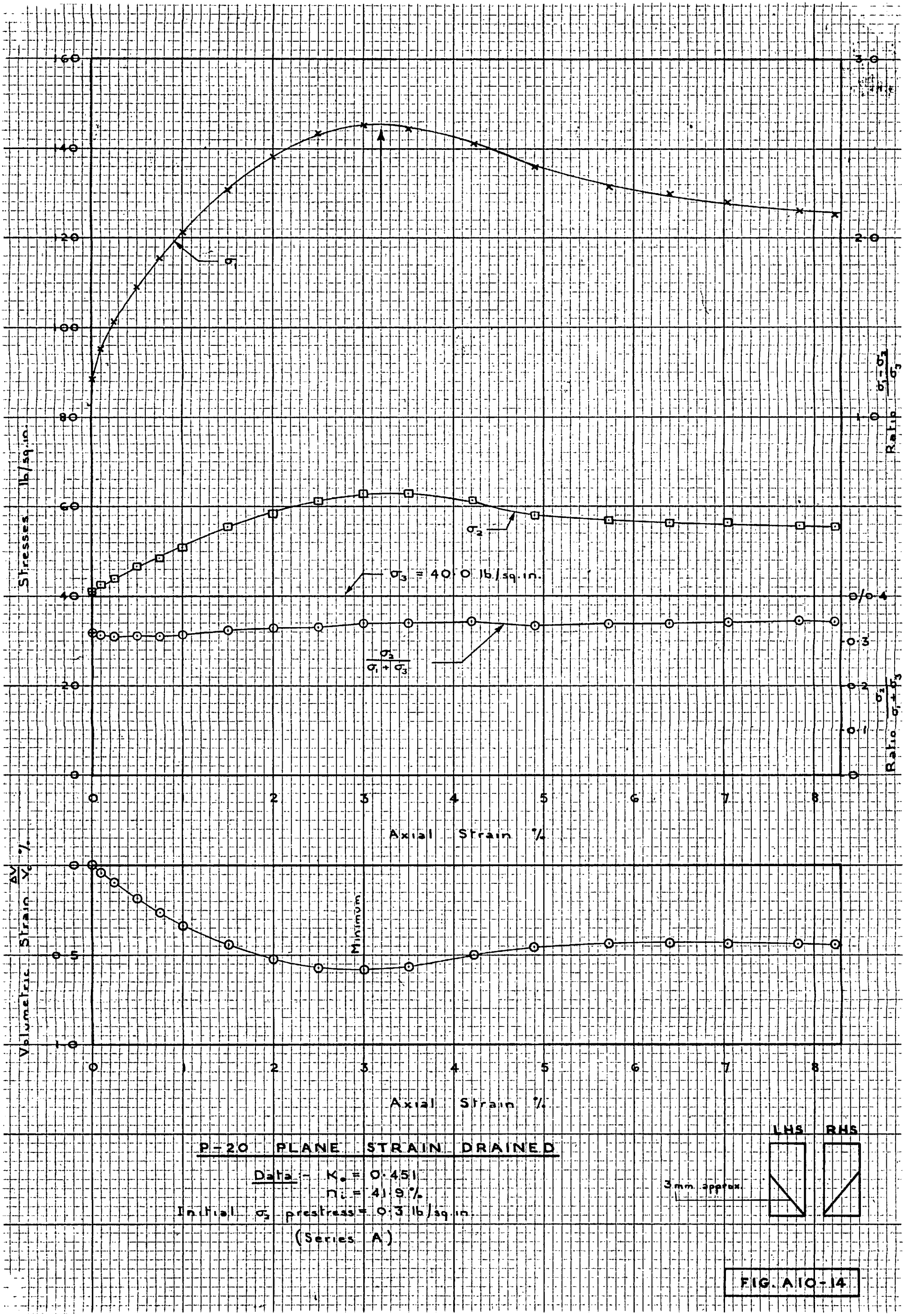
Ratio $\frac{\sigma_3}{\sigma_1 + \sigma_3}$

Ratio $\frac{\sigma_1 - \sigma_3}{\sigma_3}$

3-4 mm

LHS RHS

FIG. A10-13




P-20 PLANE STRAIN DRAINED

Data :- $K_o$ = 0·451

$n_i$ = 41·9 %

Initial $\sigma_3$ prestress = 0·3 lb/sq in.

(Series A)

FIG. A10-14

Stresses lb/sq.in.

Ratio $\frac{\sigma_1 - \sigma_3}{\sigma_3}$

$\sigma_1$

$\sigma_2$

$\sigma_3 = 40.0$ lb/sq.in.

$\frac{\sigma_2}{\sigma_1 + \sigma_3}$

Ratio $\frac{\sigma_2}{\sigma_1 + \sigma_3}$

Axial Strain %

Volumetric Strain $\frac{\Delta V}{V_c}$ %

Minimum

Axial Strain %

P-21 PLANE STRAIN DRAINED

Data :- $K_o = 0.454$

$n_i = 41.7$ %

Initial $\sigma_2$ prestress = 0.2 lb/sq.in.

(Series A)

5-6 mm

FIG. A10-15

Stresses lb/sq.in.

$\sigma_1$

$\sigma_1 - \sigma_3$

$\sigma_2$

$\sigma_3$

$\sigma_2 - \sigma_3$

Axial Strain %

Vol. Strain $\frac{\Delta V}{V_c}$ %

Minimum

$\frac{\sigma_1 - \sigma_3}{\sigma_3}$

$\frac{\sigma_2}{\sigma_1 + \sigma_3}$

$\frac{\sigma_2 - \sigma_3}{\sigma_3}$

Stress Ratios

Stress Ratio $\frac{\sigma_3}{\sigma_1 + \sigma_3}$

P-22 PLANE STRAIN DRAINED

Data:- $K_o = 0.455$

$n_i = 42.7\%$

Initial $\sigma_3$ prestress = 0.3 lb/sq.in.

(Series B)

No failure plane visible

P-25 PLANE STRAIN DRAINED

Data:- $K_o = 0.441$

$n_i = 40.2\%$

Initial $\sigma_3$ prestress = 0.3 lb/sq.in.

(Series B)

No failure plane visible

FIG. A10-16

Stresses lb/sq.in.

$\sigma_1$

$\sigma_3$

$\sigma_3$ = 40.0 lb/sq.in.

$\frac{\sigma_3}{\sigma_1 + \sigma_3}$

Axial Strain %

Ratio $\frac{\sigma_1 - \sigma_3}{\sigma_3}$

Ratio $\frac{\sigma_3}{\sigma_1 + \sigma_3}$

Volumetric Strain $\frac{\Delta V}{V_c}$ %

Minimum

Axial Strain %

P-23 PLANE STRAIN DRAINED

Data :- $K_c$ = 0.380

$n_i$ = 36.4 %

Initial $\sigma_3$ prestress = 0.4 lb/sq.in.

(Series A)

LHS RHS

2¾ - 3¾ mm

2¾ - 3¾ mm

FIG. A10-17

Stresses lb/sq.in

$\sigma_1$

$\sigma_3$ = 40·0 lb/sq.in

$\frac{\sigma_3}{\sigma_1 + \sigma_3}$

Ratio $\frac{\sigma_3}{\sigma_1 + \sigma_3}$ $\frac{\sigma_1 - \sigma_3}{\sigma_3}$

Axial Strain %

Volumetric Strain $\frac{\Delta V}{V}$ %

Minimum

Axial Strain %

P-24 PLANE STRAIN DRAINED

Data:- $K_o$ = 0·430

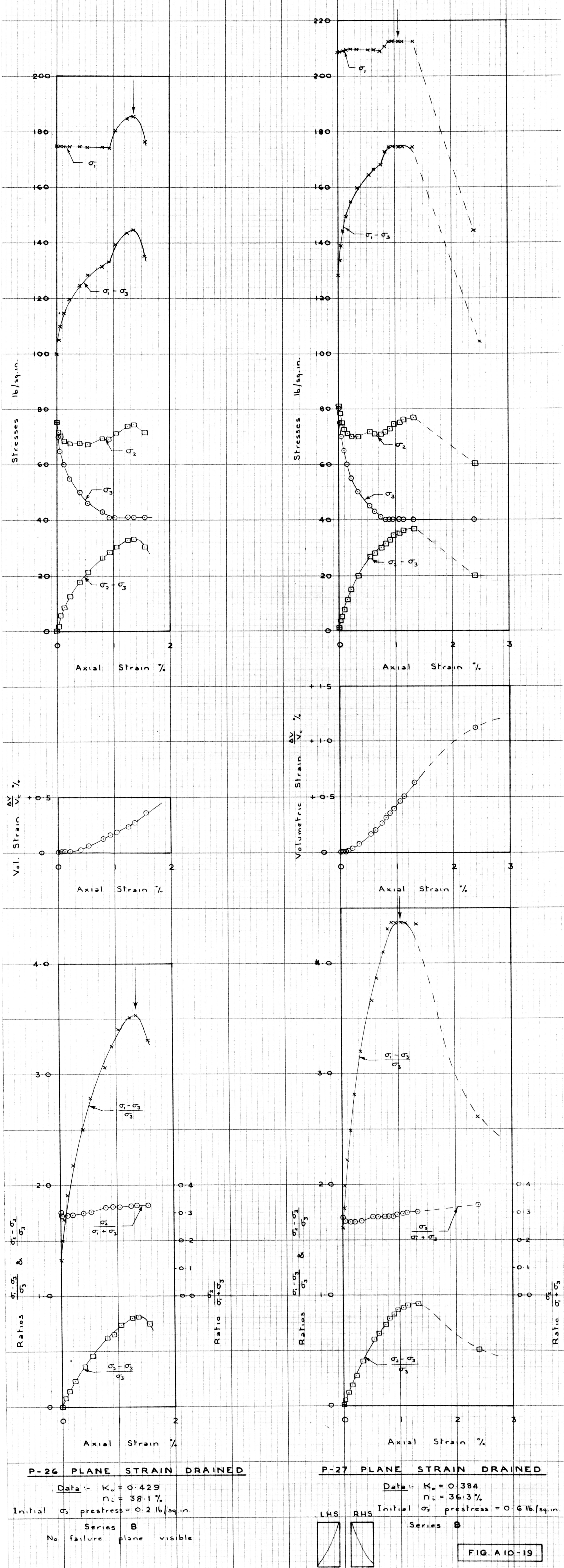
$n_i$ = 38·8 %

Initial $\sigma_3$ prestress = 0·2 lb/sq.in.

(Series A)

No failure plane visible

FIG. A10-18




P-26 PLANE STRAIN DRAINED

Data :- $K_o = 0.429$
$n_i = 38.1\%$
Initial $\sigma_2$ prestress = 0.2 lb/sq.in.

Series B
No failure plane visible

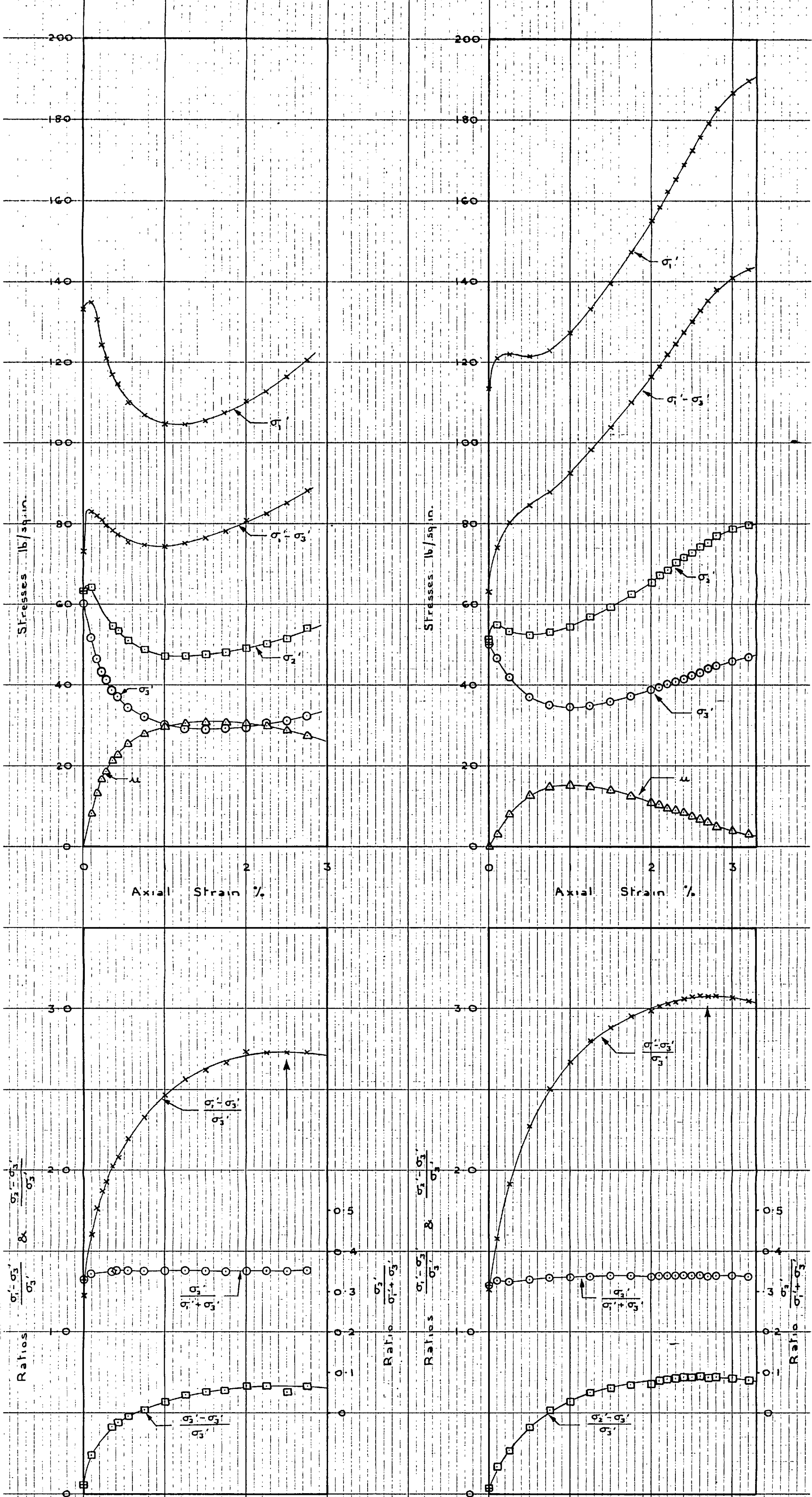
P-27 PLANE STRAIN DRAINED

Data :- $K_o = 0.384$
$n_i = 36.3\%$
Initial $\sigma_2$ prestress = 0.6 lb/sq.in.

Series B

LHS RHS

FIG. A10-19




P-28 PLANE STRAIN UNDRAINED

Data :- $K_o = 0.447$
$n_i = 41.7\%$
Initial $\sigma_3$ prestress = 0.3 lb/sq.in.

(Series D)

No failure plane visible
B value not measured.

P-29 PLANE STRAIN UNDRAINED

Data :- $K_o = 0.442$
$n_i = 39.9\%$
Initial $\sigma_3$ prestress = 0.4 lb/sq.in.

(Series D)

No failure plane visible
B value not measured.

FIG. A10-20

P-30 PLANE STRAIN UNDRAINED

Data :- $K_o$ = 0·428

$n_i$ = 38·4 %

Initial $\sigma_3$ prestress = 0·3 lb./sq.in.

(Series D)

No failure plane visible

B = 1·00




P-31 PLANE STRAIN UNDRAINED

Data :- $K_o$ = 0·402

$n_i$ = 35·0 %

Initial $\sigma_3$ prestress = 0·4 lb/sq.in.

(Series D)

No failure plane visible

B = 0·93

FIG. A10-21

Stresses lb/sq.in.

$\sigma_1'$

$\sigma_1' - \sigma_3'$

$u$

$\sigma_2'$

$\sigma_3'$

Strain $\varepsilon_1$ (%)

Stress Ratios $\frac{\sigma_1' - \sigma_3'}{\sigma_3'}$ & $\frac{\sigma_2' - \sigma_3'}{\sigma_3'}$

$\frac{\sigma_1' - \sigma_3'}{\sigma_3'}$

$\frac{\sigma_2'}{\sigma_1' + \sigma_3'}$

Stress Ratio $\frac{\sigma_2'}{\sigma_1' + \sigma_3'}$

$\frac{\sigma_2' - \sigma_3'}{\sigma_3'}$

Strain $\varepsilon_1$ (%)

P-32 PLANE STRAIN UNDRAINED

Data: $\sigma_{3c}$ = 4·0 lb/sq.in
$K_o$ = 0·432
Cell Pressure = 60·1 lb/sq.in
$\eta_i$ = 39·5%
(Series D)
B = 1·00

LHS

RHS

3-4½ mm

2-3 mm

FIG. A 10-22

Stresses lb/sq.in.

$\sigma_1'$

$\sigma_1' - \sigma_3'$

$\sigma_2'$

$\sigma_3'$

Maximum

Axial Strain %

Ratios $\frac{\sigma_1' - \sigma_3'}{\sigma_3'}$ & $\frac{\sigma_2' - \sigma_3'}{\sigma_3'}$

$\frac{\sigma_1' - \sigma_3'}{\sigma_3'}$ ($\epsilon_1 = 0-8\%$)

$\frac{\sigma_1' - \sigma_3'}{\sigma_3'}$ ($\epsilon_1 = 8-11\%$)

$\frac{\sigma_2'}{\sigma_1' + \sigma_3'}$

$\frac{\sigma_3 - \sigma_3'}{\sigma_3'}$

Ratio $\frac{\sigma_2'}{\sigma_1' + \sigma_3'}$

Axial Strain %

P-33 PLANE STRAIN UNDRAINED

Data:- $K_o = 0.448$

$n_i = 41.9\%$

Initial $\sigma_3$ prestress = 0.5 lb./sq.in.

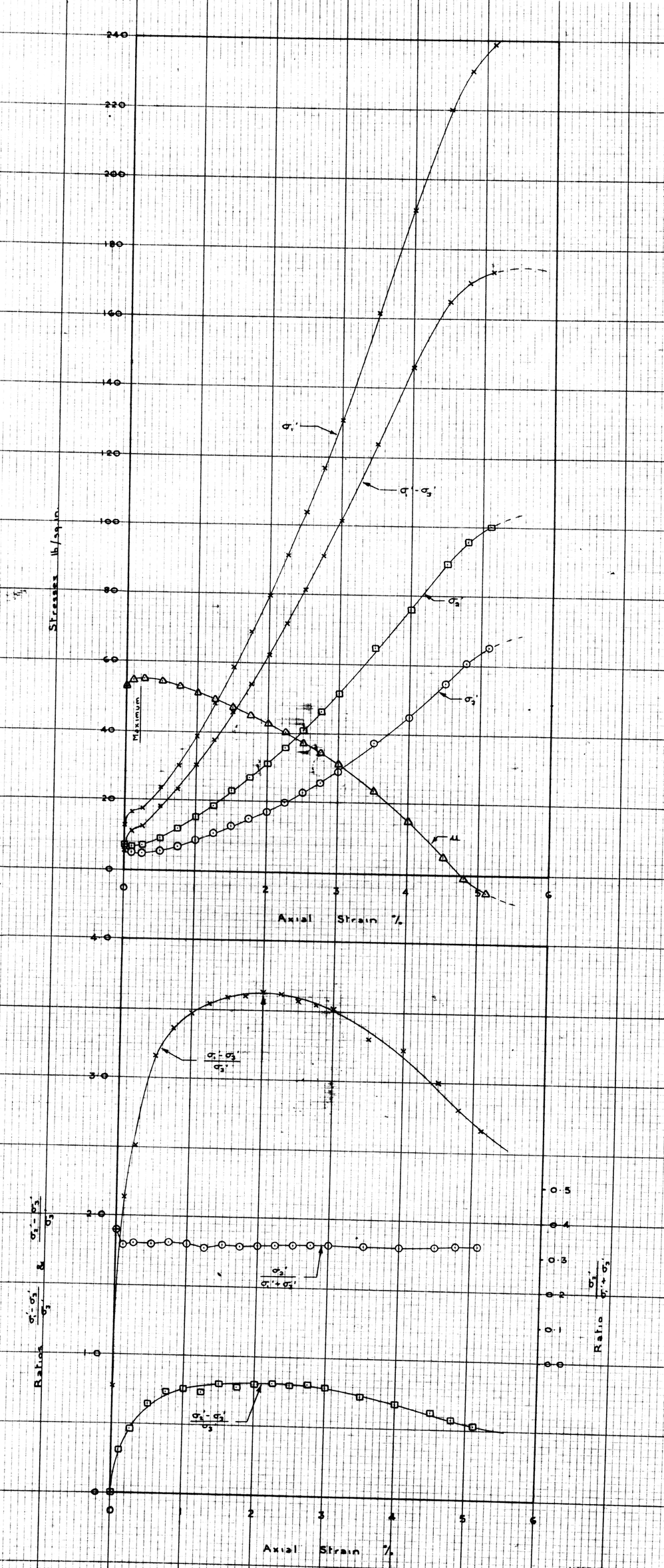
(Series D)

B value not measured.

LHS RHS

3-4 mm

FIG. A10-23




P-34 PLANE STRAIN UNDRAINED

Data:- $K_o = 0.560$

$n_i = 38.1\%$

Initial $\sigma_3$ prestress = 0.3 lb/sq.in.

(Series D)

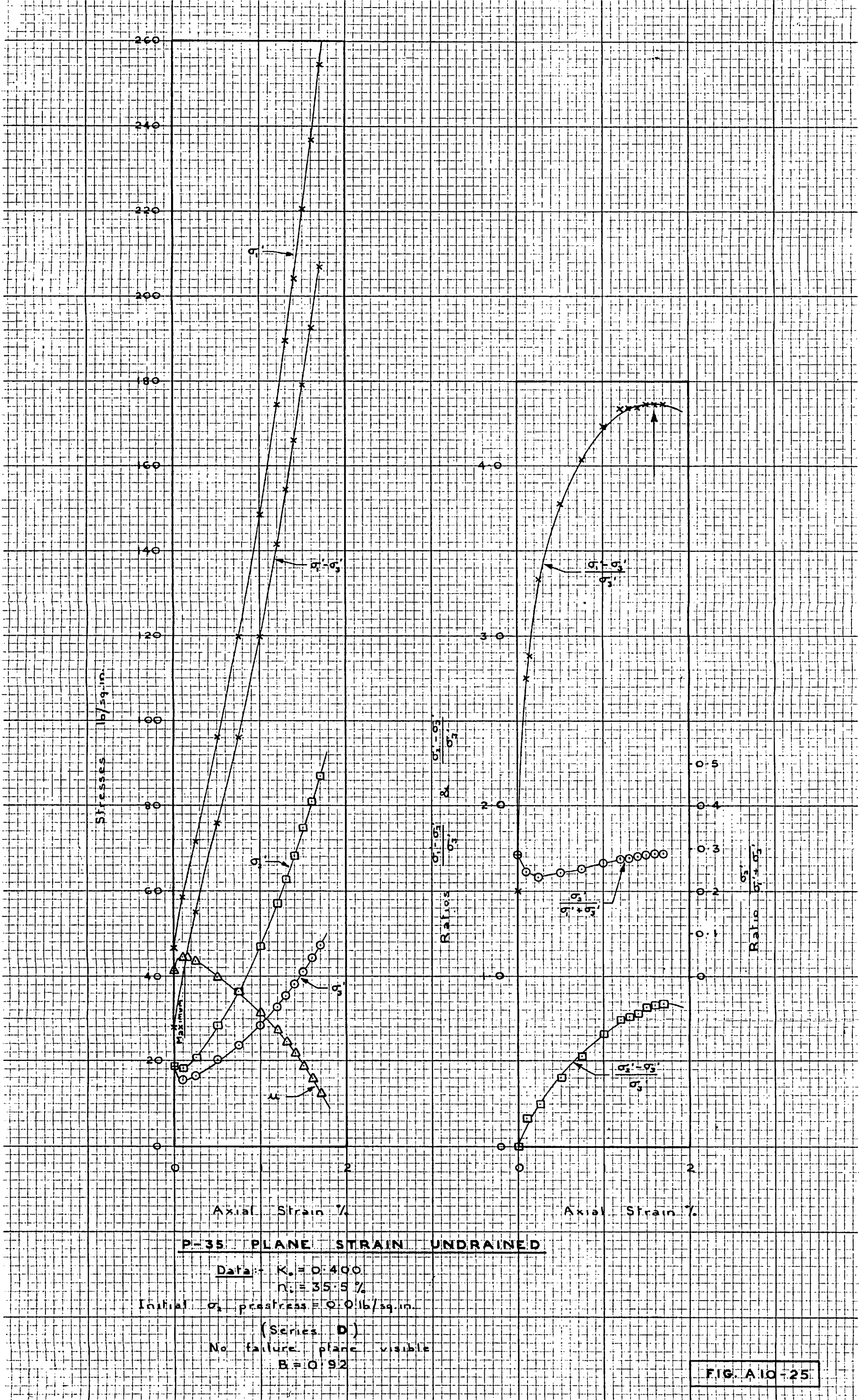
Single plane of failure visible along the length of the specimen up to 3½in. from R.H.S.

B = 0.94

LHS RHS

approx 3mm

FIG. A.10-24




P-35 PLANE STRAIN UNDRAINED

Data:- $K_o = 0.400$

$n_i = 35.5\%$

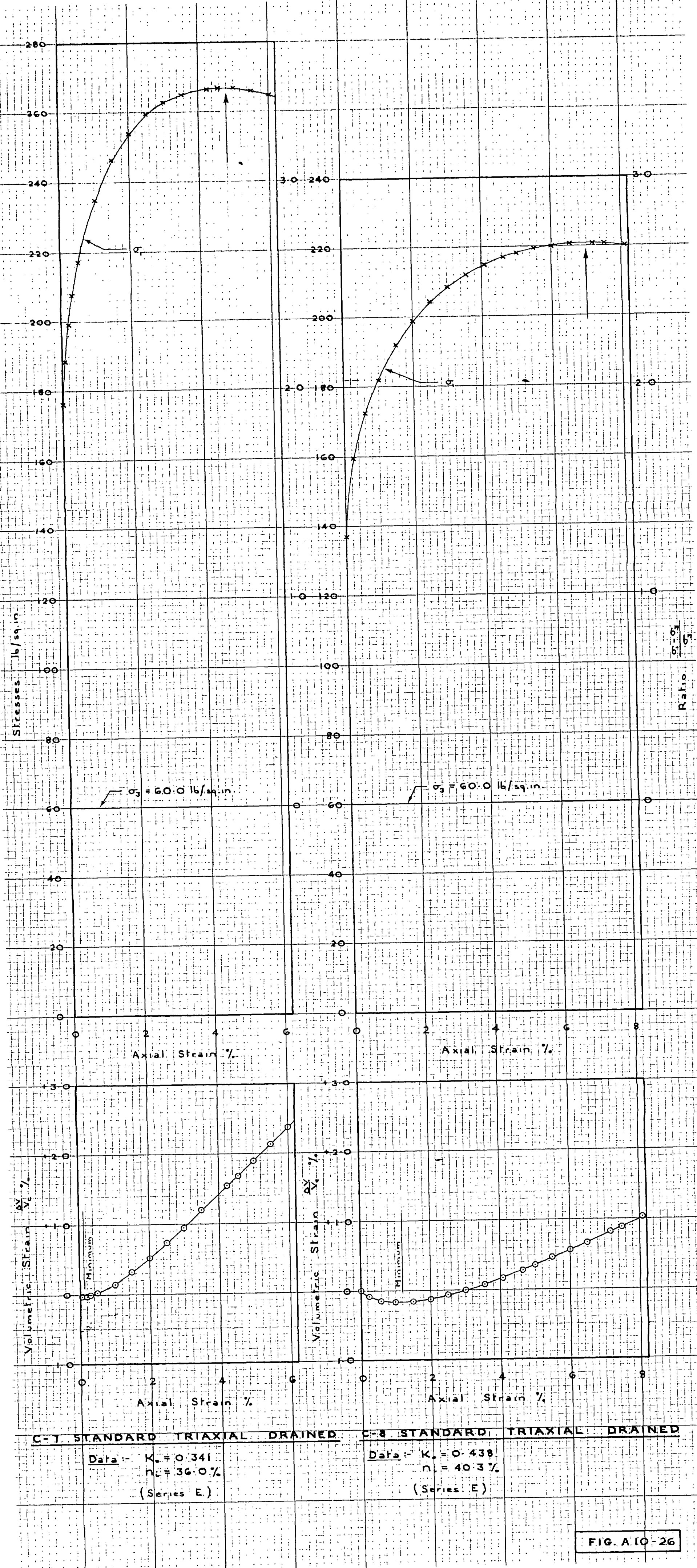
Initial $\sigma_3$ prestress = 0.0 lb/sq.in.

(Series D)

No failure plane visible

B = 0.92

FIG. A10-25



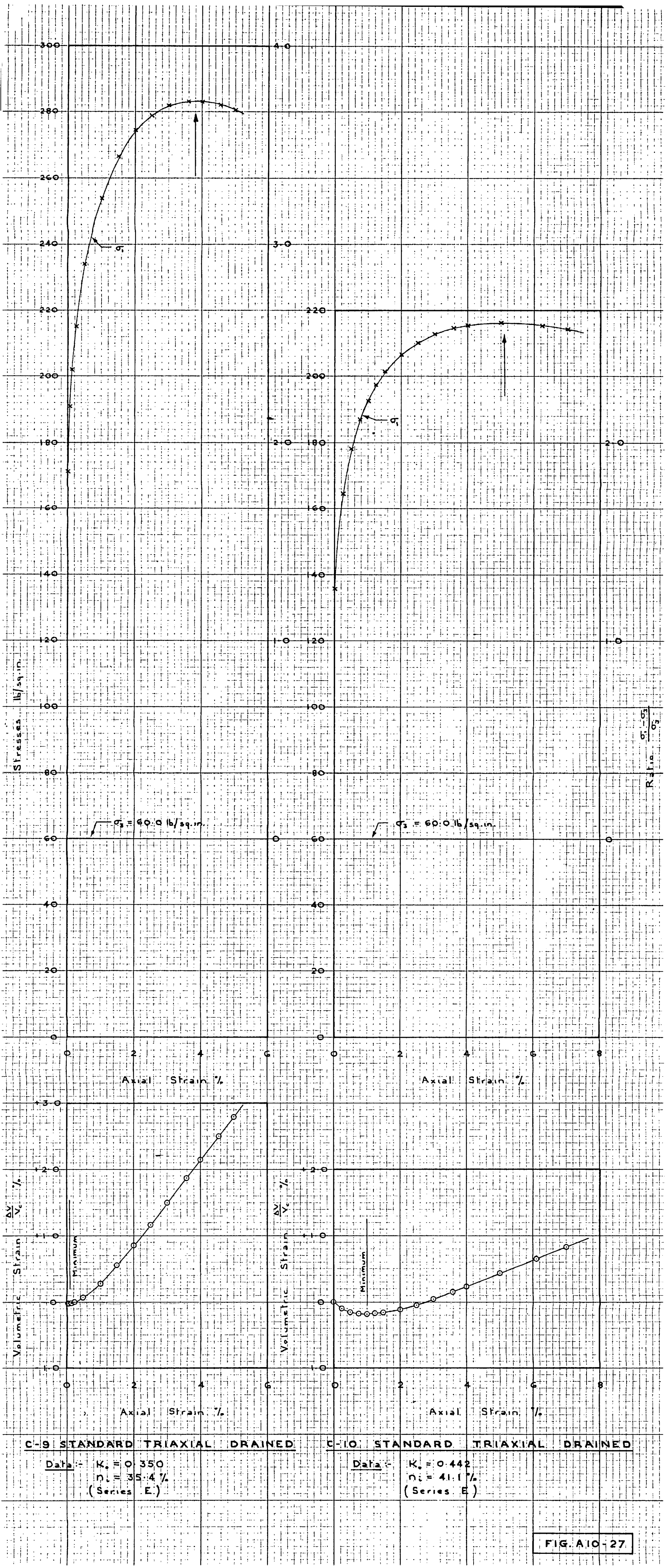

C-7 STANDARD TRIAXIAL DRAINED

Data :- $K_o$ = 0.341
$n_c$ = 36.0 %
(Series E.)

C-8 STANDARD TRIAXIAL DRAINED

Data :- $K_o$ = 0.438
$n_c$ = 40.3 %
(Series E)

FIG. A.10-26



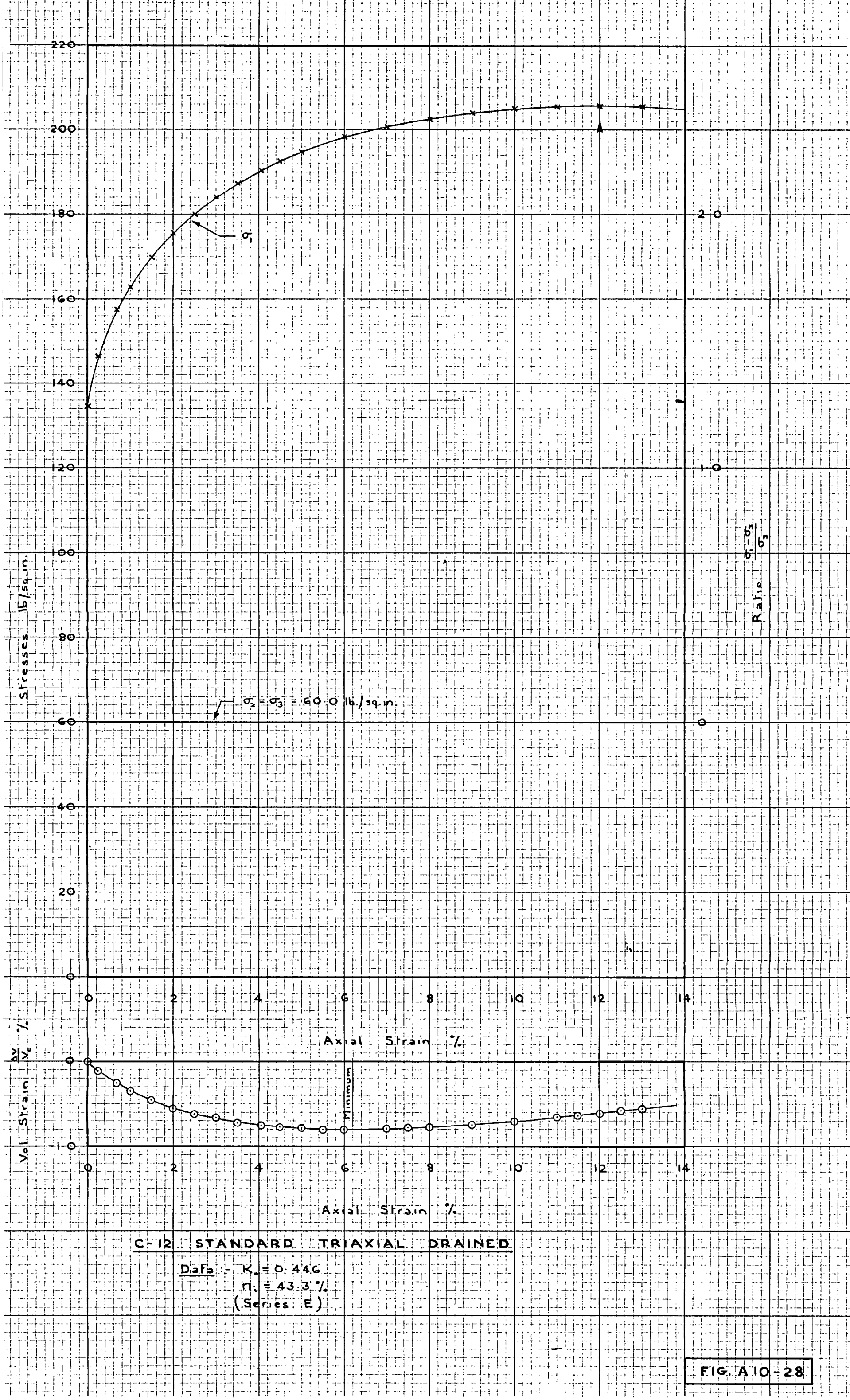

C-9 STANDARD TRIAXIAL DRAINED

Data :- $K_o$ = 0.350
$n_i$ = 35.4 %
(Series E.)

C-10 STANDARD TRIAXIAL DRAINED

Data :- $K_o$ = 0.442
$n_i$ = 41.1 %
(Series E)

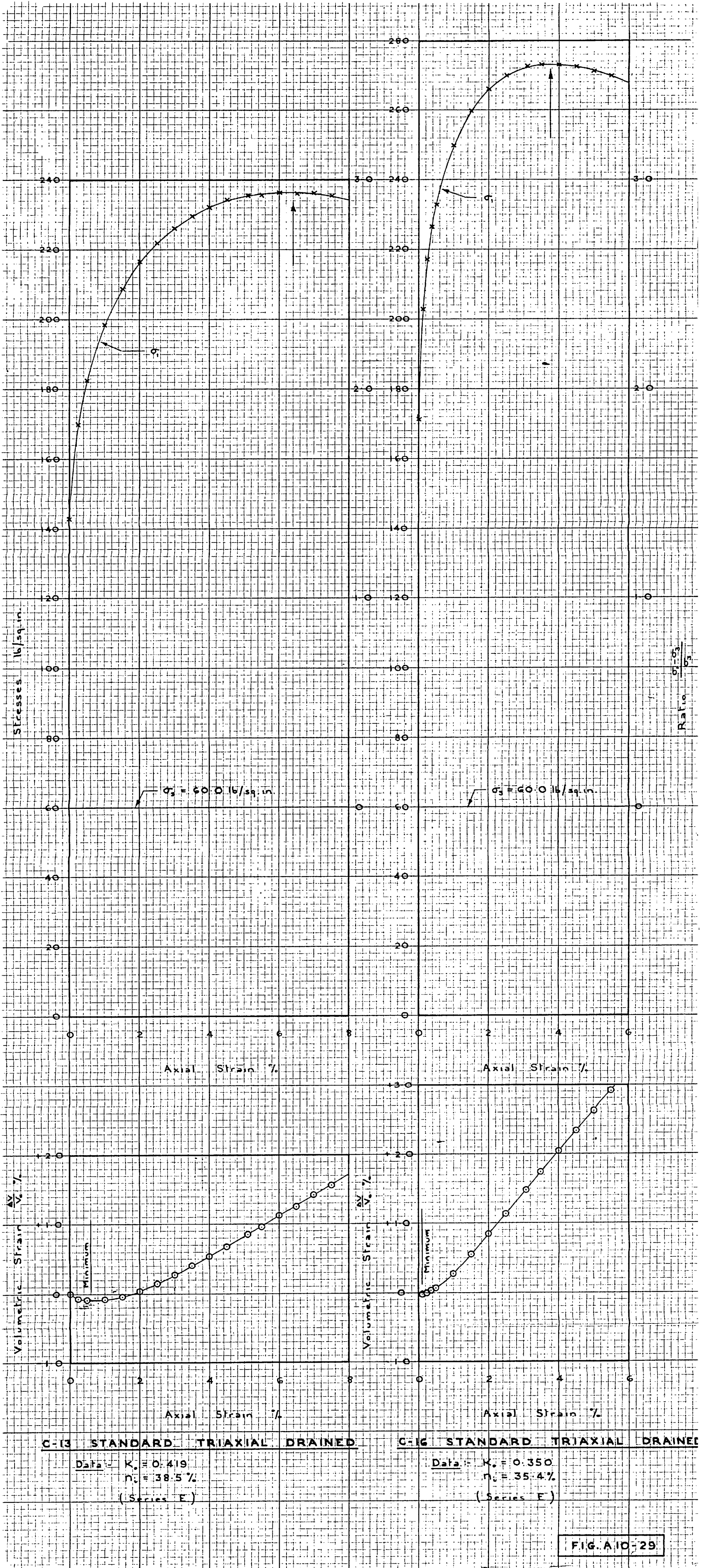
FIG. A10-27




C-12 STANDARD TRIAXIAL DRAINED

Data :- $K_o = 0.446$
$\eta_i = 43.3\%$
(Series E)

FIG. A 10-28



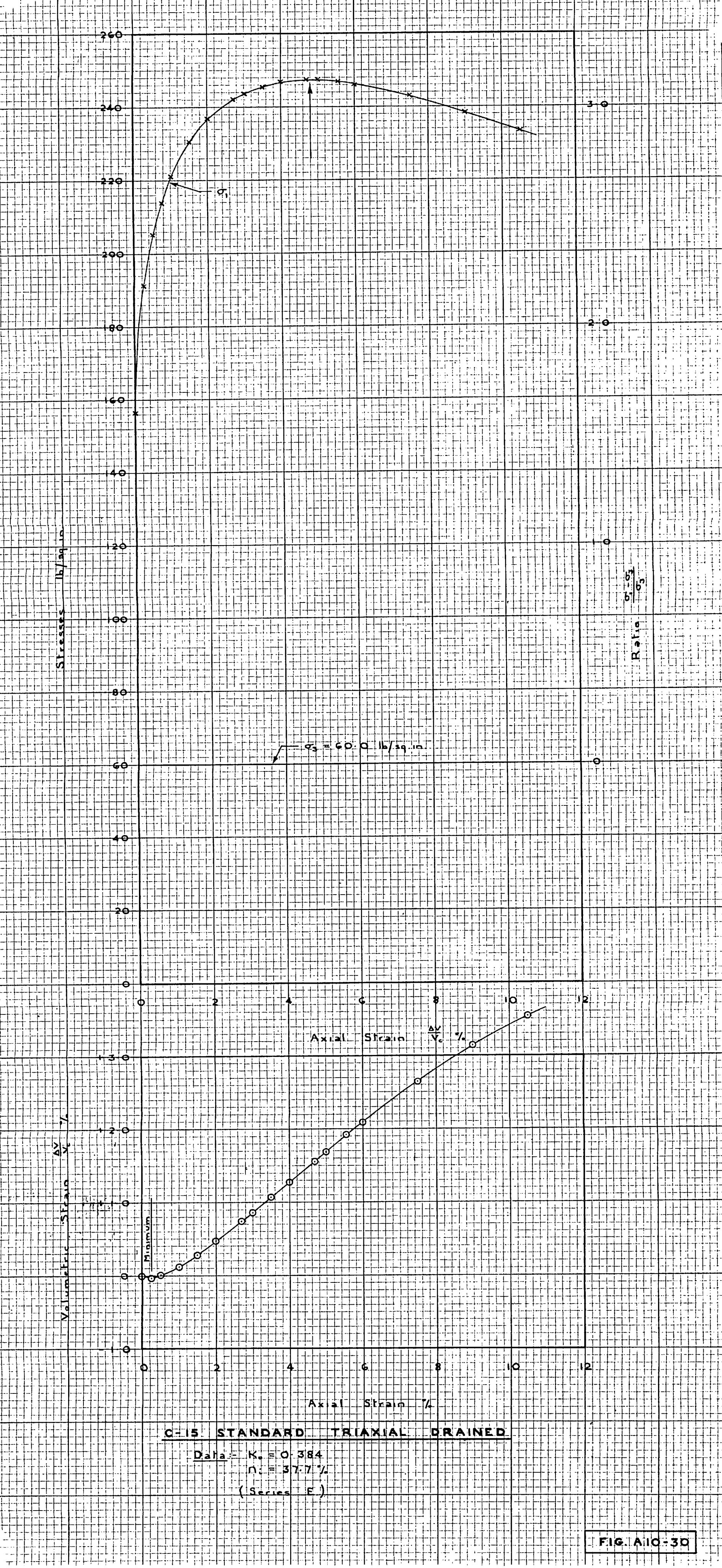

C-13 STANDARD TRIAXIAL DRAINED

Data :- $K_0 = 0.419$
$n_i = 38.5\%$
(Series E)

C-16 STANDARD TRIAXIAL DRAINED

Data :- $K_0 = 0.350$
$n_i = 35.4\%$
(Series E)

FIG. A10-29



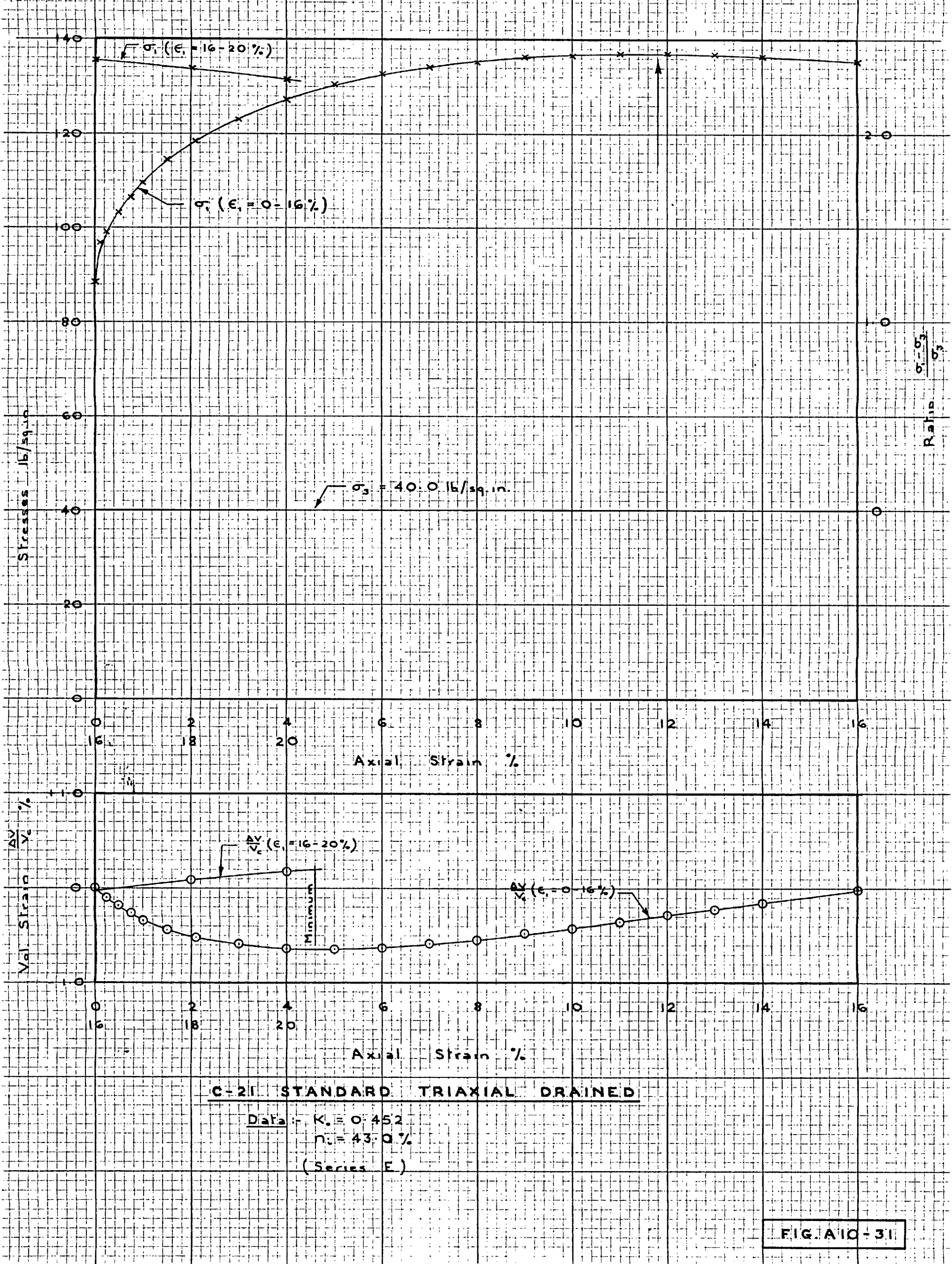

C-15 STANDARD TRIAXIAL DRAINED

Data :- $K_o = 0.384$

$n_i = 37.7\%$

(Series E)

FIG. A10-30



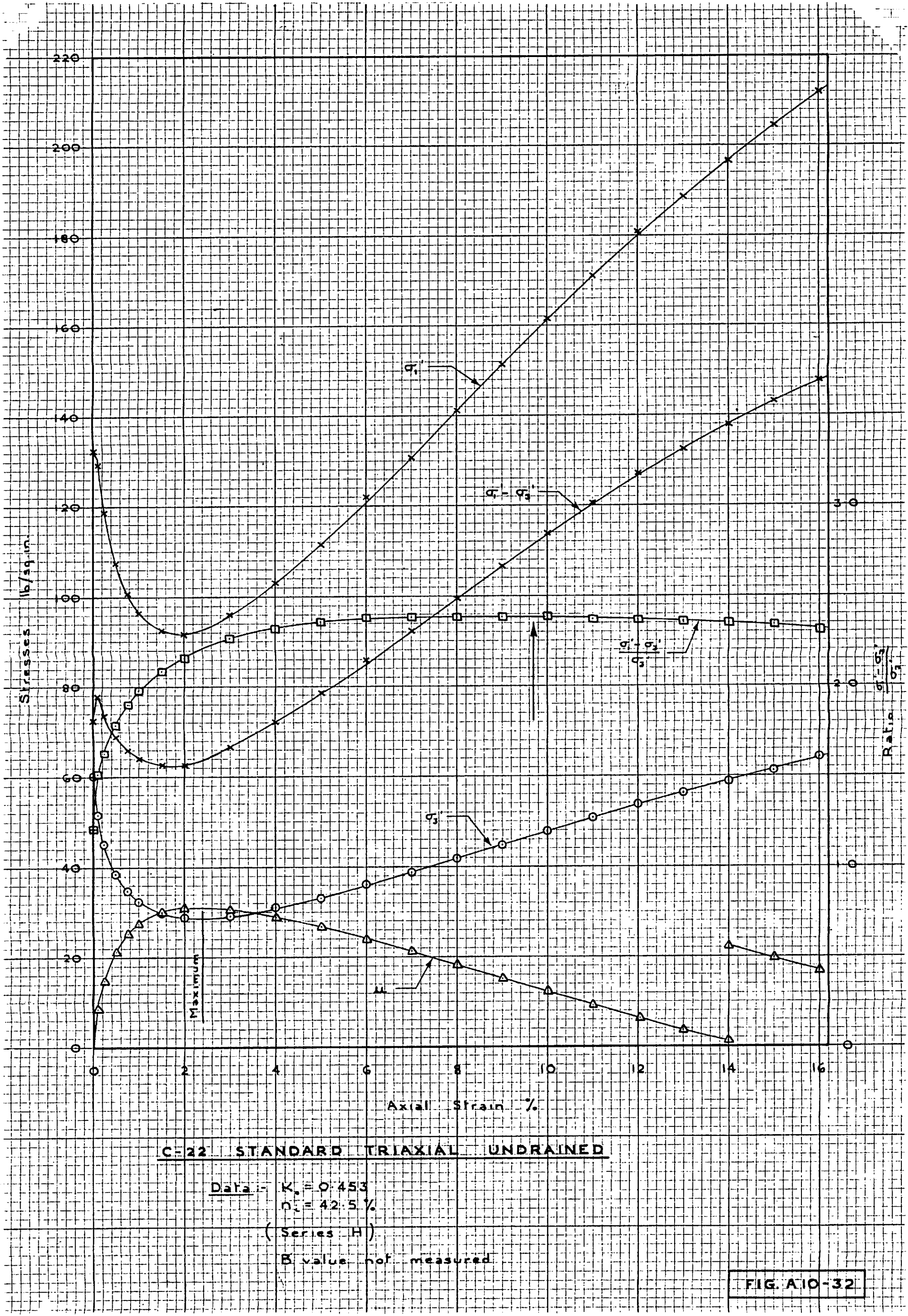

C-21 STANDARD TRIAXIAL DRAINED

Data : $K_o = 0.452$

$n_i = 43.0\ \%$

(Series E)

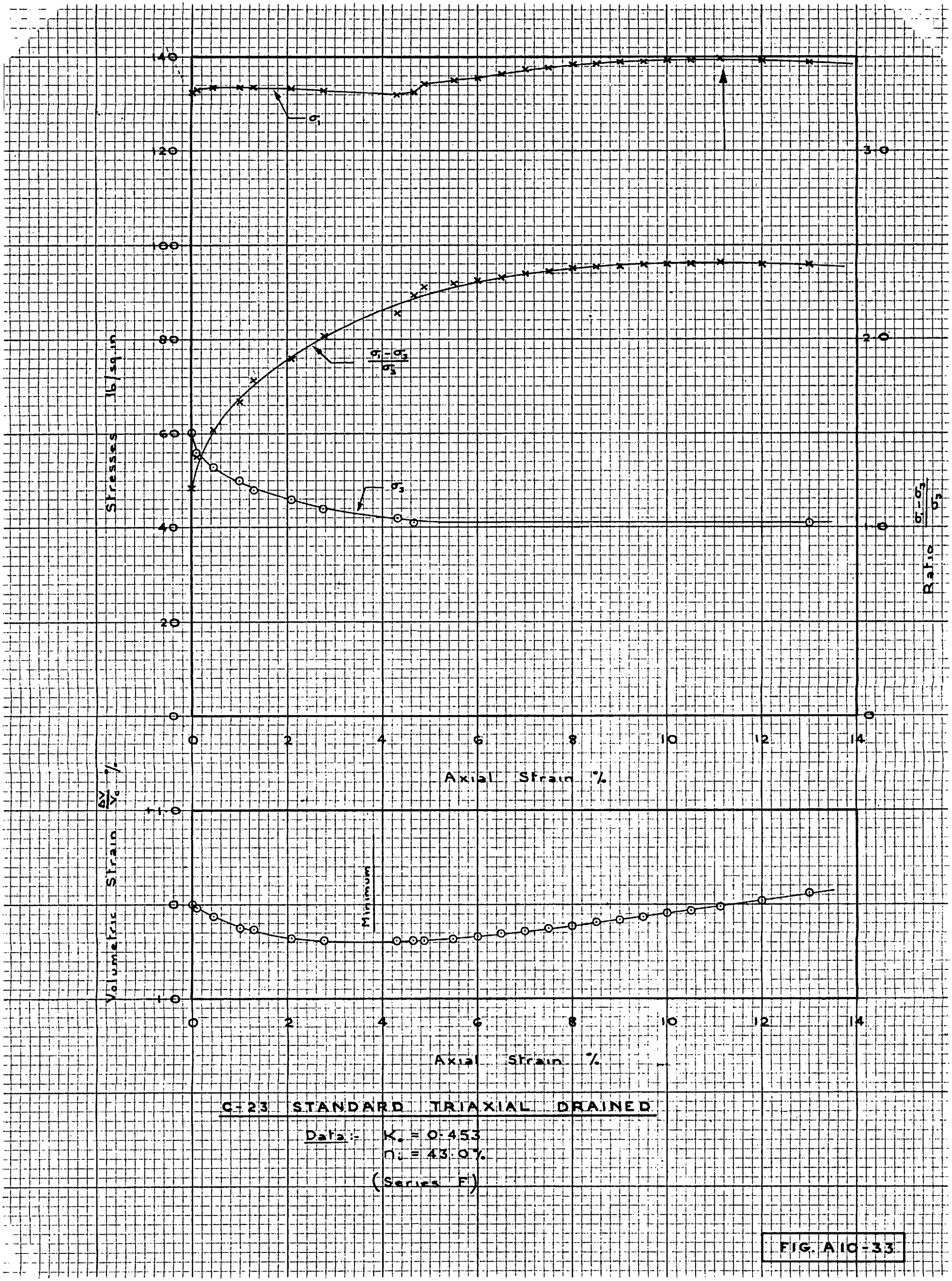
FIG. A10-31




C-22 STANDARD TRIAXIAL UNDRAINED

Data :- $K_o = 0.453$
$n_i = 42.5\%$
(Series H)
B value not measured

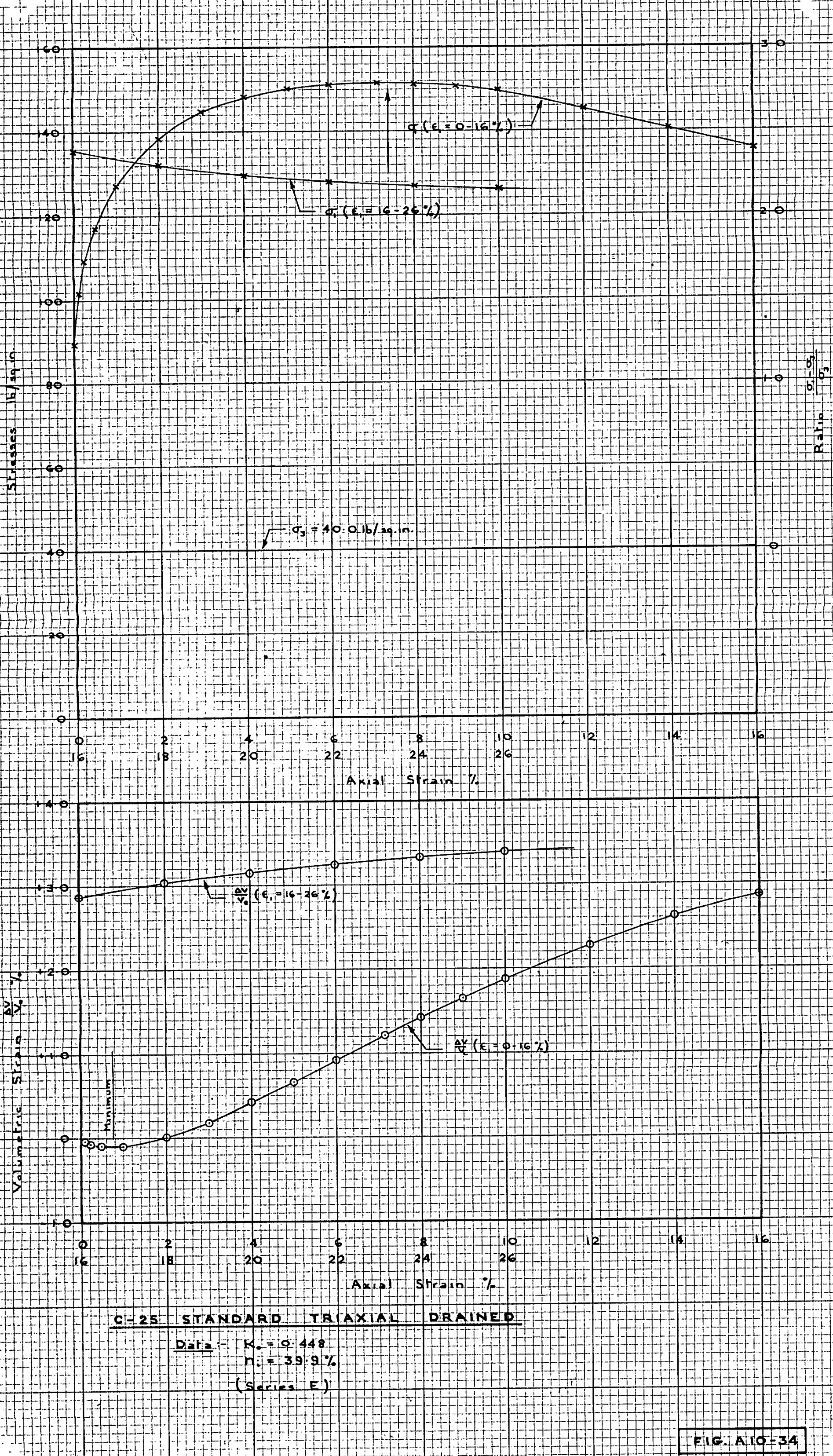
FIG. A10-32




C-23 STANDARD TRIAXIAL DRAINED

Data :- $K_o = 0{\cdot}453$
$n_i = 43{\cdot}0\%$
(Series F)

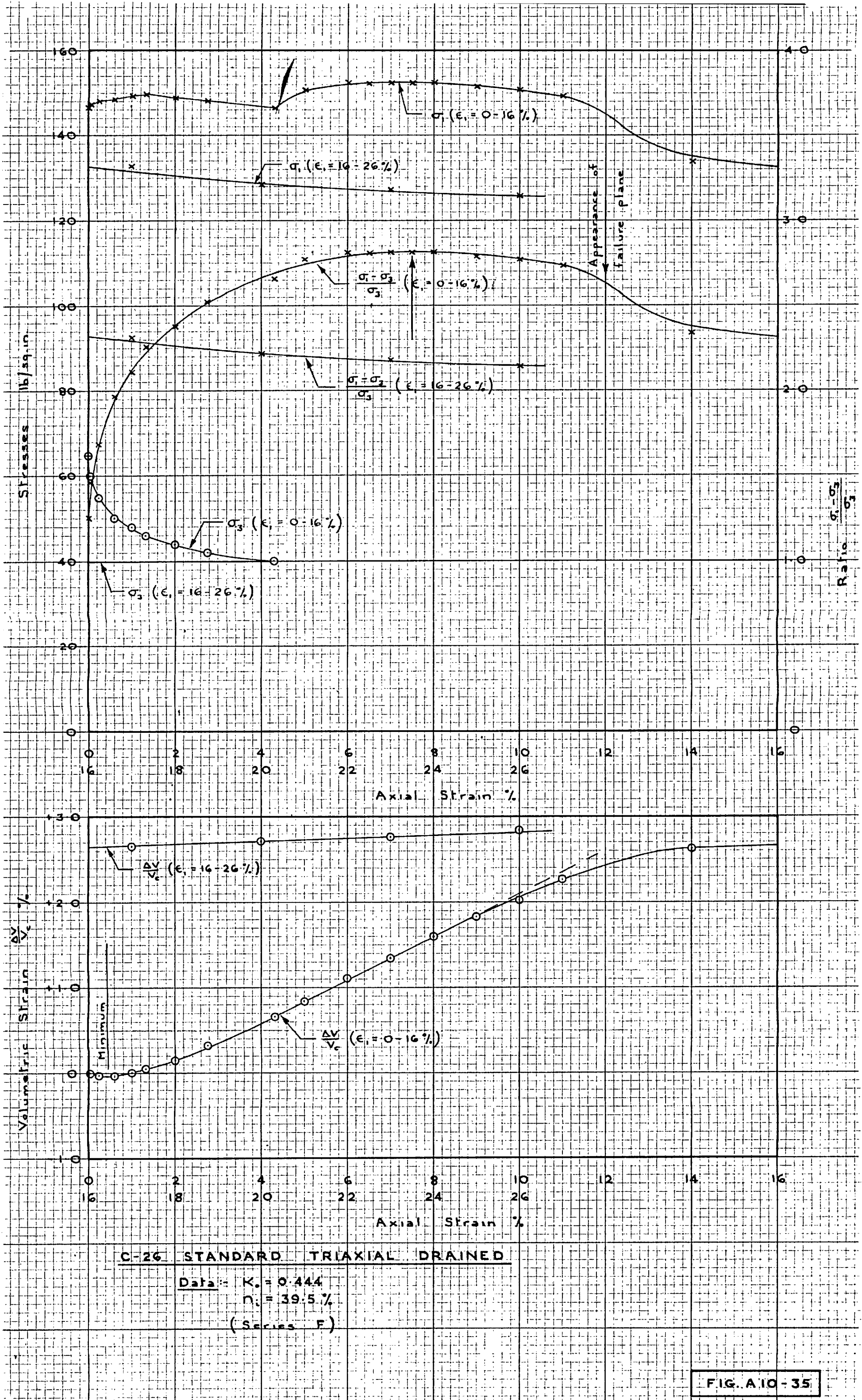
FIG. A10-33




C-25 STANDARD TRIAXIAL DRAINED

Data :- $K_o$ = 0.448
$n_i$ = 39.9 %
(Series E)

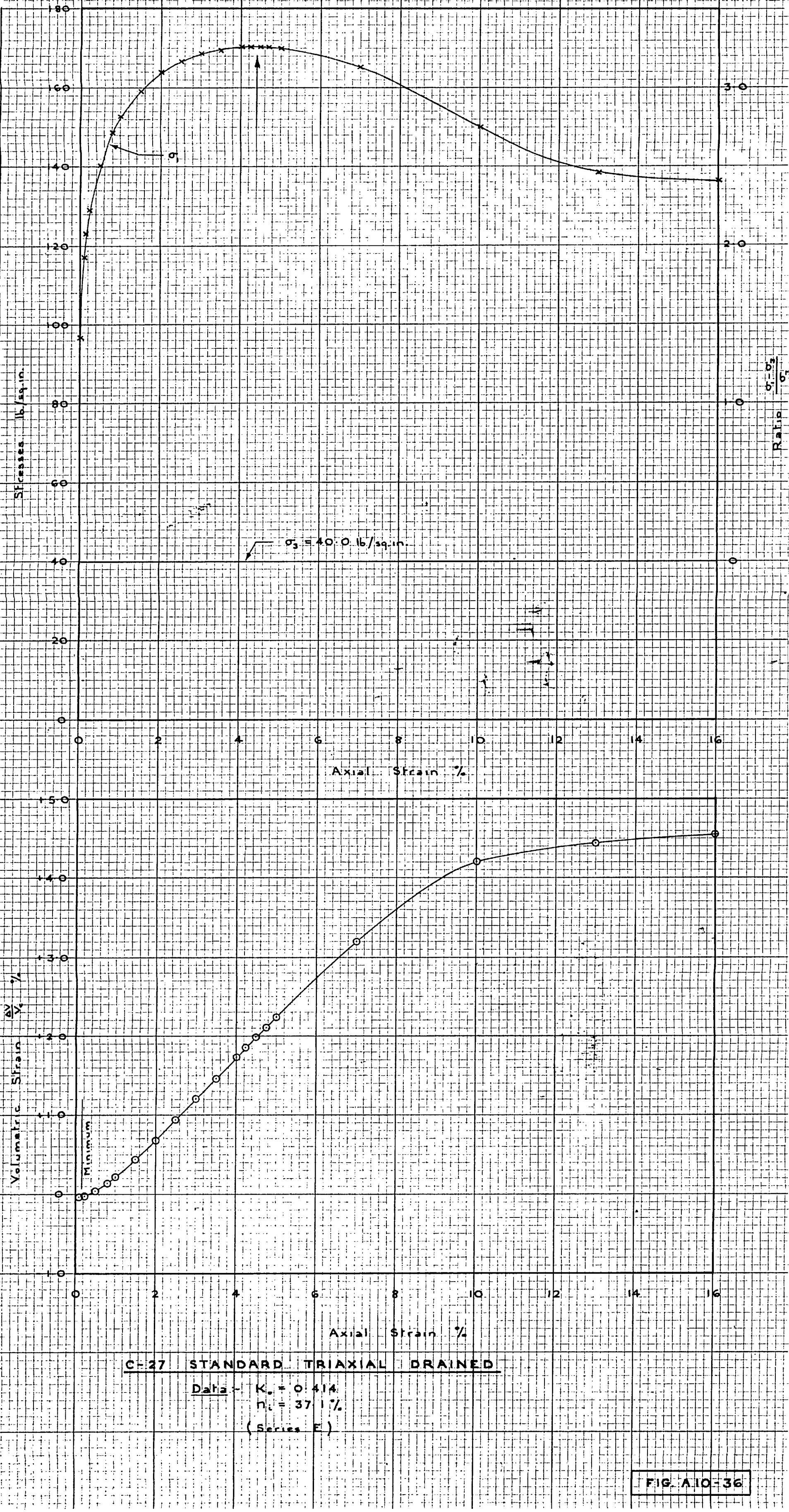
FIG. A10-34




C-26 STANDARD TRIAXIAL DRAINED

Data:- $K_o$ = 0·444
$n_i$ = 39·5 %
(Series F)

FIG. A 10 - 35




C-27 STANDARD TRIAXIAL DRAINED

Data:- $K_o$ = 0·414
$n_i$ = 37·1 %
(Series E)

FIG. A10-36

Stresses - lb/sq.in.

Ratio $\frac{\sigma_1 - \sigma_3}{\sigma_3}$

$\sigma_1$

$\sigma_3$

Appearance of failure plane

$\frac{\sigma_1 - \sigma_3}{\sigma_3}$

Axial Strain %

Volumetric Strain $\frac{\Delta V}{V_c}$ %

Axial Strain %

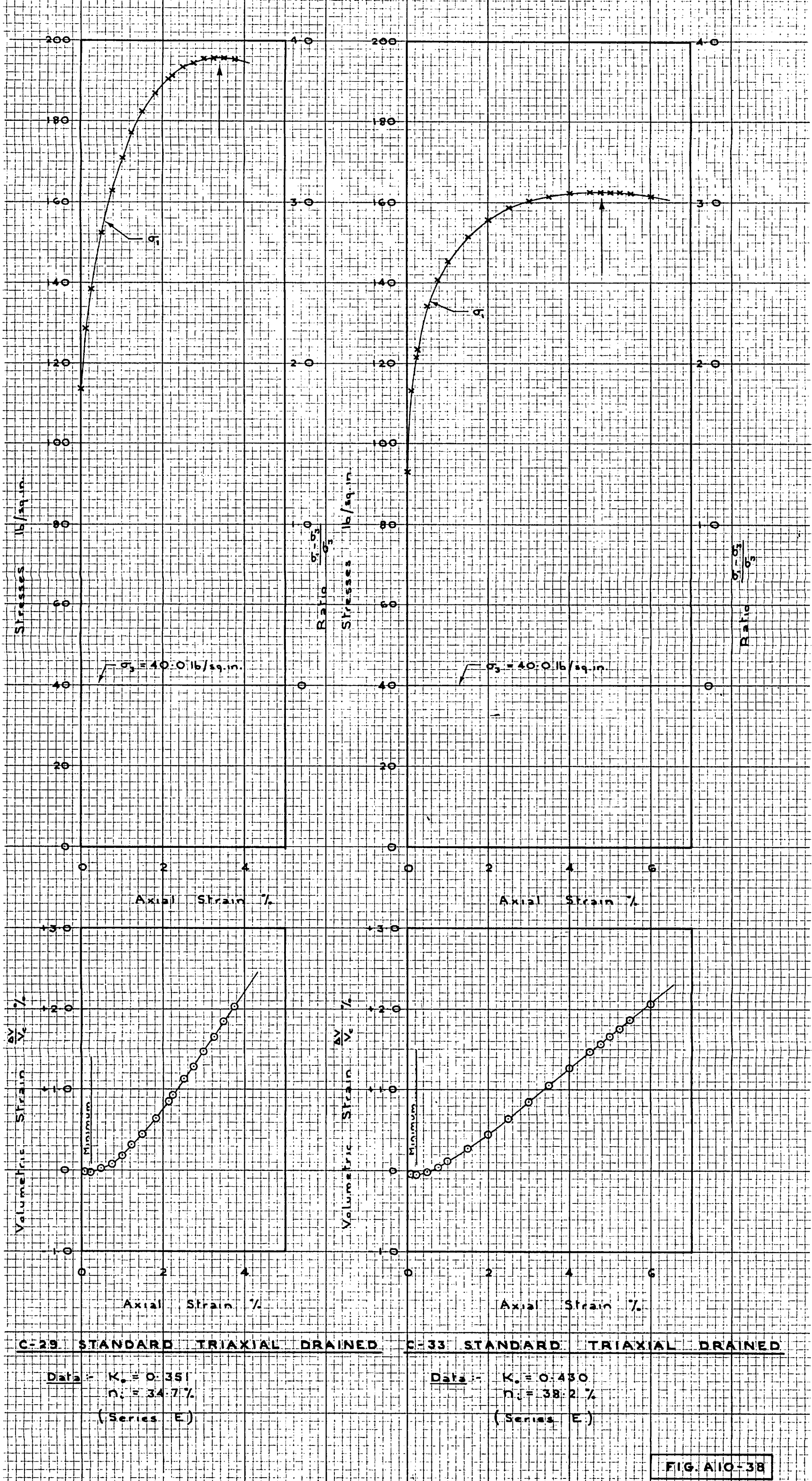
C-28 STANDARD TRIAXIAL DRAINED

Data:- $K_o = 0.416$

$n_i = 37.4\%$

(Series F)

FIG. A 10-37



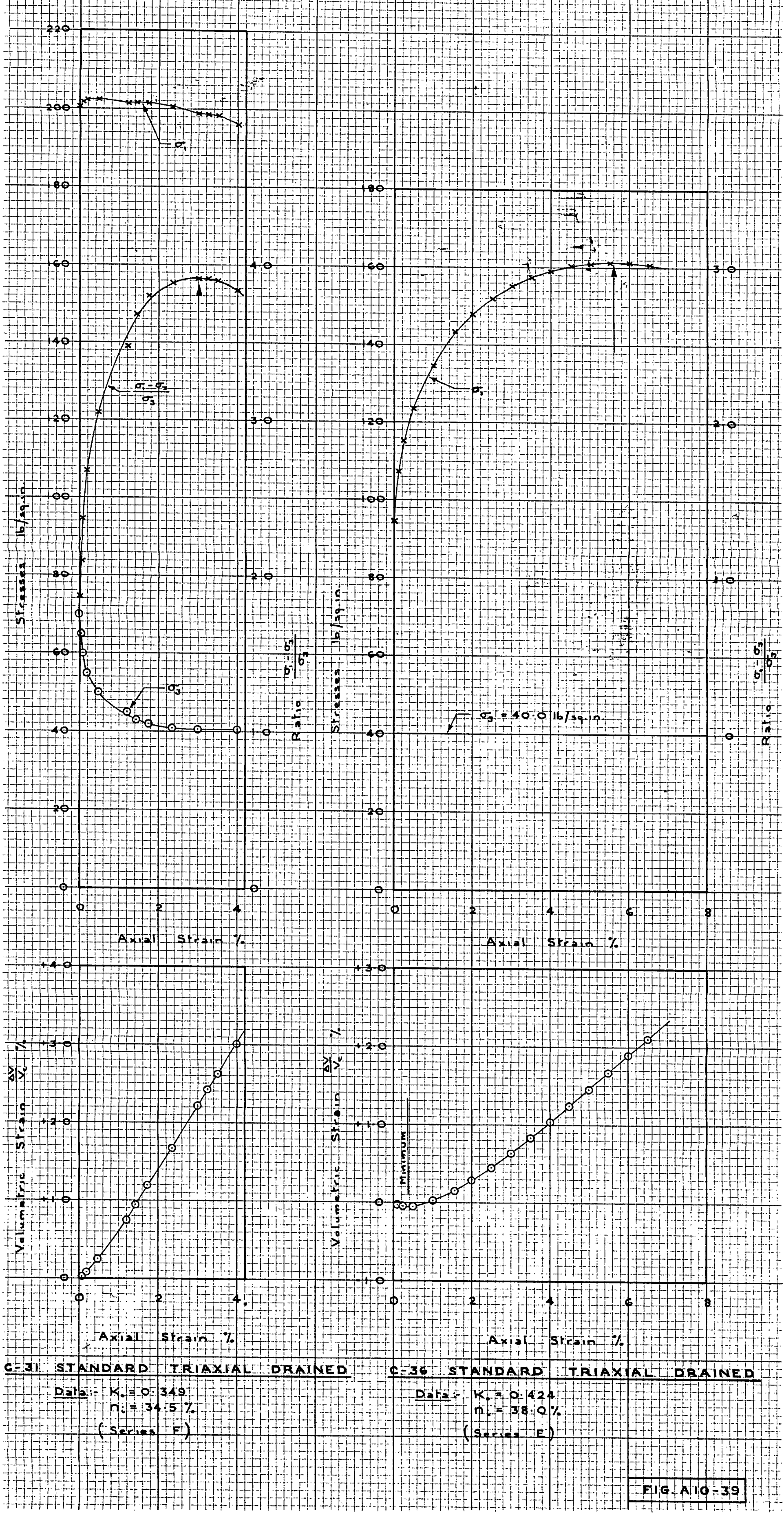

C-29 STANDARD TRIAXIAL DRAINED

Data :- $K_o$ = 0·351
$n_i$ = 34·7 %
(Series E)

C-33 STANDARD TRIAXIAL DRAINED

Data :- $K_o$ = 0·430
$n_i$ = 38·2 %
(Series E)

FIG. A10-38



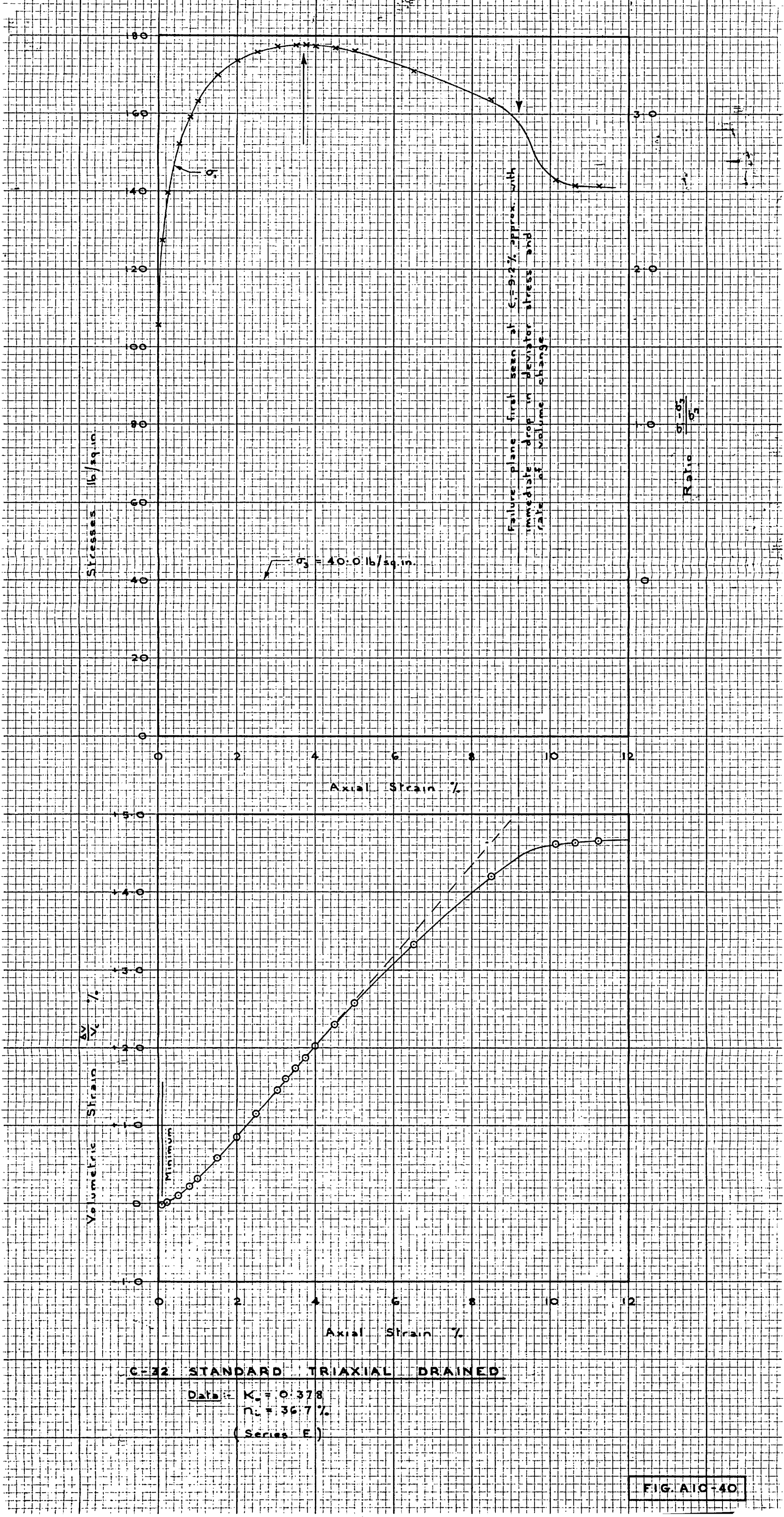

C-31 STANDARD TRIAXIAL DRAINED

Data:- $K_o = 0.349$
$n_i = 34.5\%$
(Series F)

C-36 STANDARD TRIAXIAL DRAINED

Data:- $K_o = 0.424$
$n_i = 38.0\%$
(Series E)

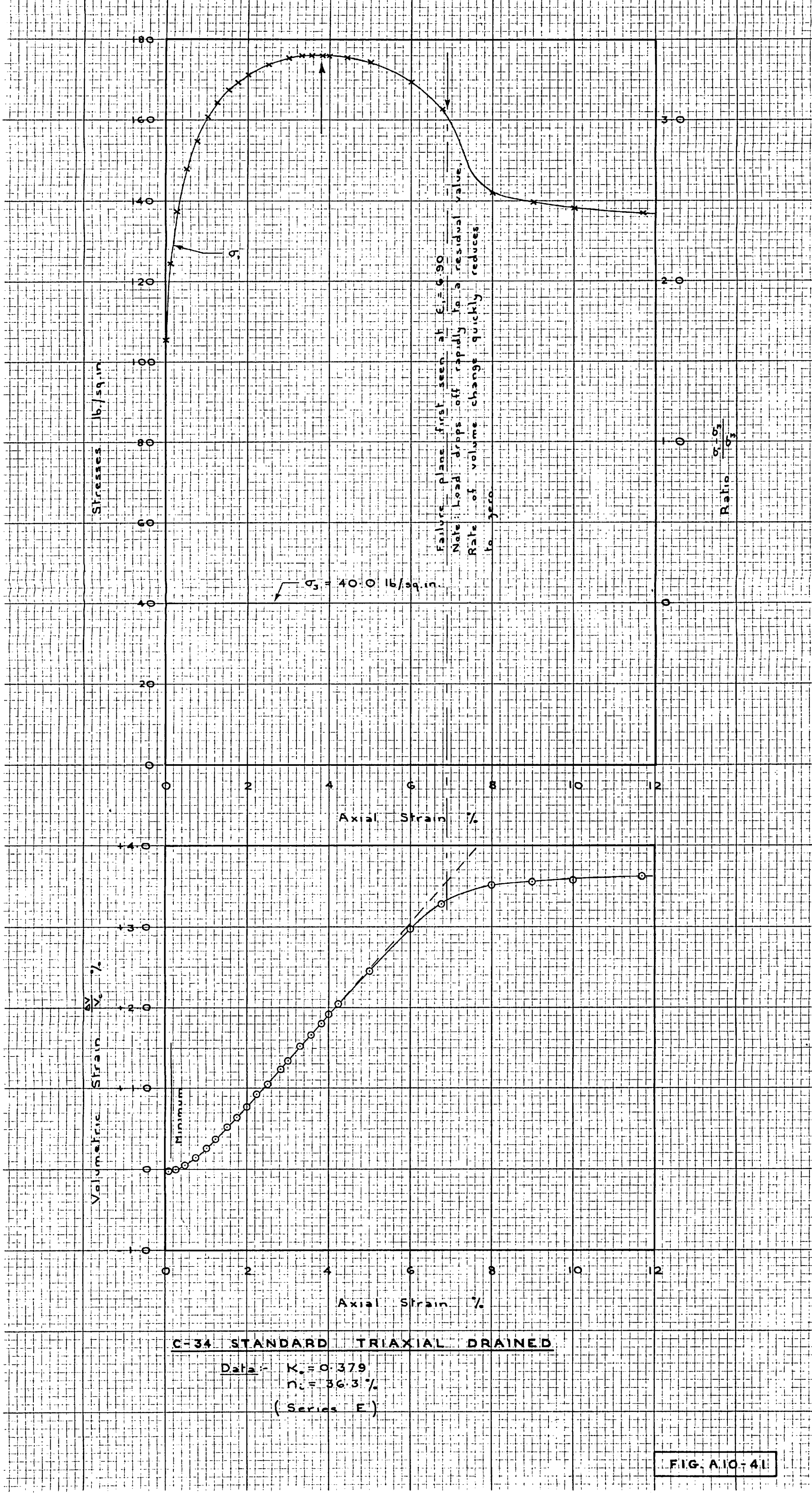
FIG. A10-39




C-32 STANDARD TRIAXIAL DRAINED

Data: $K_c$ = 0.378
$n_c$ = 36.7 %
(Series E)

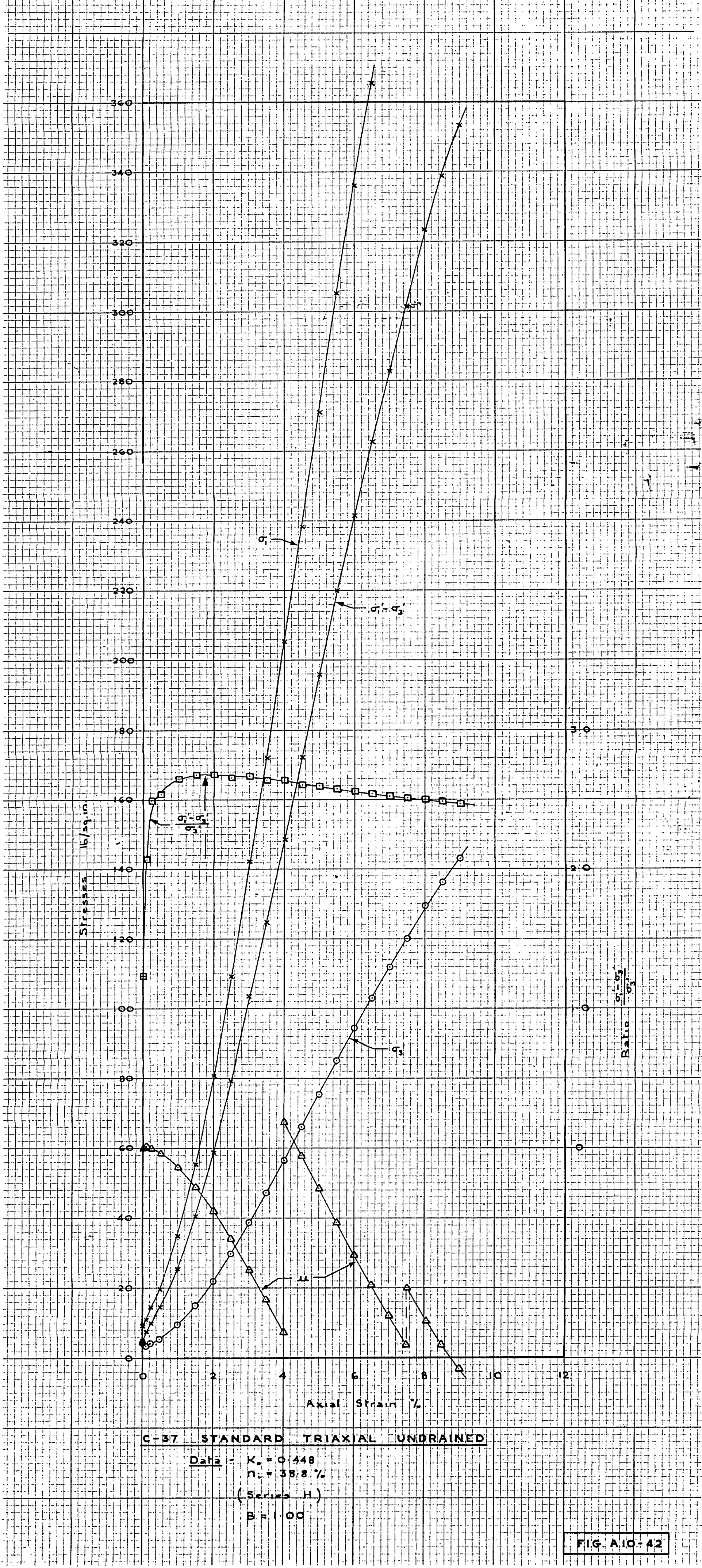
FIG. A10-40




C-34 STANDARD TRIAXIAL DRAINED

Data :- $K_o = 0.379$
$n_i = 36.3\%$
(Series E)

FIG. A.10-41




C-37 STANDARD TRIAXIAL UNDRAINED

Data :- $K_o = 0.448$
$n_i = 38.8\%$
(Series H)
$B = 1.00$

FIG. A10-42

Stresses lb/sq in

$\sigma_1' - \sigma_3'$

$\sigma_3'$

$\sigma_1'$

$u$

Axial Strain %

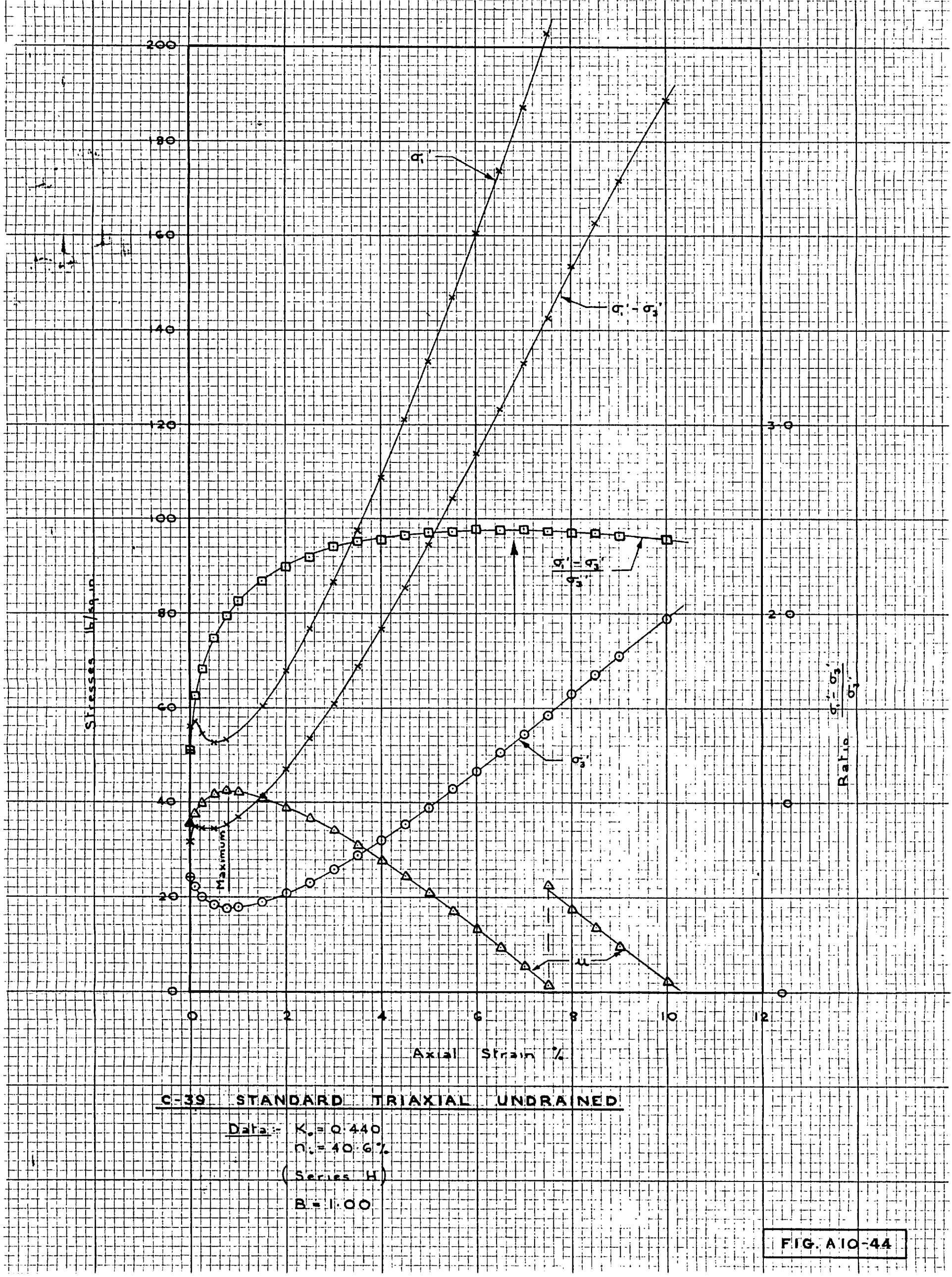
$\frac{\sigma_1' - \sigma_3'}{\sigma_3'}$ Ratio

Axial Strain %

C-38 STANDARD TRIAXIAL UNDRAINED

Data:- $K_o = 0.500$
$n_i = 38.2\ \%$
(Series H)
$B = 1.00$

FIG. A 10-43




C-39 STANDARD TRIAXIAL UNDRAINED

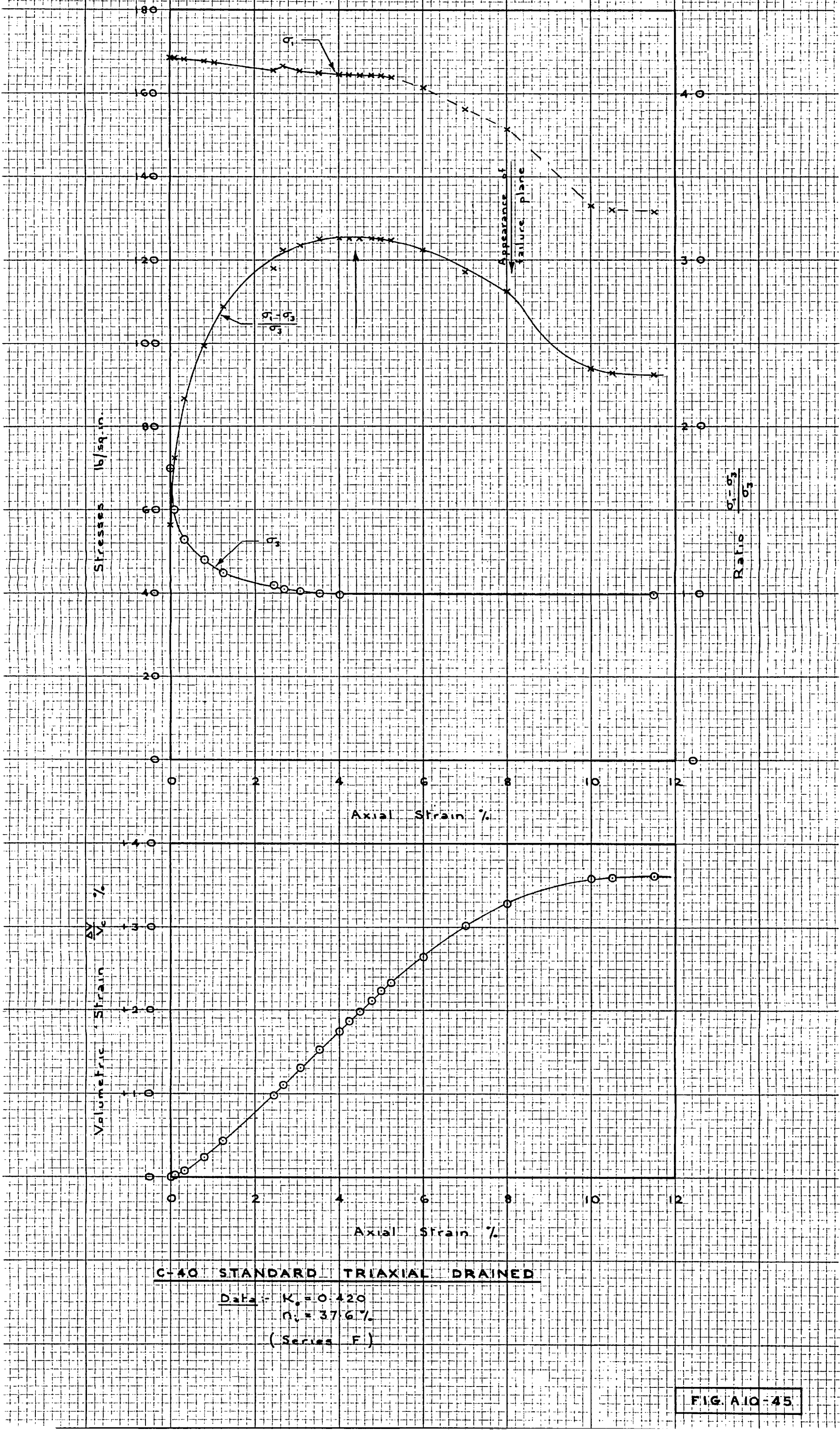
Data :- $K_o = 0.440$

$n_i = 40.6\%$

(Series H)

B = 1.00

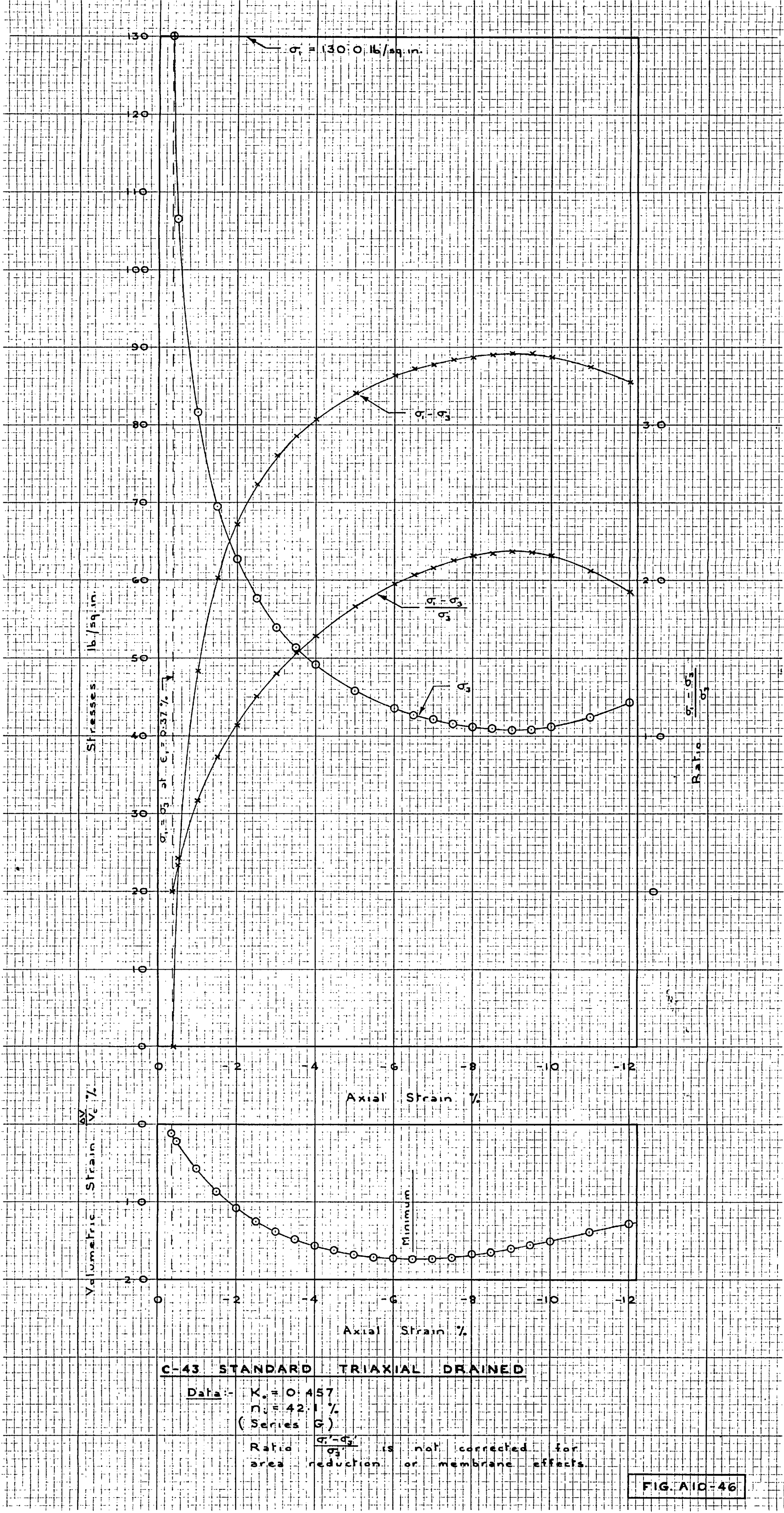
FIG. A10-44




C-40 STANDARD TRIAXIAL DRAINED

Data :- $K_o = 0.420$
$n_i = 37.6\%$
(Series F)

FIG. A10-45

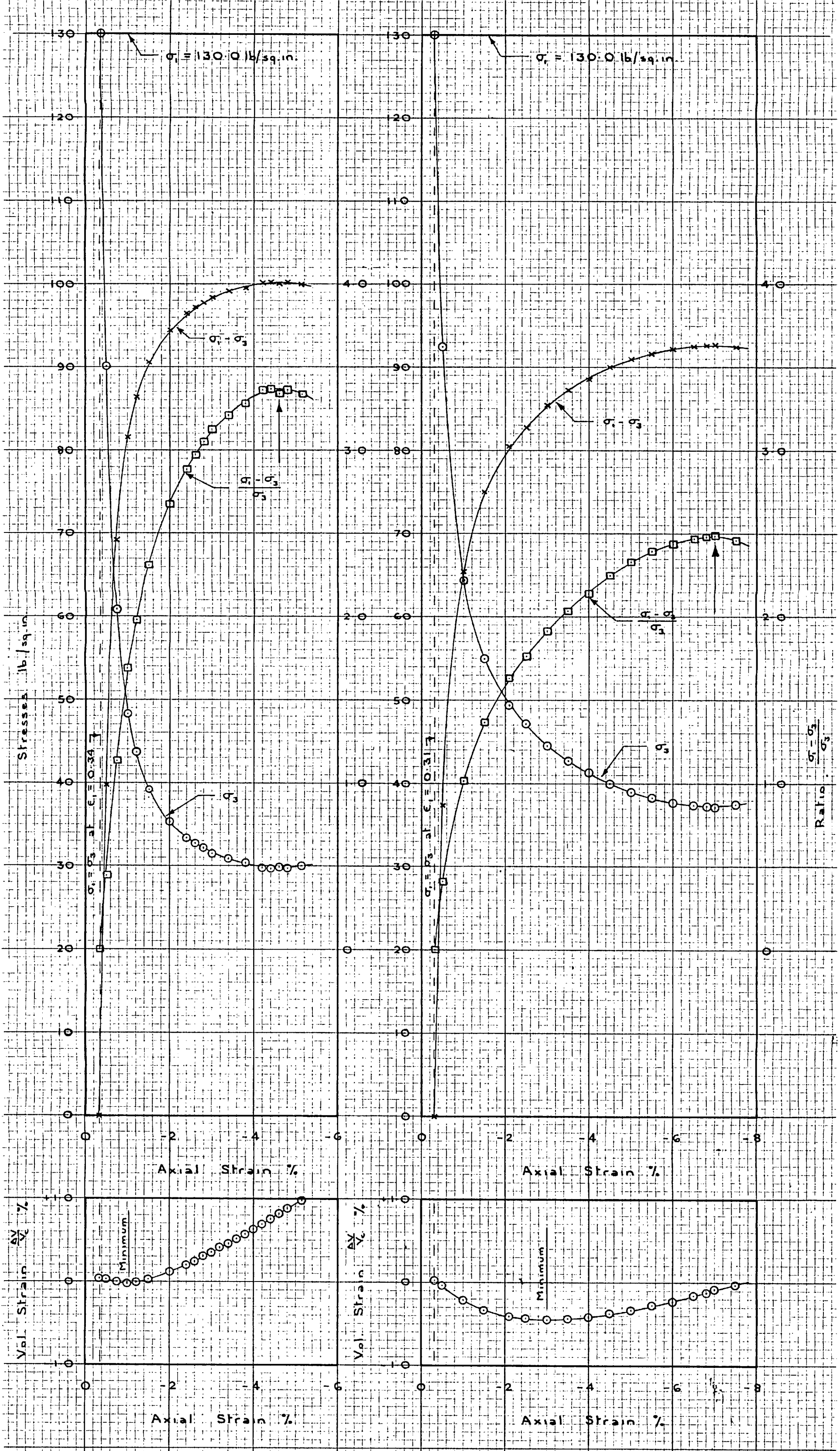



C-43 STANDARD TRIAXIAL DRAINED

Data:- $K_o$ = 0·457
$n_i$ = 42·1 %
( Series G )

Ratio $\frac{q_1' - q_3'}{q_3'}$ is not corrected for area reduction or membrane effects.

FIG. A10-46




C-44 STANDARD TRIAXIAL DRAINED

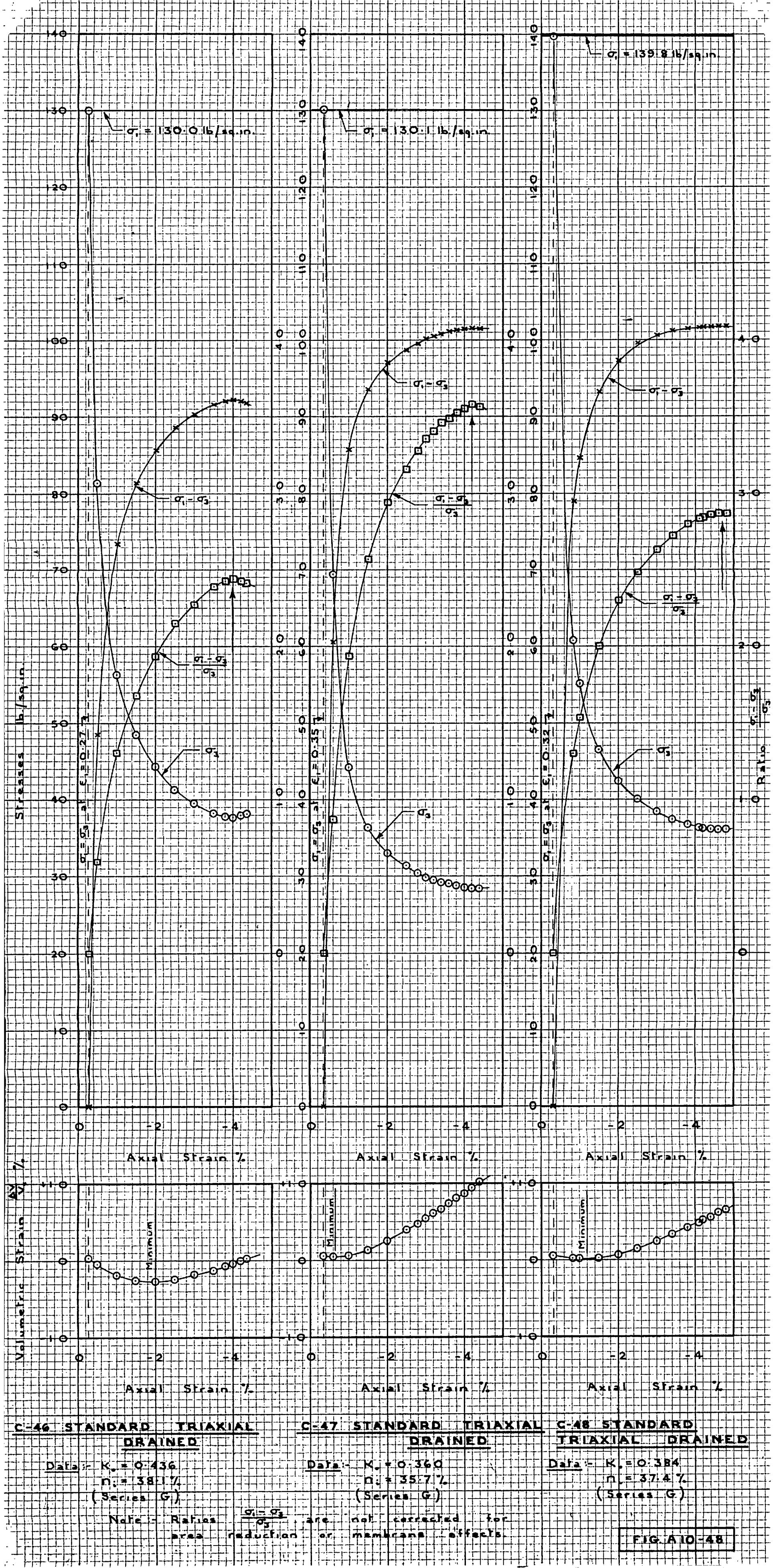
Data:- $K_o = 0.350$
$n_i = 36.0$ %
(Series G)

C-45 STANDARD TRIAXIAL DRAINED

Data:- $K_o = 0.436$
$n_i = 40.1$ %
(Series G)

Ratios $\frac{\sigma_1 - \sigma_3}{\sigma_3}$ are not corrected for area reduction or membrane effects.

FIG. A10-47




C-46 STANDARD TRIAXIAL DRAINED

Data :- $K_o$ = 0·436
$n_i$ = 38·1 %
(Series G)

C-47 STANDARD TRIAXIAL DRAINED

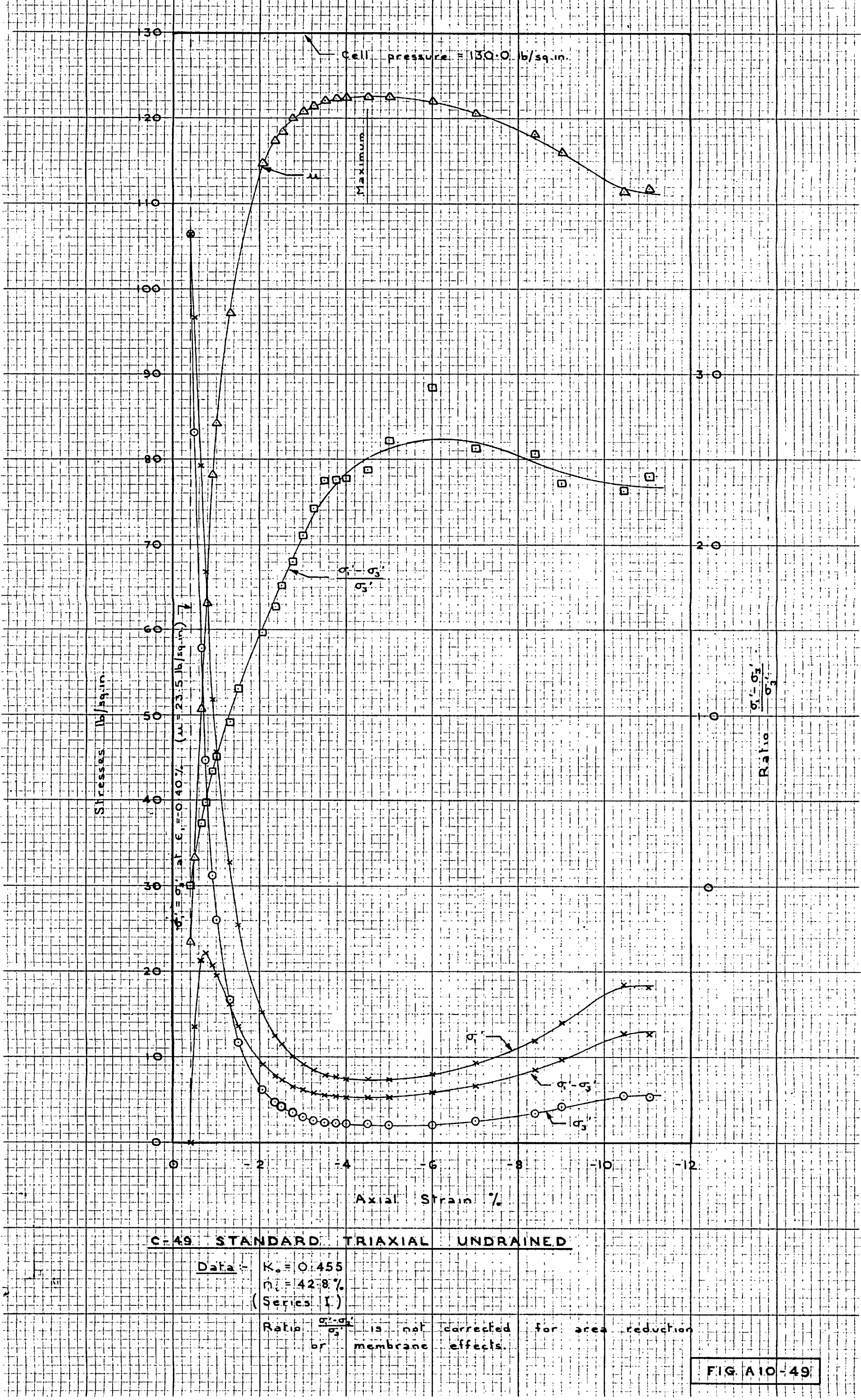
Data :- $K_o$ = 0·360
$n_i$ = 35·7 %
(Series G)

C-48 STANDARD TRIAXIAL DRAINED

Data :- $K_o$ = 0·384
$n_i$ = 37·4 %
(Series G)

Note :- Ratios $\frac{\sigma_1 - \sigma_3}{\sigma_3}$ are not corrected for area reduction or membrane effects.

FIG. A10-48




C-49 STANDARD TRIAXIAL UNDRAINED

Data :- $K_o = 0{\cdot}455$
$n_i = 42{\cdot}8\%$
(Series I.)

Ratio $\frac{\sigma_1' - \sigma_3'}{\sigma_3'}$ is not corrected for area reduction or membrane effects.

FIG. A10-49

Cell pressure = 30.0 lb/sq.in.

$\sigma_1'$

$\sigma_1' - \sigma_3'$

$\sigma_3'$

Maximum

at $\varepsilon_1 = 0.29\%$ ($\mu = -10.75$ lb/sq.in.)

$\sigma_1' = \sigma_3'$

$\mu$

Stresses lb./sq.in.

Axial Strain %

$\frac{\sigma_1' - \sigma_3'}{\sigma_3'}$

Ratio

Axial Strain %

C-50 STANDARD TRIAXIAL UNDRAINED

Data :- $K_o = 0.443$

$n_i = 39.2\%$

(Series I)

Ratio $\frac{\sigma_1' - \sigma_3'}{\sigma_3'}$ is not corrected for area reduction or membrane effects.

FIG. A.10-50

## Appendix 11. KAOLINITE TESTS

### Introduction

The first 15 months of the writer's time was spent in an unsuccessful attempt to measure the shear parameters of kaolinite under plane strain conditions. Kaolinite appears to be the ideal choice of a clay. Its most important asset is that the coefficient of consolidation is approximately 100 times greater than those of remoulded London or Weald clay and hence, the time required to carry out tests on large size specimens can be greatly reduced. In addition, kaolinite has a high clay fraction, low activity, and secondary consolidation is a small and negligible factor.

Identification tests on the soil Supreme Kaolin, produced the following results :-

| | |
|---|---|
| Liquid limit | 61% |
| Plastic limit | 38% |
| Specific gravity | 2.62 |

It contains 70-80% of soil particles within the clay sizes ( < 0.002 mm.).

The test programme fell into two main categories :-

(i) the measurement of the coefficient of earth pressure at rest ($K_o$) for kaolinite.

(ii) using the value of $K_o$ obtained in (i) to consolidate the kaolinite in the plane strain and standard triaxial apparatuses, to measure and compare the consolidated-undrained shear strength and pore-water pressure parameters A (Skempton, 1954) for a normally consolidated clay in the two types of test.

The importance of part (ii) in the stability analysis of clay slopes bears explanation. The immediate ($\phi = 0$) strength of normally consolidated clay is often the most critical condition for stability. Bishop (1954) has given theoretical reasons for believing that the effective angle of shearing resistance under undrained conditions is likely to be higher for plane strain shear than that obtained from standard triaxial compression tests. On the other hand, the greater stresses occurring in plane strain may produce an increase in pore-water pressure which would fail the plane strain specimen at a lower strength than a standard triaxial compression specimen consolidated to identical stress conditions. That this fascinating conflict was never resolved is due partly to the unsatisfactory behaviour of kaolinite (subsequently confirmed to the author from two other research organizations) and partly to the technical difficulties of testing large specimens of clay. It is hoped that some of the comments in subsequent parts of this Appendix will help others to avoid some of the difficulties experienced by the author.

Consolidation characteristics

The normal procedure in research work on clays is to remould the soil. This makes the soil uniform in consistency and gives reproducible results. To simulate natural consolidation and attain a high degree of saturation, the test specimen is initially set up at a moisture content at or near the liquid limit of the soil. Despite these precautions, the behaviour of an undisturbed and a remoulded specimen of the same soil can be quite different under identical shear conditions. This is usually attributed to a breakdown in the "structure" of the clay on remoulding. As undisturbed soil is presumably sedimented at a much higher moisture content than the liquid limit, the author attempted to find out how the consolidation behaviour of the kaolinite was affected by different initial water contents.

Specimens of kaolinite were set up in oedometer rings at moisture contents ranging from 40% to 110%. Every effort was made to avoid trapping air in the drier specimens. The usual consolidation test procedure was followed, each successive increment of load being approximately double the value of the previous load. The results are given on Fig. All-1 and the main conclusions are as follows :-

(i) the void ratio-pressure curve at any initial moisture content is unique to that moisture content. The void ratio-pressure curves at different initial moisture contents do not merge into a common virgin curve at high pressures. The compression indices decrease with decreasing initial moisture contents.

In a separate series of tests, a kaolinite-water slurry was thoroughly shaken up in a 2000 ml. glass measuring cylinder and was allowed to settle over a period of several weeks. Time-settlement readings were taken until equilibrium had been reached. Samples of the deposited kaolinite were taken at different depths of the cylinder by a 10 ml. pipette. They showed that the water content of the kaolinite at the upper surface was finite and was approximately the same at all depths. Repeat tests were consistent and the sedimentation water content was established as being approximately 260%. The water content of the pre-sedimentation mix was approximately 510%. No dispersing agents were used so the finality of the result cannot be established. However, it does show that consolidation of a naturally sedimented clay may begin at moisture contents well in excess of the liquid limit and hence one would anticipate a different void ratio-pressure relationship in the undisturbed soil to that of a laboratory remoulded soil.

(ii) the coefficients of consolidation, $c_v$, on first loading appear to be independent of the initial moisture contents over the range of moisture contents tested but increase with increasing pressure. Ignoring temperature changes and the occasional discrepancies on the first increment, the relation between the coefficient and the overburden pressure is approximately parabolic (Fig. All-1). This means that as the soil structure becomes less compressible, consolidation takes place more rapidly. This property is not a general characteristic of clays.

Measurement of $K_o$

The shear strength of the kaolinite at its liquid limit was 0.25 lb/sq.in. If the clay had been remoulded at a moisture content above the liquid limit, its consolidation (and, perhaps, shear) characteristics would conform more closely with a naturally sedimented soil. However, its strength would be insufficient for a large specimen to stand up under its own weight at the beginning of a test. At lower moisture contents than the liquid limit, the soil becomes too stiff for easy and uniform mixing and there is a danger that the soil will cease to have a sufficiently high degree of saturation. In the present context, it was decided to remould the kaolinite slightly below the liquid limit and to consolidate the soil in a large oedometer (9 inches diameter, 5 inches high) to reduce the compressibility of the soil before carrying out the shear tests. A vertical stress of 0.8 ton/sq.ft. was applied to the soil in the oedometer and this was sufficient to reduce the moisture content from 58% to 45%. When consolidation had been completed, the load was quickly removed and two core cutters (4 inches diameter, 4 inches high) were jacked into the soil. After trimming the ends of the cutters, the two specimens were joined together to form the 4 inch diameter, 8 inches high test specimen for the standard triaxial compression test. Subsequently, it was

hoped to eradicate the stress history of the oedometer stage by further consolidating the clay under stresses at least 3 to 4 times in excess of the maximum oedometer stress.

The same oedometer procedure had to be followed in preparing a $K_o$ test specimen. After weighing and measuring the specimen, ½ inch wide vertical filter drains were placed at 1 inch centres around the perimeter of the specimen. A rubber membrane was then placed on the specimen and sealed at the base pedestal and top cap by rubber O-rings.

The technique adopted for carrying out a $K_o$ test on clay differed from that described for testing sands in Bishop and Henkel (1957). The $K_o$ test on a sand can be completed in one day but for a less permeable material, the test must be carried out more slowly to keep pore-water pressure gradients as low as possible. Dr. A. W. Bishop has devized an automatic means of maintaining $K_o$ conditions (Bishop, 1958). The system makes use of the $K_o$ belt which is placed around the circumference of a 4 inch diameter triaxial test specimen at the mid-height. The belt bears on the specimen through two radiused pads, diametrically opposite to each other. A 1 mm. rise of mercury in the standpipe of the belt corresponds to a change in the specimen diameter of 0.0003 inches.* A platinum wire is placed inside the bore of the glass standpipe and is connected to an electrical terminal at the top of the standpipe. A second electrical terminal is connected to the mercury reservoir below the standpipe such that when the mercury in the standpipe makes contact with the end of the platinum wire the electric circuit is closed. The leads from the terminals pass to the electric motor of the triaxial apparatus via a mercury relay.

---

* improvements necessary to achieve this sensitivity :-
slots to allow accurate positioning of the perspex cap (on one arm of the belt) at the centre of the mercury reservoir;
rigid perspex button glued to the flexible polythene diaphragm of the mercury reservoir.

In a $K_o$ test, the belt is placed under a high vacuum to remove any air from the mercury and water in the reservoir and standpipe. The belt is then carefully placed around the specimen, ensuring that the radiused pads are not in contact with any of the filter drains. (The filter drains tend to crumple up at large strains.) It was necessary to add a pulley and weight system to the standpipe (front) side to redress the imbalance of weights between the front and back of the belt. The perspex cap on the end of the left-hand arm of the belt is adjusted until the mercury in the standpipe just makes contact with the end of the platinum wire. This is the null position of the mercury thread. The cell is then assembled and the ram brought into contact with the proving ring. After filling the cell with de-aired water, the cell pressure is slowly increased at a constant rate by a small electric motor turning the ratchet wind of the constant pressure system. The soil consolidates under the increasing cell pressure, the specimen diameter decreases and the mercury level in the standpipe rises and eventually makes contact with the end of the platinum wire. When the electric circuit closes, the triaxial motor is switched on by the servo-mechanism and a deviator stress is applied to the specimen at a constant rate-of-strain until contact between the mercury and platinum wire is broken and the motor switches off; thus, the test continues as a series of "makes" and "breaks", the value of K being greater on the "make".

Several $K_o$ tests were carried out on kaolinite covering a period of several weeks. The cell pressure was raised at a constant rate of 0.25 lb/sq.in./hour and readings were taken at each "make" and "break", where possible. In the early stages of the tests, when the soil is most compressible, several technical difficulties were encountered. Contacts were established and broken with rapidity and the hunting which occurred produced a black mark on the walls of the standpipe and made the mercury dirty. An interruptor was added to the

relay circuit to prevent too many sparks, the interruptor checking the circuit once per minute. Another snag which was predominant in the early stages of a test was the loss of deviator stress due to creep and consolidation, during the period when the triaxial motor was switched off. After the "break" had occurred, the specimen continued to deform axially at a decreasing rate until the increasing cell pressure arrested it. However, the proving ring had a 3000 lb. capacity (which was necessary for the later stages of the test) and the axial load on the ring decreased to take up the continued axial strain of the specimen. The amount of additional strain depends to some extent on the rate of loading and this is greatest at the start of the test. The result is that the difference between the $K_o$ values on the "make" and "break" can be quite large. Instead of having the proving ring in direct contact with the head of the triaxial apparatus, a large helical spring was added to work in series with the proving ring. The spring, deflecting a maximum of 1 inch under a 3000 lb. load, was compressed during the application of the deviator stress to the specimen. It had the desired effect of "softening" the proving ring and reducing the loss of load during the "break" period. The rate of strain of the electric motor was reduced from time to time during the tests so that the periods of contact and non-contact between the mercury and platinum wire were approximately equal. These periods lengthen as the specimen becomes stiffer. The $K_o$ value was taken to be the average of the readings taken at successive "make" and "break" points, the usual difference in K value on these occasions being typically 0.010. From observation, the maximum gap between the mercury and platinum wire was 2 to 3 mm. and if it is assumed that the change in mercury height was the same during the contact period, the maximum deviation of the specimen diameter

was approximately ± 0.0009 in. The radiused pads of the lateral strain indicator tended to dig into the soft clay at the start of $K_o$ tests. They may require modification in the future (e.g. increasing the bearing area).

Altogether, 4 No. $K_o$ tests were carried out on the kaolinite. Two of the tests measured only the applied stresses and the other two tests measured both the applied stresses and the pore-water pressure set up at the centre of the specimen base (radial drainage only). The cell pressure was increased at the same rate in all the tests. K values calculated from the applied stresses agreed fairly well when compared at the same cell pressure, the maximum difference being 0.05. There was a slight rise in the K values with increasing cell pressures. $K_o$ on first loading increased from approximately 0.60 initially to 0.71 at cell pressures of 130 lb/sq.in., although it is difficult to estimate the effect of the oedometer stress history on the low pressure values. A description of the $K_o$ test was published in the Brussels Conference on Earth Pressures (Bishop, 1958).

In the later $K_o$ tests, drainage was allowed from the sides and the top but not on the bottom end of the specimen. A phosphor-bronze porous probe was inserted into the centre of the lower end and the pore-water pressures set up during the test were measured (Fig. All-2). As one would expect, the pore-water pressures rose during the application of the deviator stresses and fell during the non-contact periods. Dr. R. E. Gibson, of Imperial College, has proposed a mathematical solution for this test based on radial drainage only. In it, he shows that the radial distribution of excess pore-water pressure at the non-draining ends is parabolic and that the maximum value, at the centre, becomes asymptotically constant at large values of time. However, as the maximum value is inversely proportional

to the coefficient of consolidation (which, as a necessary condition for the solution of the differential equation, is assumed to be constant in Gibson's solution) the measured values of pore-water pressure, Fig. All-2, which show a slight tendency to decrease with time, are in good agreement with the theory, since it is known that the $c_v$ of kaolinite increases with increasing effective pressures. The test result shows that the excess pore-water pressures set up in the $K_o$ tests on Kaolinite were not unduly great and that they had little effect on the $K_o$ values based on total stresses, except at the beginning of the test.

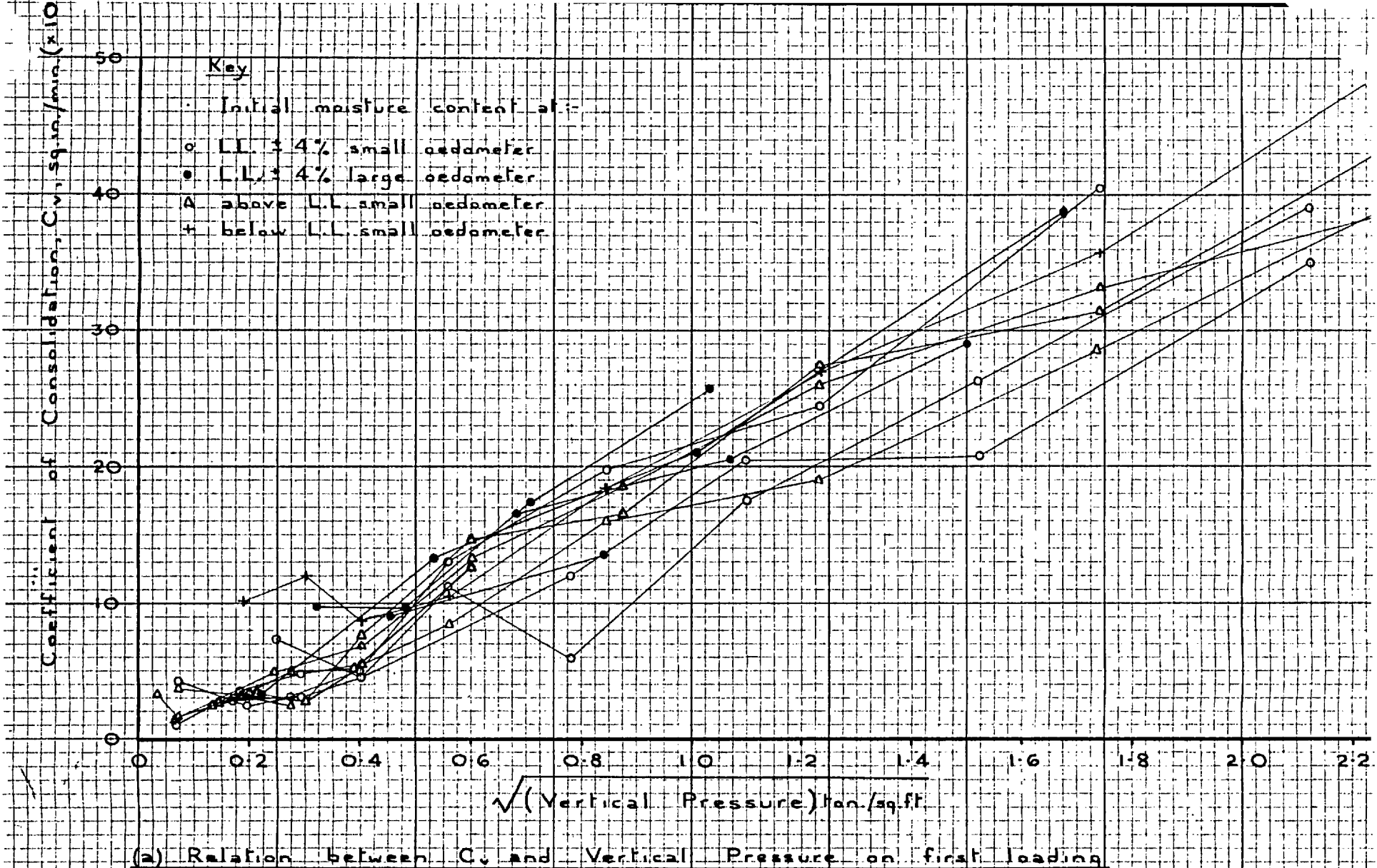
Shear strength

The preparation of a plane strain test specimen proved to be more difficult than was originally anticipated. A technique was finally evolved, but was never entirely satisfactory. A filter paper was placed between the sample and the lower porous stone in the large oedometer and a thin layer of silicone grease smeared around the circumference. The sample was then easily removed from the oedometer with a minimum of disturbance. However, it was impossible to prevent the soil from sucking back water out of the porous stones on removal of the overburden stresses, thus causing the soil to have a varying moisture content with depth. There were other difficulties associated with this technique :- the methods of cutting 2 inch wide sections by wires and knife-edge blades were not particularly successful and it was difficult to join up two or three sections to form a specimen 16 inches long; finally, an unfortunate side effect of the high coefficient of consolidation is that the soil dries out quickly when exposed to room temperatures. To sum up, the disadvantages of the large oedometer technique rule it out as a practical solution in this particular case. The alternative solution is to remould the soil at a slightly lower moisture content directly on the lower platen of the plane strain apparatus using a mould similar to the sand former.

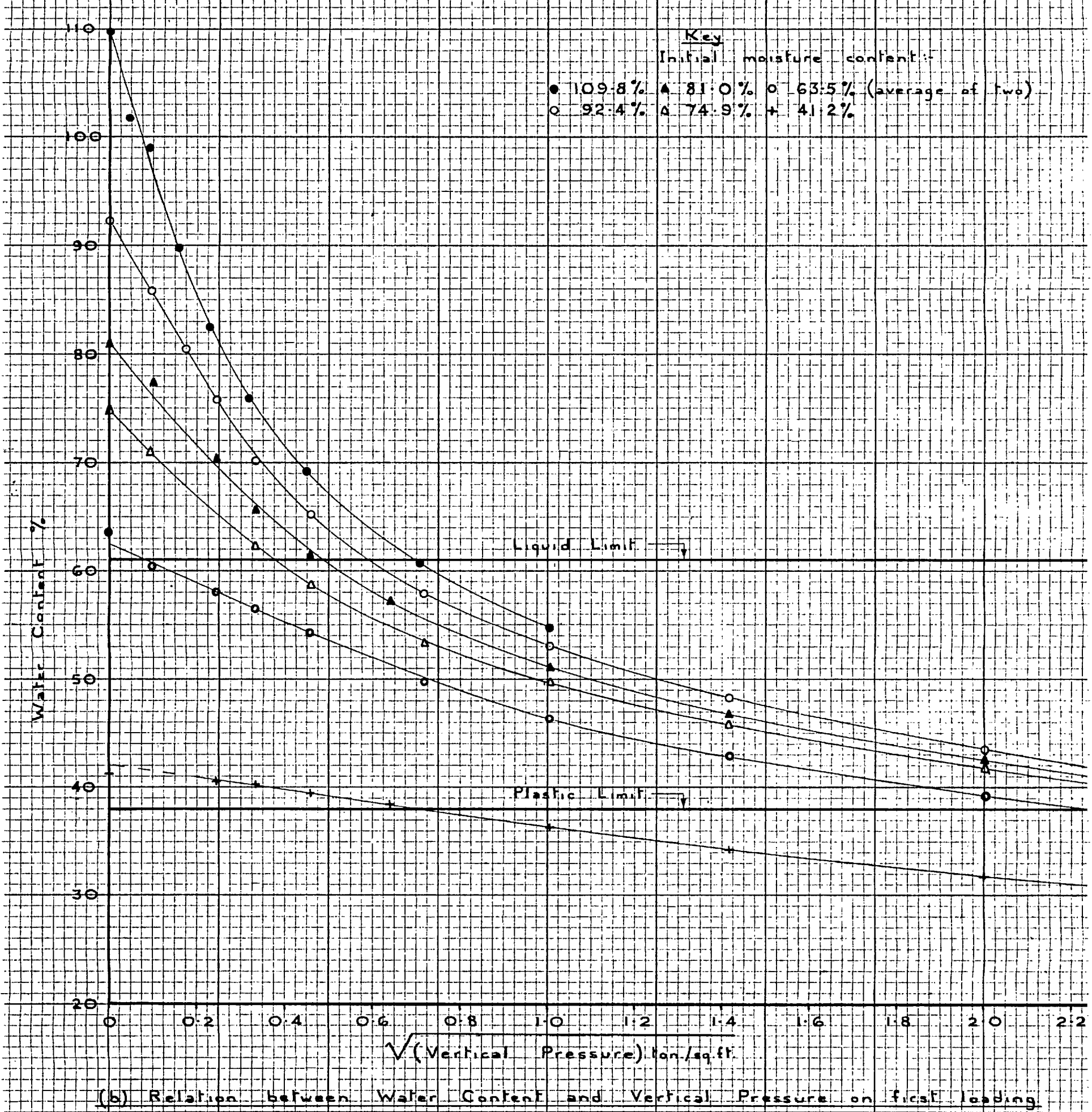
A few pilot tests were carried out on 1½ inch diameter standard triaxial test specimens to measure the shear parameters of kaolinite. The results were not consistent. The effective principal stress ratio $(\frac{\sigma_1'}{\sigma_3'})$ in the consolidated-undrained tests with pore pressure measurements varied from 1.80 to 2.05 on the same batch of clay. The axial strain at failure varied from 9 to 13%. The scatter in the principal stress ratios was larger than the anticipated difference between the effective principal stress ratios in the plane strain and standard triaxial tests. Reducing the rate-of-strain during shear had no effect on the results and consolidated-drained triaxial tests on the kaolinite were also inconsistent. The author was informed of similar scatter with kaolinite in tests carried out by the Building Research Station, Watford and the C.S.I.R.O. in Melbourne, Australia. The testing programme on the soil was abandoned.

In conclusion

The testing of large size specimens of remoulded saturated clay has not often been attempted in the past and has given rise to many technical problems. At the time of writing, Dr. D. J. Henkel and Mr. N. Wade are perfecting a device for automatically maintaining the $K_o$ and plane strain conditions on specimens of clay. The device is similar in principle to the automatic method of measuring $K_o$ values using the circumferential belt. If the technical difficulties can be overcome, the test results will be of great interest. The author also hopes that greater attention will be paid in the future to the testing of undisturbed clays and their relation to the vast amount of knowledge which has been accumulated on the behaviour of remoulded clays.



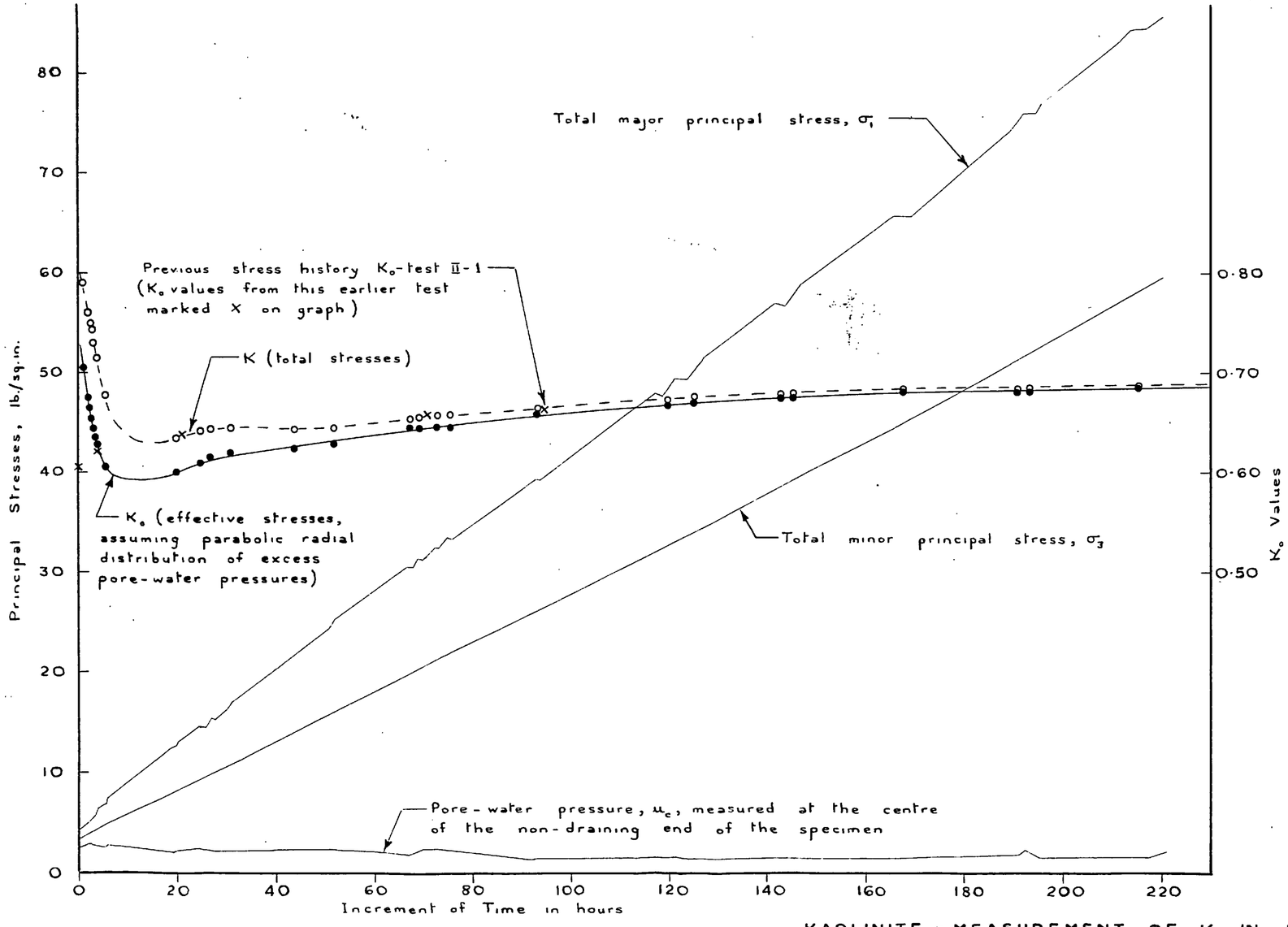

(a) Relation between $C_v$ and Vertical Pressure on first loading




(b) Relation between Water Content and Vertical Pressure on first loading

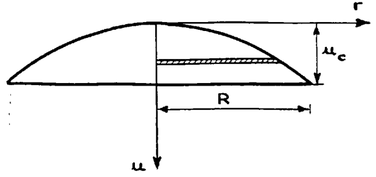
KAOLINITE - CONSOLIDATION CHARACTERISTICS

FIG. A II - 1




(a) First half of $K_o$-test on Kaolin II-2

(b) Calculation of the average pore-water pressure $\bar{u}$ in the soil specimen, given $u_c$




To find centroid $\bar{u}$ of volume of revolution:-

Volume $= \pi \int_0^{u_c} r^2 . du$

Parabolic distribution of $u$ across the diameter, 2R, of the specimen (theoretical work – Dr. R.E.Gibson)

Let $r^2 = 4a.u$ where $a$ = constant

$r = R$, $u = u_c$

$\therefore R^2 = 4a.u_c$

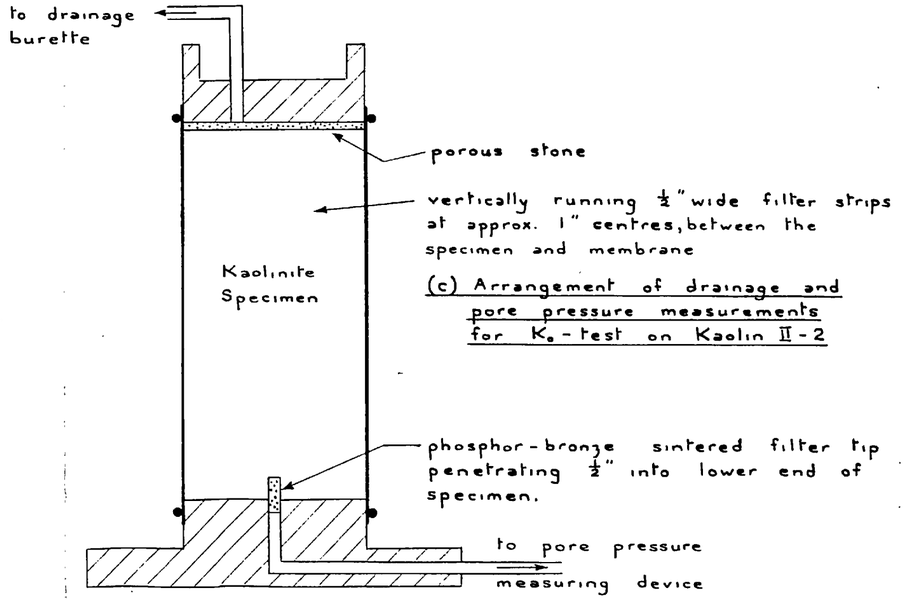
Volume $= \pi \int_0^{u_c} 4a.u.du.$

$= \pi.4a.\left\{\frac{1}{2}u^2\right\}_0^{u_c}$

$= 2\pi a.u_c^2$

Volume of disc ($r = R$, $u = u_c$) is $4\pi a.u_c^2$

$\therefore$ Average pore pressure $\bar{u}$ is given by $\bar{u} = \frac{1}{2}u_o$




(c) Arrangement of drainage and pore pressure measurements for $K_o$-test on Kaolin II-2

KAOLINITE - MEASUREMENT OF $K_o$ IN A SPECIMEN OF SATURATED CLAY

FIG. A 11-2